ROTORDYNAMIC PERFORMANCE OF A FLEXURE PIVOT PAD BEARING WITH ACTIVE AND LOCKED INTEGRAL SQUEEZE FILM DAMPER INCLUDING PREDICTIONS

A Thesis

by

JEFFREY SCOTT AGNEW

Submitted to the Office of Graduate Studies of
Texas A&M University
in partial fulfillment of the requirements for the degree of

MASTER OF SCIENCE

December 2011

Major Subject: Mechanical Engineering

Rotordynamic Performance of a Flexure Pivot Pad Bearing with Active and Locked Integral Squeeze Film Damper Including Predictions

ROTORDYNAMIC PERFORMANCE OF A FLEXURE PIVOT PAD BEARING WITH ACTIVE AND LOCKED INTEGRAL SQUEEZE FILM DAMPER INCLUDING PREDICTIONS

A Thesis

by

JEFFREY SCOTT AGNEW

Submitted to the Office of Graduate Studies of
Texas A&M University
in partial fulfillment of the requirements for the degree of

MASTER OF SCIENCE

Approved by:

Chair of Committee,	Dara W. Childs
Committee Members,	William H. Marlow
	Luis A. San Andrés
Head of Department,	Jerry Caton

December 2011

Major Subject: Mechanical Engineering

ABSTRACT

Rotordynamic Performance of a Flexure Pivot Pad Bearing with Active and Locked Integral Squeeze Film Damper Including Predictions. (December 2011)

Jeffrey Scott Agnew, B.S., Arkansas State University

Chair of Advisory Committee: Dr. Dara W. Childs

Tests are performed on a flexure-pivot-pad tilting-pad bearing with a series integral squeeze film damper in load-between-pads configuration, with both active and locked damper. The damper effects are negated when locked, resulting in a flexure-pivot-pad bearing only. Experimental tests provide static performance data and dynamic stiffnesses from which rotordynamic coefficients are extracted. The following two excitation schemes are implemented: (1) multi-frequency, single direction excitation and (2) single-frequency, rotating load excitation (or "circular excitation"). The XLTRC^2 Rotordynamics Software Suite© provides stiffness and damping coefficient, eccentricity, and power loss predictions for the locked damper bearing. Test conditions include the rotor-speed range of 4000-12000 rpm and the unit-load range of 0-862 kPa (0-125 psi).

Dynamic tests utilizing the multi-frequency excitation for the locked and active damper bearing configurations both show that the real portion of the dynamic stiffness is well modeled by a quadratic curve fit, and the imaginary portion representing the damping is a linear function of excitation frequency. This means that *frequency independent* coefficients can be obtained when an added mass term is included. While

stiffness coefficients are lower for the active damper bearing, damping coefficients remain almost constant between the locked and active damper configurations. A simulation shows that, although the damping coefficients do not change significantly, the reduced stiffness provided by the damper results in greater *effective* damping.

Static performance tests for the locked and active damper bearing indicate low cross-coupling, as shown by the eccentricity and low attitude angle measurements. Pad metal temperature measurements show a smaller temperature differential along the pad arcs for the active damper bearing, than observed for the locked damper case. Frictional power loss is estimated based on lubricant temperature rise and does not differ significantly for the two bearing configurations.

ACKNOWLEDGEMENTS

My sincere gratitude goes to all of the members on my thesis committee, including Dara Childs, Luis San Andrès, and William Marlow. Since Dr. Childs offered me a research position at the Texas A&M Turbomachinery Lab, he has been a persistent, but patient, advocate of this thesis and without his guidance and support this thesis would not have been possible. Dr. San Andrès provided practical advice and a helping hand on numerous occasions. All of my professors during both my undergraduate and graduate educations helped to further my interests and skills in engineering and science, to all of whom I am appreciative.

Bearings Plus, Incorporated (BPI) graciously supplied the test bearing, and thanks to Dr. Fouad Zeidan and Dr. Jongsoo Kim of BPI for their support of this project. Also, thanks to the Turbomachinery Research Consortium (TRC) for their funding.

Additional gratitude goes to my coworkers at the Turbomachinery Lab, namely Robert Sheets and Andy Schaible, who both helped tremendously in the testing phase and who traded many of their days and late nights for lending me a hand. Jason Wilkes was also invaluable and provided consultation relating to the rotating load section of this thesis. Steve Phillips provided technical assistance on various aspects of the project.

Finally, my wife Erin provided continual support and understanding throughout my career as a graduate student. I thank and love her for this.

TABLE OF CONTENTS

Page

Page

Page

LIST OF FIGURES

Page

Page

Page

LIST OF TABLES

Page

Page

Page

Page

Page

NOMENCLATURE

C_B	Radial bearing clearance [L]
C_P	Radial pad clearance [L]
C_{ij}	Damping coefficients [F.t/L]
ΔC_{ij}	Uncertainty in the C_{ij} coefficient [F.t/L]
$\overline{C}_{ij}$	Non-dimensionalized damping coefficient [-]
$e_{x,o}, e_{y,o}$	Eccentricities [L]
H_{ij}	Dynamic stiffness [F/L]
j	$\sqrt{-1}$
k_{ISFD}	Integral squeeze film damper structural stiffness [F/L]
$k_{\theta,pad}$	Pad rotational stiffness [F.L/rad]
$\overline{K}_{eq}$	Equivalent stiffness [F/L]
K_{ij}	Stiffness coefficients [F/L]
ΔK_{ij}	Uncertainty in the K_{ij} coefficient [F/L]
$\overline{K}_{ij}$	Non-dimensionalized stiffness coefficient [-]
$\overline{M}_{eq}$	Equivalent added mass [F.t^2/L]
M_{ij}	Added mass coefficients [F.t^2/L]
ΔM_{ij}	Uncertainty in the M_{ij} coefficient [F.t^2/L]
$\overline{M}_{ij}$	Non-dimensionalized added mass coefficient [-]
N_{rpm}	Rotor speed [rev/t]
OSI	Onset speed of instability [1/t]

P_{loss}	Power loss [F.L/t]
P_{Static}	Unit loading [F/L^2]
Re	Reynolds number [-]
S	Sommerfeld number [-]
T_{in}	Inlet temperature [T]
T_{out}	Outlet temperature [T]
W	Static load or rotor weight [F]
WFR	Whirl frequency ration [-]
x_i,y_i	Data pairs: x_i [1/t], y_i [F/L]
$\Delta x,\Delta y$	Relative rotor-bearing displacements [L]
$\Delta\dot{x},\Delta\dot{y}$	Relative rotor-bearing velocities [L/t]
$\Delta\ddot{x},\Delta\ddot{y}$	Relative rotor-bearing accelerations [L/t^2]

Subscripts

ij	Coefficient direction indicator: *xx, xy, yx,* yy
xx,yy	Indicates direct coefficients in the *x*- and *y*-directions, respectively
xy,yx	Indicates cross-coupled coefficients

Greek Symbols

β_0	Intercept of linearized curve fit of dynamic stiffness [F/L]
β_1	Slope of linearized curve fit of dynamic stiffness [F.t^2/L]
δ	Logarithmic decrement (log dec) [-]

$\varepsilon_{o,x},\varepsilon_{o,y}$	Normalized eccentricities [-]
ε_o	Eccentricity ratio [-]
κ	Bearing preload [-]
μ	Viscosity [F.t/L^2]
ρ	Density [F.t^2/L^4]
ϕ	Attitude angle [degrees]
ϕ_f	Phase angle [degrees]
$\omega_{n,pad}$	Pad natural frequency [1/t]
$\omega_{n,rotor}$	Rotor natural frequency [1/t]
Ω	Excitation frequency [1/t]
γ	Specific heat at constant pressure [L^2/t/T]
ζ	Damping ratio [-]

Abbreviations

DE	Drive End
FPJB	Flexure Pivot Journal Bearing
Im( )	Imaginary portion ( )
LBP	Load Between Pads
LOP	Load On Pad
NDE	Non-Drive End
OSI	Onset Speed of Instability
Re( )	Real portion ( )

SFD	Squeeze Film Damper
WFR	Whirl Frequency Ratio

1. INTRODUCTION

Modern turbomachines, or machines that exchange the enthalpy of a fluid for shaft power, require rotordynamic stability to operate efficiently and reliably. Examples of common turbomachines include gas and steam turbines, turbo pumps and compressors, turbochargers, and even dental drills. A primary consideration affecting the stability of these machines is the proper design and selection of their bearings. Tilting pad (TP) journal bearings are often used in commercial machinery for their high load capacity, stability, and operating speed capability. Figure 1 illustrates conventional rocker-pivot and spherical-seat TP bearings, and Fig. 2 illustrates a less typical flexure-pivot-pad TP bearing. Squeeze film dampers (SFDs) are sometimes added in series with bearings to reduce stiffness and optimize damping [1]; a typical squeeze film damper is illustrated in Fig. 3. The performance characteristics of the flexure-pivot-pad bearing with integral squeeze film damper ("damper-bearing"), shown in Fig. 4, must be known to effectively utilize them.

This thesis follows the style of the ASME Journal of Engineering for Gas Turbines and Power.

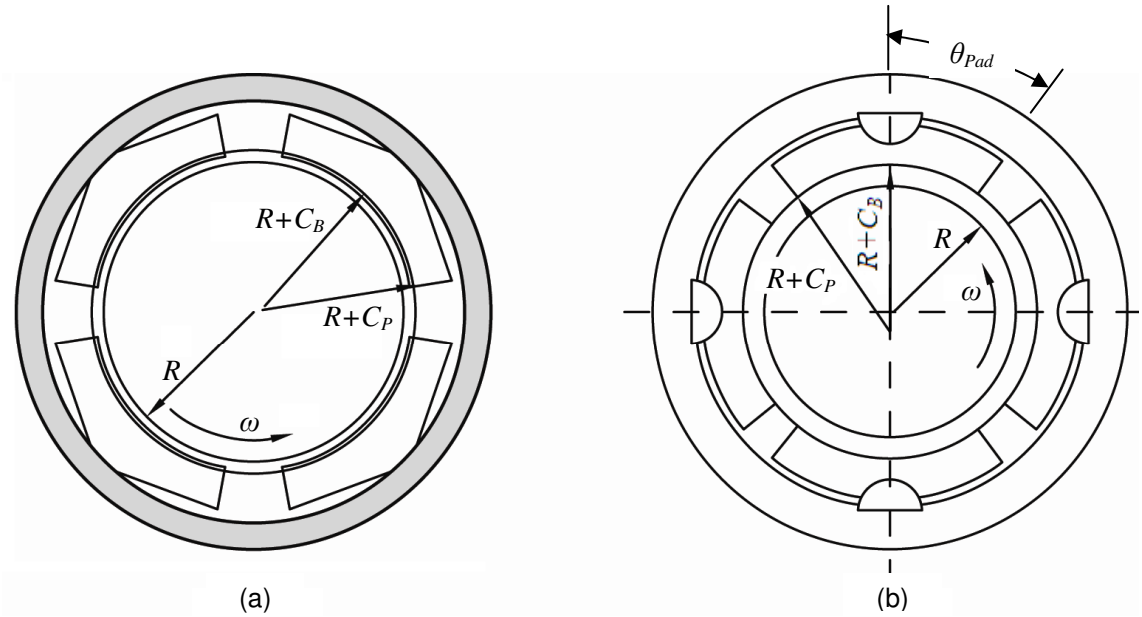

Figure 1. (a) Rocker pivot and (b) spherical pivot pad bearings (personal communication from D. Childs, July 6, 2010)

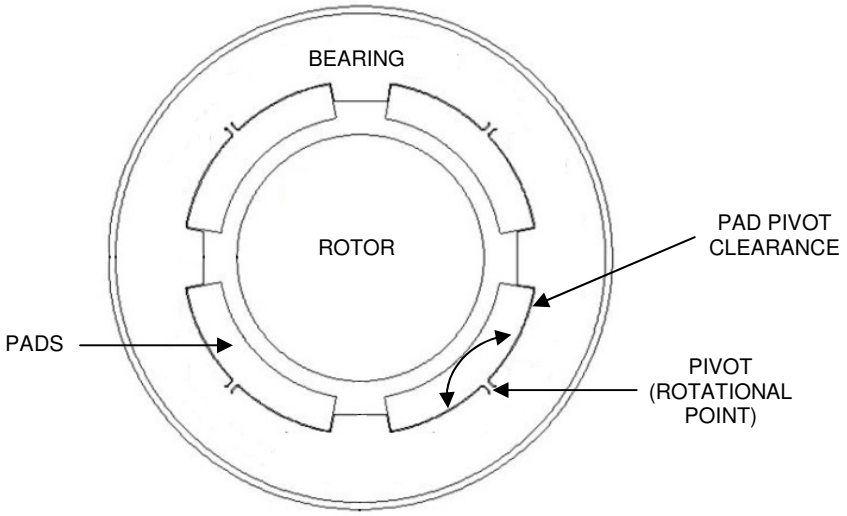

Figure 2. Flexure-pivot-pad bearing

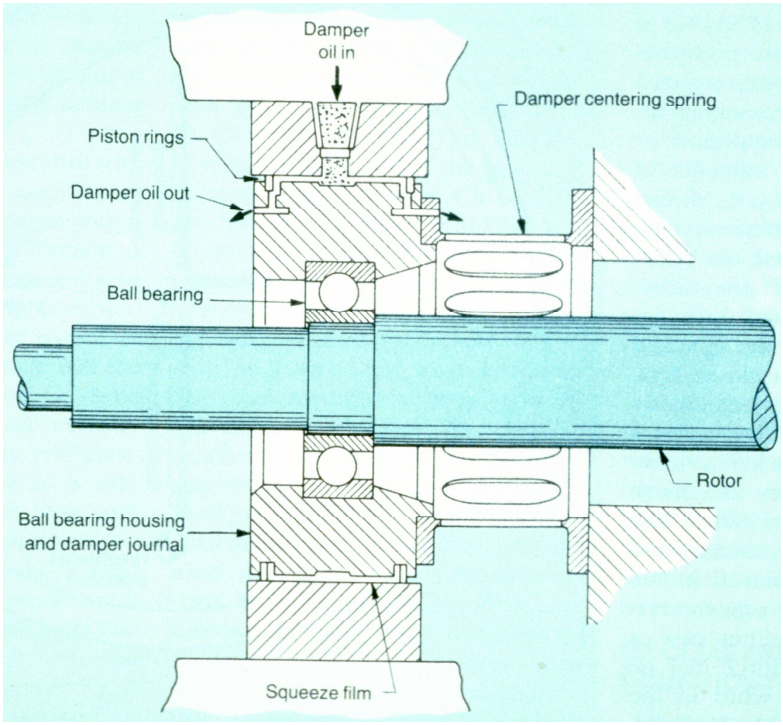

Figure 3. Conventional squeeze film damper with centering spring (personal communication from D. Childs, July 6, 2010)

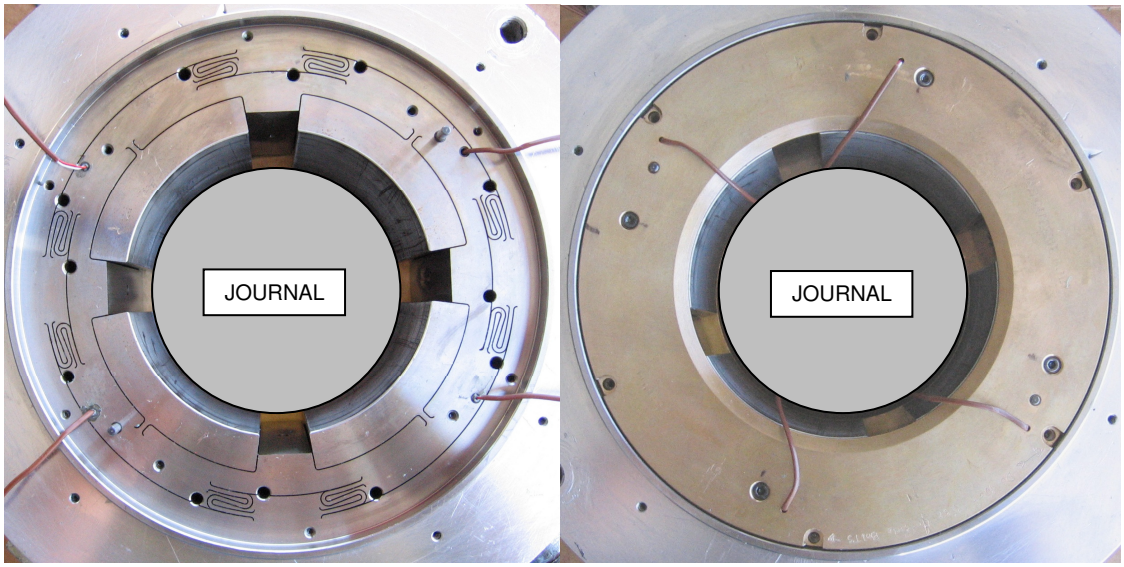

Figure 4. Flexure pivot pad bearing with integral squeeze film damper (test bearing) with seal removed for clarity (left) and with seal installed (right)

Bearing concepts and background

Unlike the conventional TP bearings shown in Fig. 1 above, flexure-pivot-pad journal bearings (FPJBs) are of a single-piece wire EDM (Electric Discharge Machine) construction as shown in Fig. 4. The advantage of FPJBs over conventional TP journal bearings is that their pivot is not a frictional interface of two moving parts that can wear, but instead is a simple beam element that flexes within its elastic region. Similarly, while standard TP bearings must be machined of multiple pieces and assembled, FPJBs practically eliminate the possibility for tolerance stackup which could lead to clearances that are not per design.

Several geometrical parameters of tilting pad journal bearings are introduced in Fig. 1, where R is the rotor radius, C_B is the radial bearing (minimum) clearance, C_P is the radial pad clearance (or the difference in the pad and rotor radii), θ_{Pad} is the pivot offset, and ω is rotor speed. Tilting pad bearing pads can be machined to a different radius than the bearing bore, resulting in the dimensionless preload κ defined below. Positive bearing preload is a common industry practice and ensures an always converging lubricant film and hydrodynamic pressure generation, thus encouraging rotor-bearing stability [2].

$$\kappa = 1 - C_P/C_B \tag{1}$$

The pivot offset, θ_{Pad}, is the circumferential location of the pad pivot as measured from the pad leading edge, and is often expressed as a percentage of the circumferential pad length. While a 50% offset (shown) is typical, offset pivots are sometimes used to

reduce operating temperatures or increase stiffness without reducing damping and increasing bearing temperature [3].

Assuming the weight of the rotor is acting downward, Fig. 1 also shows the two different loading arrangements possible with tilting pad bearings: (a) load between pads (LBP) and (b) load on pad (LOP). Load between pads is the generally preferred loading arrangement for heavy rotors spinning at relatively low speeds because of higher load capacity, decreased temperature rise due to a more uniformly distributed load, and greater lateral stiffness and damping [4].

The reaction-force model for a journal bearing is given by Eq. (2), where f_{bi} are the bearing reaction force components, K_{ij} are the stiffness coefficients, C_{ij} are the damping coefficients, M_{ij} are the apparent mass (also called "added mass") coefficients, and Δx,Δy are the relative motion (displacement) components between the rotor and bearing, with each dot representing the successive time derivatives of velocity and acceleration, respectively. The subscripts indicate the respective directions, where *xx* and *yy* are the direct coefficients and act in the *x*- and *y*-directions, and *xy* and *yx* are the cross-coupled coefficients and represent terms that cause a reaction force in a direction perpendicular to the displacement, velocity, or acceleration direction. Cross-coupled stiffnesses are undesirable because they promote self-excited vibrations and instabilities in rotating machinery. Tilting pad journal bearings are characterized by no, or low, cross-coupled stiffness due to the pads' ability to freely rotate in response to changes in load. Flexure pivot pad bearings will have some (low) cross-coupling due to the rotational stiffness of the pads [3].

$$-\begin{bmatrix} f_{bx} \\ f_{by} \end{bmatrix} = \begin{bmatrix} K_{xx} & K_{xy} \\ K_{yx} & K_{yy} \end{bmatrix} \begin{bmatrix} \Delta x \\ \Delta y \end{bmatrix} + \begin{bmatrix} C_{xx} & C_{xy} \\ C_{yx} & C_{yy} \end{bmatrix} \begin{bmatrix} \Delta \dot{x} \\ \Delta \dot{y} \end{bmatrix} + \begin{bmatrix} M_{xx} & M_{xy} \\ M_{yx} & M_{yy} \end{bmatrix} \begin{bmatrix} \Delta \ddot{x} \\ \Delta \ddot{y} \end{bmatrix} \quad (2)$$

For machines requiring stability enhancement, or with existing vibration problems, squeeze film dampers (SFDs) are often employed to provide additional damping and support flexibility to reduce vibration amplitudes, reduce forces transmitted to ground, and to shift the locations of critical speeds away from the operating range [4]. Squeeze film dampers consist of a stationary outer element, or housing, and (normally) a flexibly supported inner bearing housing. Oil is fed into the annulus between these elements, known as the squeeze film land, and perturbations to this land caused by the radial velocity of the rotor, $\vec{V}$, result in the pressure distributions causing damping forces shown in Fig. 5. Unlike hydrodynamic bearings that rely on the converging-diverging wedge for pressure generation, the pure squeezing action that takes place between the inner and outer housings of the SFD provide damping while a support structure, such as springs, normally provides the stiffness of the SFD.

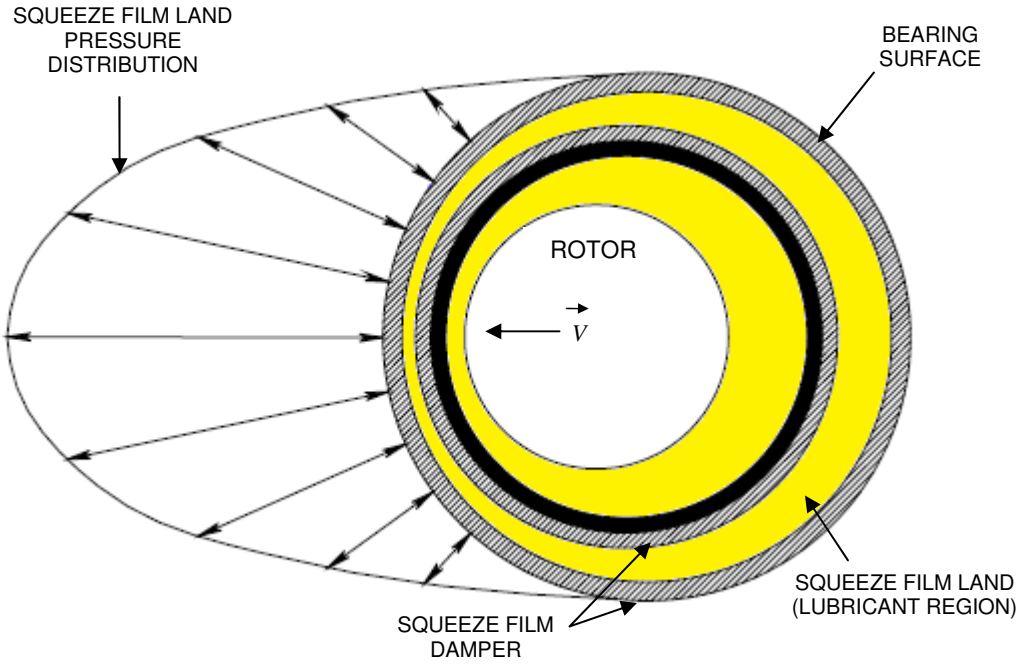

Figure 5. Simplified squeeze film damper

The additional flexibility offered by the SFD supports causes a lower resultant bearing stiffness, thus resulting in larger amplitudes of rotor vibratory motion at the rotor's first critical speed and a reduction in the second critical speed [3]. As a result, the response in the operating range and the forces transmitted to ground are reduced. Squeeze film dampers are often viewed as a "band-aid" fix due to the process industry's last resort use of SFDs to reduce vibration and enhance rotordynamic characteristics in process machinery. Because of this, SFDs are often misunderstood and misused devices [5]; however, properly designed SFDs can increase bearing life and reduce vibrations, allowing higher operating speeds and possibly longer time spans between bearing replacements [3].

A good amount of research has been performed on flexure-pivot-pad bearings (FPJBs). Al-Ghasem and Childs [6] provides perhaps the most relevant data, testing a FPJB in the same LBP loading configuration and with the same preload as the current test bearing. Al-Ghasem's curve fits for the experimental dynamic stiffnesses generally indicated good quadratic curve fits for the real portion of the dynamic stiffnesses and good linear curve fits for the imaginary portions of the dynamic stiffnesses (indicating that damping remains constant with changing excitation frequency). XLTRC^2-XLTFBrg©, a Texas A&M University rotordynamics software, was used for predicting performance, and in most cases provided good matches to experimental rotordynamic coefficients for direct coefficients, but generally poorly matched experimental cross-coupled coefficients. The code also under predicts the eccentricity and attitude angle. Power loss predictions are good, increasing with accuracy as the static load increases.

Rodriguez [7] provides test results for the same FPJB as Al-Ghasem [6], but in load-on-pad (LOP) configuration. Similar results to [6] were observed with the dynamic stiffness curve fits. The software provided good stiffness predictions, but often under-predicts damping and added mass coefficients by around 30%. Rodriguez concludes that the use of the 2x2 added mass matrix of Eq. (2) provides an improved model, and that the direct added mass terms may significantly affect rotordynamic calculations, particularly for light rotors.

San Andrès and De Santiago [8-13] supply the majority of the available literature for the damper-bearing. In one study [8], they provide test results for a rotor mounted on two identical damper bearings, for both a locked and active damper, and excited

identical imbalances. Results show higher peak amplitudes of vibration for the damper-bearing than for the FPJB (due to the extra clearance provided by the damper); however, operation with the damper (damper-bearing) resulted in increased tolerance to imbalance. In fact, the damper allowed safe operation of the rotor with imbalances twice as large as with the FPJB alone. Reductions in critical speed of up to 10% were recognized for the highest imbalance condition. Low cross-coupled stiffness was evidenced by the shaft centerline moving along a nearly vertical path during coast down tests.

San Andrés and De Santiago [10] also used imbalance masses in two planes to provide synchronous excitation to the same rotor, this time supported by a damper-bearing on one end and a plain journal bearing with a conventional SFD on the other end. Predictions made for the system estimated that coefficients change more as a function of rotor speed than of excitation frequency. At low rotor speeds, the direct stiffnesses were found to correspond to the structural support stiffnesses of the squeeze film dampers. Equivalent synchronous damping coefficients were found to decrease steadily with increased rotor speed, for most of the speed range tested.

De Santiago et al. [11] design and construct a damper-bearing and predict the imbalance response for it to show the effect on the location of critical speeds and effective damping of the series combination. Optimum selection of stiffness and damping for minimization of rotor response is described, as well as a 38-station transfer-matrix model that predicts the imbalance response of the rotor-bearing system. In a follow up paper [12], these predictions are compared to measured imbalance response

results. Results show a marked decrease in the first critical speed of the rotor-bearing system, with small variations between the experiments and predictions. The predicted peak-to-peak responses are generally close to the experimental results in the horizontal direction, but a resonance in the support is not well accounted for in the vertical direction. Results of no-imbalance coast down experiments are also shown compared to ball bearings with ISFDs and evidence very low viscous drag – taking more than 10 minutes for the decelerating rotor to come a full stop. A linear relationship between peak vibration amplitude at the critical speed and imbalance displacement is observed. Using calibrated impact hammer strikes to provide excitation at null running speed, the system damping coefficient is shown to increase by an average of 11% and 18% over the ISFD alone (mounted on ball bearings) in the horizontal and vertical directions, respectively. FPJB results are also presented and show the tilting pad bearing can tolerate imbalances less than the bearing clearances; however, the damper-bearing can handle much greater imbalances with reduced force transmissibility.

Only one paper detailing an industrial application of flexure-pivot-pad bearings with integral squeeze film dampers is presently known to the author. In this case, Locke and Faller [14] implement the bearing into the design of a high-reliability process recycle gas compressor. Suction contaminants of an abrasive and corrosive sticky material capable of *severely* eroding (nearly consuming) the radial compressor impeller in less than ten days required a machine with high stability and tolerance to imbalance, able to continue processing after significant deterioration of the impeller vanes. The damping provided by a FPJB alone was insufficient for the application, so additional

damping was provided using an ISFD. During normal operation at 10000 rpm, buildups of material from the sticky process stream routinely occur on the impeller, and the damper-bearing design tolerated the imbalance due to buildups better than a similar machine on another process line. Although buildups occasionally caused the vibration amplitude to exceed 25.4 μm (1 mil), the damper-bearing configuration sufficiently absorbs the energy to keep bearing temperatures in line with requirement and allow operation until scheduled outages. During shop testing, an imbalance corresponding to deterioration by a factor of more than ten with respect to normal balance quality was applied to the rotor. Also, the location of the critical speed was found to be at 60 percent of operating speed, while being predicted at around 40 percent, which questioned the current ability to accurately predict characteristics of the damper-bearing assembly. In the end, however, the actual test results were satisfactory with maximum vibrations being only about 10 percent above the predictions, making for a stable compressor tolerant to high imbalance.

Test Bearing: Flexure-Pivot-Pad Bearing with Integral Squeeze Film Damper

The test bearing (shown previously in Fig. 4) is a one piece, wire EDM, flexure-pivot-pad bearing with integral squeeze film damper manufactured by Bearings Plus, Inc. (BPI). Oil is fed to the bearing by two supply hoses stationed 180-degrees apart and enters a supply groove located circumferentially around the bearing. Eight ports are located in the supply groove – four supply oil to the bearing (one between each set of pads) and the other four have orifices which supply oil to the SFD. A list of the bearing parameters is provided in Table 1.

Table 1. Test bearing parameters

Type of Bearing	Flexure® Pivot Pad w/ Integral Squeeze Film Damper
Number of Pads	4
Configuration	Load Between Pads (LBP)
Pad Preload	0.25
Pad Pivot Offset	50%
Pad Arc Length	73°
Rotor Diameter	101.59 ± 0.01 mm (3.9995 ± 0.0005 in)
Pad Axial Length	76.20 ± 0.15 mm (3.000 ± 0.006 in)
Bearing Clearance (C_B)	0.1542 ± 0.0064 mm (0.0060 ± 0.00025 in)
Pad Clearance (C_P)	0.2032 ± 0.0064 mm (0.0080 ± 0.00025 in)
Lubricant Type	ISO VG32
Materials	4130 Steel Body, Babbited Pads, Bronze End Seals
Oil Inlet Orifice Diameter for SFD	1.981 mm (0.078 in)
Damper Axial Length	76.20 ± 0.15 mm (3.000 ± 0.006 in)
Squeeze Film Land Diameter	157.5 mm (6.2 in)
Squeeze Film Land Clearance	0.356 mm (0.014 in)
Axial Seal Clearance	2.437 mm (0.096 in)

Objectives

Briefly stated, the following are objectives for researching the performance characteristics of the flexure-pivot-pad bearing with integral squeeze film damper:

1. Examine the frequency-dependent nature of the dynamic stiffness coefficients for the damper-bearing.
2. Examine the frequency-dependent nature of the dynamic stiffness coefficients for the FPJB (locked damper).
3. Quantify the effect of the damper on the performance of the FPJB.

4. Evaluate the accuracy of available predictive rotordynamic software, namely the XLTRC^2-XLTFBrg© Rotordynamics Suite to predict static and dynamic bearing parameters for the FPJB.

2. TEST RIG DESCRIPTION

Bearing performance is measured using an existing hydrodynamic bearing test rig located at the Texas A&M University Turbomachinery Laboratory. Kaul [15] provides a detailed description of the test rig, originally designed for testing oil seals and extracting rotordynamic coefficients.

Main Test Rig

The main sectional of the test rig is shown in Fig. 6. A mild steel plate box supports a 76.2 mm (3 in) T-slot top, forming the foundation for the main section and prime mover. The stainless steel test rotor is precision machined to a diameter of 101.59 mm (3.9995 in) and was dynamically balanced immediately prior to the testing described hereafter. The rotor is supported by high-speed ball bearings pressed onto each end. Two steel pedestals, spaced approximately 381 mm (15 in) apart and fixed to the base, cradle the shaft at the support bearing locations. A framework attached to the pedestals encases and secures the support bearings, provides a mounting place for electro-hydraulic actuators, and ties the main test rig together. An oil mist generator provides lubrication to the support bearings, and two air buffer seals between the pedestals prevent the oil mist from leaking into the test bearing lubricant discharge chambers. A vacuum seal on the drive end (DE) and draining rotor end cap on the non-drive end (NDE) are used to evacuate the support bearing lubricant oil.

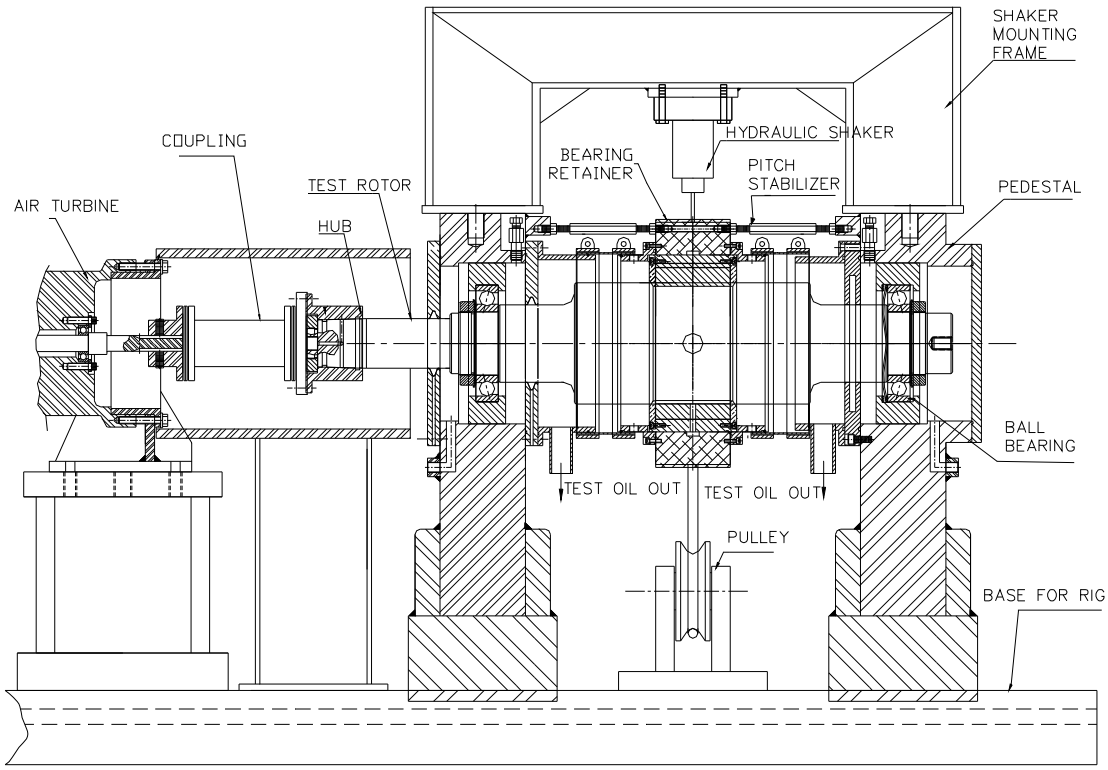

Figure 6. Bearing test rig main sectional

The test bearing is stationed on the rotor between the support bearings and is pressed into a one-piece aluminum stator housing, which provides a place to attach the oil supply hoses, sensors, static loading device, and electro-hydraulic actuators. Unlike a real system where the bearing is stationary and supports a "floating" rotor, the test rig is set up such that the rotor can be assumed rigidly supported (radially stationary) and the test bearing "floats" about it. Six pitch stabilizers link the stator housing to the pedestals and are used to ensure alignment and restrict axial movement of the test bearing, while having minimal impact on radial movement.

The oil supply system feeds temperature controlled ISO VG32 turbine oil to the test bearing via two hoses attached to the bearing housing, located horizontally opposite each other. Lubricant flow rate is adjusted by means of a user-controlled pneumatic valve, and lubricant temperature is controlled by a forced air heat exchanger. A maximum practical oil flow rate of 61 l/min (16 gpm) is achievable. Supply oil exits the test bearing axially and is contained in the test rig by rubber sleeves connecting the test bearing to the pedestals. The oil exits the test rig through the discharge chambers located against the pedestals on either side of the test bearing.

A high-speed flexible disc coupling attaches the rotor to a direct-drive air turbine, which runs on externally supplied compressed air. The turbine can run to 17000 rpm and deliver 67 kW (90 hp) of power. Shaft speed is adjustable via a user-controlled electro-pneumatic valve that regulates the air flow to the turbine.

Static and Dynamic Loading

Static loading is applied to the bearing stator housing by a pneumatic cylinder, with a spring and cable system linking the cylinder's piston to the stator housing via a pulley, as shown in Fig. 7. The spring ensures a constant load by isolating the motion of the bearing from that of the piston, and the pulley guarantees that the load is purely radial and in one direction. A user-controlled electro-pneumatic valve adjusts the static load produced by the cylinder from zero to 20 kN (4500 lbf), using the 827 kPa (120 psi) air supply pressure.

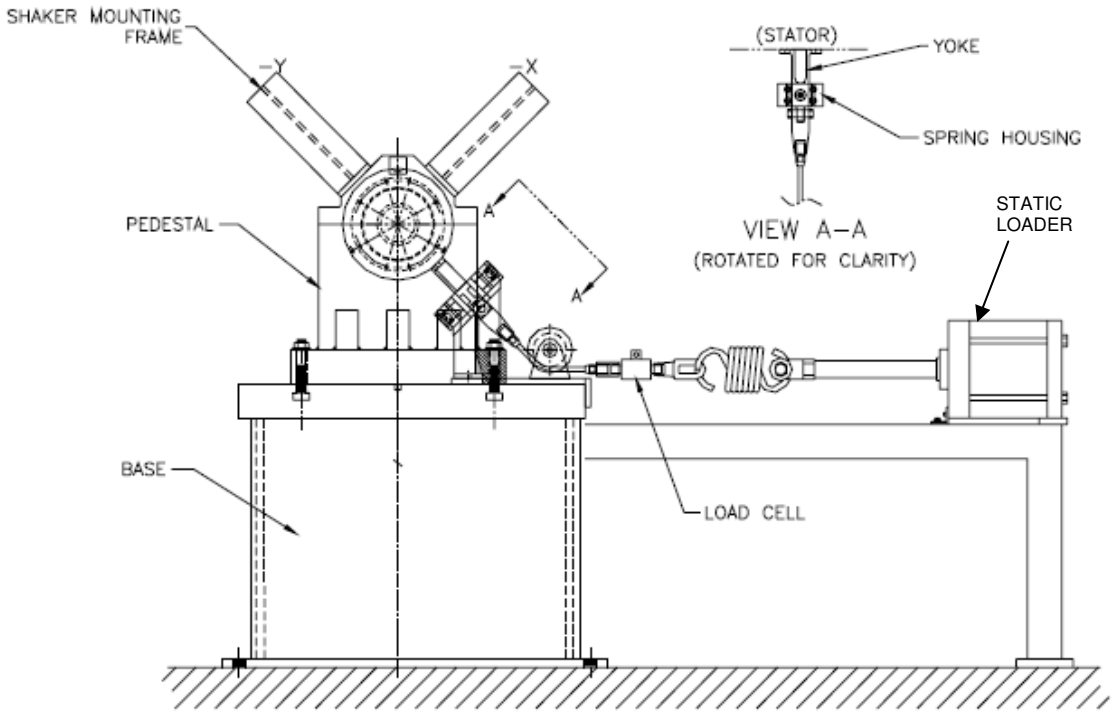

Figure 7. Static loader as viewed from the NDE

Two orthogonally mounted electro-hydraulic shakers, each oriented 45° from the horizontal as shown in Fig. 8, are used to provide support and apply dynamic loading to the test bearing. In this figure, $+x$ and $+y$ show the positive x- and y-directions, F_S is the static load provided by the pneumatic cylinder, and ω is the rotor speed. The x-direction shaker can excite the stator housing with dynamic loads up to 4.45 kN (1000 lb_f) in tension and compression, while the y-direction shaker can excite up to 4.45 kN (1000 lb_f) in tension and 11.1 kN (2500 lb_f) in compression. Both shakers can excite at frequencies to 1000 Hz (60,000 rpm). "Stingers" are the simple bar elements that connect the hydraulic shaker heads to the stator housing.

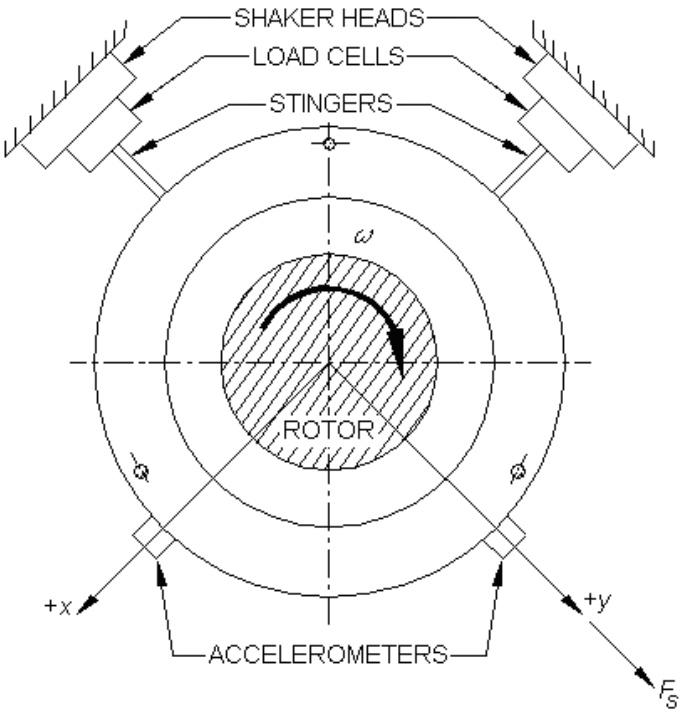

Figure 8. Stator-shaker arrangement viewed from the non-drive end (NDE)

A dual-loop master controller, supplied by the hydraulic shaker manufacturer, enables independent control of the static and dynamic force amplitudes of the shakers. The master controller incorporates automatic gain control in the dynamic loop, allowing a constant force amplitude to be maintained even as the excitation frequency is changed. The system is driven by manufacturer supplied individual *x*- and *y*-direction hydraulic pumps, capable of providing a constant 20.7 MPa (3000 psi) supply pressure under varying frequency and load demands.

Instrumentation

Several measurements of the oil conditions and relative rotor-bearing movements are required to determine bearing performance. The ISO VG32 supply oil flow rate is measured via a flow meter. Inlet oil supply temperature is measured using a K-type thermocouple in the bearing oil supply groove, and outlet temperature is measured by two similar thermocouples, located in the end caps immediately on either side of the stator housing. Static pressure transducers measure the inlet oil pressure in the bearing oil supply groove (around 165 kPa, or 24 psi) and the outlet oil pressure in the bearing end caps (close to ambient). A series of fourteen thermocouples located within the bearing pads and eight thermocouples along the squeeze film land record the metal temperatures at these locations.

Four non-contacting eddy current proximity probes measure the relative rotor-bearing position in two orthogonal directions (x- and y-directions) and in two parallel planes (in each of the two bearing end caps). Position measurements in two planes allow for assessment of bearing pitch and yaw, while orthogonal directions provides measurements in both dimensions of travel. A strain gauge attached between the spring and cable on the static loader measures the static load applied to the bearing. Rotor speed is measured using a keyphasor arrangement.

Dynamic loading of the hydraulic shakers is measured by load cells located between the stinger-shaker assemblies, shown in Fig. 8. Accelerometers mounted to the stator housing measure the absolute acceleration of the bearing-stator in the x- and y-directions.

3. PRELIMINARY TESTING AND RESULTS

Preliminary testing was required to determine the bearing pad rotational (structural) stiffness and damping values, and the squeeze film damper spring stiffness, for later use as inputs in the rotordynamic predictive software. Prior to this testing, compressed air was blown through all of the bearing and squeeze film damper grooves to ensure a clean and dry bearing.

Bearing Pad Rotational Stiffness and Damping

Beam Theory Pad Stiffness

The rotational stiffness and damping of the bearing pads are not directly measured, but rather are calculated using measured values. Two methods are presented for determining rotational stiffness, and one is further refined to determine pad damping. First, the beam theory for a cantilever beam is used to calculate rotational stiffness; then, a pad mounted accelerometer is used to measure the vibratory response of the pad to an impact, from which the rotational stiffness and damping can be calculated.

The calculation of the pad rotational stiffness using beam theory assumes the pad's web behaves like a cantilever beam, fixed at one end and with a moment applied at the free end, as shown in Fig. 9. Note that h is the height of the web and w is the width of the web.

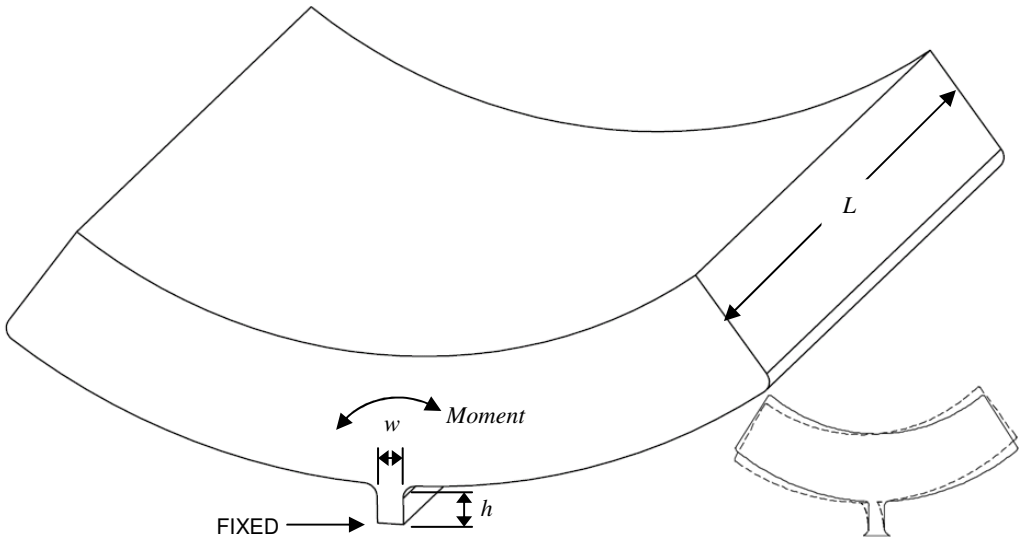

Figure 9. Cantilever beam model of pad web (modified from [7])

The equation for the rotational stiffness of a cantilever beam can be found in most texts on mechanics of materials, such as Hibbeler [16], and is given in Eq. (3) where $k_{\theta,pad}$ is the rotational stiffness, E is the material modulus of elasticity, I_a is the area moment of inertia of the web cross-section defined in Eq. (4), and L is the web length (in this case equal to the pad length). The fillets shown at the top and bottom of the web are assumed to add some flexibility, so h is presented as the centerline distance between the top and bottom fillets. Using measured pad dimensions, application of these equations yields a pad rotational stiffness of 1758 N.m/rad.

$$k_{\theta,pad} = \frac{EI_a}{h} \tag{3}$$

$$I_a = \frac{1}{12} L w^3 \tag{4}$$

Experimental Pad Stiffness and Damping

An alternate method for determining the rotational stiffness of the pads is to use Eq. (5), where $\omega_{n,pad}$ is the measurable pad natural frequency and I_m is the mass moment of inertia of a pad. D. Wilde and B. Doud (personal communication from L. San Andrès, June 1, 2009) provide the calculation for the mass moment of inertia of the pad in Eq. (6), where m_{pad} is the mass of the pad, $r_{i,pad}$ and $r_{o,pad}$ are the inner and outer pad radii, respectively, ρ is the bearing material density, l is the pad axial length, and $L_{arc,pad}$ is the arc length of the pad.

$$k_{\theta,pad} = \omega_{n,pad}^2 I_m \tag{5}$$

$$I_m = \frac{1}{2} m_{pad}\left(3r_{o,pad}^2 + r_{i,pad}^2\right) - \frac{4}{3} r_{o,pad}\rho l\left(r_{o,pad}^3 - r_{i,pad}^3\right)\sin\left(\frac{L_{arc,pad}}{2}\right) \tag{6}$$

Measuring the pad natural frequency is accomplished by attaching a miniature, adhesive-backed, accelerometer near the middle edge of the pad as shown in Fig. 10. The pad is then either impacted, or flexed and released, to make it resonate. Several impact methods were tried to obtain "clean" vibratory responses, while the most consistent responses were obtained by flexing (deflecting) the pad by using thumbnails on both sides and releasing. All four pads were tested this way and the accelerometer was moved to test both ends of each pad.

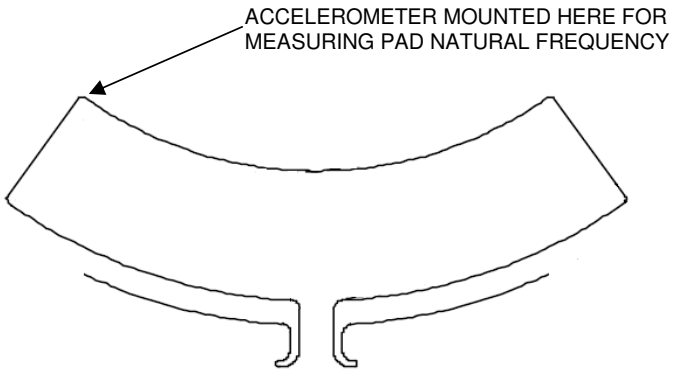

Figure 10. Accelerometer location on bearing pad (modified from [7])

Figure 11 shows one of the pad responses obtained on the dry bearing. Following Eq. (7), where n is the number of cycles in a chosen time t, the pad natural frequency of 320 Hz (2011 rad/s) is determined. This natural frequency is typical, or very close, for all of the pads. This particular response was chosen for the log-decrement calculations below because of its especially clean response.

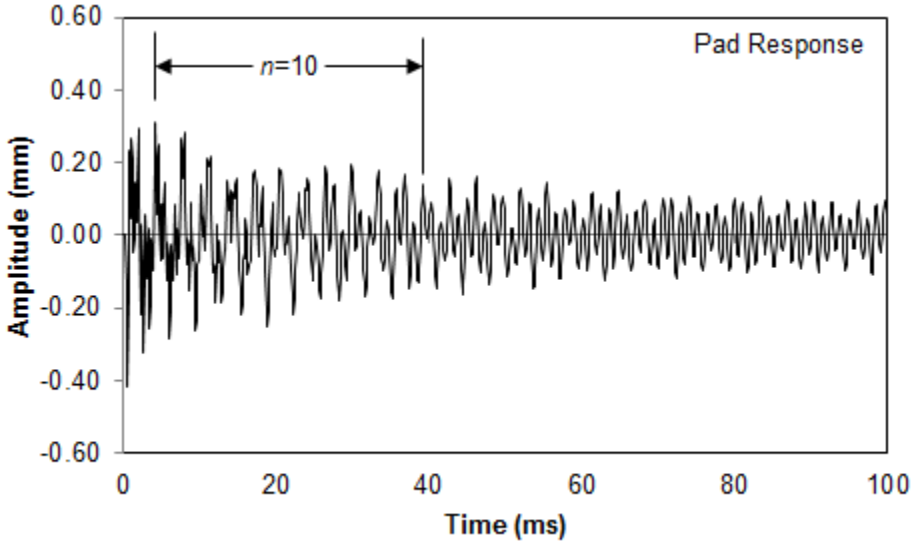

Figure 11. Typical dry bearing pad response to an impact

$$\omega_{n,pad} = 2\pi\left(\frac{n}{t}\right) \tag{7}$$

Following Eq. (6), the pad mass moment of inertia is calculated to be $295(10^{-6})$ kg-m^2. Combining this with the natural frequency just found, Eq. (5) results in a pad stiffness of 1194 N.m/rad. Although this stiffness is considerably (32%) lower than the 1758 N.m/rad calculated previously using beam theory, it is used as the rotational stiffness in the predictive software since it is the most accurate (experimental), and the method also provides pad damping (described next). To satisfy scientific curiosity, beam theory and experimental rotational stiffnesses were compared by predicting rotordynamic coefficients using the prediction software, and the experimental rotational stiffness provided the best (closest to experimental) overall results.

Pad damping is determined using Fig. 11, and Eqs. (8) and (9), where δ is the logarithmic decrement, N is the number of peaks in the desired response period ($N = n - 2$, using Fig. 11), y_1 and y_N are are the beginning and ending response amplitudes, respectively, ζ is the damping ratio, C_{pad} is pad damping, and the other symbols are previously defined. Using the range and corresponding values in Fig. 11, the mass moment of inertia calculated using Eq. (6), and either of the previously determined rotational stiffnesses results in practically zero pad damping (approximately 0.01 N.s/m).

$$\delta = \frac{1}{N-1}\ln\left(\frac{y_1}{y_N}\right) = \frac{2\pi\zeta}{\sqrt{1-\zeta^2}} \tag{8}$$

$$C_{pad} = 2\zeta\sqrt{k_{\theta,pad} I_{m,pad}} \tag{9}$$

Squeeze Film Damper Structural Stiffness

The squeeze film damper structural stiffness is an input used in the rotordynamic prediction software. The stiffness was experimentally measured, and verified using finite element analysis (FEA) software.

Measured of Damper Stiffness

The subject bearing is tested in a load-between-pads (LBP) configuration, meaning that two pads are loaded. For measuring the SFD stiffness, the loaded pads were shimmed using strips of brass sheet to negate their deflection, as shown in Fig. 12. The end seals are left off the bearing and the test rig is normally assembled, except that all unnecessary items are left unattached. Two displacement probes are used (DE and NDE), both measuring in the *y*-direction (direction of load) but in separate planes, and are averaged for each reading.

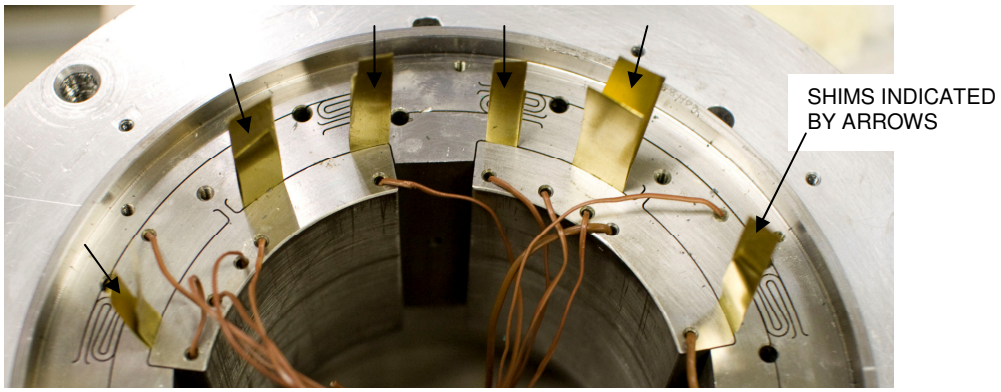

Figure 12. Loaded pads shimmed for damper stiffness measurements

A minimal initial load of about 400 N (90 lb_f) applied to the stator housing "seated" the bearing against the shaft. The proximity probes were adjusted until they touch the rotor, and were then backed out so that the loading would be within the range of the probes. The initial proximity probe readings were averaged, and (together with the initial load) were subtracted from additional measurements to determine the true displacements and loads. The force-displacement plot for the damper is shown in Fig. 13. The linear regression feature of Microsoft Excel was used to find the equation representing the data; the damper structural stiffness is the slope of this line. The experimental damper stiffness is linear within the test range and is equal to k_{ISFD} = 47.79 MN/m (273,000 lb_f/in).

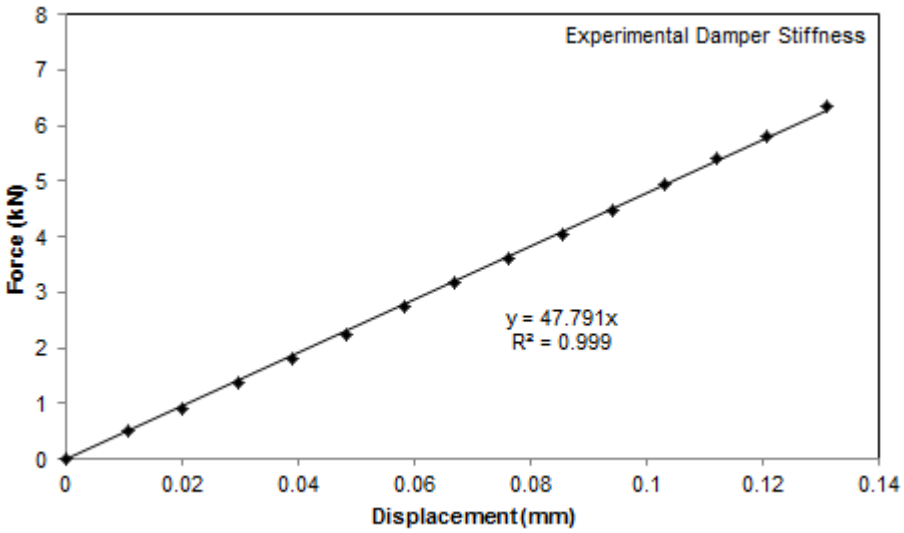

Figure 13. Experimental load versus displacement for squeeze film damper

Predicted Damper Stiffness

As an exercise in confirming the measured results, finite element analysis (FEA) was used to predict the damper structural stiffness. Key dimensions of the test bearing were measured and used to create a solid model in SolidWorks and the COSMOSXpress package was used for the analysis. In the analysis, four different loads were applied to the damper, and the displacements were estimated at the squeeze film land near the load location, from which the damper stiffness was determined. For analysis efficiency, some damper-bearing features were not included or were modified in the model. For example, the cuts forming the bearing pads are filled in, and the axial length is reduced from 76.2 mm to 25.4 mm (3 in to 1 in). The bearing pad outline cuts have no effect on the damper stiffness, and the change in axial length is easily accounted for by multiplying the resulting stiffness by the ratio of the reduction in axial length (3). These modifications result in a model that is both smaller and less complex, meaning that a greater number of smaller elements can be used, resulting in a more accurate and equally (or more) time efficient analysis.

Figure 14 shows the bearing model and how it is (a) restrained and (b) loaded in the analyses. Individual loads of 0.4, 0.8, 1.2, and 1.6 kN were used in the analyses. Each analysis generates an exaggerated deformation plot that uses a color scale to determine the deformation, as shown in Fig. 15; the predicted deflection is estimated from this deformation plot.

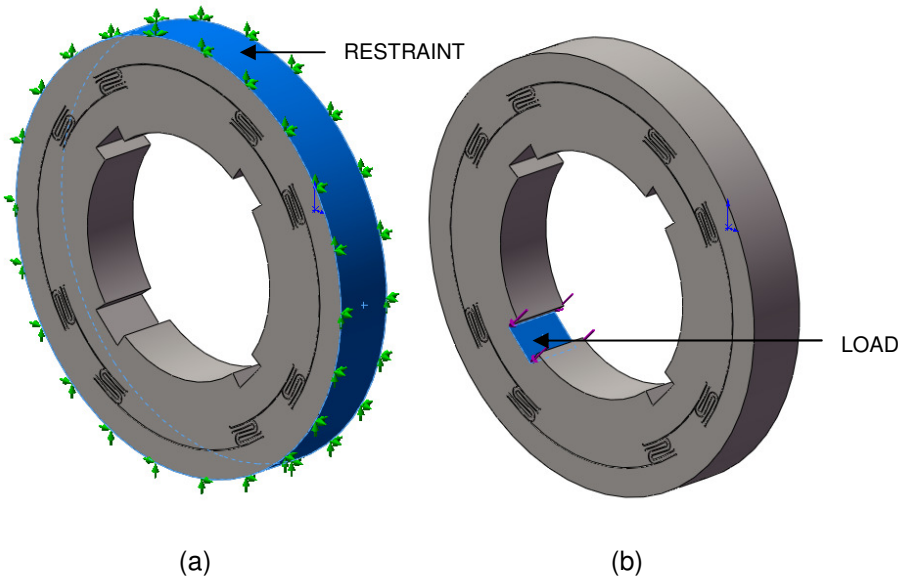

Figure 14. (a) Restraint and (b) load locations for FEA damper analysis

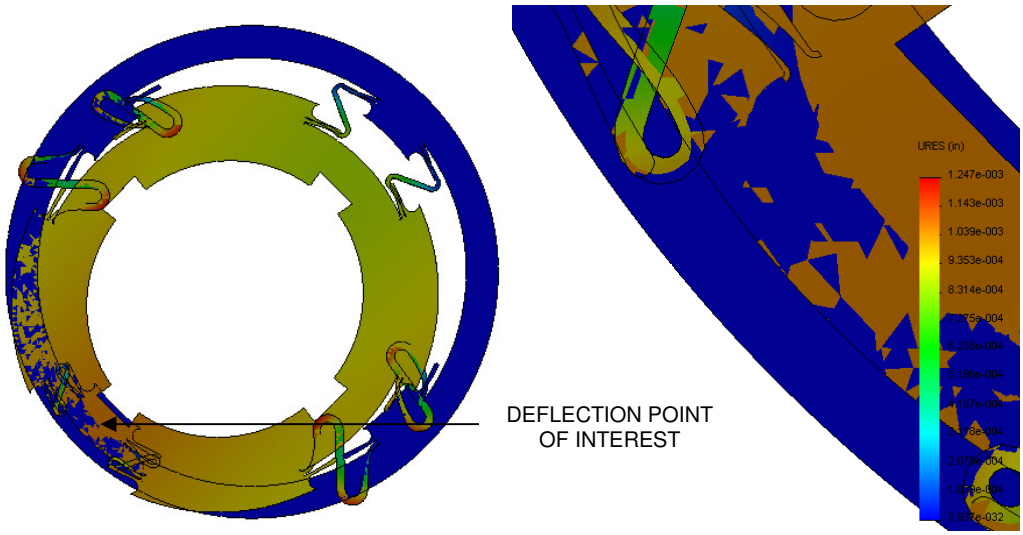

Figure 15. Exaggerated scale damper deformation for 0.4 kN load

The applied loads and displacements predicted by COSMOS are plotted in Fig. 16. As with the measured results, the predicted damper stiffness is the slope of this graph, or 43.29 MN/m (247,216 lbf/in). This value differs from the measured damper

stiffness by about 9.5%, thereby confirming the previously measured results and suggesting that FEA can provide good results for the complex design of integral squeeze film dampers.

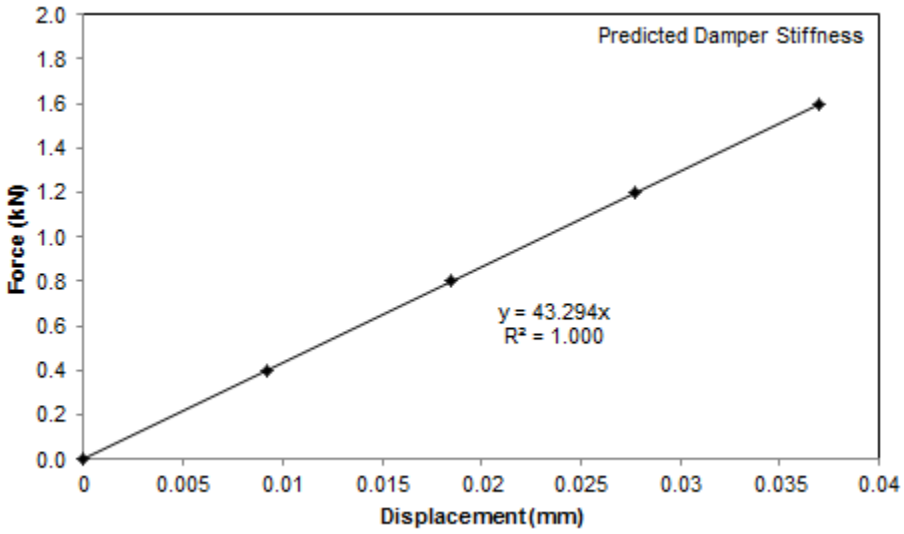

Figure 16. Predicted damper stiffness results using FEA

4. EXPERIMENTAL PROCEDURES AND PARAMETER IDENTIFICATION

As stated previously, two different bearing configurations are tested – locked and active squeeze film damper. For the first case, the damper was locked by inserting pins into all of the holes along the squeeze film land, as shown in Fig. 17. Care was taken to fit individual pins to each hole to avoid adversely affecting bearing dimensions. Pins were used rather than shims because they are easily removable (can be removed), yet still allow the end seals to be installed (shims would have to be folded at the end to be removable, which would prevent the seal from fully seating).

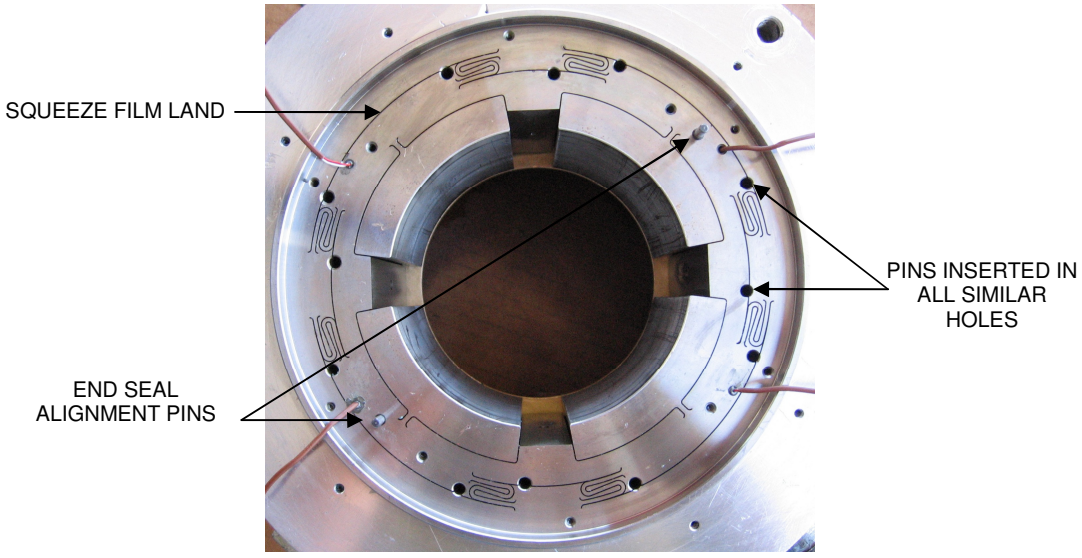

Figure 17. Damper is locked using pins

The test procedures for both bearing configurations are the same, except for minor differences concerning the bearing centering process and squeeze film land temperature measurements are taken for the active damper case, as discussed below.

Data reduction and parameter identification processes are identical for both bearing configurations.

Centering the Bearing

Prior to initiating the static and dynamic testing, the bearing center must be found. This process consists of moving the bearing to its extremes about two perpendicular axes and marking these points on an oscilloscope readout. The bearing center is then the center of the extremes. The centering process is depicted in Fig. 18 and a summary follows.

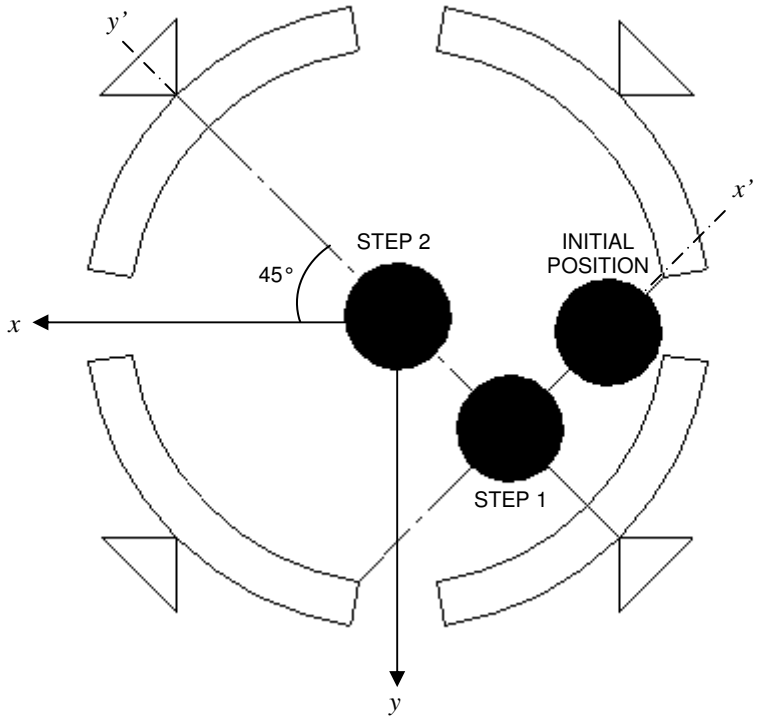

Figure 18. Process for finding bearing center

Step 1: The bearing is moved from an initial position along an axis at a 45° angle relative to the *x*-axis until contact is made with the rotor. The bearing is then moved along the same axis in the opposite direction until contact is made. Note that determining contact FPJB (locked damper) is relatively easy using the oscilloscope; however, the additional flexibility of the active damper (damper-bearing) makes this difficult. For the damper-bearing, contact between the bearing and rotor is determined by touch – the shaft is rotated by hand and the bearing is pulled just to the point where it can no longer be easily turned.

Step 2: The middle of the two extremes found in step 1 is determined, and the bearing is moved to the perpendicular extremes of the middle of that axis. The middle of this axis *should* be the same as the bearing center.

Step 3: The center of the bearing is verified by checking that the bearing clearance is equal along orthogonal axes oriented 45° relative to the *x*-axis (this is the distance from the rotor to the circumferential pad center).

Step 4: If the clearances are not equal in step 3, steps 1-3 are repeated.

Static Load Test Procedure

After completing the bearing centering procedure, pitch and yaw are adjusted using the pitch stabilizers until the DE and NDE displacement probes have equivalent readings to ensure the bearing is properly aligned with the rotor. The oil flow rate is set to a constant 45.4 l/min (12 gpm) for all tests to ensure a flooded bearing. After other initial test rig startup procedures, the air turbine is ramped up to test speed, and the

appropriate static load is applied to the bearing. Identical shaft speed and load conditions are used to test both bearing configurations, which are summarized in Table 2; however, some data are incomplete at certain conditions. The static load supported by a bearing is often described as the average pressure exerted on the bearing oil lands and is approximated as P_{Static} defined in Eq. (10) where W is the static force, L is the pad length, and D is the bearing diameter. Note that the highest load of 862 kPa is not used for the 4000 rpm rotor speed due to rubbing concerns during dynamic testing.

$$P_{Static} = \frac{W}{LD} \tag{10}$$

Table 2. Test conditions for both locked and active damper configurations

	Unit Load (kPa)					
Speed (rpm)	0	172	345	517	689	862
4000	X	X	X	X	X	-
6000	X	X	X	X	X	X
8000	X	X	X	X	X	X
10000	X	X	X	X	X	X
12000	X	X	X	X	X	X

Once steady state thermal conditions are reached, the following data are recorded:

(a) Nominal rotor speed

(b) Bearing static load

(c) Pad metal temperatures

(d) Squeeze film land temperatures (active damper only)

(e) Oil supply and exit temperatures

(f) Oil supply pressure

(g) *x*- and *y*-direction DE and NDE displacement probe readings

Static Load Parameter Identification

Eccentricity Ratio and Attitude Angle

Eccentricity ratio and attitude angle describe the location of the rotor relative to the bearing center, as shown in Fig. 19. The eccentricity consists of the measured rotor-bearing *x*- and *y*-direction displacements, $e_{x,0}$ and $e_{y,0}$ which are often normalized by the radial bearing clearance, C_B, as in Eqs. (11) and (12). The normalized eccentricity components are used to define the eccentricity ratio in Eq. (13), which is simply the magnitude of the eccentricity. Equation 14 defines the attitude angle, ϕ, which is the angular location of the center of the shaft, as measured from the *y*-axis.

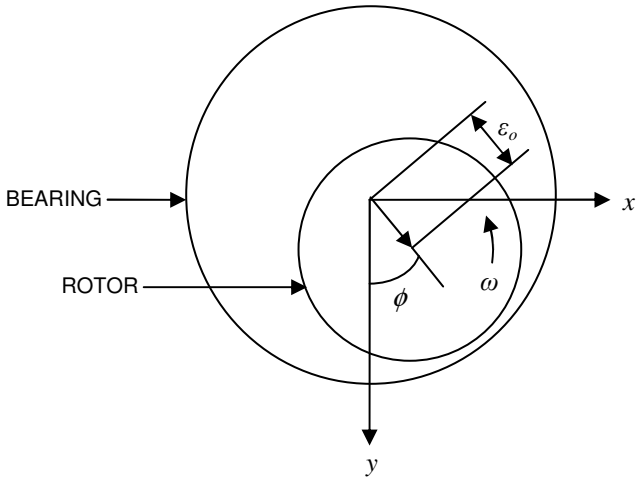

Figure 19. Eccentricity and attitude angle

$$\varepsilon_{x,o} = \frac{e_{x,o}}{C_B} \tag{11}$$

$$\varepsilon_{y,o} = \frac{e_{y,o}}{C_B} \tag{12}$$

$$\varepsilon_o = \sqrt{\varepsilon_{x,o}^2 + \varepsilon_{y,o}^2} \tag{13}$$

$$\phi = \tan^{-1}\left(\frac{e_{x,o}}{e_{y,o}}\right) \tag{14}$$

Temperature Dependent Lubricant Properties

Some calculations require temperature dependent lubricant properties for the supply oil (ISO VG32). The XLTRC^2© help menu contains the temperature dependent relationships for viscosity (μ), density (ρ), and specific heat (c_P) in Eqs. (15), (16), and (17) where T is the temperature in Kelvin that the property is evaluated at.

$$\mu = 0.045336e^{-0.030069(T-294.2611)} \ [Pa.s] \tag{15}$$

$$\rho = -0.6616 \ \ T + 1064 \quad [kg/m^3] \tag{16}$$

$$\gamma = 3.6273 \ \ T + 811.75 \ [kJ/kg.K] \tag{17}$$

Power Loss

Frictional power loss in fluid film bearings occurs primarily due to the no slip condition on the rotor and bearing surfaces, resulting in shearing action between the lubricant film layers. The shear stresses that develop produce a resistive (drag) torque on the shaft and dissipate this energy as heat. Since the test rig cannot measure drag

torque, a thermal approach is instead used to *estimate* the bearing power loss. This approach is considered an estimate because it assumes that all of the frictional energy goes directly and only into heating the oil, and therefore assumes no heat is lost through any other part of the test rig. The estimated frictional power loss, P_{loss}, is found using Eq. (18) where $\dot{Q}$ is the volumetric flow rate of the lubricant, T_{in} and T_{out} are the lubricant supply and exit temperatures, and the other terms are defined above. Since the test rig allows oil to exit on both the drive end and non-drive end, temperatures are measured at both locations and averaged to obtain T_{out}.

$$P_{loss} = \dot{Q}\left[(\rho\gamma)_{T_{out}} T_{out} - (\rho\gamma)_{T_{in}} T_{in}\right] \tag{18}$$

Sommerfeld Number

The Sommerfeld number is a useful parameter for comparing similar bearings and is defined in Eq. (19), where μ is the lubricant viscosity at the average inlet-exit temperature, D is the bearing diameter, L is the bearing pad length, N_{rpm} is the rotor speed in rpm, W is the static load on the bearing, and C_P is the radial pad clearance. The equation is not all-encompassing and does not include effects for preload or support stiffness, but enables similar bearings to be compared at the same Sommerfeld number. Non-dimensionalized rotordynamic coefficients are later compared to coefficients for a similar bearing to the locked damper case tested by Al-Ghasem [6] at similar Sommerfeld numbers.

$$S = \frac{\mu DL}{W}\left(\frac{N_{rpm}}{60}\right)\left(\frac{D}{2C_P}\right)^2 \tag{19}$$

Dynamic Load Test Procedure

Dynamic load tests are performed on the FPJB and damper-bearing for the same conditions as listed in Table 2. After ensuring steady state conditions, the test bearing is excited in the *x*- and *y*-directions in 10 Hz increments from 20 to 320 Hz. Only one shaker is used during each test so that excitation occurs exclusively in the *x*- or *y*-direction. The "pseudo-random periodic" multi-frequency sinusoidal signal described by Rouvas and Childs [17] is used for excitation, which consists of adjusting the phase to minimize the peak factor. Rather, the phase ϕ_f is adjusted in Eq. (20) to minimize $(F_{max} - F_{min})$ so that the amplitude of the prescribed force remains approximately constant across the frequency range.

$$F = \sum_{f=20}^{320} f_f \cos(2\pi f t + \phi_f) \tag{20}$$

Each set of ten consecutive shakes in each direction is averaged in the frequency domain to yield one set of frequency-dependent dynamic stiffness coefficients. Sampling occurs at a rate of 10240 samples per second over 0.1 seconds per frequency channel, yielding 1024 samples per channel and a 3.2 second time per test. The excitation force is manually adjusted to keep the excitation motion acceptably below the bearing clearance, ensuring linear bearing operation and repeatability of results.

Before the test rig is fully started, *baseline* dynamic data are taken with the bearing dry and at zero shaft speed. The baseline stiffness accounts for the stator-bearing assembly mass and the stiffness due to the turnbuckles (used for pitch and yaw

adjustment), unused shaker, hoses, ect. and is subtracted from subsequent tests so that stiffness and damping results are for the bearing only.

Rotordynamic Parameter Identification

A parameter identification model originally developed by Rouvas and Childs [17] for hydrostatic bearings is used to determine the direct and cross-coupled stiffness, damping, and added mass coefficients. The testing scheme utilizes multi-frequency excitation and noise reduction techniques, and power cross-spectral densities are applied to the data to effectively eliminate the effects of fluid flow induced vibration on the results. A brief description of the dynamic data reduction model follows.

The equation of motion for the bearing stator is given in Eq. (21), where M_s is the bearing-stator mass, a_x and a_y are stator acceleration components measured by stator-mounted accelerometers, f_x and f_y are the dynamic forces measured by load cells on each hydraulic shaker, $f_{b,x}$ and $f_{b,y}$ are the bearing reaction forces, and the x and y subscripts refer to the x- and y-directions of Fig. 8. Combining and rearranging the terms in the force-reaction model of Eq. (2) and the equation of motion for the stator housing given in Eq. (21), yields Eq. (22). The stiffness, damping, and added mass terms are given by K_{ij}, C_{ij}, and M_{ij}, respectively, while the subscripts (xx, yy) and (xy, yx) refer to the direct and cross-coupled terms.

$$M_s \begin{Bmatrix} a_x \\ a_y \end{Bmatrix} = \begin{Bmatrix} f_x \\ f_y \end{Bmatrix} - \begin{Bmatrix} f_{b,x} \\ f_{b,y} \end{Bmatrix} \tag{21}$$

$$\begin{Bmatrix} f_x - M_s a_x \\ f_y - M_s a_y \end{Bmatrix} = -\begin{bmatrix} K_{xx} & K_{xy} \\ K_{yx} & K_{yy} \end{bmatrix} \begin{Bmatrix} \Delta x \\ \Delta y \end{Bmatrix} - \begin{bmatrix} C_{xx} & C_{xy} \\ C_{yx} & C_{yy} \end{bmatrix} \begin{Bmatrix} \Delta \dot{x} \\ \Delta \dot{y} \end{Bmatrix} - \begin{bmatrix} M_{xx} & M_{xy} \\ M_{yx} & M_{yy} \end{bmatrix} \begin{Bmatrix} \Delta \ddot{x} \\ \Delta \ddot{y} \end{Bmatrix} \tag{22}$$

The terms making up the left side vector of Eq. (22) are entirely known, measured functions of time, as is the relative motion of the stator given by $\Delta x(t)$ and $\Delta y(t)$ on the right side. The Fast Fourier Transform, F, converts Eq. (22) to the frequency domain version of Eq. (23), where $F_k = F(f_k)$, $A_k = F(a_k)$, and $D_k = F(\Delta k)$ is the k-direction displacement.

$$\begin{Bmatrix} F_x - M_s A_x \\ F_y - M_s A_y \end{Bmatrix} = -\begin{bmatrix} \boldsymbol{H}_{xx} & \boldsymbol{H}_{xy} \\ \boldsymbol{H}_{yx} & \boldsymbol{H}_{yy} \end{bmatrix} \begin{Bmatrix} D_x \\ D_y \end{Bmatrix} \tag{23}$$

The frequency dependent terms for the complex stiffness function H are related to the coefficients in Eq. (22) by:

$$\begin{aligned} &\boldsymbol{H}_{ij} = (K_{ij} - \Omega^2 M_{ij}) + \boldsymbol{j}(\Omega C_{ij}) \\ &\mathrm{Re}(\boldsymbol{H}_{ij}) = K_{ij} - \Omega^2 M_{ij}, \mathrm{Im}(\boldsymbol{H}_{ij}) = \boldsymbol{j}(\Omega C_{ij}) \end{aligned} \tag{24}$$

where Ω is the excitation frequency and $\boldsymbol{j}$ is the complex number $\sqrt{-1}$. Equation (23) provides only two equations for four unknowns – $\boldsymbol{H}_{xx}$, $\boldsymbol{H}_{xy}$, $\boldsymbol{H}_{yx}$, and $\boldsymbol{H}_{yy}$. Therefore, two additional independent equations are needed to solve the system; so, alternate shakes are made about orthogonal directions (x and y) to give Eq. (25).

$$\begin{bmatrix} F_{xx} - M_s A_{xx} & F_{xy} - M_s A_{xy} \\ F_{yx} - M_s A_{yx} & F_{yy} - M_s A_{yy} \end{bmatrix} = -\begin{bmatrix} \boldsymbol{H}_{xx} & \boldsymbol{H}_{xy} \\ \boldsymbol{H}_{yx} & \boldsymbol{H}_{yy} \end{bmatrix} \begin{bmatrix} D_{xx} & D_{xy} \\ D_{yx} & D_{yy} \end{bmatrix} \tag{25}$$

Curve Fitting and Uncertainty Analysis

Assuming that the real part of the dynamic stiffness of Eq. (24) is a quadratic function of Ω, while the imaginary part is a linear function, by setting $\Lambda = \Omega^2$, the $\mathrm{Re}(\boldsymbol{H}_{ij})$ relationship in Eq. (24) is curve fitted to the linearized form:

$$\hat{y} = \beta_0 + \beta_1 x \tag{26}$$

where $\hat{y}$ is the predicted value, β_0 is the *y*-intercept, and β_1 is the slope. Other values used to compile Eq. (26) are found in Eqs. (27), (28), and (29), where (x_i,y_i) are data pairs, $\bar{x}$ and $\bar{y}$ are those mean values, and N_D is the number of data pairs.

$$\bar{x} = \frac{1}{N_D}\sum_{i=1}^{N} x_i$$
$$\bar{y} = \frac{1}{N_D}\sum_{i=1}^{N} y_i \tag{27}$$

$$\beta_1 = \frac{\sum_{i=1}^{N} y_i x_i - N_D \overline{yx}}{\sum_{i=1}^{N} x_i^2 - N_D \bar{x}^2} \tag{28}$$

$$\beta_0 = \bar{y} - \beta_1 \bar{x} \tag{29}$$

Referring to the previous equations, K_{ij} is estimated as the *y*-intercept, β_0, of the real portion of the regression given by Eq. (26), the added-mass M_{ij} is estimated as the slope, β_1, of the real portion of the regression, and the damping coefficient C_{ij} is estimated as the slope, β_1, of the imaginary portion of the regression. The *y*-intercept of the imaginary portion regression has no physical meaning. These values are referred to as "estimates" because they are extracted from sets of data that contain sampling errors and do not present perfect parabolas. Examples showing the graphical representations of the coefficients are shown in Fig. 20.

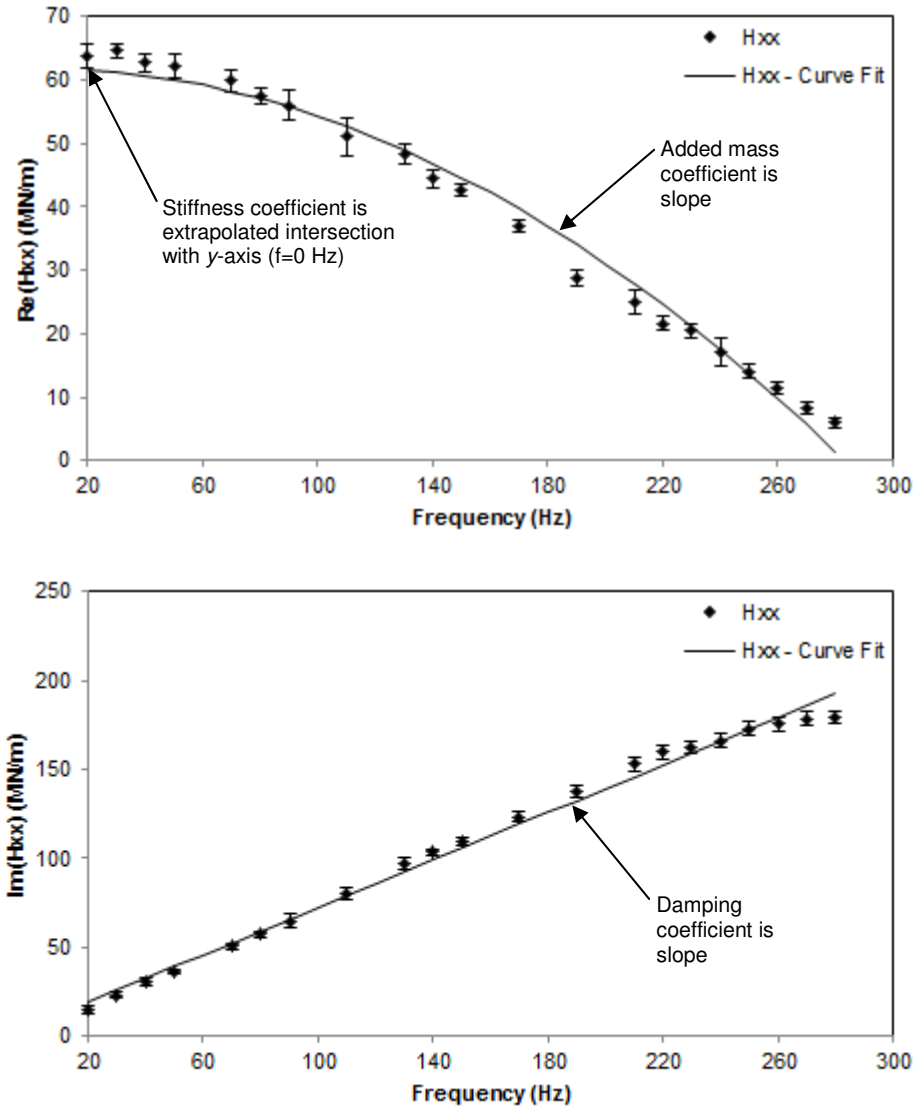

Figure 20. Coefficients extraction from dynamic stiffness

Obviously, a high degree of certainty in the results is desirable, so "confidence intervals" are used to help numerically and visually quantify the amount of uncertainty present. The uncertainty of the data points in the dynamic stiffness, ΔH_{ij}, is quantified as two times the standard deviation ($2S_{xx}$). A 95% confidence interval is achieved by setting q=1.96 in Eqs. (30-32), where 95% of the area under a normal distribution curve

lies within approximately 1.96 standard deviations of the mean. The equations used to calculate the uncertainties in the rotordynamic coefficients are:

$$\Delta K_{ij} = q \times \sqrt{\hat{\sigma}^2 \left(\frac{1}{N_D} + \frac{\bar{x}^2}{S_{xx}} \right)} \tag{30}$$

$$\Delta C_{ij} = q \times \sqrt{\frac{\hat{\sigma}^2}{S_{xx}}} \tag{31}$$

$$\Delta M_{ij} = q \times \sqrt{\frac{\hat{\sigma}^2}{S_{xx}}} \tag{32}$$

$$\hat{\sigma}^2 = \frac{\sum_{i=1}^{N} \left(y_i - \bar{y}_i \right)^2}{N_D - 2} \tag{33}$$

$$S_{xx} = \sum_{i=1}^{N} x_i^2 - N_D \, \bar{x}^2 \tag{34}$$

Note that the values of the excitation frequency points and average, x_i and $\bar{x}$ respectively, in the above equations depend on what coefficient is being determined. Rather, x_i and $\bar{x}$ refer to Ω^2 for the stiffness and added mass coefficients, and to Ω for the damping coefficients.

Non-Dimensionalization of Rotordynamic Coefficients

Non-dimensionalization of rotordynamic coefficients is sometimes useful for comparing similar bearings. The following non-dimensional stiffness ($\overline{K}_{ij}$), damping ($\overline{C}_{ij}$), and added mass ($\overline{M}_{ij}$) terms are defined, where C_P is the radial pad clearance, ω is

the running speed, W is the static load, and K_{ij}, C_{ij}, and M_{ij} are the dimensional stiffness, damping, and added mass coefficients, respectively.

$$\overline{K}_{ij} = \frac{C_P}{W} K_{ij} \tag{35}$$

$$\overline{C}_{ij} = \frac{C_P \omega}{W} C_{ij} \tag{36}$$

$$\overline{M}_{ij} = \frac{C_P \omega^2}{W} M_{ij} \tag{37}$$

Whirl Frequency Ratio

Whirl frequency ratio (WFR) is a stability indicator originally introduced by Lund [18]. WFR relates the natural frequency of a flexible rotor, supported at its ends by identical bearings, to the onset speed of instability (OSI), or the limiting upper operating speed of a bearing, as shown in Eq. (38). The equation shows that a low WFR is indicative of a high OSI; in other words, the lower the WFR the higher the maximum stable rotor running speed. For example, a bearing with a WFR of 0.25 would have an OSI of four times the rotor natural frequency. Permanent stability is indicated by a WFR of zero, meaning that the bearing imposes no upper operating limit for the rotor.

$$WFR = \frac{\Omega_{n,rotor}}{OSI}, \text{ or } OSI = \frac{\Omega_{n,rotor}}{WFR} \tag{38}$$

Lund's equation does not account for added-mass terms; however, San Andrés [19] updated this equation. After some lengthy manipulations, San Andrés' equation reduces to the polynomial given in Eq. (39), where a_{WFR}, b_{WFR}, and c_{WFR} are the terms defined below and $\overline{K}_{ij}$, $\overline{C}_{ij}$, and $\overline{M}_{ij}$ are the non-dimensionalized bearing coefficients

defined previously. Note that removing the cross-coupled added mass terms reduces the polynomial to that of Lund's equation.

$$a_{WFR} WFR^4 + b_{WFR} WFR^2 + c_{WFR} = 0 \tag{39}$$

$$a_{WFR} = M_{eq}^2 + \left(\overline{M}_{xx}\overline{M}_{yy} - \overline{M}_{xy}\overline{M}_{yx}\right) - \left(\overline{M}_{xx} + \overline{M}_{yy}\right)M_{eq} \tag{40}$$

$$\begin{aligned} b_{WFR} = {} & \left(\overline{K}_{xx} + \overline{K}_{yy}\right)\overline{M}_{eq} + \left(\overline{M}_{xx} + \overline{M}_{yy}\right)\overline{K}_{eq} - 2\overline{K}_{eq}\overline{M}_{eq} + \\ & - \overline{K}_{xx}\overline{M}_{yy} - \overline{K}_{yy}\overline{M}_{xx} - \overline{C}_{xx}\overline{C}_{yy} + \overline{K}_{xy}\overline{M}_{yx} + \overline{K}_{yx}\overline{M}_{xy} + \overline{C}_{xy}\overline{C}_{yx} \end{aligned} \tag{41}$$

$$c_{WFR} = \overline{K}_{xx}\overline{K}_{yy} - \overline{K}_{yx}\overline{K}_{yx} + \overline{K}_{eq}^2 - \left(\overline{K}_{xx} + \overline{K}_{yy}\right)\overline{K}_{eq} \tag{42}$$

$$\overline{M}_{eq} = \frac{\overline{C}_{xx}\overline{M}_{yy} + \overline{C}_{yy}\overline{M}_{xx} - \overline{C}_{xy}\overline{M}_{yx} - \overline{C}_{yx}\overline{M}_{xy}}{\overline{C}_{xx} + \overline{C}_{yy}} \tag{43}$$

$$\overline{K}_{eq} = \frac{\overline{C}_{xx}\overline{K}_{yy} + \overline{C}_{yy}\overline{K}_{xx} - \overline{C}_{xy}\overline{K}_{yx} - \overline{C}_{yx}\overline{K}_{xy}}{\overline{C}_{xx} + \overline{C}_{yy}} \tag{44}$$

Realizing that San Andrés' equation is a fourth order polynomial, two types of solutions are possible – real positive values and their negatives, and purely imaginary values and their complex conjugates. If a real positive root is found, that number is the WFR; however, if all roots are purely imaginary or equal to zero, the WFR for that condition is zero.

5. ANALYTICAL PROCEDURE

Rotordynamics software is available to provide predictions for some of the parameters obtained through testing for the flexure-pivot-pad bearing. Developed at the Texas A&M Turbomachinery Laboratory, the XLTRC^2-XLTFPBrg Rotordynamics Suite© is used to predict rotordynamic coefficients, power loss, and eccentricity for the FPJB. A brief description of the program and its modeling options follows.

XLTRC^2-XLTFPBrg Rotordynamics Suite©

The XLTRC^2-XLTFPBrg© software predicts rotordynamic coefficients, power loss, and eccentricity for the FPJB at all shaft speed and static load conditions tested. The code is based on San Andrès [20] and uses a bulk flow model that includes axial and circumferential momentum, mass, and energy conservation. Both laminar and turbulent flows are modeled in the thin film region between the bearing pads and rotor. Temporal and convective acceleration terms can be included. Temperature dependent functions are used for the bulk lubricant density and viscosity. The model includes the effects of pad rotational stiffness, damping, and inertia.

A perturbation analysis is used, in which small journal displacements are imposed about the bearing center, to solve the momentum and continuity equations for the flow fields including pressure and temperature. The fluid film forces and moments on each pad are found by integration of the pressure field, which are used to determine the stiffness and damping coefficients for the bearing. An iterative approach is needed to find the journal static equilibrium coordinates and pad rotation angles which satisfy the load and moment constraints, and a Newton-Raphson algorithm is used for quick

convergence. Perturbations and pad motions are assumed to occur at the same frequency, as chosen by the user and selected as synchronous or non-synchronous in the menu. A discussion of the primary modeling options in the software follows.

XLTRC^2-XLTFPBrg Modeling Options

Pad Inertia, Rotational Stiffness, and Damping

The pad inertia, rotational stiffness, and damping values determined earlier in the Preliminary Testing and Results section are used as inputs for the XLTFPBrg software. Because two different rotational stiffness (1194, 1758 N.m/rad) values varying by 47%, and a corresponding damping value of approximately 0.01 N.s.m/rad for both rotational stiffnesses were found, both stiffnesses were modeled in the software. After testing, the predicted coefficients using each pair of pad stiffness and damping values were compared to the experimental results, which showed that the majority of results were better predicted using the lower (experimentally obtained) pad rotational stiffness of 1194 N.m/rad. Therefore, all of the results presented later were obtained using the experimental values as inputs in the prediction software.

Fluid Inertia

Fluid inertia is usually included when the operating speed is high. As an exercise, the code was run both including and excluding fluid inertia. An error analysis between the predicted and measured rotordynamic coefficients showed that 66% of the direct coefficients (stiffness, damping, and added mass) were better predicted by including the fluid inertia. In instances where the *exclusion* of fluid inertia provided

better results, usually only small differences existed between the predictions with and without including fluid inertia. Hence, the effects of fluid inertia were included.

Thermal Analysis

The software has several thermal-analysis options. Based on the data measured during testing and the required inputs for the software, the adiabatic journal and adiabatic bearing option was chosen. This assumes that no heat is transferred to or from the journal or bearing and that all heat is carried away from the bearing by the oil. Although the bearing and shaft were observed to warm up during testing, based on their estimated temperatures and the temperature rise of the oil the rate of heat transfer was assumed negligible.

Oil-Mixing Parameter

The thermal mixing coefficient λ is defined in Eq. (45) and represents the amount of hot oil carry over between adjacent pads, where $\dot{Q}_{up}$ and $\dot{Q}_{down}$ are the upstream and downstream flows, and T_{up} and T_{down} are the upstream and downstream temperatures, respectively. The value of the mixing coefficient normally ranges from 0.6 to 0.9 [21]; λ=0.65 was used in all software predictions.

$$\dot{Q}_{down} T_{inlet} = \dot{Q}_{\sup\ ply} T_{\sup\ ply} + \lambda \dot{Q}_{up} T_{up} \tag{45}$$

XLTFPBrg Chosen Input Parameters

Figures 21 and 22 show the XLTFPBrg software input and output screens, respectively. All of the entries (gray highlighted cells) in both figures remain unchanged

except for those accounting for rotor speed and static load, which are changed to match the nominal experimental test conditions. Note that the loading in Fig. 22 is described as a force (N) rather than a unit loading (kPa) as used later in the results sections. The excitation frequencies are essentially the same frequencies (20-320 Hz) used in testing, but converted to cpm.

The theoretical stiffness and added mass coefficients are reduced in a similar manner as those shown in the experimental dynamic data reduction procedures. Because of the relative linearity of the stiffness curves, choosing the stiffness coefficient to be the *y*-intercept of the second order curve fit of the stiffness values yields stiffness coefficients that are less than those actually predicted by the software. Therefore, the stiffness coefficients are taken as the stiffnesses predicted at 60 rpm, or 1 Hz. Added mass coefficients are still determined as the second-order curve fit, as outlined in the dynamic data reduction procedures.

The software produces damping coefficients at various frequencies, rather than the coefficient as the slope of the imaginary portion of the dynamic stiffness versus excitation frequency, as in the experiments. Experiments indicated frequency *independent* damping, and as a reasonable approximation, the predicted damping coefficients are evaluated at running speed (synchronous).

XLTFPBrg Spreadsheet for Tilting, Flexure, and Rigid Pad Bearing Coefficients

Version 2.0, Copyright 1998-1999 by Texas A&M University. All rights reserved.

Flexure Pivot Pad Bearing

Journal Diameter	0.1016	meters
Bearing Axial Length	0.0762	meters
Diametral Pad Clearance	0.0004064	meters
Radial Preload Clearance	0.0001524	meters
Number of Pads	4	--
Pad Arc Length	73	degrees
Pad Pivot Offset	0.5	--
Bearing Type Option	Tilting Pads	
Pad Inertia	0.000295	kg-m^2
Pad Stiffness	1194	N-m/rad
Pad Damping	0.006	N-s-m/rad

Supply Pressure	1.65E+05	N/m^2
Supply Temperature	309.8	deg. K

Selected Lubricant		
ISO 32		
Viscosity at Tsupply	0.031	N-s/m^2
Density at Tsupply	860.9	kg/m^3
Compressibility	0.000	m^2/N
Specific Heat	1925.0	J/(kg-K)
Thermal Conductivity	0.132	W/(m-K)
Coef Therm Exp	0.00076	1/K
Temp Visc Coef	0.029	1/K

Pad Geometry Option	Load Between Pad (-Y)	
Lead Edge of Pad 1	7	degrees

Fluid Inertia Option	Include Fluid Inertia	
It Max	199	--
Momentum Relaxation Factor	0.9	--
Pressure Relaxation Factor	0.5	--
Temperature Relaxation Factor	0.8	--
Oil Mixing Parameter	0.65	--
Thermal Analysis Option	Adiabatic, Qj=Qb=0	
Shaft Temperature	310	deg K
Bearing Temperature	310	deg K
Pad Back Temperature	315.7	deg K
Pad Outer Radius	0.0635	meters
Pad Material	Steel - 4340	
Pad Therm Cond	50.190377	W/(m-K)

EccX Initial Guess	0.02	--
EccY Initial Guess	-0.4	--
Rotor Relative Roughness	0	--
Bearing Relative Roughness	0	--
Moody's Coef Amod	0.001375	--
Moody's Coef Bmod	500000	--
Moody's Coef Expo	0.33333	--
Frequency Analysis Option	Nonsynchronous Analysis	
Constant Shaft Rpm	12000	rpm

Figure 21. Input parameters for XLTFPBrg used to model FPJB (locked damper)

X Load Newtons	Y Load Newtons	Freq cpm	Kxx N/m	Kxy N/m	Kyx N/m	Kyy N/m	Cxx N-s/m	Cxy N-s/m	Cyx N-s/m	Cyy N-s/m
0	-5338	60	1.09E+08	-1.39E+07	-2.86E+07	1.02E+08	6.45E+04	-1.66E+04	-5.82E+03	7.10E+04
0	-5338	1200	1.08E+08	-1.38E+07	-2.82E+07	1.01E+08	6.49E+04	-1.67E+04	-6.06E+03	7.13E+04
0	-5338	1800	1.07E+08	-1.36E+07	-2.79E+07	1.00E+08	6.54E+04	-1.68E+04	-6.34E+03	7.17E+04
0	-5338	2400	1.06E+08	-1.34E+07	-2.74E+07	9.94E+07	6.61E+04	-1.69E+04	-6.72E+03	7.22E+04
0	-5338	3000	1.05E+08	-1.32E+07	-2.67E+07	9.80E+07	6.70E+04	-1.71E+04	-7.21E+03	7.28E+04
0	-5338	3600	1.03E+08	-1.29E+07	-2.60E+07	9.64E+07	6.79E+04	-1.72E+04	-7.75E+03	7.35E+04
0	-5338	4200	1.00E+08	-1.26E+07	-2.51E+07	9.46E+07	6.91E+04	-1.74E+04	-8.36E+03	7.43E+04
0	-5338	4800	9.80E+07	-1.22E+07	-2.42E+07	9.25E+07	7.03E+04	-1.77E+04	-9.01E+03	7.53E+04
0	-5338	5400	9.54E+07	-1.19E+07	-2.33E+07	9.03E+07	7.16E+04	-1.79E+04	-9.69E+03	7.63E+04
0	-5338	6000	9.26E+07	-1.15E+07	-2.23E+07	8.78E+07	7.30E+04	-1.81E+04	-1.04E+04	7.73E+04
0	-5338	6600	8.97E+07	-1.11E+07	-2.13E+07	8.52E+07	7.44E+04	-1.83E+04	-1.11E+04	7.85E+04
0	-5338	7200	8.66E+07	-1.06E+07	-2.02E+07	8.24E+07	7.59E+04	-1.86E+04	-1.18E+04	7.96E+04
0	-5338	7800	8.33E+07	-1.02E+07	-1.91E+07	7.95E+07	7.75E+04	-1.88E+04	-1.25E+04	8.09E+04
0	-5338	8400	8.00E+07	-9.72E+06	-1.81E+07	7.65E+07	7.90E+04	-1.90E+04	-1.32E+04	8.21E+04
0	-5338	9000	7.66E+07	-9.27E+06	-1.70E+07	7.34E+07	8.05E+04	-1.92E+04	-1.39E+04	8.34E+04
0	-5338	9600	7.31E+07	-8.80E+06	-1.60E+07	7.02E+07	8.21E+04	-1.94E+04	-1.45E+04	8.46E+04
0	-5338	10200	6.96E+07	-8.33E+06	-1.49E+07	6.69E+07	8.36E+04	-1.96E+04	-1.52E+04	8.59E+04
0	-5338	10800	6.60E+07	-7.86E+06	-1.39E+07	6.36E+07	8.51E+04	-1.98E+04	-1.57E+04	8.72E+04
0	-5338	11400	6.24E+07	-7.39E+06	-1.29E+07	6.03E+07	8.66E+04	-2.00E+04	-1.63E+04	8.84E+04
0	-5338	12000	5.88E+07	-6.91E+06	-1.19E+07	5.69E+07	8.80E+04	-2.02E+04	-1.69E+04	8.97E+04
0	-5338	12600	5.52E+07	-6.43E+06	-1.09E+07	5.35E+07	8.95E+04	-2.03E+04	-1.74E+04	9.09E+04
0	-5338	13200	5.16E+07	-5.94E+06	-9.91E+06	5.01E+07	9.08E+04	-2.05E+04	-1.79E+04	9.21E+04
0	-5338	13800	4.80E+07	-5.46E+06	-8.96E+06	4.67E+07	9.22E+04	-2.06E+04	-1.84E+04	9.33E+04
0	-5338	14400	4.44E+07	-4.96E+06	-8.01E+06	4.33E+07	9.35E+04	-2.08E+04	-1.88E+04	9.44E+04
0	-5338	15000	4.08E+07	-4.46E+06	-7.09E+06	3.99E+07	9.47E+04	-2.09E+04	-1.92E+04	9.55E+04
0	-5338	15600	3.73E+07	-3.97E+06	-6.18E+06	3.65E+07	9.59E+04	-2.10E+04	-1.96E+04	9.66E+04
0	-5338	16200	3.37E+07	-3.46E+06	-5.28E+06	3.31E+07	9.71E+04	-2.11E+04	-2.00E+04	9.76E+04
0	-5338	16800	3.02E+07	-2.96E+06	-4.39E+06	2.97E+07	9.82E+04	-2.12E+04	-2.04E+04	9.86E+04
0	-5338	17400	2.66E+07	-2.44E+06	-3.52E+06	2.63E+07	9.93E+04	-2.13E+04	-2.07E+04	9.96E+04
0	-5338	18000	2.31E+07	-1.92E+06	-2.65E+06	2.29E+07	1.00E+05	-2.14E+04	-2.10E+04	1.01E+05
0	-5338	18600	1.96E+07	-1.40E+06	-1.79E+06	1.95E+07	1.01E+05	-2.15E+04	-2.13E+04	1.01E+05
0	-5338	19200	1.61E+07	-8.62E+05	-9.33E+05	1.61E+07	1.02E+05	-2.16E+04	-2.16E+04	1.02E+05
0	-5338	12000	5.88E+07	-6.91E+06	-1.19E+07	5.69E+07	8.80E+04	-2.02E+04	-1.69E+04	8.97E+04

Freq	Somm Number	Reynolds Number	Loading	Ecc X	Ecc Y	Min P	Max P	Min T	Max T	Power Loss
cpm	--	--	N/m2	--	--	N/m2	N/m2	Deg. K	Deg. K	kW
60	0.56	234.33	6.89E+05	0.0381	-0.2820	-3.06E+05	2.25E+06	313.2	326.6	13.485

Figure 22. Output screen (predictions) for FPJB (locked damper) using XLTFPBrg

Prediction Post Processing

The prediction software uses a coordinate system that is different from that used in the experiments. Comparing the experimental and theoretical rotordynamic coefficients and eccentricities requires a transformation between the coordinates shown in Fig. 23. These transformations are provided by the following equations.

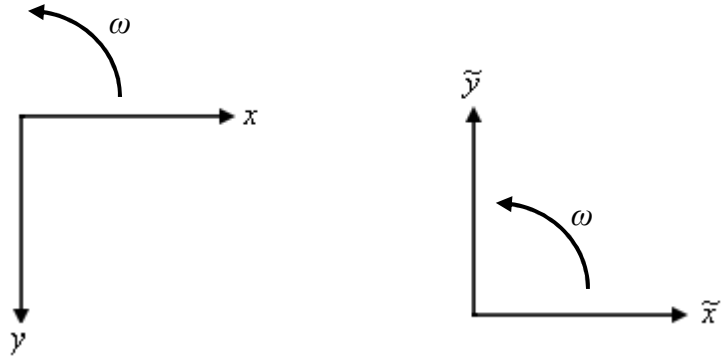

Figure 23. (a) Experimental and (b) analytical coordinate systems

$$\begin{bmatrix} K_{xx} & K_{xy} \\ K_{yx} & K_{yy} \end{bmatrix} = \begin{bmatrix} K_{\tilde{x}\tilde{x}} & -K_{\tilde{x}\tilde{y}} \\ -K_{\tilde{y}\tilde{x}} & K_{\tilde{y}\tilde{y}} \end{bmatrix} \tag{46}$$

$$\begin{bmatrix} C_{xx} & C_{xy} \\ C_{yx} & C_{yy} \end{bmatrix} = \begin{bmatrix} C_{\tilde{x}\tilde{x}} & -C_{\tilde{x}\tilde{y}} \\ -C_{\tilde{y}\tilde{x}} & C_{\tilde{y}\tilde{y}} \end{bmatrix} \tag{47}$$

$$\begin{bmatrix} M_{xx} & M_{xy} \\ M_{yx} & M_{yy} \end{bmatrix} = \begin{bmatrix} M_{\tilde{x}\tilde{x}} & -M_{\tilde{x}\tilde{y}} \\ -M_{\tilde{y}\tilde{x}} & M_{\tilde{y}\tilde{y}} \end{bmatrix} \tag{48}$$

$$\begin{Bmatrix} \varepsilon_x \\ \varepsilon_y \end{Bmatrix} = \begin{bmatrix} 1 & 0 \\ 0 & -1 \end{bmatrix} \begin{Bmatrix} \varepsilon_{\tilde{x}} \\ \varepsilon_{\tilde{y}} \end{Bmatrix} \tag{49}$$

6. STATIC RESULTS: MEASURED AND PREDICTED

Static performance characteristics are those occurring with the rotor at its stationary equilibrium position and at steady state conditions. This section presents representative measured static results for both bearing configurations, and predictions for the FPJB (locked damper) obtained using the XLTRC^2-XLTFPBrg© software described in the previous section. Parameters discussed include eccentricity, attitude angle, pad metal temperatures, squeeze film land metal temperatures, and power loss. All tests are conducted using ISO VG32 turbine oil and occur at an oil flow rate of 45 L/min (12 gpm).

Eccentricity and Attitude Angle

Journal loci plots show measured and predicted eccentricity results for the FPJB and damper-bearing in Fig. 24; the damper-bearing predictions use the FPJB predictions with an added *y*-direction deflection calculated using the known static load and damper structural stiffness. As expected, increasing the static load on the bearing causes a displacement in the direction of the load, ε_y, except for the FPJB in (c) and (d), where ε_y remains approximately constant or actually decreases slightly between certain loads. Similarly, while some displacement in the *x*-direction ε_x is expected due to cross-coupled forces, some of the conditions appear excessive. Alternating static and dynamic tests at each condition (with the possibility of some static lag in the shaker heads), rather than performing all the static tests for a given running speed and then all of the dynamic tests,

is the suspected cause of this. At higher loads, however, the eccentricities typically move closer to the loaded axis as expected.

Experiments were conducted for shaft speeds from 4000-12000 rpm and to a maximum static load of 862 kPa, except for 4000 rpm where rubbing was suspected due to an audible "tapping" during dynamic testing. Extrapolation of the eccentricity in Fig. 24(a) after the incident indicates that rubbing is clearly a concern at 862 kPa, as the rotor would be very close to the limit of the bearing clearance, C_B = 152.4 μm (0.006 in), and likely at or beyond the clearance during dynamic testing. This is an important lesson of how bearing eccentricity must be considered for anticipated loading. No significant damage to the bearing was noted after testing.

The software under predicts the eccentricity of the FPJB. The software also predicts that, under no load, the bearing is concentric with the rotor, while all measurements show there to be some eccentricity in the *x*-direction possibly due to an imperfect bearing centering, residual displacement in the shakers left over from previous tests, or slightly different pad preloads due to machining tolerances. The predicted results better follow the expected trend of the bearing center moving closer to the loaded axis with increasing load. This might also be explained by an imperfect bearing centering process or a small static lag in the *x*-direction hydraulic shaker imparting a slight load in that direction.

The eccentricities in Fig. 24 for the damper-bearing confirm that this configuration is much softer than the FPJB alone. While the FPJB displacements tend to get closer together with increasing load (indicating the fluid film is stiffening), the

damper-bearing displacement increments are almost equal regardless of load. This is a result of the nearly constant stiffness due to the series bearing-damper stiffness. The significantly lower series stiffness of the damper-bearing is evident in eccentricities that are on the order of two times the locked damper case. Note that the added flexibility of the damper allows the journal eccentricity for the damper-bearing to extend beyond the bearing clearance; the clearance of the damper is not shown for clarity.

Eccentricity predictions for the damper-bearing are provided using the predictions for the FPJB and adding a *y*-direction deflection equal to the static load divided by the damper structural stiffness. While the measurements show a significant *x*-direction eccentricity component and an initial *y*-direction component, this is not predicted. There are several possible reasons for this, such as an imperfectly centered bearing, unequal pad preloads due to tolerances, ect. If the damper-bearing eccentricity measurements were moved so that the zero load data points matched with the predictions, the predicted eccentricities at higher loads match very well.

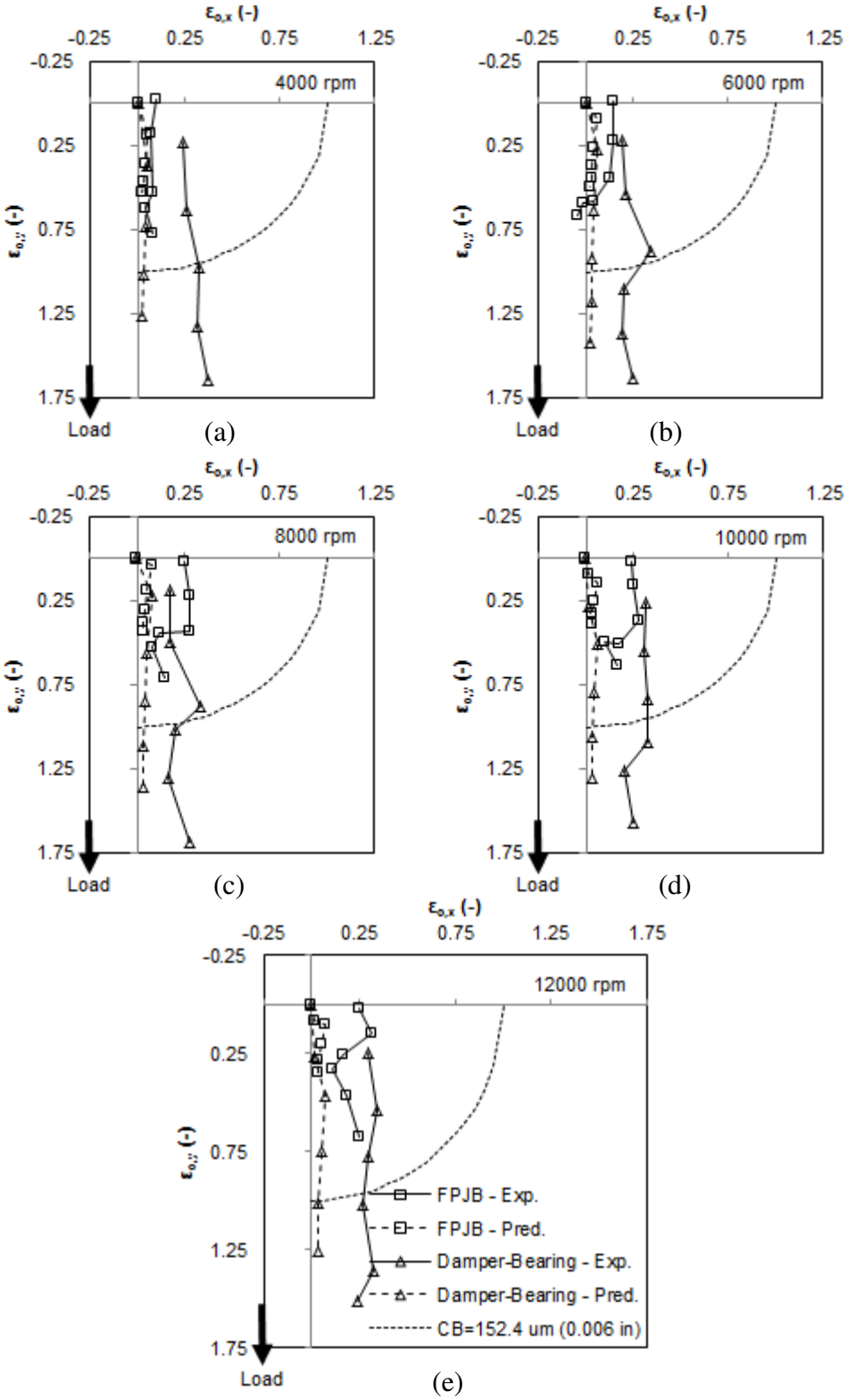

Figure 24. Experimental and predicted loci plots for all test conditions

Journal eccentricity ratio (or the magnitude of the eccentricity) and attitude angle are shown as functions of load for a shaft speed of 12000 rpm in Fig. 25. Figure 25 (top) confirms the stiffnesses for both bearing configurations is approximately linear, and that the stiffness of the damper-bearing is typically about half that of the FPJB alone. The predicted journal eccentricity ratio for both bearing configurations is normally under predicted by about 0.25-0.40 of the bearing clearance (C_B = 152.4 µm, 0.006 in).

Attitude angle versus load for both bearing configurations is given in Fig. 25 (bottom) and approaches 0-degrees with increasing static load. As expected, the softer damper-bearing has a lower attitude angle for all loads, since a given load pulls this bearing in the *y*-direction (the 0° mark) greater than the FPJB. Attitude angles are typically under predicted at low loads (0-172 kPa), but accuracy tends to increase with load.

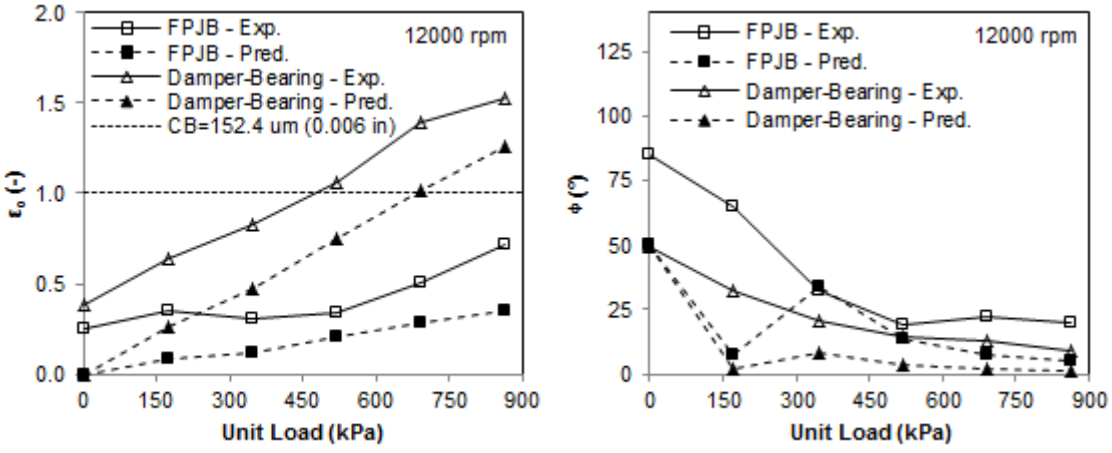

Figure 25. Experimental and predicted eccentricity ratio (top) and attitude angle (bottom) versus load at a shaft speed of 12000 rpm

Eccentricity ratio and attitude angle as functions of shaft speed are given in Fig. 26. Similar to the results above, the eccentricity ratios and attitude angles are usually under predicted. The eccentricity ratio decreases with increasing running speed for both bearing configurations, indicating an increase in centering force. The attitude angle increases slightly with speed; a sign that the effects of the cross-coupling are stronger at higher running speeds. Note that the damper-bearing has a relatively constant attitude angle compared to the FPJB, indicating lower cross-coupling forces.

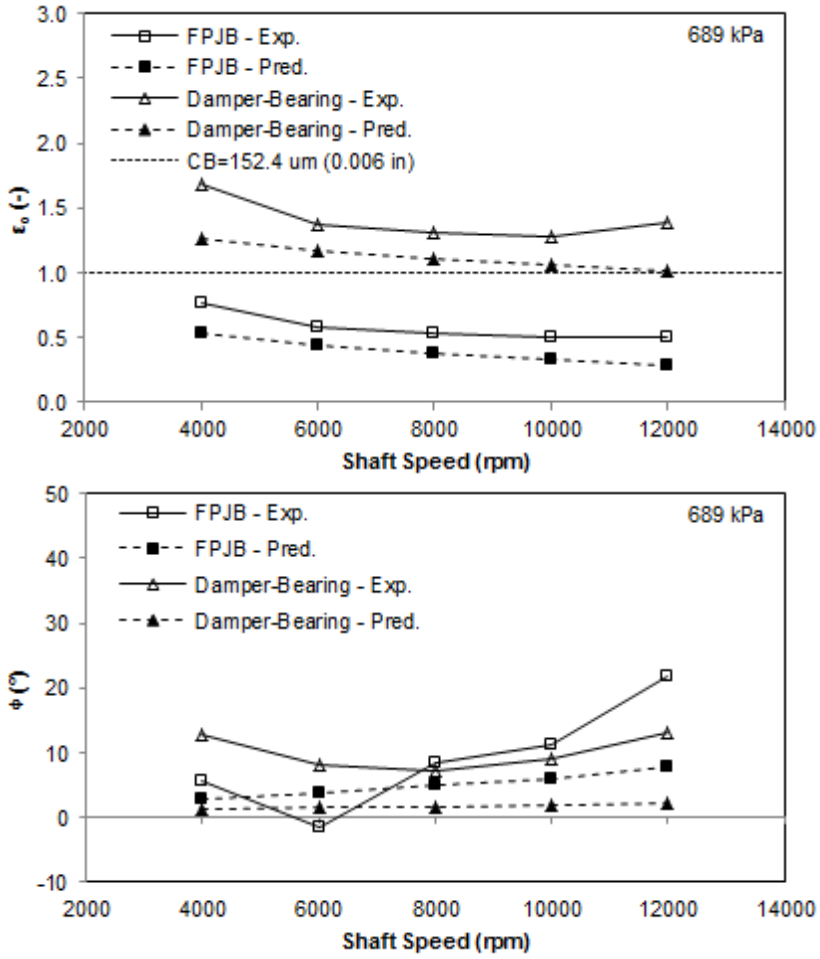

Figure 26. Experimental and predicted eccentricity ratio (top) and attitude angle (bottom) versus shaft speed at a sample load of 689 kPa

Pad Metal and Squeeze Film Land Metal Temperatures

The temperature distribution in a bearing is analogous to the pressure distribution, which is useful for understanding the behavior of a bearing. This pressure distribution is dependent on lubricant properties, which are temperature dependent and therefore vary throughout the bearing film lands. The temperature distribution is key to understanding the pressure distribution without directly measuring pressures, since the high pressures in lubricant film increase the temperatures. Thermocouples located near the inside surface of the pads are used for measuring the pad metal temperatures and give an indication of the lubricant temperature distribution within the bearing lands. Similarly, knowledge of the squeeze film land temperatures can help better understand of heat transfer in the bearing, and temperatures at two different axial positions can help identify misalignment.

Figure 27 shows the fourteen thermocouple locations used for measuring the pad metal temperatures, located approximately 3.175 mm (0.125 in) from the pad surface. A similar arrangement of eight thermocouples is used to measure temperatures along the squeeze film land, except that the devices are paired at four different circumferential locations with one each on the drive end (DE) and non-drive end (NDE), as shown in Fig. 27 and 28.

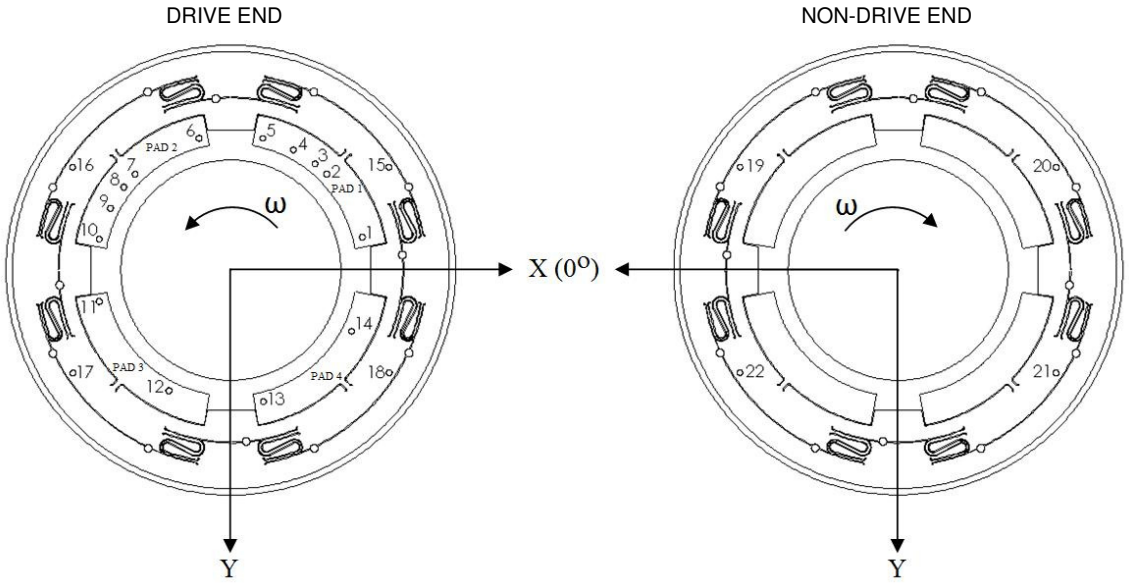

Figure 27. Bearing and squeeze film land thermocouple locations

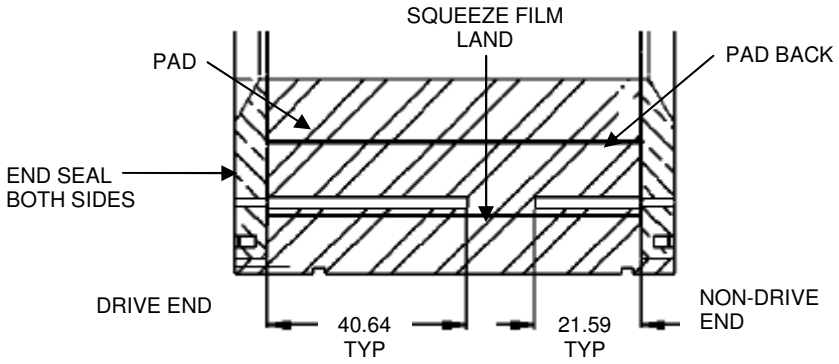

Figure 28. Squeeze film land thermocouple DE and NDE locations

Measured pad metal temperatures for both bearing configurations and their corresponding oil supply temperatures are given at different loads in Fig. 29 for a sample shaft speed of 4000 rpm. The static load is applied between pads 1 and 2, so the peak pad metal temperatures occurring on these pads is expected. Supply oil injected between the pads is shown to have a significant cooling effect on the downstream pads and a

slight effect on the upstream pads, as evidenced by the temperature drops at these locations. Note that the leading edge temperatures are all greater than the oil supply temperatures, indicating hot oil carry over and mixing from the previous pad.

Observation of the pad metal temperatures for both bearing configurations suggests a linear temperature increase with load, although this is not as obvious with the damper-bearing due to the more variable oil supply temperatures shown in Fig. 29. Although attempts were made to keep the supply oil temperature constant, warm ambient conditions around the oil coolers resulted in sometimes varying temperatures. The temperature distributions across the pads of the damper-bearing tend to be "flatter" than those of the FPJB; rather, the temperature changes along the pad circumference are less for the damper-bearing. Note the dashed line in Fig. 29, which is the oil supply temperature used for the prediction software and is shown to be a reasonable representation of average test conditions.

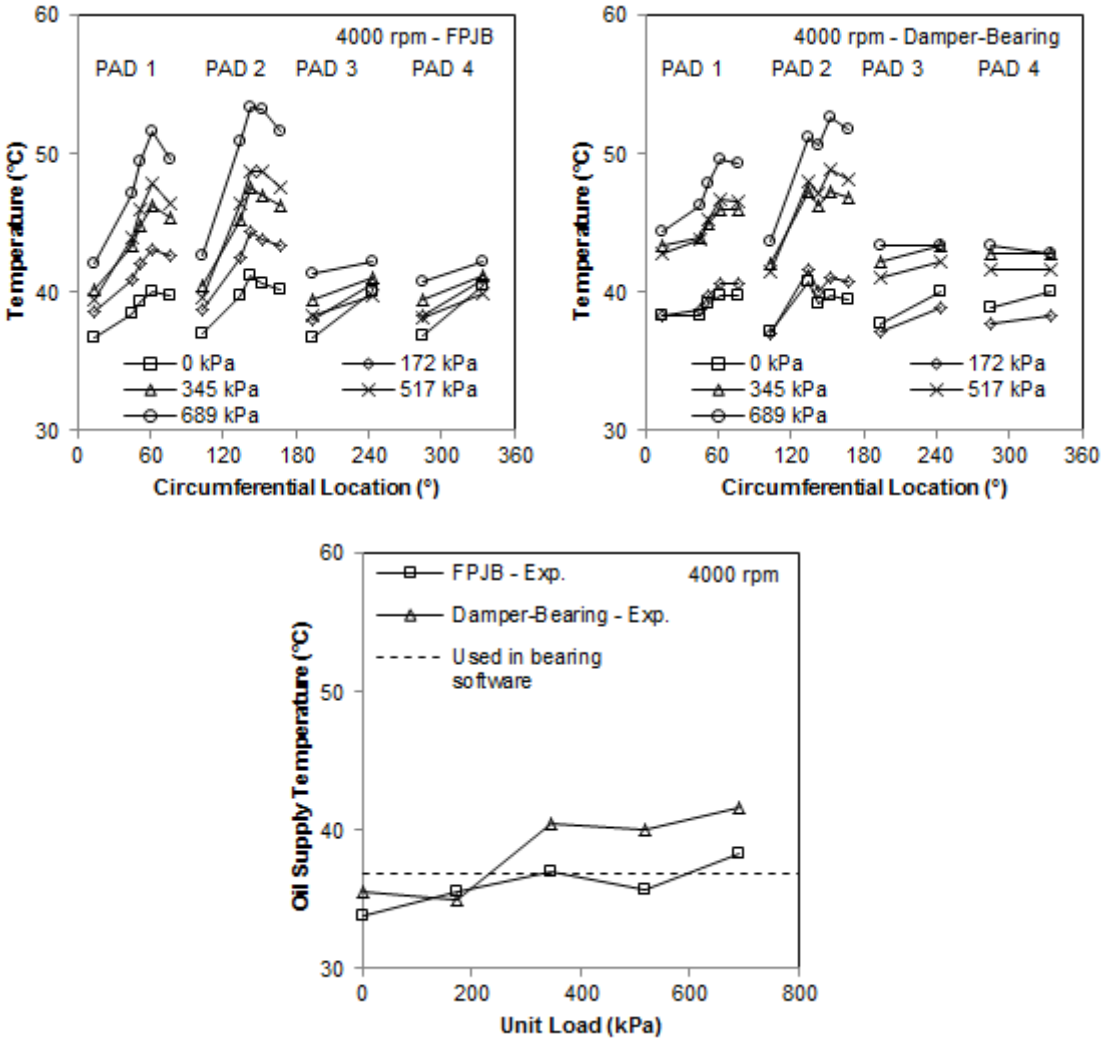

Figure 29. Measured pad metal temperatures and corresponding oil supply temperatures for both bearing configurations at 4000 rpm

As with the previous figure, Fig. 30 shows pad metal and corresponding oil supply temperatures but at different running speeds for a sample load of 517 kPa. As expected, the temperatures increase with running speed due to the greater shearing action. Although some of the pad temperatures decrease at certain running speeds, this is again explained by the changes in oil supply temperature below.

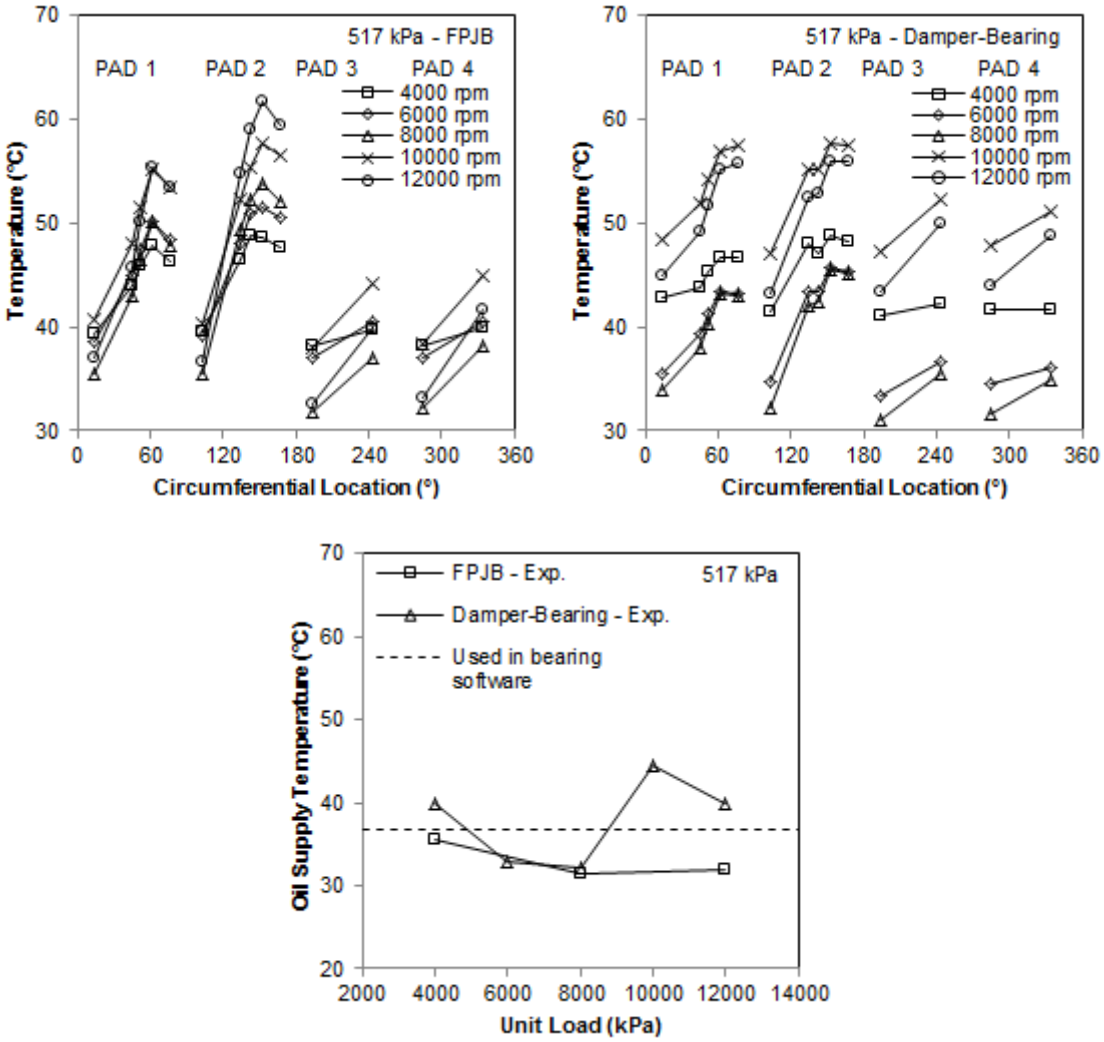

Figure 30. Measured pad metal temperatures and corresponding oil supply temperatures for both bearing configurations at 517 kPa

Squeeze-film land metal temperatures are shown in Fig. 31 at a sample shaft speed of 4000 rpm (top) and load of 517 kPa (bottom). These temperatures were recorded for both the drive-end (DE – solid lines) and non-drive end (NDE – dashed lines). The DE temperatures experience a noticeable temperature spike above pad 2. This is observed at all test conditions, including zero loading, which might indicate a

slight misalignment or a thermocouple that was not inserted completely in its hole. Other than this temperature spike, the squeeze film land remains at approximately constant temperature for both the DE and NDE. Unlike the pad metal temperatures, the squeeze film land temperature distribution is not a good representation of the pressure distribution in the lands since the damper is segmented resulting in non-rotational flow. A constant squeeze film land temperature suggests a homogeneous squeeze film land lubricant viscosity and constant outer bearing surface temperature, which could be used to simplify modeling.

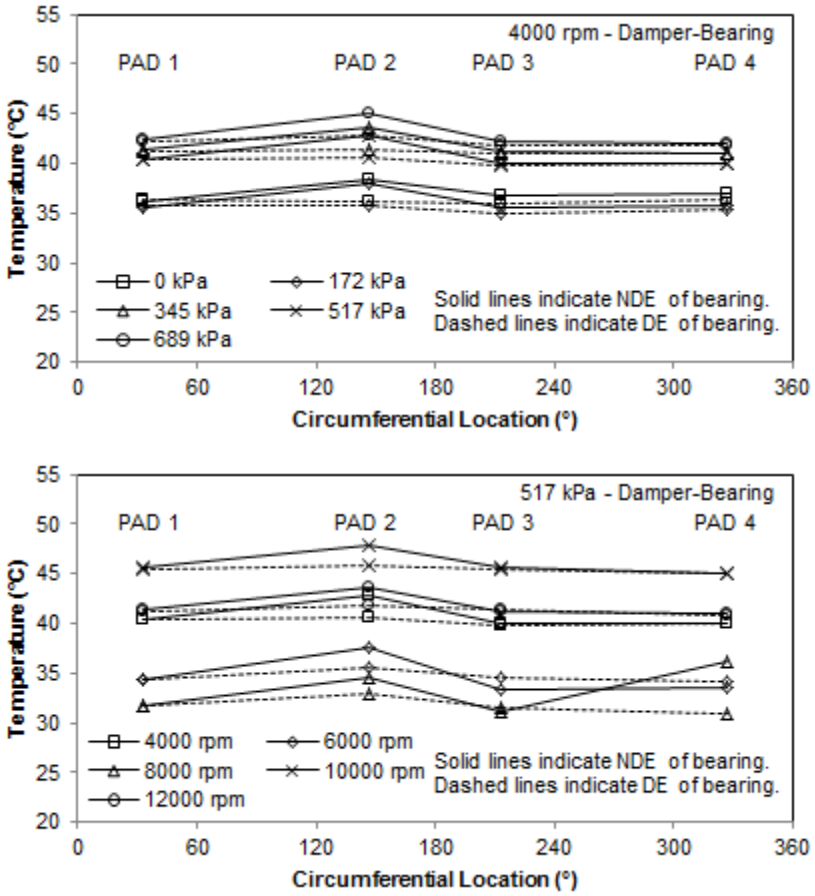

Figure 31. Damper bearing squeeze film land temperatures at 4000 rpm (top) and 517 kPa (bottom)

Estimated Power Loss

Power loss in bearings is important because it affects machine efficiency and operating cost. Since the test rig is not setup to measure the drag torque, the power loss is instead estimated using the temperature dependent specific heat capacity of the oil and the measured inlet and average outlet oil temperatures, described earlier in Section 4.

The estimated power loss for both bearing configurations is shown in Fig. 32 at different loads and shaft speeds on the left and the corresponding temperature rise on the right. At lower shaft speeds, the damper-bearing appears to yield lower power losses than with the FPJB alone. However, at higher running speeds the results for both configurations seem to converge. A similar trend is apparent viewing the power loss versus shaft speed for the two sample loads shown. Power loss for the FPJB is typically under predicted by about 2 kW, resulting in errors of up to 62% at 4000 rpm and decreasing with increased shaft speed to less than 16% at 12000 rpm. Where the experimental trends are apparent (i.e. smooth curves), the predictions do a good job of following those trends. While the measured temperature rises are often erratic, when used with the temperature dependent densities and specific heats they produce almost constant power loss values.

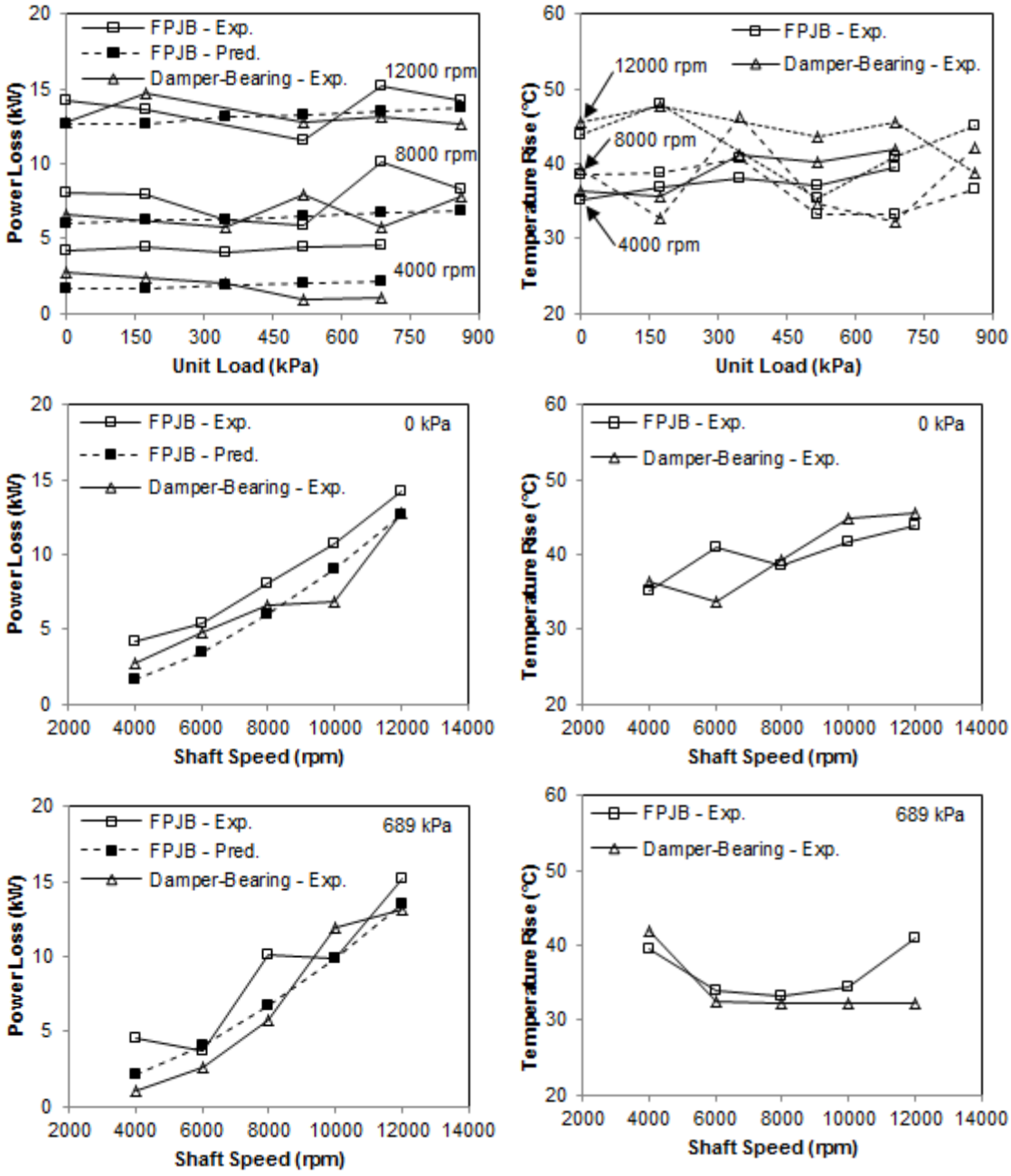

Figure 32. Experimental and predicted power loss for different shaft speeds and static loads

7. MEASURED AND PREDICTED MULTI-FREQUENCY RESULTS

This section details the dynamic stiffness coefficients and the derived rotordynamic coefficients for the test bearing. Measured and predicted data are provided for the FPJB, and measured data only are provided for the damper-bearing. Whirl frequency ratio (WFR) as a stability indicator is also presented. Results for both bearing configurations are presented together to gauge the effect of the squeeze film damper. Finally, non-dimensionalized rotordynamic coefficients for the locked damper bearing are compared to those obtained by Al-Ghasem [6] on a similar bearing to verify results and to see how effective non-dimensionalization using the Sommerfeld number is.

Baseline Data

Dynamic tests are used to measure rotordynamic coefficients for the FPJB and damper bearing. Due to the design of the test rig, before the dynamic tests are performed, "baseline" tests are conducted for each bearing configuration at zero rotor speed, zero load, and no oil (dry bearing). The baseline tests account for external factors, such as the stiffness of the pitch stabilizers, stiffness of the unused hydraulic shaker, and the mass of the bearing and bearing housing. These baseline dynamic stiffnesses are subtracted from each subsequent dynamic test, so that only effects of the fluid film bearing are determined.

Figures 33 and 34 show the baseline Re($\boldsymbol{H_{ij}}$) and Im($\boldsymbol{H_{ij}}$) coefficients, respectively, for the FPJB (left) and damper bearing (right); the direct stiffnesses are shown at the top and cross-coupled are on the bottom of each figure. Data points occurring at frequencies of multiples of 60 Hz and beyond 300 Hz are removed for

clarity due to high uncertainties. The baseline data accounts for factors external to the test bearing, so this data should be approximately equal for both bearing configurations. In Fig. 33, the baseline stiffness coefficients (intersection with the *y*-axis) are very close for both configurations; however, the slopes of the stiffnesses increase greatly from the FPJB to the damper bearing and is accounted for by the added mass terms. The reason for this is uncertain, but this should have little effect on the calculation of the stiffness coefficients, since the stiffness values at the lower frequency range for both bearings are similar. However, this might have resulted in some error with the calculation of the added mass coefficients due to the differences in stiffness at higher frequencies. The baseline damping coefficients, as provided by the slopes of the imaginary portions of the dynamic stiffnesses, are presented in Fig. 34. The baseline direct damping coefficients are close for both bearing configurations, and the cross-coupled damping is similar when the measurement uncertainties are considered.

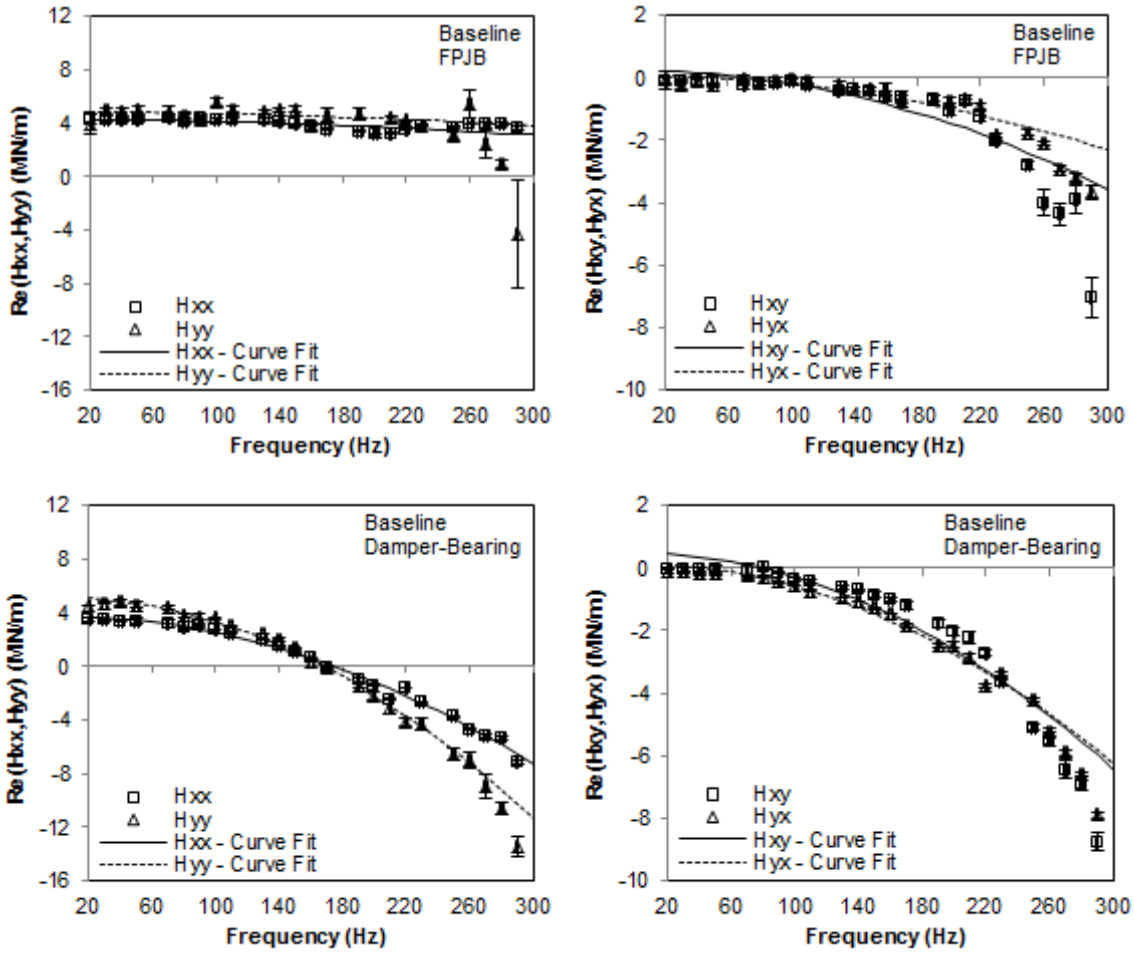

Figure 33. Baseline real dynamic stiffnesses for FPJB (top) and damper-bearing (bottom)

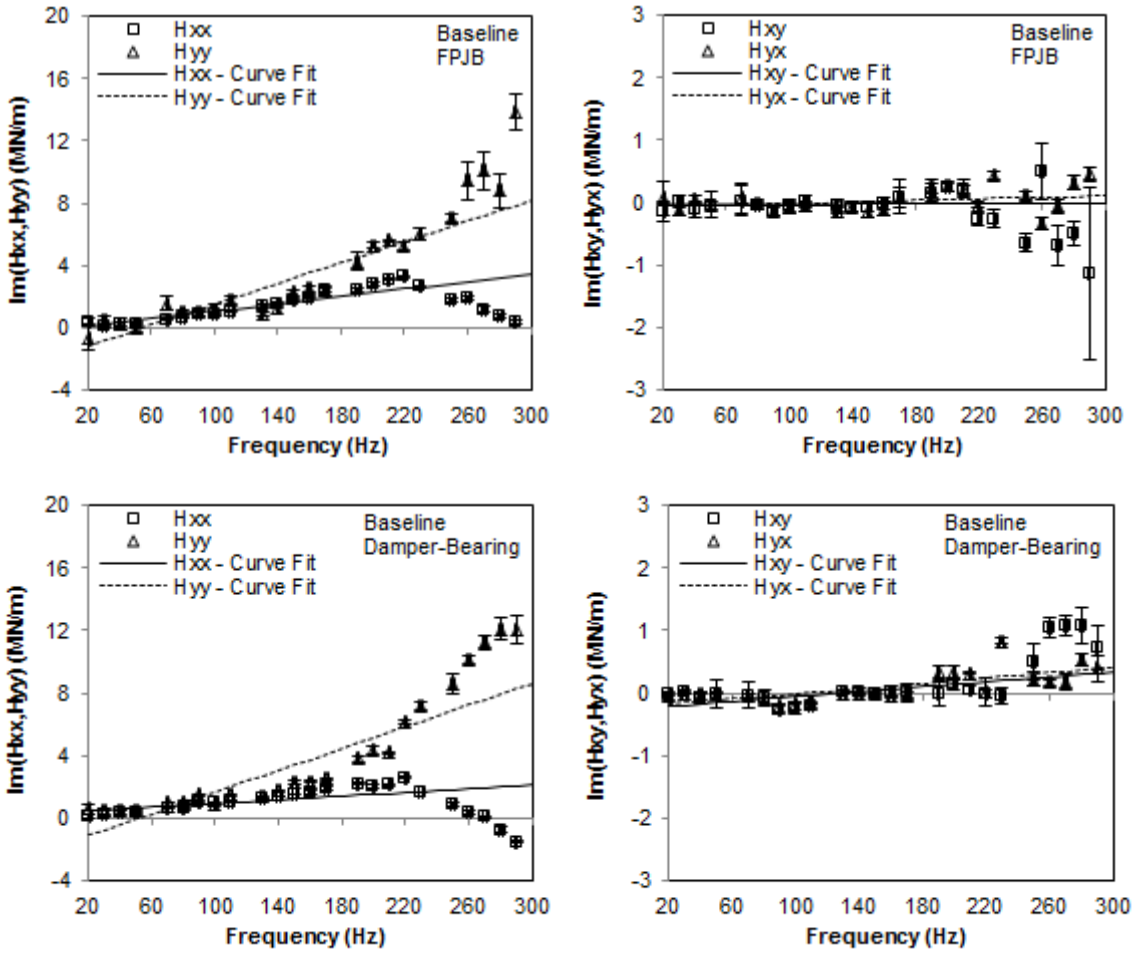

Figure 34. Baseline imaginary dynamic stiffnesses for FPJB (top) and damper-bearing (bottom)

Dynamic Stiffnesses

Figures 35 and 36 provide experimental dynamic stiffnesses for both bearing configurations, and predicted dynamic stiffnesses for the FPJB, at a sample test condition of 4000 rpm and 172 kPa unit load. The real portions of the dynamic stiffnesses for the damper-bearing are generally flatter than those for the FPJB, meaning that the stiffness changes less with excitation frequency. As expected, the stiffness is lower for the damper-bearing due to the softer support of the damper. The imaginary

portions of the dynamic stiffness are nominally linear, meaning that the damping remains constant with changes in excitation frequency. The quadratic stiffness and linear damping curve fits given by the least squares regression method described earlier fit the data well. Up to at least 1X running speed (4000 rpm or 70 Hz in this case), the stiffness curves for both bearing configurations are relatively flat, suggesting that ignoring the added mass terms and using a stiffness-damping only (no added mass) approach is a reasonable method of modeling.

Defining the stiffness coefficients as where the real portions of the dynamic stiffnesses intersect the *y*-axis, the software [20] does a good job of predicting the direct stiffness coefficients, as suggested by the closeness of the experimental and predicted stiffnesses at the 20 Hz mark. Although the predictions follow the same trends as the experimental results to about 150 Hz (2.25X running speed), at higher frequencies the predictions are "too linear" and over predict the stiffness. Also, being "too linear," the predictions do not lend themselves well to the curve fitting procedure used to determine the added mass coefficients, since a quadratic curve fit is used; this is obvious when reviewing the added mass coefficients presented later. Cross-coupled stiffness predictions are often "hit or miss," with the software [20] generally predicting close to the measured magnitude but not always the correct direction, as shown at the bottom right of Fig. 35. Note the particularly small uncertainties, especially at lower excitation frequencies; large uncertainties occurred on most tests at frequencies beyond 220 Hz and these data points were removed during the data reduction process. The high

uncertainties around 220 Hz have been observed before and may be due to a resonance of the test rig.

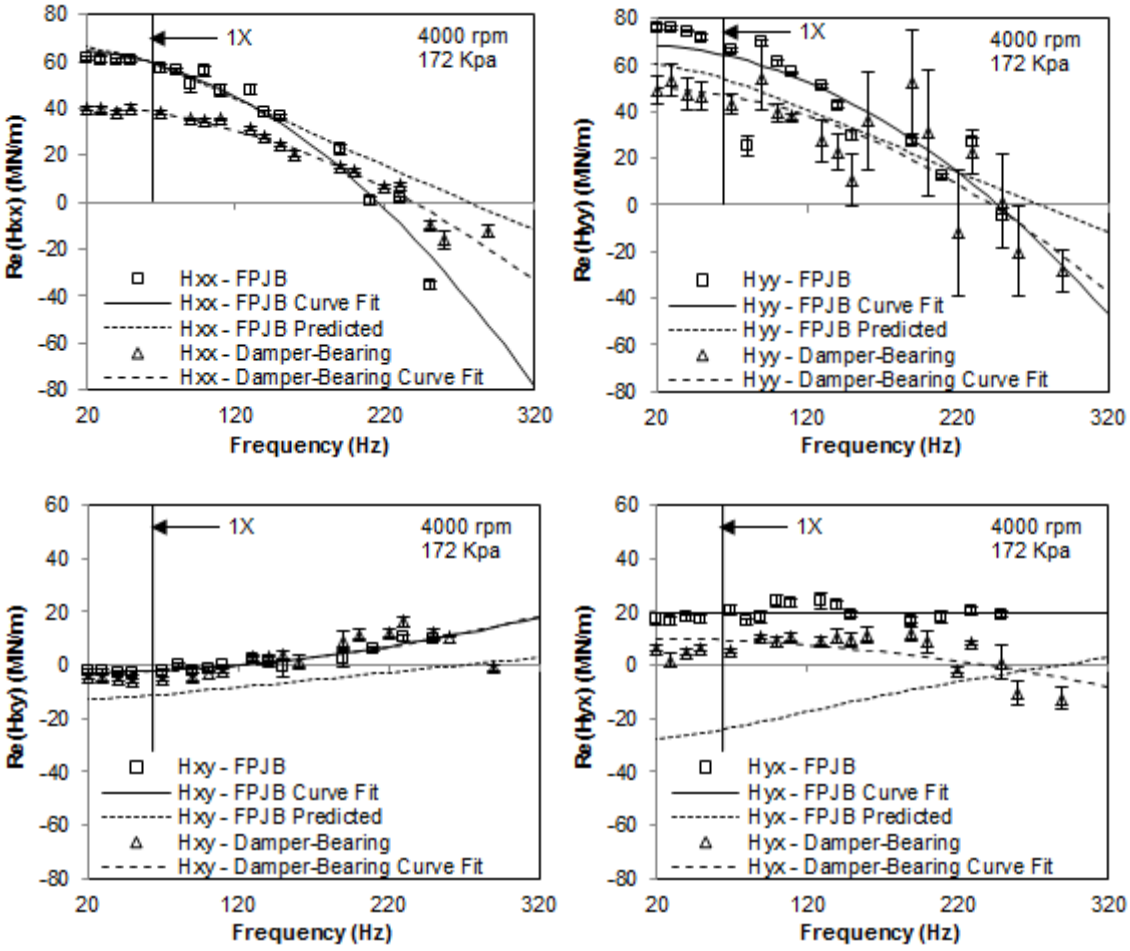

Figure 35. Real direct (top) and cross-coupled (bottom) dynamic stiffnesses at 4000 rpm and 172 kPa

The predicted slopes of the imaginary portions of the dynamic stiffnesses are shown in Fig. 36 and are linear like the experimental values. This is always the case since the predicted synchronous damping coefficient is transformed into a line to match the format of experimental data. Due to differences in loading, the slope for Im($\boldsymbol{H_{xx}}$) is

normally over-predicted and the slope for Im($\boldsymbol{H_{yy}}$) is normally under-predicted. The slopes of the cross-coupled terms Im($\boldsymbol{H_{xy}}$) and Im($\boldsymbol{H_{yx}}$) are often over-predicted in magnitude and of opposite direction from the experimental values. This is more clearly shown with the rotordynamic coefficients derived from this data presented in the next section.

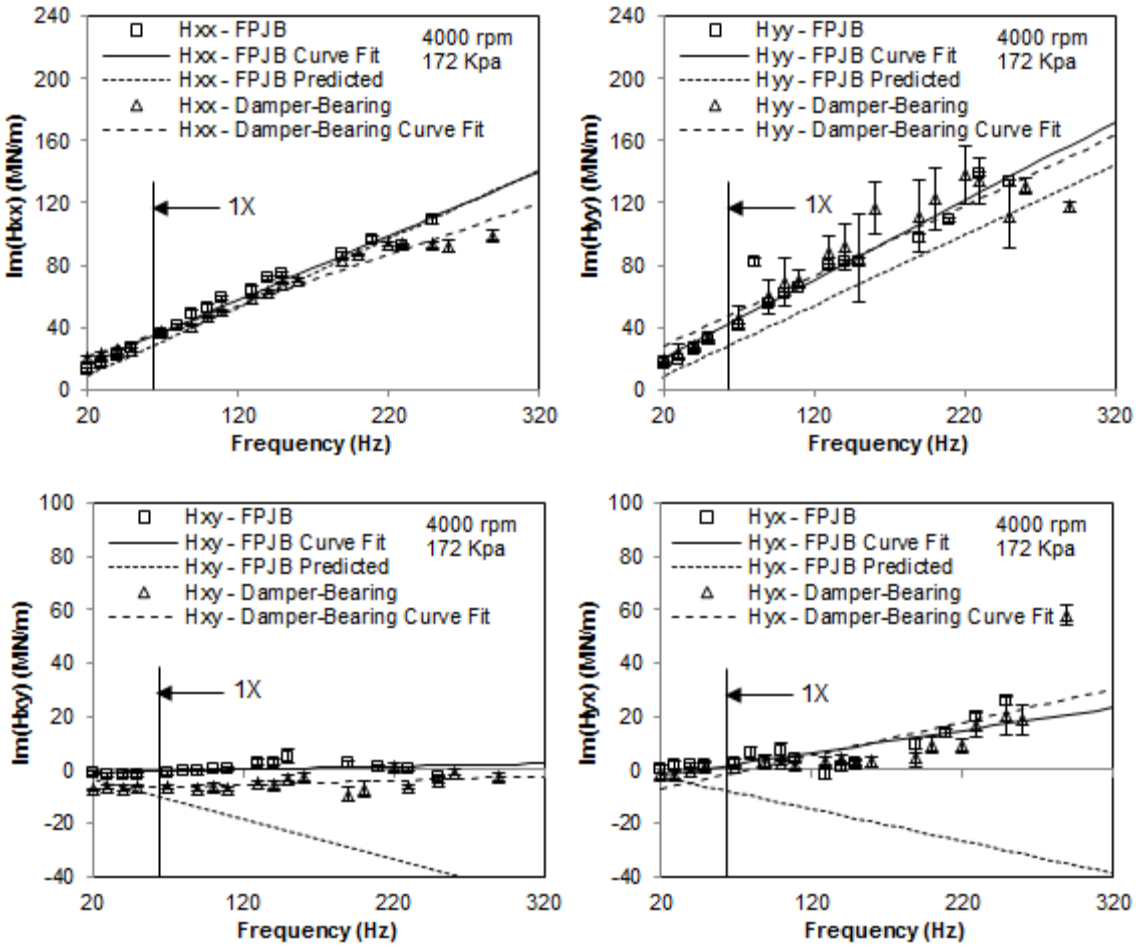

Figure 36. Imaginary direct (top) and cross-coupled (bottom) dynamic stiffnesses at 4000 rpm and 172 kPa

Rotordynamic Coefficients

This section presents the measured rotordynamic coefficients for both bearing configurations, and predictions for the FPJB. The results for each bearing configuration are shown on top of each other for comparison, and are then compared at the end of the section to show the effect of the damper on the rotordynamic coefficients. Also, as an exercise to increase confidence in the data obtained, non-dimensionalized data for the FPJB (locked damper case) is compared to previous tests on a similar bearing. For brevity, only representative data are presented, however, complete data can be found in the appendix.

Measurements and Predictions

Figure 37 presents rotordynamic coefficients for the FPJB (left) and damper-bearing (right), as well as predicted coefficients for the FPJB, at a sample shaft speed of 8000 rpm. For the FPJB, the direct stiffness and damping coefficients increase with load, while the cross-coupled coefficients remain approximately constant. The added mass coefficients remain constant with increasing load. The software [20] does a good job of predicting the stiffness and damping coefficients, and a fair job of predicting direct damping coefficients, but poorly predicts added mass coefficients, which is expected since the dynamic stiffnesses predicted by the software are *almost* linear rather than quadratic like those measured. Added mass coefficients are often under predicted, and the wrong sign (+/-) is usually predicted for one or both of the cross-coupled terms.

For the damper-bearing, the stiffness, damping, and added mass coefficients remain almost constant with increasing static load (except for the apparent damping

coefficient outlier at 345 kPa). The significantly softer and constant stiffness of the SFD in series with the increasing fluid film stiffness results in a combined stiffness that is less than damper stiffness (k_{ISFD} = 47.79 MN/m) and nearly constant for the given range. As expected, the stiffness of the damper-bearing is less than that of the FPJB. The damping coefficients for the damper-bearing are close to (or even less than) those of the FPJB; this is elaborated on near the end of this chapter. The direct added mass coefficients are slightly less for the damper-bearing. While the cross-coupled stiffness coefficients are usually less for the damper-bearing, the cross-coupled damping and added mass coefficients are very close to, or larger in magnitude than, those coefficients for the FPJB. This suggests that a rotor supported by FPJBs alone *might* actually be more stable than the same rotor supported by damper-bearing (FPJBs in series with ISFDs), which is explored at the end of this chapter.

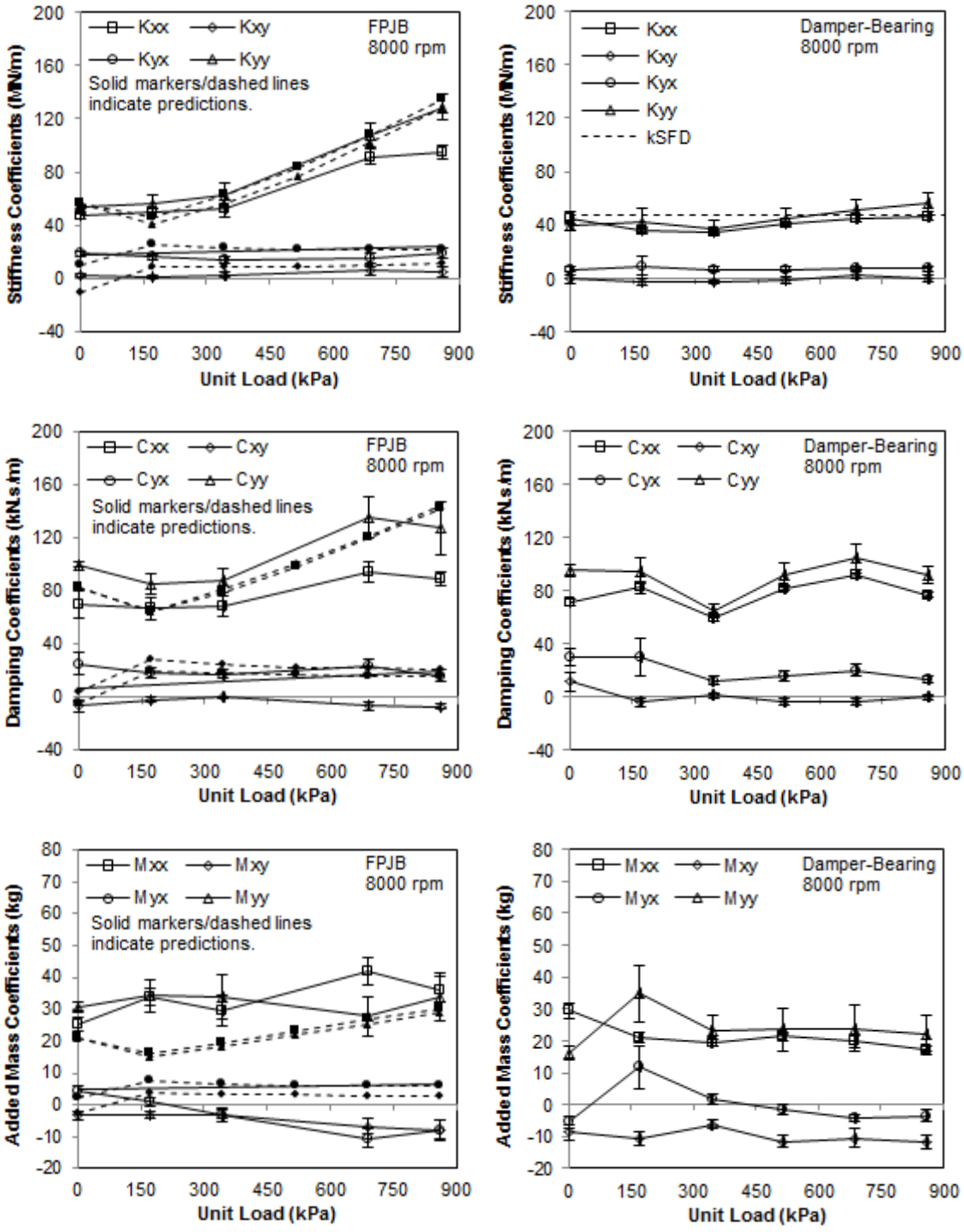

Figure 37. Stiffness, Damping, and added mass coefficients for a sample shaft speed of 8000 rpm for FPJB (left) and damper-bearing (right)

Measured and predicted rotordynamic coefficients are presented as a function of shaft speed in Fig. 38 at a sample load of 517 kPa for the FPJB (left), and measured coefficients are presented for the damper-bearing (right). For the FPJB, the measured direct stiffness coefficients increase with shaft speed, while the predictions for these remain approximately constant. The cross-coupled stiffnesses are predicted well, particularly at lower shaft speeds. The overall downward trend of the direct damping coefficients and the flat trend of the cross-coupled damping coefficients are predicted, and the magnitudes are predicted reasonably well. The added mass coefficients are generally poorly predicted.

For the damper-bearing, the measured direct stiffness coefficients increase with speed, but at a lesser rate than the FPJB due to the softer support of the SFD. Cross-coupled stiffnesses remain relatively constant with speed, and are lower than those measured for the FPJB. Damper-bearing test results show almost constant added mass coefficients, regardless of shaft speed.

The quality of this experimental data might be described by both the uncertainty (repeatability of the results) and the data curve fits. The multi-frequency test data for both bearing configurations generally exhibits low uncertainty. Both bearing configurations also yield similar quality curve fits, although those for the damper-bearing are slightly better overall. Curve fits for direct coefficients are good, with R^2 values typically greater than 0.9, while curve fits for cross-coupled coefficients vary but often yield R^2 values of 0.5 or more.

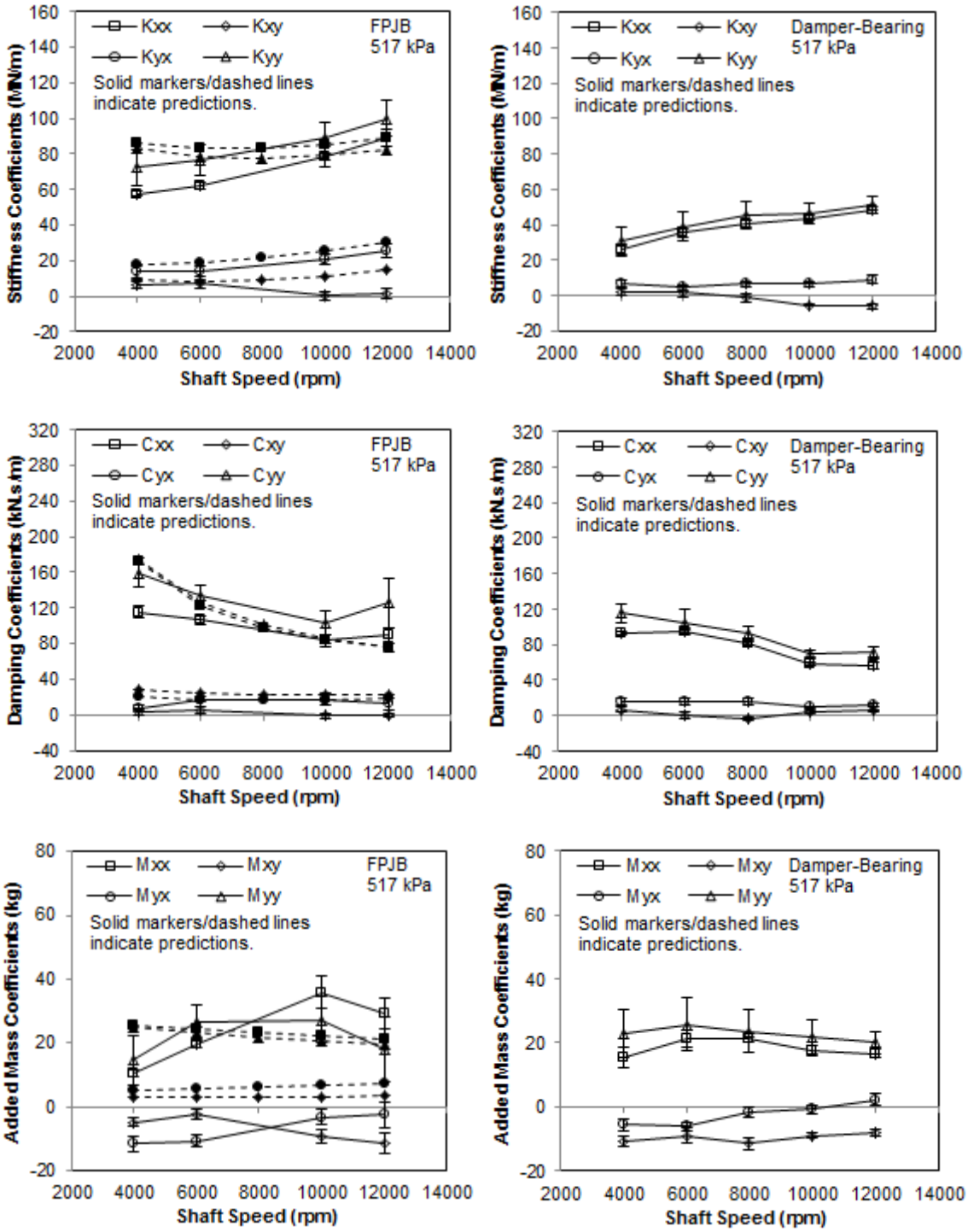

Figure 38. Stiffness, damping, and added mass coefficients for a sample load of 517 kPa for FPJB (left) and damper-bearing (right)

Effect of Integral Squeeze Film Damper on Rotordynamic Coefficients

Experimental rotordynamic coefficients for both bearing configurations are presented for a sample loading of 345 kPa in Fig. 39, so that the effect of the SFD can be observed. The stiffness coefficients are expectedly lower for the damper-bearing, and the direct added mass coefficients are also lower and remain almost constant with load. Cross-coupled added mass terms are approximately equal for the FPJB and damper-bearing. The damping coefficients are almost equal for the two configurations, or even less for the damper-bearing. The beneficial effect of the damper is explained using with the simulation that follows.

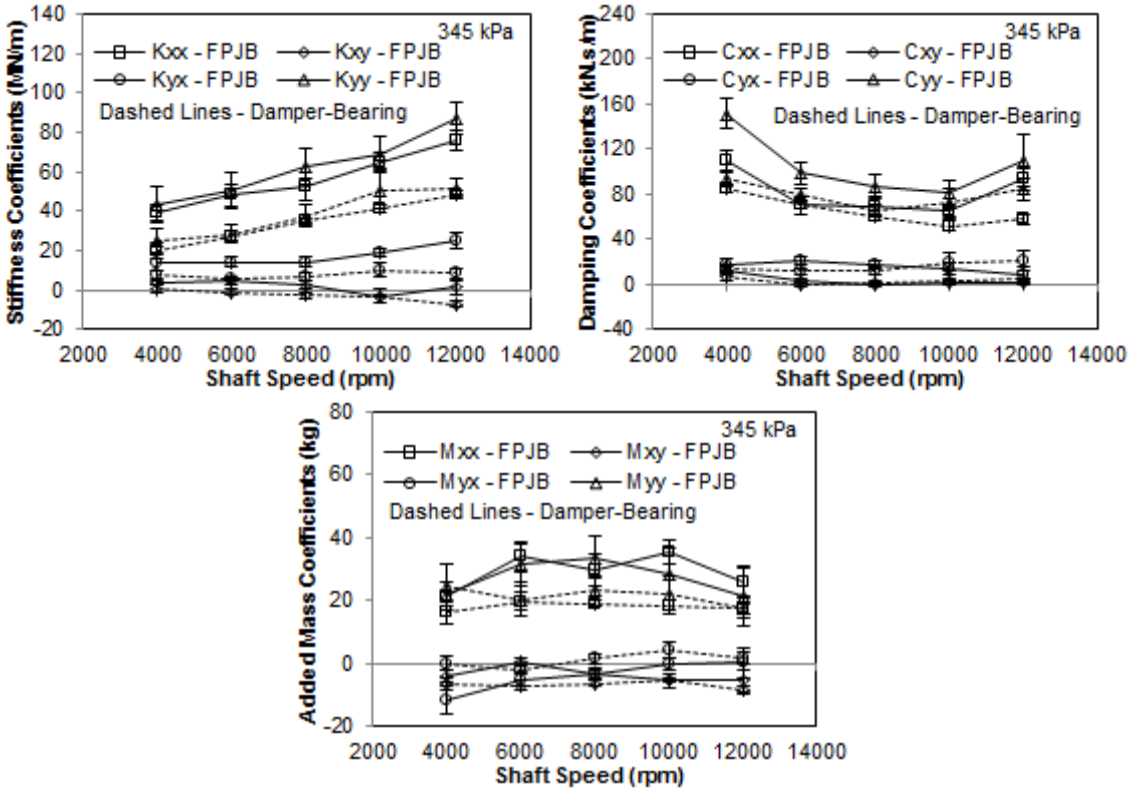

Figure 39. Effect of squeeze film damper on bearing coefficients at a static load of 345 kPa (FPJB - solid lines; damper-bearing - dashed lines)

The simple rotor-bearing model shown in Fig. 40 was created using XLTRC^2 and the measured bearing coefficients in Fig. 39 for both bearing configurations. The rotor-bearing system is not representative of any specific type of machine, but rather was designed to produce an arbitrary critical speed of approximately 10000 rpm (running speed = 10000 rpm; rotor-bearing natural frequency = 10438 cpm) and "reasonable" (less than the bearing clearance) responses at the bearing locations using the rotordynamic coefficients for FPJB. Figure 41 shows the mode shape for the shaft supported on FPJBs (locked damper bearings) at this condition, which indicates the first bending mode. Since rigid-rotor operation is required in most machines, this is obviously undesirable. The rotor responses (peak-to-peak amplitudes versus shaft speed) are given in Fig. 42 for the FPJB (top) and damper-bearing (bottom), at a bearing location (left) and at the mid-span of the rotor (right).

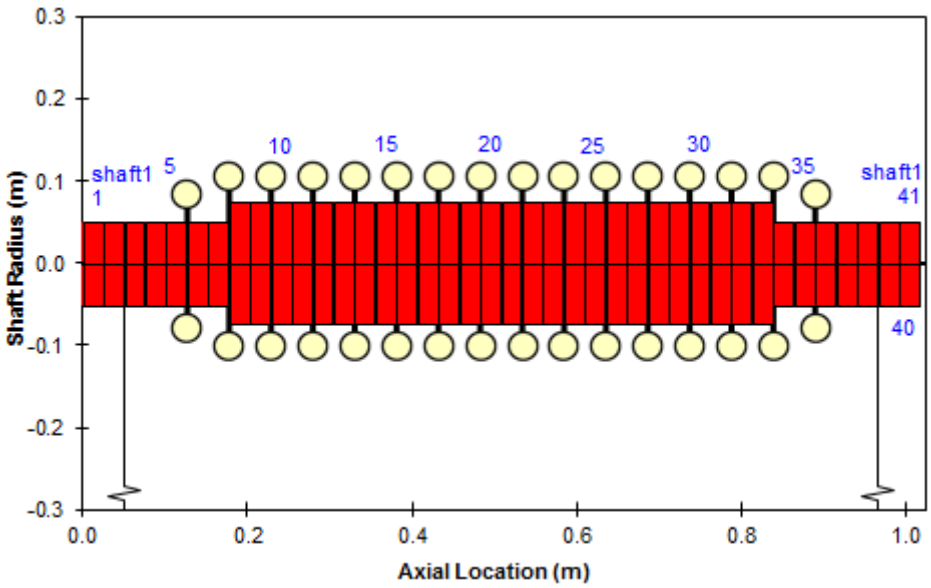

Figure 40. XLTRC^2 rotor model

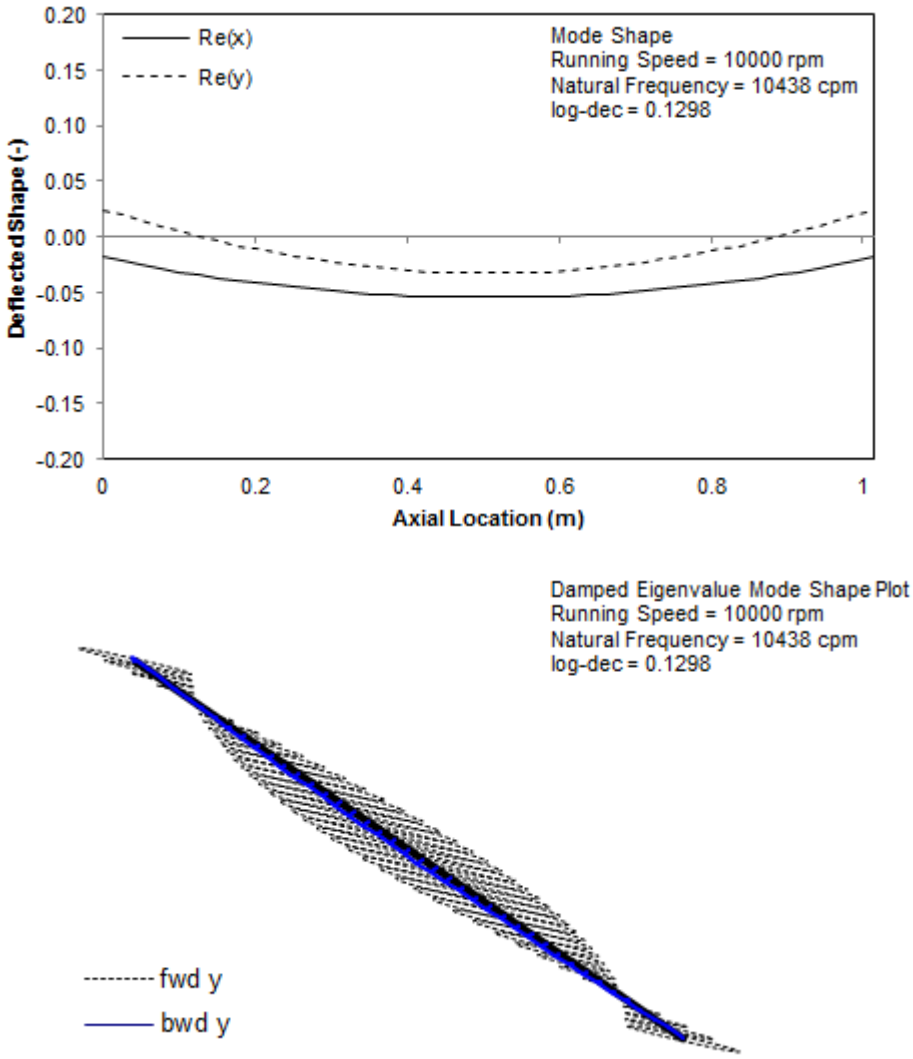

Figure 41. Mode shape for a shaft speed of 10000 rpm

For the FPJB, Fig. 42 shows a peak-to-peak response of about 22 µm (0.9 mils) at the bearing locations and 58 µm (2.3 mils) at the rotor mid-span, at 10000 rpm. Utilizing the squeeze film damper, the amplitude at the bearings is barely reduced at all – to 21 µm (0.8 mils); however, the rotor mid-span vibration is only 23 µm (0.9 mils) – more than a 50% reduction! Although all of the damping coefficients for the damper-

bearing used in the simulation are less than or close to those of the FPJB, the accompanying reduction in stiffness clearly results in greater *effective* damping. The softer support of the combined damper-bearing makes the damping provided by the bearing closer to optimum for the rotor-bearing system [22]. A common use of SFDs – shifting critical speeds away from the operating range – is also shown in Fig. 42. The SFD not only gives a much greater operating range between the second and third critical speeds (10000 rpm versus 3700 rpm), but also results in reduced response vibration amplitude in that range.

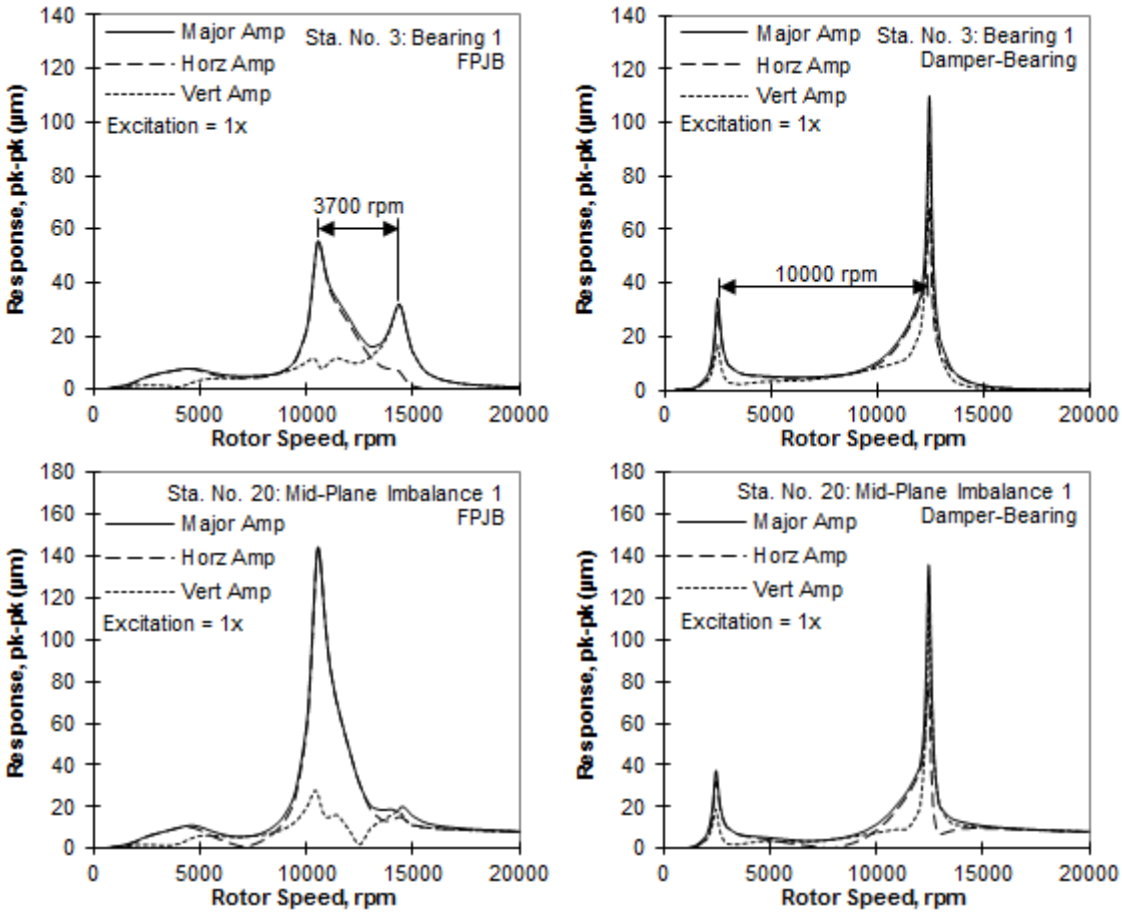

Figure 42. Simulated peak-to-peak response for FPJB (left) and damper-bearing (right)

Similar FPJB Non-Dimensionalized Results Comparison

To investigate the accuracy of the test results, the FPJB coefficients are non-dimensionalized and compared to coefficients obtained from a similar bearing tested by Al-Ghasem [6]. The bearing tested by Al-Ghasem is a flexure pivot pad bearing with larger clearances $C_B = 0.1905 \pm 0.0127$ mm (0.0075 ± 0.0005 in), $C_P = 0.2540 \pm 0.0127$ mm (0.0100 ± 0.0005 in), to give an identical preload of $\kappa = 0.25$, and an identical pad length of 76.2 mm (3.0 in), but is made to accept a 116.8 mm (4.6 inch) rotor instead of the current test bearing that is made for a 101.6 mm (4 inch) rotor. The bearing coefficients are plotted against the Sommerfeld number, defined previously in Eq. (19), because similar bearings should behave similarly at identical Sommerfeld numbers.

Figure 43 shows non-dimensionalized stiffness, damping, and added mass coefficients for the FPJB and a similar bearing tested previously by Al-Ghasem, at a sample shaft speed of 10000 rpm. Generally, the non-dimensional stiffness and damping coefficients follow similar trends for both bearings, but the current FPJB results are usually of lower magnitude. Similarly, the direct added mass coefficients match well for both bearings, and the cross-coupled added mass terms are close at lower Sommerfeld numbers. The best overall agreement between the measured coefficients for the bearings is at the lower Sommerfeld numbers. At lower Sommerfeld numbers, the stiffness coefficients compare reasonably well, and the added mass coefficients agree very well. Damping coefficients are less for the current test bearing than for Al-Ghasem, regardless of Sommerfeld number, but are also closer at lower Sommerfeld numbers. Overall, the

results show the bearing coefficients for the similar bearings to be reasonably close on a non-dimensional basis, which act as validation for the current results.

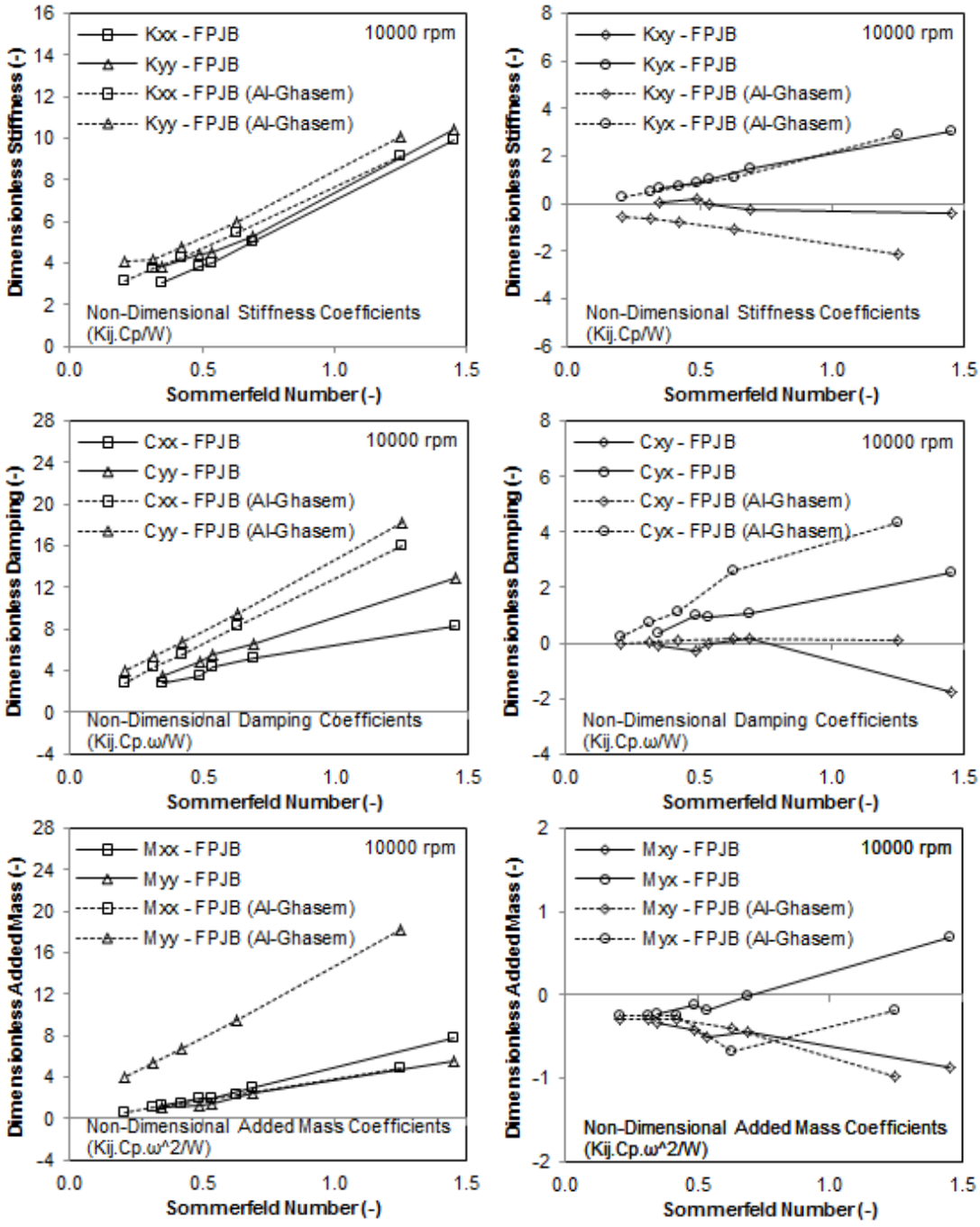

Figure 43. Non-dimensional rotordynamic coefficients versus Sommerfeld number

Whirl Frequency Ratio (WFR)

The whirl frequency ratio (WFR) was calculated from the rotordynamic coefficients to quantify the stability at the various test conditions. The WFRs indicate infinite stability for both bearing configurations at many test conditions, including all loads at 4000 rpm and 6000 rpm for FPJB and all but one load for the damper-bearing at the same shaft speeds. Experimental and predicted WFRs, as well as corresponding WFRs for the similar bearing tested by Al-Ghasem [6], are shown at sample shaft speeds of 8000 rpm and 10000 rpm in Fig. 44. Using the rotordynamic coefficients predicted following [20] for the FPJB, stability is normally over-predicted with WFRs equal to zero, except at lower loads where the predictions normally over-predict the WFR slightly. Unlike Al-Ghasem's data which exhibits almost linear trends until the highest loading, there is no obvious WFR trend in the current results for either bearing configuration. However, the WFRs for both current bearing configurations are almost always lower than those found by Al-Ghasem.

Whirl frequency ratio versus shaft speed is also shown in Fig. 44, for sample unit loads of 172 kPa and 689 kPa. Increases in WFR typically accompany increases in shaft speed for a given load, although it has zero magnitude at lower speeds in the given examples. In cases where the predicted WFRs for the FPJB are non-zero, such as 0 kPa at all shaft speeds and 172 kPa at 10000 rpm, the WFR is almost always over-predicted, as illustrated below. As stated above, the WFRs for Al-Ghasem's data are normally much higher than those measured in the current experiments, but still do not exceed 0.2 for the data presented.

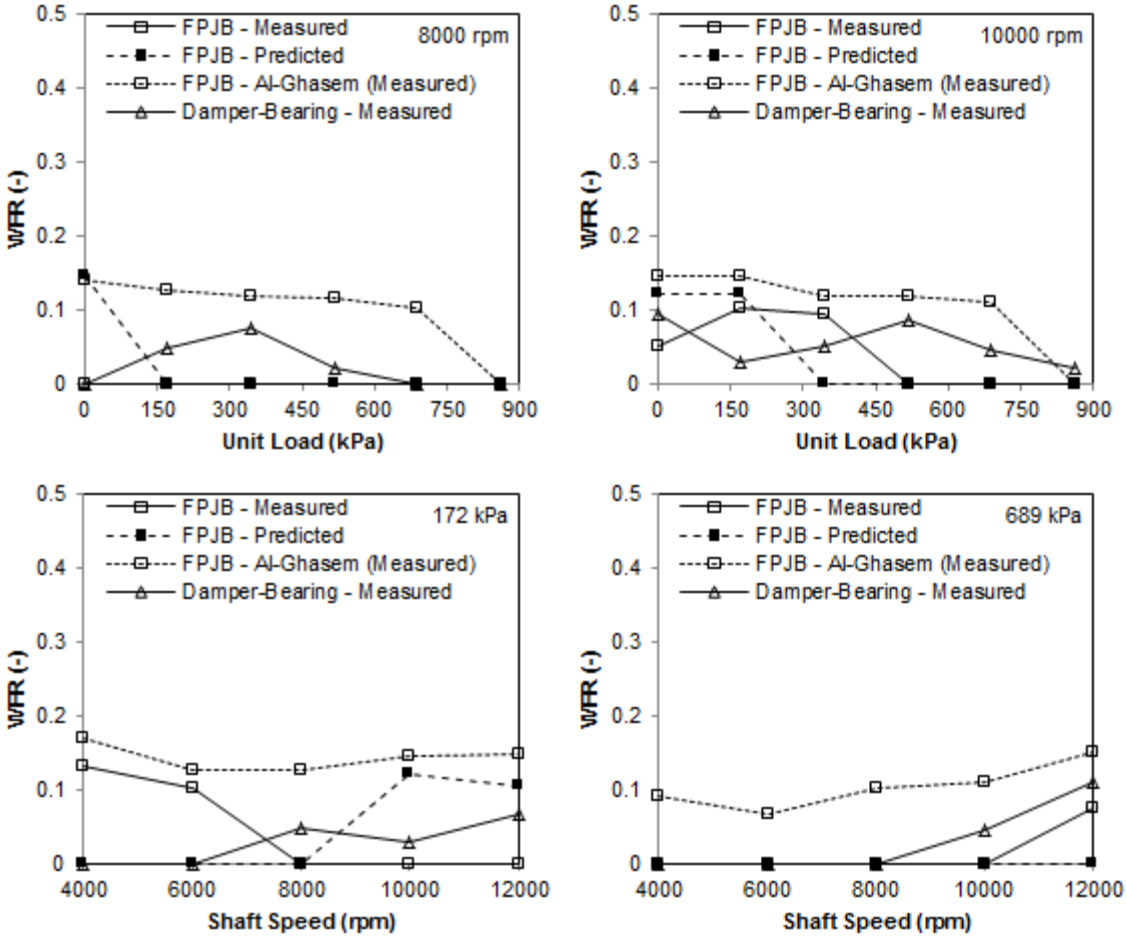

Figure 44. WFR at different static loads and shaft speeds

The maximum *experimental* WFR under the test conditions occurred at 12000 rpm and was 0.13 and 0.11 for the FPJB and damper-bearing, respectively, while the maximum *prediction* for the FPJB was 0.25 and occurred at 4000 rpm. While the FPJB has a higher maximum WFR, interestingly, the damper-bearing experiences a significantly greater number of instances of non-zero WFRs from 8000-12000 rpm (six non-zero WFRs for the FPJB; fifteen non-zero WFRs for the damper-bearing). Regardless, the WFR remained low for both bearing configurations throughout all tests.

For example, the maximum WFR of 0.13 corresponds to an onset speed of instability (OSI) of 7.7X the rotor natural frequency. Note that while conventional tilting pad bearings have WFRs = 0 due to very low or non-existent cross-coupling, flexure-pivot-pad journal bearings normally have a low WFR due to the cross-coupling present because of the pivot stiffness.

As a side note, while WFR calculations were performed both excluding and included the added mass term (Lund [18] and San Andrès [19] models, respectively), only the San Andrès version is presented in this section. Identical values were found using both models in all but one test condition for each bearing configuration, and even these WFRs varied by only 0.01.

8. ROTATING LOAD TEST RESULTS

The rotating load test imposes a two-dimensional excitation force onto the unloaded damper-bearing in a circular fashion, like that encountered by an unbalanced shaft. Unlike the multi-frequency testing which forces the bearing in only one direction at a time, the rotating load forces in two directions (*x*- and *y*-directions) simultaneously, ideally forcing the bearing into a circular centered orbit (CCO) about the rotor. This type of testing is of particular interest for squeeze film dampers, since the damper is displaced about its full range of motion, thereby capturing its full damping ability. In the current test program, the excitation scheme was developed and first implemented by Schaible [23], who provides a more detailed description of the test regime that follows.

Polar coordinates best represent the rotating load, which requires a constant magnitude radial force with a varying angular direction. Since excitation is accomplished via two electro-hydraulic shakers orthogonally located in the plane of the bearing, a more convenient approach uses rectangular coordinates utilizing both shakers to produce sinusoidal forces with a phase difference of 90°, identical frequencies, and amplitudes that result in the excitation amplitude. This rectangular representation of the force signals (F_x,F_y) is given in Eqs. (50) and (51), where f_o is the force magnitude (or radius), Ω is the excitation frequency, and t is time.

$$F_x = f_o \cos(\Omega t) = f_o \sin(\Omega t + \pi/2) \tag{50}$$

$$F_y = f_o \sin(\Omega t) \tag{51}$$

Ideally, plotting F_y versus F_x yields a force plot like that shown in Fig. 45. Actually, achieving this force proves difficult due to the necessity of some manner of

phase control to ensure the shakers work in harmony to produce the desired force at the desired time. Unlike the multi-frequency testing that utilizes only a single actuator at a time, phase control can be a significant problem for the rotating load excitation method since it requires the actuators to work together to produce a two-directional force. Schaible determined that the slow nature of the phase lag drift did not necessitate a real time correction, so instead a phase lag correctional scheme is included in the LabView controller software. Essentially, this correctional scheme assumes a starting phase difference of 90°, measures the actual phase difference after a test, and corrects to that test. Schaible found average phase differences for tests to be typically within ±2.5°, which was found to be similar in the current tests.

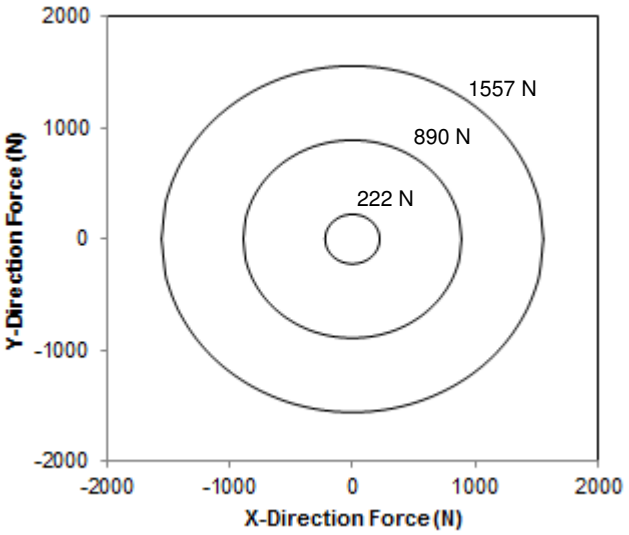

Figure 45. Ideal rotating excitation force at sample amplitudes

Unlike the multi-frequency (single-direction) excitation tests that have the effect of exciting at multiple frequencies automatically, the rotating load testing regime requires that tests are performed individually at each excitation frequency. This makes for a very time intensive process to obtain data necessary to adequately define the rotordynamic coefficients. Data were taken and are presented for a shaft speed of 12000 rpm and at excitation frequencies of 20-160 Hz, and for magnitudes of 222-1779 N; zero static load is used to best achieve CCOs. Higher frequency excitations were not recorded because circular force plots were not obtained.

Contrary to the ideal excitation force shown above, a typical example of the real excitation force is shown in Fig. 46, along with the corresponding acceleration and displacement plots. Raw (unfiltered) signals are shown on the left and signals passed through a ±1 Hz band pass filter are shown on the right. Only the raw data is used to calculate the rotordynamic force coefficients – the filtered data is presented solely for reference to show that the excitation force is truly circular. Note that the centroids of the force and displacement raw data are not located at (0,0) – for the force, this is due to the centering process used and really has no significance; for the displacement, it is simply a matter of how the probes are adjusted (the probes cannot read a negative displacement so they must be adjusted to avoid contact with the rotor). The filtered force plot is clearly circular, which proves the loading method was a success. Figure 47 shows the FFT for the *x*- and *y*-direction force data that compose the rotating load, confirming that the 100 Hz excitation frequency is dominant (approximately).

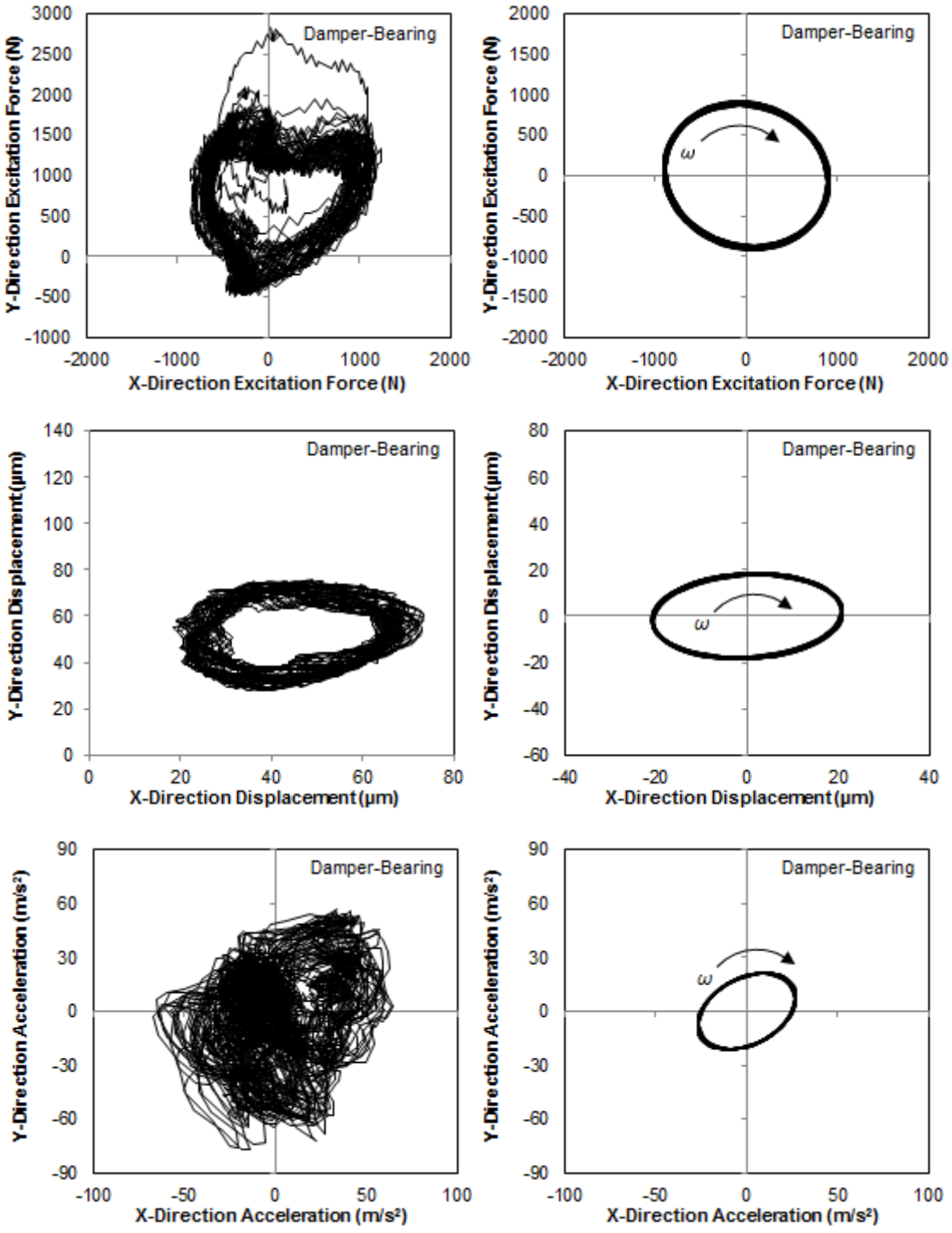

Figure 46. Raw and filtered signals at a sample excitation of 100 Hz and 890 N

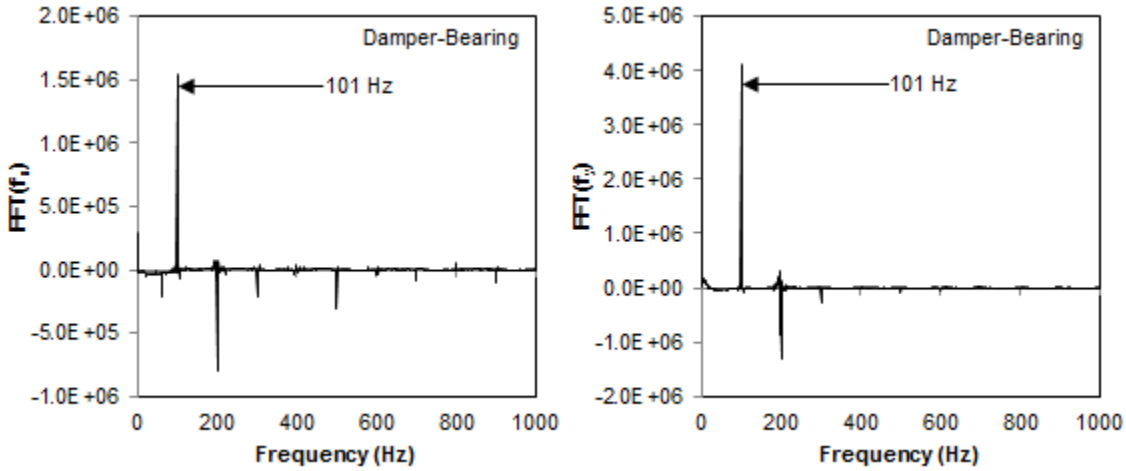

Figure 47. Force frequency spectrum for *x*- (left) and *y*-directions (right) for 100 Hz and 890 N sample excitation

Figure 48 shows sample displacement orbits for the rotating load tests at 100 Hz excitation and filtered using the same ±1 Hz band pass filter as Fig. 46. The bearing clearance, C_B, is not shown for clarity but is provided for reference – at the maximum excitation force of 1557 N the relative rotor-bearing displacement is 20% of the bearing clearance. The figure shows elliptical orbits that increase linearly with increasing excitation amplitude.

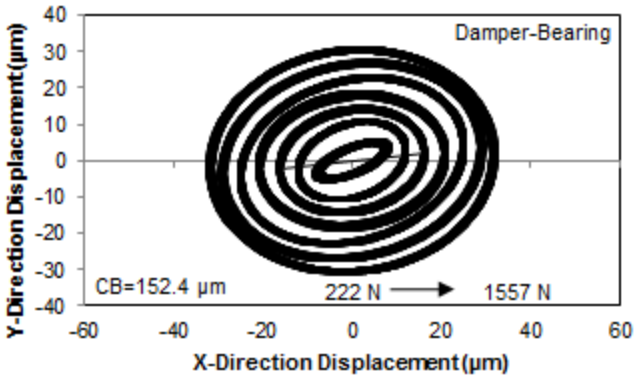

Figure 48. Filtered displacement orbits for multiple excitation forces at 100 Hz

Using a code developed by J. Wilkes (personal communication, May 4, 2011), the data extraction method assumes the elliptic displacements and accelerations of Eqs. (52) and (53), which are used to solve for the rotordynamic coefficients in Eq. (54). The equations in Eq. (54) use the data as-is and do not *necessarily* assume a circular excitation force (rather an ellipse), although this is the result based on the filtered excitation force plot shown in Fig. 47. The equations in Eq. (54) provide four equations for twelve unknowns – at least three frequencies are required to solve for all of the coefficients. For tests where data for more than three frequencies was collected, a least squares approach was used to best approximate the coefficients.

$$\begin{aligned} x(t) &= x_c \cos(\Omega_f t) + x_s \sin(\Omega_f t) \\ y(t) &= y_c \cos(\Omega_f t) + y_s \sin(\Omega_f t) \end{aligned} \tag{52}$$

$$\begin{aligned} a_x(t) &= a_{xc} \cos(\Omega_f t) + a_{xs} \sin(\Omega_f t) \\ a_y(t) &= a_{yc} \cos(\Omega_f t) + a_{ys} \sin(\Omega_f t) \end{aligned} \tag{53}$$

$$\begin{aligned} (K_{xx} - \Omega_i^2 M_{xx}) x_{ci} + (K_{xy} - \Omega_i^2 M_{xy}) y_{ci} + C_{xx}\Omega_i x_{si} + C_{xy}\Omega_i y_{si} &= f_{xc} - M_s a_{xc} \\ (K_{xx} - \Omega_i^2 M_{xx}) x_{si} + (K_{xy} - \Omega_i^2 M_{xy}) y_{si} - C_{xx}\Omega_i x_{ci} - C_{xy}\Omega_i y_{ci} &= f_{xs} - M_s a_{xs} \\ (K_{yy} - \Omega_i^2 M_{yy}) y_{ci} + (K_{yx} - \Omega_i^2 M_{yx}) x_{ci} + C_{yx}\Omega_i x_{si} + C_{yy}\Omega_i y_{si} &= f_{yc} - M_s a_{yc} \\ (K_{yy} - \Omega_i^2 M_{yy}) y_{si} + (K_{yx} - \Omega_i^2 M_{yx}) x_{si} - C_{yx}\Omega_i x_{ci} - C_{yy}\Omega_i y_{ci} &= f_{yc} - M_s a_{yc} \end{aligned} \tag{54}$$

Coefficients are calculated for each of the twenty runs per test condition, from which uncertainties are determined. Similar to the multi-frequency data presented earlier, the coefficient uncertainties are calculated to a 95% confidence interval using Eq. (55), where 1.96 is a statistical parameter corresponding to the confidence interval used, S_{ij} is the standard deviation of the tests for each coefficient, and n_t is the number of tests (20 in this case).

$$\Delta K_{ij} = \frac{1.96 S_{ij}}{\sqrt{n_t}}$$
$$\Delta C_{ij} = \frac{1.96 S_{ij}}{\sqrt{n_t}} \quad (55)$$
$$\Delta M_{ij} = \frac{1.96 S_{ij}}{\sqrt{n_t}}$$

Figure 48 shows all of the rotordynamic coefficients measured using the rotating load excitation and the corresponding multi-frequency excitation results measured previously at 12000 rpm and zero static load. The direct stiffness results for the *x*- and *y*-directions show low orthotropy for the rotating load. These stiffnesses decrease with increasing excitation force and seem to converge to about 30 MN/m. At similar excitation forces, the direct stiffness coefficients are about 30% less for the rotating load method than for the multi-frequency tests. Cross-coupled stiffness coefficients range from low to relatively high (compared with the direct terms) and there is no clear trend with excitation force. Cross-coupled stiffness coefficients vary, but fall within the same range as with the multi-frequency tests. At the highest excitation force, there is a hint that the cross-coupled stiffnesses are converging toward zero, but additional testing at higher excitation forces would be required to confirm this.

Direct damping coefficients do not follow an obvious trend relative to excitation force. At similar excitation forces, the rotating load direct damping coefficients are higher than those found with the rotating load tests – C_{xx} is about 40% higher and C_{yy} is close to 65% higher. Cross-coupled damping coefficients are generally very high relative to the direct terms (in excess of 50% at some excitation amplitudes). While these coefficients initially diverge with increasing excitation force, it is unclear whether this

continues at higher excitation forces or if they have converged to some value. Cross-coupled damping coefficients are three to four times larger for the rotating load than for the multi-frequency results at similar excitation forces.

Direct added mass coefficients increase with excitation force and at similar excitation forces are significantly larger than the multi-frequency results (two to six times larger). This means that at higher frequencies the stiffness is lower for the rotating load method. Cross-coupled added mass coefficients are erratic and do not correspond well with the multi-frequency values at similar excitation amplitude.

As stated above, the direct stiffness and damping coefficients found with the rotating load method are practically equivalent for each direction (low orthotropy) and excitation amplitude. This is in contrast to the coefficients obtained using the multi-frequency excitation which often differ somewhat in each direction. The coefficients of determination for the rotating load stiffness, damping, and added mass coefficients is excellent for all cases and ranges from R^2 = 0.98 to 1.00. Three to six excitation frequencies were used to calculate the rotordynamic coefficients (six at the lower excitation amplitudes, decreasing to three at the higher amplitudes).

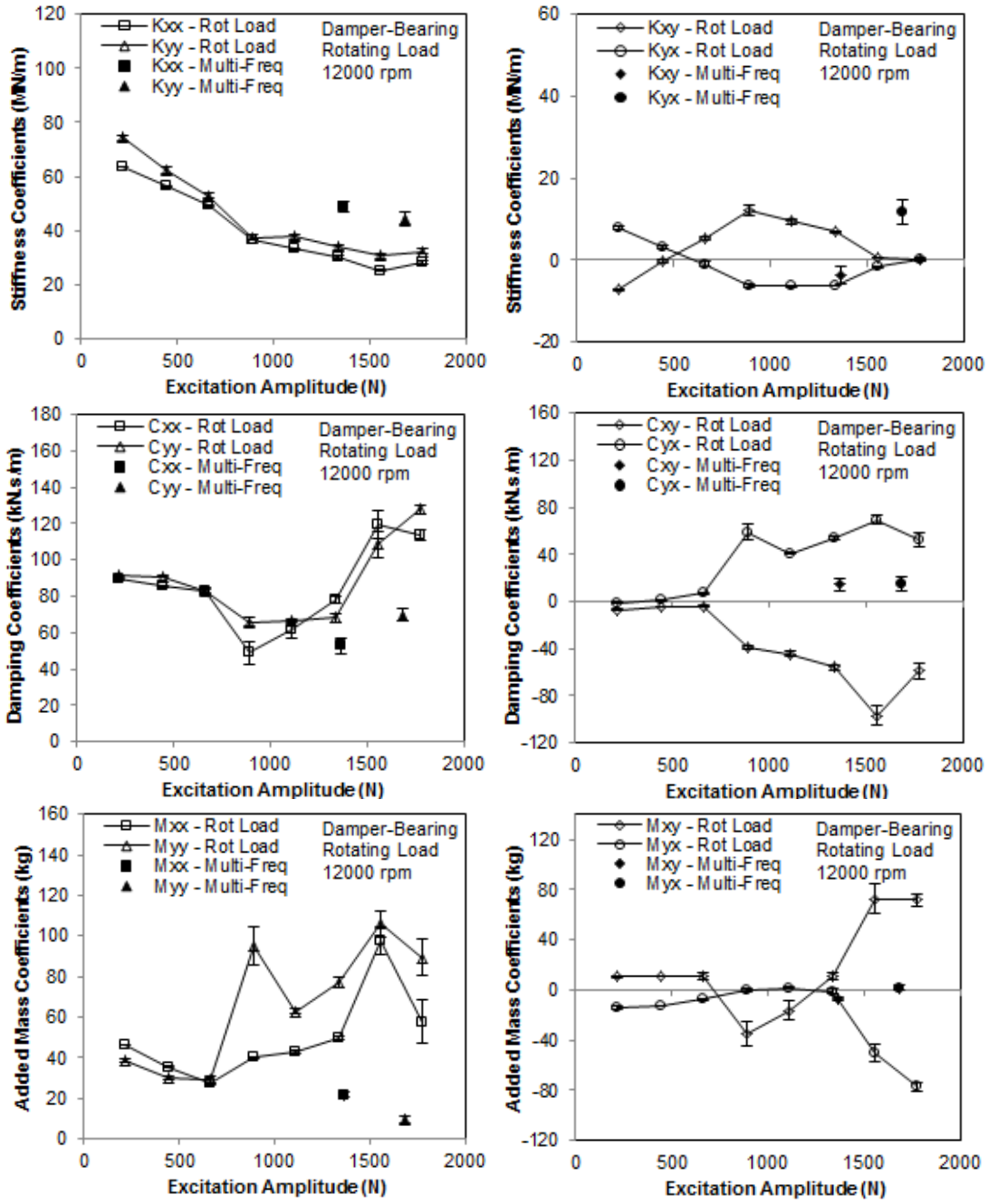

Figure 49. Stiffness, damping, and added mass coefficients at different excitation amplitudes

9. CONCLUSIONS

A four pad flexure-pivot-pad journal bearing in series with both a locked and active ISFD was tested in load-between-pads (LBP) configuration to determine performance characteristics of the bearing, and particularly, the effect of the ISFD on these characteristics. Multiple test conditions (running speed and static load combinations) and two excitation schemes are used to produce data, and compared to predictions from appropriate models. For the FPJB (locked damper configuration), rotordynamic coefficients from a similar bearing measured by another tester are compared on a non-dimensional basis and increase the confidence in the results.

Static tests on both bearing configurations show low cross-coupling, as evidenced by eccentricities that follow the loaded axis relatively well. Eccentricities increase and attitude angles decrease with increasing load, as expected. The added flexibility provided by the ISFD results in a lower stiffness for the damper-bearin (active damper configuration), resulting in larger eccentricities on the order of 2-3 times those measured for the FPJB alone. In fact, the addition of the damper allows eccentricities in excess of the bearing clearance, C_B. Attitude angles are not significantly different between the FPJB and damper-bearing. For the FPJB, the commercial software under-predicted the eccentricity but did an OK job of predicting the attitude angle.

Pad metal temperatures increase linearly with increasing load and running speed. The pad metal temperatures are “flatter” for the damper-bearing than for the FPJB alone, in that the temperatures change less along the circumference of the pads. Squeeze film land metal temperatures recorded for the active damper tests increase linearly with load

and shaft speed, and the temperatures are nearly constant about the circumference of the land. Power consumption for both bearing configurations remain approximately constant with load, and increase almost linearly with increasing running speed. Both bearing configurations consume the same amount of power, except at the lowest running speed of 4000 rpm where the damper-bearing has a reduced power consumption of 1 to 2 kW. The power loss of the FPJB is under-predicted by about 1 to 2 kW, resulting in relatively high errors at low shaft speeds; however, the accuracy increases to produce good predictions at higher shaft speeds.

Although not realized during testing, a different order of testing the different loads and shaft speeds might have provided slightly better results (i.e. eccentricities and rotordynamic coefficients that follow the apparent trends better). Normally, both static and dynamic data were collected at each test condition before changing test conditions; however, after dynamic loading, the bearing did not always return to its precise location about the rotor center, probably due to some residual loads on the shakers (as observed at test rig shut down). Performing all static tests at a given shaft speed and then performing all dynamic tests would likely have proven a better method, and at least should have resulted in better eccentricity trends.

Both the FPJB and damper-bearing configurations were excited using the multi-frequency excitation scheme. For both bearing configurations, the frequency dependency of the real portions of the dynamic stiffnesses were found to be quadratic and of the imaginary portions, linear. This means that the inclusion of added mass coefficients creates *frequency independent* stiffness and damping coefficients.

Rotordynamic coefficients for the FPJB alone (locked damper configuration) indicate an increase in stiffness and damping with increasing static load, and an increase in stiffness and decrease in damping with increasing shaft speed. Cross-coupled stiffnesses remain constant with increased load and diverge slightly with increased running speed. Cross-coupled damping terms remain constant with both increased load and running speed. Trends vary for the added mass coefficients. For the damper-bearing, the measured rotordynamic coefficients change little with increased static loading, although the direct stiffness tends to increase slightly, and the direct damping tends to decrease slightly with increasing shaft speed.

A comparison of the rotordynamic coefficients for the FPJB and damper-bearing results shows that the damping coefficients for the damper-bearing are often close to or even less than the damping coefficients for the FPJB alone. Synchronous-response analysis shows that, although the damping coefficients are on par with each other, the reduced stiffness of the series damper-bearing produces greater *effective* damping. This is clear in the analysis by a significant reduction in vibration amplitude of a simple rotor at both the bearing and rotor mid-span locations.

For the FPJB, the intersections of the real direct stiffnesses are well predicted and the intersections of the cross-coupled stiffnesses are predicted OK. Predictions following [20] show a more linear change in stiffness with excitation frequency than what the experimental results indicate. Since the synchronous damping value is used from predictions as the damping coefficient, the software always yields a linear slope for the imaginary portions of the dynamic stiffnesses; these curve fits are fair to good

depending on the test condition. Although not usually significant, the inclusion of the fluid inertia option in the software [20] provides results overall closer to those obtained experimentally.

Rotating load (single-frequency) tests performed on the damper-bearing force the bearing into whirl about the rotor at prescribed excitation forces and frequencies, and are used to calculate rotordynamic coefficients for comparison with the multi-frequency excitation method at 12000 rpm and zero static load. Rotating load stiffness coefficients are lower, and damping coefficients are higher, than those found with the multi-frequency tests. The rotating load direct stiffness coefficients seem to head toward convergence, but additional data would be required to confirm this. Added mass coefficients increase with excitation force and are much higher than those found with the multi-frequency tests.

Unlike the multi-frequency excitation method where the magnitudes of the direct coefficients sometimes varied slightly between the *x*- and *y*-directions, the coefficients are practically identical with the rotating load excitation, except for the added mass coefficients which vary. The data suggests that the stability of a rotor-bearing system might be significantly different than implied by the multi-frequency excitation method, as evidenced by the difference in rotordynamic coefficients.

REFERENCES

[1] Grey, G.G., Hess, T.D. Jr., Leader, M.E., Whalen, J.K., 1996, "The Design and Application of a Squeeze Film Damper Bearing to a Flexible Steam Turbine Rotor," *Proceedings of the Twenty-Fifth Turbomachinery Symposium*, Turbomachinery Laboratory, Texas A&M University, pp. 49-57.

[2] Edney, S.L., 2003, "Pad Temperature in Tilting Pad Journal Bearings Influenced By Operation High Speed and Light Load," TP104, Dresser-Rand, Wellsville, NY.

[3] Zeidan, F.Y., and Paquette, D.J., 1994, "Application of High Speed and High Performance Fluid Film Bearings in Rotating Machinery," *Proceedings of the Twenty-Third Turbomachinery Symposium*, Turbomachinery Laboratory, Texas A&M University, pp. 209-233.

[4] Szeri, A.Z., 1998, *Fluid Film Lubrication Theory & Design*, Cambridge University Press, New York, NY, Chap. 4.

[5] Zeidan, F.Y., San Andrés, L., and Vance, J.M., 1996, "Design and Application of Squeeze Film Dampers in Rotating Machinery," *Proceedings of the Twenty-Fifth Turbomachinery Symposium*, Turbomachinery Laboratory, Texas A&M University, pp. 169-188.

[6] Al-Ghasem, A.M., 2004, "Measurement of Rotordynamic Coefficients for a High Speed Flexure-Pivot Tilting-Pad Bearing (Load Between Pad) Configuration," M.S. Thesis, Texas A&M University, College Station, TX.

[7] Rodriguez Colmenares, L.E., 2004, "Experimental Frequency-Dependent Rotordynamic Coefficients for a Load-On-Pad, High-Speed, Flexible-Pivot Tilting-Pad Bearing," M.S. Thesis, Texas A&M University, College Station, TX.

[8] San Andrés, L., and De Santiago, O., 2003, "Imbalance Response of a Rotor Supported on Flexure Pivot Tilting Pad Journal Bearings in Series With Integral Squeeze Film Dampers," ASME J. Engr. for Gas Turb. Power, **125**, pp. 1026-1032.

[9] De Santiago, O., and San Andrés, L., 2007, "Field Methods for Identification of Bearing Support Parameters – Part I: Identification From Transient Rotor Dynamic Response due to Impacts," ASME J. Engr. for Gas Turb. Power, **129**, pp. 205-212.

[10] De Santiago, O., and San Andrés, L., 2007, "Field Methods for Identification of Bearing Support Parameters – Part II: Identification From Rotor Dynamic

Response due to Imbalances," ASME J. Engr for Gas Turb. Power, **129**, pp. 213-219.

[11] De Santiago, O., and San Andrés, L., 1999, "Design of a Series Tilting Pad Bearing and Squeeze Film Damper for NSF-TRC Rotordynamic Test Rig and Analysis for Optimum Damping at Bearing Supports," Turbomachinery Research Consortium Annual Report, Texas A&M University, TRC-SFD-1-99, May.

[12] De Santiago, O., and San Andrés, L., 2000, "Measurements of the Imbalance Response in a Rotor Supported on Tilting Pad Bearings and Integral Squeeze Film Dampers," Turbomachinery Research Consortium Annual Report, Texas A&M University, TRC-SFD-1-00, May.

[13] De Santiago, O., and San Andrés, L., 2001, "Parameter Identification of Bearing Supports from Imbalance Response and Impact Excitations," Turbomachinery Research Consortium Annual Report, Texas A&M University, TRC-RD-1-01, May.

[14] Locke, S., and Faller, W., 2003, "Recycle Gas Compressor Designed for High Unbalance Tolerance and Stability," *Proceedings of the Thirty-Second Turbomachinery Symposium*, Turbomachinery Laboratory, Texas A&M University, pp. 137-144.

[15] Kaul, A., 1999, "Design and Development of a Test Setup for the Experimental Determination of the Rotordynamic and Leakage Characteristics of Annular Bushing Oil Seals," M.S. Thesis, Texas A&M University, College Station, TX.

[16] Hibbeler, R.C., 2003, *Mechanics of Materials*, Pearson Education, Inc., Upper Saddle River, NJ.

[17] Rouvas, C., and Childs, D.W., 1993, "A Parameter Identification Method for the Rotordynamic Coefficients of a High Reynolds Number Hydrostatic Bearing," ASME J. Vib. and Acou., **115**, pp. 264-270.

[18] Lund, J., 1967, "A Theoretical Analysis of Whirl Instability and Pneumatic Hammer for a Rigid Rotor in Pressurized Gas Journal Bearings," ASME J. Lubr. Tech., **89**, pp. 154-166.

[19] San Andrés, L., 1991, "Effect of Eccentricity on the Force Response of a Hybrid Bearing, STLE Tribology Transactions, **34**, pp. 537-544.

[20] San Andrés, L., 1995, "Bulk-Flow Analysis of Flexure and Tilting Pad Fluid Film Bearings," Turbomachinery Research Consortium Annual Report, Texas A&M University, TRC-B&C-3-95, May.

[21] Pinkus, O., 1990, *Thermal Aspects of Fluid Film Tribology*, ASME Press, New York, NY.

[22] Allaire, P.E., Barrett, L.E., and Gunter, E.J., 1978, "Optimum Bearing and Support Damping for Unbalance Response and Stability of Rotating Machinery," ASME J. Engr. for Power, **100**, pp. 89-94.

[23] Schaible, A., 2008 (Draft), "Static and Excitation-Amplitude-Dependent Dynamic Parameters of a Tilting Pad Journal Bearing with Ball-in-Socket Pivots in Load-On-Pad Configuration Measured Using Two Excitation Schemes," M.S. Thesis Draft, Texas A&M University, College Station, TX.

APPENDIX

NOTE: All off the dynamic stiffnesses and corresponding rotordynamic coefficients presented in this section already have the baseline data subtracted from them.

Table 3. FPJB measured loci data

EXPERIMENT											
Running Speed (rpm)	Unit Load (kPa)	X_{DE} (μm)	X_{NDE} (μm)	Y_{DE} (μm)	Y_{NDE} (μm)	$e_{x,ave}$ (μm)	$e_{y,ave}$ (μm)	$\varepsilon_{o,x}$ (-)	$\varepsilon_{o,y}$ (-)	ε_{o} (-)	φ (deg)
4000	0	17.0	12.5	-3.2	-3.8	14.8	-3.5	0.10	-0.02	0.10	103.3
4000	172	12.3	9.6	27.6	25.3	11.0	26.4	0.07	0.17	0.19	22.5
4000	345	14.4	10.2	84.1	75.2	12.3	79.6	0.08	0.52	0.53	8.8
4000	517	8.1	4.5	100.7	90.2	6.3	95.5	0.04	0.63	0.63	3.8
4000	689	13.3	9.7	121.8	111.8	11.5	116.8	0.08	0.77	0.77	5.6
6000	0	26.0	17.2	0.1	-3.0	21.6	-1.5	0.14	-0.01	0.14	93.9
6000	172	26.4	18.5	34.9	31.5	22.5	33.2	0.15	0.22	0.26	34.1
6000	345	26.3	13.3	71.3	62.3	19.8	66.8	0.13	0.44	0.46	16.5
6000	517	10.8	1.0	93.1	83.7	5.9	88.4	0.04	0.58	0.58	3.8
6000	689	0.8	-5.3	92.4	86.6	-2.3	89.5	-0.01	0.59	0.59	-1.5
6000	862	-6.3	-6.3	104.0	97.7	-6.3	100.9	-0.04	0.66	0.66	-3.6
8000	0	43.7	31.2	-1.4	7.2	37.4	2.9	0.25	0.02	0.25	85.6
8000	172	48.9	34.6	30.6	37.7	41.7	34.1	0.27	0.22	0.35	50.7
8000	345	49.3	34.3	62.8	69.9	41.8	66.4	0.27	0.44	0.51	32.2
8000	517	22.3	14.3	63.7	70.5	18.3	67.1	0.12	0.44	0.46	15.3
8000	689	15.3	9.2	77.3	84.8	12.2	81.0	0.08	0.53	0.54	8.6
8000	862	22.2	20.8	104.9	110.2	21.5	107.6	0.14	0.71	0.72	11.3
10000	0	40.5	33.2	-1.8	8.4	36.8	3.3	0.24	0.02	0.24	84.9
10000	172	43.0	34.3	21.7	26.7	38.6	24.2	0.25	0.16	0.30	57.9
10000	345	47.8	37.1	52.3	59.8	42.4	56.1	0.28	0.37	0.46	37.1
10000	517	30.4	23.2	73.0	79.9	26.8	76.4	0.18	0.50	0.53	19.3
10000	689	17.1	12.6	70.2	79.4	14.9	74.8	0.10	0.49	0.50	11.2
10000	862	24.4	26.5	91.0	101.1	25.4	96.0	0.17	0.63	0.65	14.8
12000	0	45.6	31.3	-1.3	7.8	38.5	3.3	0.25	0.02	0.25	85.2
12000	172	51.8	43.4	17.7	27.0	47.6	22.4	0.31	0.15	0.35	64.8
12000	345	29.4	20.0	35.7	43.0	24.7	39.3	0.16	0.26	0.30	32.1
12000	517	19.3	14.8	43.0	56.2	17.0	49.6	0.11	0.33	0.34	18.9
12000	689	29.1	27.9	66.1	75.4	28.5	70.8	0.19	0.46	0.50	21.9
12000	862	36.1	38.6	95.9	108.7	37.4	102.3	0.25	0.67	0.71	20.1

Table 4. Damper-bearing measured loci data

EXPERIMENT											
Running Speed (rpm)	Unit Load (kPa)	X_{DE} (μm)	X_{NDE} (μm)	Y_{DE} (μm)	Y_{NDE} (μm)	$e_{x,ave}$ (μm)	$e_{y,ave}$ (μm)	$\varepsilon_{o,x}$ (-)	$\varepsilon_{o,y}$ (-)	ε_{o} (-)	φ (deg)
4000	0	36.6	36.0	25.8	43.9	36.3	34.9	0.24	0.23	0.33	46.2
4000	172	38.9	38.8	88.5	104.4	38.9	96.5	0.26	0.63	0.68	21.9
4000	345	49.4	49.3	139.8	157.0	49.3	148.4	0.32	0.97	1.03	18.4
4000	517	50.8	44.9	190.8	212.1	47.9	201.5	0.31	1.32	1.36	13.4
4000	689	59.6	52.9	236.0	264.1	56.2	250.1	0.37	1.64	1.68	12.7
6000	0	29.1	28.7	24.3	41.6	28.9	33.0	0.19	0.22	0.29	41.2
6000	172	33.9	31.2	73.1	92.3	32.5	82.7	0.21	0.54	0.58	21.5
6000	345	53.1	50.1	124.1	144.3	51.6	134.2	0.34	0.88	0.94	21.0
6000	517	31.9	30.8	158.5	176.0	31.3	167.3	0.21	1.10	1.12	10.6
6000	689	31.2	28.0	197.4	217.6	29.6	207.5	0.19	1.36	1.38	8.1
6000	862	36.7	38.2	236.4	262.0	37.4	249.2	0.25	1.64	1.65	8.5
8000	0	22.4	30.3	18.6	37.1	26.4	27.8	0.17	0.18	0.25	43.5
8000	172	26.6	27.6	67.1	84.2	27.1	75.6	0.18	0.50	0.53	19.7
8000	345	51.6	49.5	124.5	144.4	50.6	134.5	0.33	0.88	0.94	20.6
8000	517	31.0	29.9	145.6	164.7	30.5	155.2	0.20	1.02	1.04	11.1
8000	689	27.1	23.6	188.5	207.3	25.4	197.9	0.17	1.30	1.31	7.3
8000	862	43.3	39.9	246.1	268.2	41.6	257.2	0.27	1.69	1.71	9.2
10000	0	48.0	48.8	30.8	49.2	48.4	40.0	0.32	0.26	0.41	50.4
10000	172	47.9	44.3	72.8	93.4	46.1	83.1	0.30	0.55	0.62	29.0
10000	345	50.5	48.5	116.5	138.5	49.5	127.5	0.32	0.84	0.90	21.2
10000	517	52.0	46.1	155.9	176.8	49.1	166.4	0.32	1.09	1.14	16.4
10000	689	30.2	31.9	182.0	200.9	31.0	191.4	0.20	1.26	1.27	9.2
10000	862	37.7	37.0	228.2	248.8	37.4	238.5	0.25	1.56	1.58	8.9
12000	0	41.5	47.7	29.5	46.3	44.6	37.9	0.29	0.25	0.38	49.6
12000	172	54.1	50.7	72.7	92.9	52.4	82.8	0.34	0.54	0.64	32.3
12000	345	45.9	43.3	108.3	127.2	44.6	117.8	0.29	0.77	0.83	20.7
12000	517	41.8	40.4	145.6	166.0	41.1	155.8	0.27	1.02	1.06	14.8
12000	689	52.4	44.6	194.5	218.6	48.5	206.5	0.32	1.36	1.39	13.2
12000	862	37.2	35.5	218.6	241.6	36.3	230.1	0.24	1.51	1.53	9.0

Table 5. FPJB temperature and power loss data

EXPERIMENT										
Running Speed (rpm)	Unit Load (kPa)	P_{in} (kPa)	T_{in} (°C)	$T_{out,DE}$ (°C)	$T_{out,NDE}$ (°C)	$T_{out,ave}$ (°C)	$T_{in-out,ave}$ (°C)	Flow Rate (L/min)	Sommerfeld Number (-)	Estimated Power Loss (kW)
4000	0	-	33.9	36.1	36.7	36.4	35.1	45.4	-	4.2
4000	172	-	35.6	37.8	38.6	38.2	36.9	45.4	1.23	4.4
4000	345	-	36.9	38.9	39.7	39.3	38.1	45.5	0.59	4.0
4000	517	-	35.7	37.8	38.8	38.3	37.0	46.0	0.41	4.5
4000	689	-	38.3	40.6	41.2	40.9	39.6	46.4	0.28	4.5
6000	0	-	39.4	42.2	43.0	42.6	41.0	45.8	-	5.4
6000	172	-	40.7	43.3	44.2	43.8	42.2	45.5	1.57	5.2
6000	345	-	42.0	45.0	45.9	45.4	43.7	45.9	0.75	5.9
6000	517	-	-	-	-	-	-	-	-	-
6000	689	-	32.7	34.4	35.4	34.9	33.8	45.0	0.51	3.7
6000	862	-	31.4	34.4	34.8	34.6	33.0	45.9	0.41	5.5
8000	0	-	36.1	40.6	41.0	40.8	38.4	45.6	-	8.0
8000	172	-	36.4	40.6	41.6	41.1	38.7	45.4	2.33	7.9
8000	345	-	38.9	41.7	43.6	42.6	40.8	45.6	1.09	6.2
8000	517	-	31.4	33.9	36.1	35.0	33.2	44.3	0.91	5.8
8000	689	-	30.2	35.0	37.5	36.3	33.2	45.2	0.69	10.1
8000	862	-	34.1	37.8	40.3	39.0	36.6	45.7	0.50	8.3
10000	0	-	38.5	44.4	45.1	44.8	41.6	45.9	-	10.8
10000	172	-	41.4	47.2	48.3	47.8	44.6	45.0	2.44	10.6
10000	345	-	43.4	50.3	48.9	49.6	46.5	45.6	1.15	10.5
10000	517	-	-	-	-	-	-	-	-	-
10000	689	-	31.5	36.1	38.8	37.5	34.5	44.6	0.83	9.9
10000	862	-	35.7	41.1	44.1	42.6	39.1	45.2	0.57	11.7
12000	0	-	39.6	47.8	48.3	48.0	43.8	45.2	-	14.3
12000	172	-	43.9	51.7	52.1	51.9	47.9	45.6	2.65	13.6
12000	345	-	-	-	-	-	-	-	-	-
12000	517	-	31.9	37.8	39.9	38.8	35.4	44.6	1.29	11.5
12000	689	-	36.5	44.4	46.6	45.5	41.0	45.0	0.81	15.2
12000	862	-	40.9	48.3	50.3	49.3	45.1	45.2	0.58	14.3

Table 6. Damper-bearing measured temperature and power loss data

EXPERIMENT										
Running Speed (rpm)	Unit Load (kPa)	P_{in} (kPa)	T_{in} (°C)	$T_{out,DE}$ (°C)	$T_{out,NDE}$ (°C)	$T_{out,ave}$ (°C)	$T_{in-out,ave}$ (°C)	Flow Rate (L/min)	Sommerfeld Number (-)	Estimated Power Loss (kW)
4000	0	162.3	35.6	37.2	37.1	37.2	36.4	45.3	-	2.7
4000	172	165.0	35.0	36.1	36.7	36.4	35.7	45.3	1.27	2.3
4000	345	155.8	40.6	41.7	41.7	41.7	41.1	45.7	0.54	1.9
4000	517	175.5	40.0	40.6	40.4	40.5	40.3	46.6	0.37	0.9
4000	689	160.0	41.7	42.2	42.3	42.3	42.0	45.9	0.26	1.0
6000	0	172.5	32.2	35.0	35.1	35.1	33.6	45.6	-	4.8
6000	172	167.1	30.6	33.3	33.2	33.3	31.9	43.6	2.14	4.4
6000	345	176.7	43.3	44.4	45.1	44.8	44.0	47.9	0.74	2.5
6000	517	182.4	32.8	33.3	33.7	33.5	33.2	45.4	0.69	1.3
6000	689	172.0	31.7	32.8	33.7	33.3	32.5	44.8	0.53	2.6
6000	862	171.6	34.4	39.4	37.7	38.6	36.5	46.3	0.37	7.1
8000	0	172.6	37.2	41.1	41.2	41.2	39.2	44.7	-	6.6
8000	172	184.1	31.7	33.9	33.2	33.5	32.6	43.8	2.80	3.0
8000	345	149.7	44.4	47.2	48.4	47.8	46.1	45.5	0.93	5.8
8000	517	189.8	32.2	36.1	37.6	36.8	34.5	46.5	0.88	8.0
8000	689	181.9	30.6	33.3	34.7	34.0	32.3	45.3	0.71	5.8
8000	862	-	40.0	43.3	45.6	44.4	42.2	47.0	0.42	7.8
10000	0	143.8	42.8	46.7	46.9	46.8	44.8	45.1	-	6.8
10000	172	168.5	40.0	42.2	43.6	42.9	41.4	45.5	2.68	4.9
10000	345	150.3	41.1	46.7	48.0	47.3	44.2	45.7	1.23	10.7
10000	517	156.7	44.4	48.9	50.7	49.8	47.1	47.1	0.75	9.4
10000	689	168.4	31.7	37.2	40.1	38.6	35.2	45.8	0.81	11.9
10000	862	149.7	-	-	-	-	-	46.0	-	-
12000	0	156.5	41.7	48.9	49.4	49.2	45.4	45.5	-	12.8
12000	172	151.2	43.3	51.7	52.1	51.9	47.6	45.8	2.67	14.7
12000	345	-	-	-	-	-	-	-	-	-
12000	517	161.4	40.0	46.7	48.1	47.4	43.7	46.3	1.00	12.8
12000	689	163.6	41.7	48.3	50.1	49.2	45.4	46.6	0.71	13.2
12000	862	158.0	35.0	41.7	43.3	42.5	38.8	45.4	0.70	12.7

Table 7. FPJB measured pad metal temperatures

EXPERIMENT		Pad Metal Temperatures (°C)													
		Pad 1		Pad 2		Pad 3					Pad 4				
Thermocouple Number:		1	2	3	4	5	6	7	8	9	10	11	12	13	14
Thermcouple Location (deg):		14	45	52	62	76	104	135	142	153	167	193	243	284	333
Running Speed (rpm)	Unit Load (kPa)														
4000	0	36.7	38.5	39.3	40.1	39.8	37.0	39.8	41.2	40.7	40.2	36.7	40.1	36.8	40.5
4000	172	38.6	41.0	42.1	43.2	42.7	38.8	42.5	44.3	43.9	43.4	38.1	40.6	38.3	40.9
4000	345	40.2	43.4	44.9	46.3	45.4	40.4	45.3	47.6	47.1	46.3	39.5	41.1	39.5	41.2
4000	517	39.4	43.9	46.0	47.9	46.4	39.6	46.4	48.8	48.7	47.6	38.3	39.8	38.2	39.9
4000	689	42.1	47.2	49.5	51.6	49.7	42.7	51.0	53.4	53.2	51.6	41.3	42.3	40.8	42.2
6000	0	42.3	44.7	45.8	46.9	46.6	42.6	46.3	47.7	47.4	47.0	42.4	46.6	42.4	47.1
6000	172	43.8	47.0	48.4	49.9	49.4	44.3	48.6	50.3	50.6	50.2	43.4	47.0	43.4	47.3
6000	345	45.4	49.2	51.0	52.9	52.1	45.9	51.3	53.5	53.7	53.0	44.7	47.4	44.6	47.5
6000	517	38.7	44.9	47.5	50.2	48.4	39.1	48.1	50.9	51.6	50.5	37.0	40.5	37.1	40.6
6000	689	36.8	44.5	48.0	51.4	48.8	36.7	49.5	52.7	53.9	52.0	34.0	37.6	34.3	38.0
6000	862	36.3	45.2	49.3	53.1	49.8	36.5	51.1	54.0	55.9	53.3	33.2	36.5	33.3	36.7
8000	0	41.7	45.3	46.9	48.5	48.1	42.1	47.5	48.6	49.4	49.0	41.9	48.2	41.9	49.4
8000	172	44.8	48.9	50.8	52.7	52.2	45.1	51.3	52.6	53.4	53.0	44.4	49.3	44.4	49.9
8000	345	47.4	52.1	54.3	56.6	55.8	47.8	54.9	56.2	57.3	56.6	46.8	50.8	46.7	51.0
8000	517	35.5	42.9	46.4	50.1	47.9	35.4	49.4	52.2	53.9	52.0	31.8	37.1	32.3	38.2
8000	689	35.9	44.8	49.1	53.4	50.5	36.1	52.2	55.4	57.8	55.3	31.8	36.5	32.1	37.6
8000	862	40.4	49.4	53.7	58.0	54.9	40.6	56.2	59.2	61.5	58.9	37.2	41.4	37.3	41.4
10000	0	42.1	47.1	49.2	51.6	51.0	42.7	49.8	51.2	52.5	52.1	42.4	50.9	42.3	52.1
10000	172	45.4	50.6	52.9	55.4	54.8	45.6	52.8	54.4	55.9	55.4	45.1	51.9	45.0	52.7
10000	345	47.4	52.9	55.4	58.2	57.5	47.5	55.3	57.1	58.6	58.0	46.8	52.5	46.7	52.9
10000	517	40.7	48.1	51.5	55.2	53.4	40.4	52.3	55.3	57.7	56.4	38.1	44.2	38.3	44.9
10000	689	37.7	47.4	52.4	57.7	54.8	37.7	56.3	61.0	63.9	60.7	32.6	38.7	33.0	39.7
10000	862	42.2	51.6	56.2	61.0	58.0	41.9	58.6	62.9	65.4	62.6	38.6	43.9	38.6	43.9
12000	0	43.3	49.0	51.6	54.4	53.8	43.9	51.6	54.0	55.2	54.6	44.3	54.5	43.6	54.8
12000	172	47.6	53.6	56.2	59.1	58.6	47.9	56.3	58.1	59.5	59.4	48.3	57.2	47.5	56.8
12000	345	-	-	-	-	-	-	-	-	-	-	-	-	-	-
12000	517	37.0	45.7	50.1	55.4	53.4	36.6	54.8	59.1	61.7	59.4	32.6	40.0	33.2	41.6
12000	689	43.5	52.2	56.5	61.3	59.3	42.7	57.4	61.9	64.9	63.2	40.3	47.9	40.2	48.2
12000	862	47.4	56.1	60.2	64.9	63.2	47.7	61.3	65.1	67.6	65.8	46.2	52.9	45.5	52.0

Table 8. Damper-bearing measured pad metal temperatures

EXPERIMENT		Pad Metal Temperatures (°C)													
		Pad 1		Pad 2		Pad 3					Pad 4				
Thermocouple Number:		1	2	3	4	5	6	7	8	9	10	11	12	13	14
Thermcouple Location (deg):		14	45	52	62	76	104	135	142	153	167	193	243	284	333
Running Speed (rpm)	Unit Load (kPa)														
4000	0	38.3	38.4	39.1	39.7	39.7	37.2	40.8	39.2	39.8	39.5	37.8	40.0	38.9	40.0
4000	172	38.3	38.8	39.7	40.6	40.6	36.9	41.6	40.1	41.1	40.7	37.2	38.9	37.8	38.3
4000	345	43.3	44.0	45.0	46.1	46.0	42.1	47.3	46.2	47.3	46.9	42.2	43.3	42.8	42.8
4000	517	42.8	43.9	45.3	46.7	46.6	41.4	48.0	47.2	48.8	48.2	41.1	42.2	41.7	41.7
4000	689	44.4	46.2	47.8	49.6	49.3	43.7	51.2	50.7	52.7	51.8	43.3	43.3	43.3	42.8
6000	0	35.6	37.0	38.3	39.7	39.8	34.5	39.6	38.5	39.9	39.5	35.0	40.0	35.6	40.0
6000	172	34.4	36.7	38.3	40.0	40.0	33.2	39.5	38.6	40.4	40.1	32.8	37.2	33.9	37.2
6000	345	45.6	47.5	48.9	50.3	50.4	44.9	50.7	50.0	51.5	51.1	44.4	46.7	45.6	46.1
6000	517	35.6	39.3	41.2	43.5	43.3	34.8	43.5	43.4	45.8	45.4	33.3	36.7	34.4	36.1
6000	689	36.1	37.9	40.4	43.3	43.3	33.1	43.0	43.5	46.6	46.1	33.3	36.7	34.4	35.0
6000	862	38.9	42.4	45.1	48.4	48.2	37.4	48.0	48.6	52.2	51.4	36.1	38.3	36.7	37.8
8000	0	40.6	42.3	43.7	45.3	45.5	39.6	45.0	44.0	45.5	45.3	40.0	45.6	41.1	45.6
8000	172	36.1	38.2	40.0	42.1	42.0	33.6	41.0	40.5	42.6	42.1	33.3	39.4	35.0	39.4
8000	345	47.2	49.7	51.4	53.4	53.7	46.4	52.9	52.4	54.2	54.0	46.1	50.0	47.2	48.9
8000	517	33.9	37.9	40.3	43.2	43.1	32.1	42.0	42.4	45.6	45.1	31.1	35.6	31.7	35.0
8000	689	35.6	39.8	42.5	45.9	45.8	34.0	44.5	45.3	48.9	48.5	32.2	36.1	32.8	35.6
8000	862	45.0	48.5	51.2	54.7	54.5	43.4	53.5	54.2	57.7	57.1	42.8	45.6	43.3	44.4
10000	0	47.8	50.8	52.3	54.1	54.4	47.5	53.5	52.9	54.3	54.1	45.6	52.2	46.7	53.3
10000	172	44.4	50.0	51.8	54.0	54.0	45.5	52.9	52.4	54.1	53.8	41.7	48.3	42.8	49.4
10000	345	46.1	49.0	51.1	53.8	54.3	44.4	52.1	51.9	54.1	54.0	44.4	49.4	45.6	49.4
10000	517	48.3	51.9	54.1	57.0	57.5	47.1	55.2	55.2	57.7	57.5	47.2	52.2	47.8	51.1
10000	689	37.2	41.8	44.9	49.0	49.4	35.3	46.3	47.5	51.9	52.1	33.3	39.4	33.9	38.3
10000	862	42.8	47.1	50.3	54.6	54.8	40.5	52.0	53.2	57.6	57.5	40.0	45.6	40.6	43.3
12000	0	46.1	49.2	51.1	53.5	53.9	45.1	52.1	51.8	53.7	53.6	45.6	53.3	46.1	53.3
12000	172	47.8	51.5	53.6	56.3	56.9	46.5	54.4	54.3	56.5	56.4	47.2	55.6	48.3	55.0
12000	345	43.3	47.3	49.7	53.1	53.8	41.4	50.3	50.4	53.3	53.5	41.1	48.9	42.2	48.3
12000	517	45.0	49.1	51.7	55.3	55.8	43.3	52.5	52.8	55.9	55.9	43.3	50.0	43.9	48.9
12000	689	47.2	51.6	54.3	58.1	58.8	45.5	55.4	55.9	59.2	59.0	45.6	51.7	46.1	50.0
12000	862	41.1	46.1	49.7	54.7	55.3	38.6	51.2	53.1	58.1	58.5	37.2	43.9	37.8	42.2

Table 9. Damper-bearing squeeze film land metal temperatures

EXPERIMENT		Squeeze Film Land Metal Temperatures (°C)								
		Non-Drive End (NDE)					Drive End (DE)			
Thermocouple Number:		15	16	17	18		19	20	21	22
Thermcouple Location (deg):		33	147	213	327		33	147	213	327
Running Speed (rpm)	Unit Load (kPa)									
4000	0	36.2	38.3	36.7	36.9		36.3	36.2	36.0	36.3
4000	172	35.6	37.9	35.6	35.8		35.7	35.8	35.0	35.4
4000	345	41.4	43.6	41.1	41.1		41.2	41.5	40.9	41.0
4000	517	40.4	42.8	40.0	40.1		40.3	40.6	39.8	39.9
4000	689	42.4	45.1	42.2	41.9		42.3	42.8	41.8	41.9
6000	0	32.9	35.2	32.8	33.6		33.0	33.2	32.8	33.3
6000	172	31.7	34.2	31.7	31.8		31.7	32.1	31.3	31.6
6000	345	43.9	46.1	43.3	43.5		43.8	43.9	43.4	43.6
6000	517	34.4	37.6	33.3	33.6		34.4	35.5	34.5	34.1
6000	689	31.3	34.3	31.7	31.1		31.2	32.4	30.8	30.4
6000	862	35.2	37.9	35.0	34.4		35.2	35.6	34.5	34.4
8000	0	38.2	40.3	38.3	38.8		38.1	38.2	37.9	38.2
8000	172	33.0	35.8	32.8	32.8		33.1	33.8	33.0	32.9
8000	345	45.2	47.3	45.0	44.4		45.0	45.3	44.8	44.7
8000	517	31.7	34.6	31.1	36.2		31.6	32.8	31.6	31.0
8000	689	32.3	35.1	31.7	31.2		32.3	33.1	31.7	31.3
8000	862	41.5	44.2	41.1	40.7		41.4	41.8	41.1	40.6
10000	0	46.3	48.5	45.0	46.1		46.2	46.2	46.1	46.2
10000	172	45.8	48.4	42.2	43.5		45.6	46.0	46.0	45.7
10000	345	42.8	45.3	42.8	42.7		42.7	42.8	42.6	42.4
10000	517	45.6	47.8	45.6	45.0		45.4	45.9	45.5	44.9
10000	689	33.2	35.9	32.2	32.1		33.1	33.9	32.7	32.0
10000	862	38.2	41.0	38.3	37.7		38.1	38.9	38.2	37.2
12000	0	43.7	45.9	43.3	43.6		43.7	43.9	43.7	43.5
12000	172	44.9	47.3	45.0	45.2		44.8	45.3	45.0	44.6
12000	345	40.0	42.6	39.4	39.7		40.0	40.5	40.1	39.7
12000	517	41.5	43.6	41.1	41.0		41.3	41.7	41.5	40.8
12000	689	43.4	45.7	43.3	42.2		43.2	43.9	43.7	42.6
12000	862	36.3	39.1	36.1	35.4		36.2	37.1	36.5	35.2

Table 10. FPJB measured stiffness coefficients summary

EXPERIMENT		*Rotordynamic Coefficients*				*Uncertainties*			
		Stiffness (MN/m)				Stiffness (MN/m)			
Running Speed (rpm)	Unit Load (kPa)	Kxx	Kxy	Kyx	Kyy	ΔKxx	ΔKxy	ΔKyx	ΔKyy
4000	0	26.0	3.0	11.6	28.0	3.1	1.3	2.0	2.1
4000	172	30.2	3.3	13.3	31.4	5.2	1.2	3.2	5.8
4000	345	39.2	4.1	14.3	43.5	4.4	1.7	4.2	9.2
4000	517	57.7	6.5	13.7	72.4	1.4	1.7	3.2	10.3
4000	689	69.5	14.2	19.5	94.4	2.1	2.2	2.4	8.1
4000	862	-	-	-	-	-	-	-	-
6000	0	31.3	2.7	13.3	38.2	6.7	1.8	1.0	2.6
6000	172	39.8	2.5	14.3	43.2	4.6	1.6	2.0	4.7
6000	345	48.5	4.5	14.3	50.6	6.2	1.6	2.8	9.4
6000	517	62.0	6.9	14.3	76.6	1.7	2.6	2.8	8.8
6000	689	78.4	7.8	14.1	101.9	1.6	3.3	4.0	8.1
6000	862	95.2	6.6	12.0	136.9	1.2	3.0	2.8	7.9
8000	0	47.1	2.2	18.6	54.3	2.0	1.2	1.4	1.3
8000	172	49.4	1.2	16.1	56.3	3.3	1.1	1.6	5.8
8000	345	52.1	2.5	14.4	63.0	6.5	1.9	2.8	9.2
8000	517	-	-	-	-	-	-	-	-
8000	689	91.4	5.9	15.3	107.6	6.0	3.4	4.1	8.7
8000	862	94.6	4.9	19.4	128.8	4.9	3.6	3.7	9.2
10000	0	58.0	-1.6	20.1	65.5	2.7	1.6	2.7	2.3
10000	172	65.2	-2.6	20.2	68.6	9.6	1.2	2.3	5.5
10000	345	65.1	-2.8	19.3	69.0	3.9	0.9	1.9	8.7
10000	517	78.2	0.4	21.0	88.9	5.8	2.5	2.9	8.4
10000	689	100.4	5.1	23.6	117.3	11.4	4.0	4.3	9.5
10000	862	100.7	2.3	22.3	124.4	4.9	3.8	2.8	9.2
12000	0	74.7	1.1	18.5	75.1	17.6	9.1	2.0	3.2
12000	172	74.6	-7.0	19.7	82.6	4.5	1.3	2.2	7.6
12000	345	75.9	1.3	24.9	87.1	4.6	3.1	4.4	8.4
12000	517	89.2	1.2	25.3	99.7	4.6	3.0	3.9	10.1
12000	689	97.2	-4.6	24.2	108.9	3.3	2.9	4.0	12.3
12000	862	103.5	-4.5	30.0	123.6	3.5	5.4	6.1	8.6

Table 11. FPJB measured damping coefficients summary

EXPERIMENT		*Rotordynamic Coefficients*				*Uncertainties*			
		Damping (kN.s/m)				Damping (kN.s/m)			
Running Speed (rpm)	Unit Load (kPa)	Cxx	Cxy	Cyx	Cyy	ΔCxx	ΔCxy	ΔCyx	ΔCyy
4000	0	110.8	10.3	24.1	129.8	6.6	2.6	2.7	3.6
4000	172	89.0	12.7	20.7	117.3	12.2	3.0	3.1	8.8
4000	345	109.3	12.5	17.0	151.5	10.2	4.2	5.2	13.2
4000	517	115.6	3.2	8.0	159.6	7.2	4.2	2.8	15.9
4000	689	97.8	7.1	8.6	148.8	8.6	4.3	3.7	18.7
4000	862	-	-	-	-	-	-	-	-
6000	0	79.0	0.0	25.2	104.3	6.3	1.2	6.1	4.2
6000	172	64.1	-1.3	20.0	95.7	11.2	2.4	4.5	6.5
6000	345	70.7	3.7	21.9	98.5	7.8	2.0	3.5	10.2
6000	517	106.2	4.7	17.0	133.5	4.1	4.0	2.9	12.5
6000	689	105.8	0.8	13.0	144.1	5.5	4.9	3.6	17.9
6000	862	110.8	-3.5	8.3	153.9	4.4	6.7	3.3	16.5
8000	0	70.1	-6.6	25.3	100.2	10.5	4.9	8.6	2.1
8000	172	67.1	-1.8	18.5	85.8	8.3	1.9	3.3	7.9
8000	345	68.4	-0.1	17.8	87.8	7.6	0.9	3.7	9.3
8000	517	-	-	-	-	-	-	-	-
8000	689	95.1	-6.6	23.1	135.9	7.7	2.8	5.2	15.6
8000	862	89.6	-6.6	16.6	127.4	5.3	2.0	4.4	20.2
10000	0	72.5	0.6	8.0	90.9	8.7	4.1	5.0	6.5
10000	172	52.2	-11.2	16.0	80.8	14.1	7.7	4.8	6.1
10000	345	65.5	1.8	13.4	80.8	4.9	2.2	5.3	11.2
10000	517	83.1	-1.1	17.1	103.6	6.6	2.7	6.6	12.9
10000	689	87.0	-6.5	25.2	120.8	13.6	2.6	9.3	17.9
10000	862	88.5	-2.6	11.3	110.5	10.3	5.4	5.3	13.1
12000	0	34.9	-6.9	27.9	93.8	21.9	11.9	7.3	5.5
12000	172	53.3	-5.8	6.9	81.1	9.7	9.6	4.1	8.7
12000	345	93.5	2.2	8.7	110.1	10.0	3.2	6.6	22.5
12000	517	89.0	-0.4	12.1	126.0	9.2	2.2	6.6	27.6
12000	689	76.7	5.2	8.7	114.8	5.4	3.6	6.8	24.7
12000	862	84.6	-17.7	-9.1	122.9	9.4	6.3	10.9	13.4

Table 12. FPJB measured added mass coefficients summary

EXPERIMENT		*Rotordynamic Coefficients*				*Uncertainties*			
		Added Mass (kg)				Added Mass (kg)			
Running Speed (rpm)	Unit Load (kPa)	Mxx	Mxy	Myx	Myy	ΔMxx	ΔMxy	ΔMyx	ΔMyy
4000	0	31.2	3.8	-4.5	33.5	3.9	1.6	2.5	2.6
4000	172	30.0	0.3	-5.8	28.4	4.1	1.0	2.5	4.6
4000	345	21.6	-4.0	-11.4	22.3	4.5	1.7	4.3	9.4
4000	517	10.4	-4.8	-11.4	14.8	1.1	1.3	2.4	7.9
4000	689	5.3	-0.8	-4.8	11.6	1.5	1.5	1.7	5.8
4000	862	-	-	-	-	-	-	-	-
6000	0	25.2	4.0	1.8	37.3	7.3	2.0	1.1	2.8
6000	172	33.6	0.6	-2.3	33.4	3.8	1.3	1.6	3.9
6000	345	34.0	0.3	-5.0	31.4	4.6	1.2	2.1	6.9
6000	517	19.6	-2.2	-10.6	26.6	1.1	1.6	1.7	5.6
6000	689	18.9	-3.0	-11.0	24.2	1.0	2.0	2.4	4.9
6000	862	19.7	-5.0	-14.4	29.7	0.8	2.1	1.9	5.3
8000	0	25.5	-3.4	4.4	30.8	2.2	1.2	1.5	1.4
8000	172	33.9	-3.2	0.9	34.2	2.9	1.0	1.4	5.2
8000	345	29.8	-3.1	-3.1	33.8	4.8	1.4	2.0	6.8
8000	517	-	-	-	-	-	-	-	-
8000	689	41.9	-6.6	-10.4	27.9	4.2	2.4	2.9	6.2
8000	862	36.2	-7.9	-8.0	33.9	4.0	2.9	3.1	7.6
10000	0	31.8	-2.3	7.5	35.0	3.8	2.2	3.7	3.2
10000	172	46.5	-5.2	4.1	33.0	6.7	0.8	1.6	3.9
10000	345	35.4	-5.2	-0.1	28.7	3.7	0.8	1.8	8.2
10000	517	36.0	-9.2	-3.2	27.4	5.1	2.2	2.5	7.4
10000	689	47.6	-10.0	-2.6	28.7	7.4	2.6	2.8	6.1
10000	862	37.6	-9.7	-6.6	31.4	4.4	3.4	2.5	8.2
12000	0	37.5	11.1	-3.0	19.3	10.4	5.4	1.2	1.9
12000	172	35.2	-6.4	0.8	35.4	4.2	1.2	2.0	7.0
12000	345	26.2	-5.3	0.4	21.2	5.1	3.4	4.8	9.1
12000	517	29.4	-11.4	-2.5	18.1	4.6	3.0	3.9	10.1
12000	689	32.9	-10.6	-4.8	27.5	3.1	2.8	3.9	11.9
12000	862	35.9	-12.0	-3.8	31.7	3.2	4.9	5.6	7.9

Table 13. FPJB predicted static and dynamic data

PREDICTIONS																		
Running Speed (rpm)	Unit Load (kPa)	K_{xx} (MN/m)	K_{xy} (MN/m)	K_{yx} (MN/m)	K_{yy} (MN/m)	C_{xx} (kN.s/m)	C_{xy} (kN.s/m)	C_{yx} (kN.s/m)	C_{yy} (kN.s/m)	M_{xx} (kg)	M_{xy} (kg)	M_{yx} (kg)	M_{yy} (kg)	$\varepsilon_{o,x}$ (-)	$\varepsilon_{o,y}$ (-)	Power Loss (kW)	Somm. No. (-)	Re (-)
4000	0	29.6	-9.8	9.8	29.6	91.8	10.9	-10.9	91.8	14.7	-1.8	1.8	14.7	0.000	0.000	1.62	-	58.3
4000	172	33.6	2.7	15.2	28.9	84.8	31.2	17.7	89.6	14.3	2.5	5.0	13.4	0.056	0.187	1.69	0.75	63.8
4000	345	57.6	6.2	16.1	53.9	127.0	29.1	19.1	130.2	20.1	2.9	5.1	19.3	0.041	0.362	1.82	0.37	75.3
4000	517	86.4	9.0	17.8	83.3	173.0	28.5	20.1	175.3	25.6	3.2	5.2	24.8	0.032	0.461	1.95	0.25	81.9
4000	689	118.8	11.5	19.6	116.0	220.8	28.4	20.9	222.5	30.7	3.4	5.3	30.0	0.028	0.530	2.07	0.19	86.8
6000	0	43.5	-10.0	10.0	43.5	86.4	7.0	-7.0	86.4	18.3	-2.2	2.2	18.3	0.000	0.000	3.49	-	91.5
6000	172	39.6	5.7	20.4	34.1	69.8	29.1	18.9	73.2	15.4	3.2	6.5	14.2	0.063	0.094	3.61	1.12	92.6
6000	345	58.5	6.3	18.9	53.3	94.0	26.0	17.5	97.5	19.8	3.0	5.9	18.7	0.044	0.262	3.74	0.56	106.4
6000	517	82.8	8.0	19.1	78.1	122.4	24.6	17.3	125.4	24.4	3.1	5.7	23.3	0.035	0.369	3.92	0.37	117.3
6000	689	110.4	9.8	19.9	106.1	152.6	23.8	17.3	155.1	28.8	3.2	5.6	27.8	0.030	0.442	4.09	0.28	124.9
6000	862	140.3	11.7	21.1	136.3	183.8	23.4	17.5	186.0	33.1	3.3	5.6	32.1	0.027	0.497	4.25	0.22	130.7
8000	0	56.2	-10.1	10.1	56.2	82.8	4.8	-4.8	82.8	21.0	-2.4	2.4	21.0	0.000	0.000	5.99	-	126.5
8000	172	45.7	9.2	26.1	41.3	64.9	28.3	20.3	65.1	16.3	3.8	7.9	15.3	0.076	0.037	6.19	1.49	125.8
8000	345	62.2	8.9	23.1	56.1	78.7	24.8	18.1	81.4	19.7	3.3	6.8	18.3	0.050	0.192	6.29	0.75	136.2
8000	517	83.1	9.0	22.0	77.2	98.2	23.0	16.9	100.9	23.2	3.1	6.3	21.8	0.038	0.300	6.48	0.50	151.2
8000	689	107.6	9.9	22.0	102.0	119.7	22.0	16.4	122.2	26.8	3.0	6.0	25.5	0.032	0.377	6.68	0.37	162.1
8000	862	134.2	10.9	22.2	128.9	142.0	21.1	15.9	144.4	30.3	3.0	5.8	29.0	0.029	0.435	6.89	0.30	170.3
10000	0	68.0	-10.1	10.1	68.0	80.0	3.4	-3.4	80.0	22.6	-2.5	2.5	22.6	0.000	0.000	9.04	-	163.3
10000	172	71.3	-10.1	10.8	71.7	82.4	4.2	-2.9	82.3	23.0	-2.5	2.7	23.0	0.014	0.095	9.08	1.87	169.5
10000	345	66.8	12.7	27.8	60.7	70.2	24.2	19.2	72.1	19.6	3.9	7.6	18.1	0.058	0.141	9.44	0.93	165.8
10000	517	85.5	11.6	25.9	79.0	84.4	22.1	17.4	86.6	22.3	3.3	6.9	20.7	0.043	0.246	9.61	0.62	184.3
10000	689	107.5	11.2	24.8	100.9	100.4	20.8	16.4	102.6	25.1	3.1	6.4	23.5	0.034	0.325	9.81	0.47	198.6
10000	862	131.8	11.7	24.6	125.4	117.5	20.0	15.7	119.7	27.9	2.9	6.1	26.3	0.031	0.385	10.06	0.37	209.2
12000	0	79.1	-10.1	10.1	79.1	77.7	2.4	-2.4	77.7	23.4	-2.6	2.6	23.4	0.000	0.000	12.61	-	201.7
12000	172	81.9	-10.1	10.6	82.2	79.4	2.8	-2.0	79.3	23.6	-2.6	2.7	23.7	0.011	0.083	12.65	2.24	207.8
12000	345	71.9	17.1	32.7	66.0	64.7	24.0	20.4	65.9	19.4	4.3	8.3	17.9	0.068	0.101	13.18	1.12	198.5
12000	517	88.9	15.2	30.2	82.1	75.6	21.7	18.3	77.1	21.4	3.7	7.5	19.7	0.049	0.203	13.30	0.75	217.1
12000	689	108.9	13.9	28.6	101.8	88.0	20.2	16.9	89.7	23.5	3.2	6.9	21.8	0.038	0.282	13.48	0.56	234.3
12000	862	131.4	13.5	27.8	124.2	101.6	19.2	16.0	103.3	25.8	2.9	6.5	24.0	0.033	0.344	13.71	0.45	247.9

Table 14. Damper-bearing measured stiffness coefficients summary

EXPERIMENT		*Rotordynamic Coefficients*				*Uncertainties*			
		Stiffness (MN/m)				Stiffness (MN/m)			
Running Speed (rpm)	Unit Load (kPa)	Kxx	Kxy	Kyx	Kyy	ΔKxx	ΔKxy	ΔKyx	ΔKyy
4000	0	24.0	1.0	6.8	16.1	3.8	3.0	2.1	5.7
4000	172	18.0	0.6	5.6	22.0	2.5	3.0	2.7	5.5
4000	345	19.9	0.7	7.6	24.7	3.6	2.1	2.4	6.7
4000	517	26.0	2.2	6.7	30.6	3.4	1.9	2.0	7.8
4000	689	32.0	5.2	7.7	38.5	1.8	1.4	1.8	9.6
4000	862	-	-	-	-	-	-	-	-
6000	0	37.2	-1.6	5.6	29.9	3.9	4.2	2.3	4.8
6000	172	30.5	3.7	4.1	34.8	2.9	5.7	3.1	6.7
6000	345	27.3	-1.1	5.6	28.3	2.6	1.4	1.2	4.7
6000	517	35.2	1.9	4.8	39.0	2.6	2.5	1.5	8.2
6000	689	40.2	2.3	5.7	46.6	2.3	2.8	1.6	9.4
6000	862	41.2	3.6	6.7	53.7	2.2	3.2	1.8	6.7
8000	0	45.3	-0.1	5.9	39.4	4.6	4.6	3.0	3.7
8000	172	35.6	-2.7	9.3	42.6	1.7	2.2	7.1	9.4
8000	345	34.9	-2.6	6.9	37.7	1.5	1.4	1.9	5.9
8000	517	40.5	-1.3	6.4	45.3	1.5	2.1	1.8	7.3
8000	689	44.8	2.7	7.1	51.0	2.4	3.5	1.5	8.3
8000	862	45.7	-0.6	7.3	56.5	1.7	2.7	2.2	7.0
10000	0	45.4	-4.2	9.3	39.4	2.7	2.6	1.4	2.6
10000	172	39.4	-1.6	6.2	44.5	2.6	4.6	4.3	5.8
10000	345	41.4	-3.2	10.2	50.7	2.3	3.5	3.7	9.0
10000	517	43.7	-5.4	6.4	46.3	1.5	0.8	1.4	5.7
10000	689	50.1	-2.3	7.4	50.5	1.7	1.5	2.2	8.3
10000	862	51.5	-2.1	8.4	59.2	1.8	2.7	2.7	6.5
12000	0	49.0	-3.6	11.6	44.4	1.9	2.2	2.9	2.8
12000	172	49.0	-4.1	7.7	53.2	1.7	4.2	1.9	13.3
12000	345	48.2	-7.2	8.6	51.8	1.9	1.6	2.3	4.4
12000	517	48.4	-6.1	9.2	51.3	1.8	1.6	2.6	4.9
12000	689	52.2	-7.7	10.8	54.0	1.9	1.5	5.8	7.2
12000	862	54.3	-3.2	11.0	60.8	2.1	2.4	5.3	6.6

Table 15. Damper-bearing measured damping coefficients summary

EXPERIMENT		*Rotordynamic Coefficients*				*Uncertainties*			
		Damping (kN.s/m)				Damping (kN.s/m)			
Running Speed (rpm)	Unit Load (kPa)	Cxx	Cxy	Cyx	Cyy	ΔCxx	ΔCxy	ΔCyx	ΔCyy
4000	0	71.6	9.6	12.7	106.9	3.2	9.8	5.8	7.5
4000	172	87.2	5.4	18.4	100.7	6.5	2.3	6.5	12.0
4000	345	85.0	7.5	13.5	94.8	2.6	3.5	3.6	6.7
4000	517	92.4	6.8	16.0	115.3	1.9	3.2	3.9	10.9
4000	689	84.1	13.3	18.6	123.1	2.0	2.9	3.1	9.9
4000	862	-	-	-	-	-	-	-	-
6000	0	73.0	17.0	22.4	97.2	4.0	9.3	5.6	6.0
6000	172	77.9	6.3	36.3	104.6	6.0	6.8	10.4	12.5
6000	345	70.8	0.2	11.7	79.7	2.5	1.7	2.5	4.9
6000	517	94.6	0.1	16.0	105.1	2.3	3.5	3.8	14.5
6000	689	99.7	-0.9	15.0	119.4	2.9	4.1	3.3	10.8
6000	862	94.9	2.1	14.8	118.3	1.7	3.3	2.9	9.0
8000	0	71.0	11.6	30.0	95.3	2.4	7.3	6.8	4.7
8000	172	82.5	-4.0	30.0	95.0	4.1	3.2	14.1	9.9
8000	345	59.9	1.3	12.5	64.8	3.1	1.8	3.3	5.3
8000	517	81.1	-3.4	16.0	92.6	1.2	2.1	4.2	8.2
8000	689	91.6	-3.6	20.4	105.3	1.7	2.7	4.7	9.4
8000	862	76.8	0.0	13.3	91.8	1.6	2.1	2.7	6.9
10000	0	50.5	15.1	15.6	65.7	2.8	5.2	5.3	3.8
10000	172	57.3	2.0	29.0	74.6	5.3	2.4	9.6	12.0
10000	345	52.2	2.6	20.0	71.9	4.3	1.9	8.1	12.6
10000	517	58.6	4.0	9.4	69.4	1.9	1.7	1.5	4.0
10000	689	80.6	-1.1	11.6	94.3	1.8	2.5	3.1	8.5
10000	862	71.2	1.1	11.6	86.0	3.0	1.8	1.6	5.8
12000	0	52.7	14.4	15.0	69.8	4.5	5.1	6.5	3.0
12000	172	53.0	17.6	23.1	83.0	3.0	6.6	8.8	9.6
12000	345	57.7	4.5	20.9	84.6	4.5	1.2	8.4	9.7
12000	517	56.2	5.7	11.5	70.9	4.2	1.3	2.2	6.7
12000	689	54.2	8.1	10.6	79.5	4.8	1.6	2.4	12.8
12000	862	68.2	2.0	13.1	101.2	5.3	1.6	2.7	15.4

Table 16. Damper-bearing measured added mass coefficients summary

EXPERIMENT		*Rotordynamic Coefficients*				*Uncertainties*			
		Added Mass (kg)				Added Mass (kg)			
Running Speed (rpm)	Unit Load (kPa)	Mxx	Mxy	Myx	Myy	ΔMxx	ΔMxy	ΔMyx	ΔMyy
4000	0	22.3	-1.6	-4.1	12.4	3.5	2.8	1.9	5.3
4000	172	17.5	-2.2	-0.1	28.1	2.3	2.8	2.5	5.1
4000	345	16.3	-6.4	0.2	24.8	3.6	2.0	2.4	6.5
4000	517	15.4	-10.8	-5.6	23.0	3.3	1.8	1.9	7.6
4000	689	11.4	-8.2	-3.3	18.6	1.7	1.4	1.7	9.4
4000	862	-	-	-	-	-	-	-	-
6000	0	28.2	-7.2	-6.3	16.3	2.3	2.5	1.4	2.8
6000	172	23.7	5.3	-2.2	33.1	2.1	4.2	2.3	5.0
6000	345	19.7	-6.8	-1.7	20.4	3.0	1.6	1.3	5.3
6000	517	21.3	-8.9	-6.2	25.8	2.5	2.5	1.5	8.1
6000	689	19.7	-12.0	-7.9	24.6	2.4	2.8	1.6	9.6
6000	862	16.0	-10.9	-7.0	24.6	1.8	2.6	1.5	5.5
8000	0	29.4	-8.7	-5.5	16.2	2.6	2.6	1.7	2.1
8000	172	20.9	-10.6	11.7	34.9	1.6	2.1	6.8	8.9
8000	345	19.3	-6.2	1.6	23.3	1.2	1.2	1.5	4.8
8000	517	21.4	-11.6	-1.6	23.7	1.4	2.0	1.6	6.7
8000	689	19.7	-10.5	-4.3	23.9	2.1	3.0	1.3	7.1
8000	862	17.2	-11.6	-3.5	22.4	1.3	2.1	1.7	5.5
10000	0	23.5	-6.5	0.8	11.8	1.6	1.6	0.8	1.5
10000	172	20.6	-2.3	4.2	30.4	1.8	3.2	3.0	4.1
10000	345	18.4	-5.3	4.5	21.9	1.6	2.4	2.5	6.2
10000	517	17.6	-8.9	-0.7	21.8	1.4	0.7	1.4	5.5
10000	689	17.6	-14.8	-2.6	15.4	1.7	1.5	2.1	8.1
10000	862	14.9	-11.6	-1.5	19.2	1.2	1.9	1.8	4.4
12000	0	21.8	-7.8	1.4	9.3	1.2	1.4	1.9	1.8
12000	172	19.3	-0.3	-1.7	27.8	1.1	2.8	1.3	9.0
12000	345	17.6	-8.1	1.7	18.0	1.5	1.3	1.8	3.5
12000	517	16.7	-8.3	2.1	20.1	1.3	1.1	1.9	3.5
12000	689	15.8	-9.3	3.8	17.2	1.2	1.0	3.9	4.8
12000	862	11.9	-12.5	1.8	16.1	1.4	1.6	3.6	4.4

Table 17. FPJB measured baseline dynamic stiffnesses for 0 rpm and 0 kPa

Ω (Hz)	Ω/ω	EXPERIMENT															
		Dynamic Stiffness (MN/m)								Uncertainty (MN/m)							
		$Re(H_{xx})$	$Im(H_{xx})$	$Re(H_{xy})$	$Im(H_{xy})$	$Re(H_{yx})$	$Im(H_{yx})$	$Re(H_{yy})$	$Im(H_{yy})$	$Re(U_{xx})$	$Im(U_{xx})$	$Re(U_{xy})$	$Im(U_{xy})$	$Re(U_{yx})$	$Im(U_{yx})$	$Re(U_{yy})$	$Im(U_{yy})$
20	N/A	4.34	0.41	-0.10	-0.13	-0.07	0.07	3.93	-0.63	0.39	0.27	0.09	0.16	0.27	0.27	0.69	0.85
30	N/A	4.17	0.10	-0.08	0.02	-0.25	-0.12	4.96	0.53	0.09	0.09	0.06	0.09	0.14	0.08	0.22	0.26
40	N/A	4.20	0.27	-0.10	-0.10	-0.13	0.05	4.87	0.29	0.09	0.11	0.12	0.13	0.10	0.06	0.28	0.38
50	N/A	4.27	0.27	-0.10	-0.03	-0.21	-0.04	4.95	-0.04	0.12	0.11	0.16	0.20	0.06	0.08	0.29	0.24
60	N/A	10.23	-12.49	2.04	-3.13	2.73	-3.17	6.20	-0.27	87.60	22.77	67.36	45.49	23.46	12.21	20.72	12.99
70	N/A	4.38	0.56	-0.23	0.02	-0.06	0.07	4.85	1.57	0.33	0.06	0.15	0.24	0.14	0.25	0.39	0.44
80	N/A	4.07	0.67	-0.19	-0.04	-0.17	-0.01	4.56	0.97	0.07	0.10	0.05	0.06	0.08	0.06	0.24	0.12
90	N/A	4.34	0.85	-0.19	-0.14	-0.12	-0.14	4.22	0.97	0.05	0.13	0.07	0.05	0.11	0.08	0.26	0.23
100	N/A	4.26	0.94	-0.14	-0.04	-0.07	-0.08	5.60	1.13	0.19	0.08	0.09	0.09	0.08	0.09	0.31	0.34
110	N/A	4.18	1.06	-0.27	0.02	-0.10	-0.06	5.05	1.73	0.14	0.09	0.06	0.09	0.10	0.08	0.23	0.26
120	N/A	4.21	1.37	-0.26	0.03	-0.23	0.03	4.65	2.18	0.37	0.32	0.73	0.69	0.38	0.36	0.74	1.08
130	N/A	4.23	1.38	-0.41	-0.04	-0.23	-0.13	4.89	0.92	0.10	0.10	0.09	0.10	0.11	0.06	0.15	0.11
140	N/A	4.12	1.58	-0.38	-0.09	-0.38	-0.08	4.95	1.33	0.10	0.04	0.06	0.06	0.06	0.06	0.14	0.12
150	N/A	3.89	1.76	-0.42	-0.08	-0.34	-0.13	5.00	2.24	0.03	0.09	0.11	0.07	0.07	0.10	0.21	0.20
160	N/A	3.83	1.94	-0.60	-0.01	-0.35	-0.10	3.83	2.54	0.10	0.10	0.15	0.10	0.21	0.12	0.28	0.18
170	N/A	3.54	2.40	-0.63	0.08	-0.73	0.09	4.59	2.39	0.04	0.09	0.17	0.17	0.20	0.27	0.50	0.34
180	N/A	4.54	1.71	-1.22	3.26	-3.23	0.15	8.90	0.95	9.65	9.34	15.83	15.77	22.35	15.30	35.35	28.89
190	N/A	3.39	2.46	-0.72	0.15	-0.66	0.23	4.64	4.26	0.08	0.11	0.17	0.14	0.12	0.16	0.47	0.55
200	N/A	3.17	2.79	-1.05	0.25	-0.72	0.27	3.37	5.31	0.06	0.09	0.13	0.06	0.10	0.08	0.43	0.24
210	N/A	3.25	3.13	-0.77	0.22	-0.69	0.21	4.32	5.61	0.09	0.06	0.06	0.14	0.11	0.08	0.21	0.06
220	N/A	3.52	3.31	-1.28	-0.26	-0.90	-0.04	4.19	5.30	0.09	0.05	0.08	0.10	0.09	0.05	0.11	0.24
230	N/A	3.84	2.65	-2.03	-0.26	-1.85	0.44	3.85	6.02	0.05	0.08	0.09	0.15	0.06	0.06	0.10	0.33
240	N/A	3.96	2.70	-3.22	0.68	-0.88	0.15	6.84	8.35	0.09	0.06	0.72	0.59	0.14	0.25	1.58	1.27
250	N/A	3.70	1.80	-2.81	-0.65	-1.75	0.12	3.24	7.02	0.12	0.09	0.15	0.14	0.09	0.06	0.59	0.22
260	N/A	3.91	1.87	-4.00	0.50	-2.08	-0.33	5.44	9.45	0.04	0.12	0.42	0.45	0.06	0.11	1.09	1.20
270	N/A	3.88	1.18	-4.38	-0.69	-2.91	-0.06	2.44	10.11	0.20	0.18	0.37	0.32	0.11	0.12	1.08	1.20
280	N/A	3.92	0.78	-3.92	-0.50	-3.18	0.32	0.94	8.79	0.14	0.14	0.46	0.19	0.12	0.12	0.28	1.05
290	N/A	3.57	0.35	-7.04	-1.13	-3.65	0.46	-4.32	13.87	0.15	0.13	0.67	1.38	0.22	0.11	3.99	1.12
300	N/A	3.15	-1.27	-5.55	2.15	-5.94	1.17	1.87	13.49	2.31	1.76	5.30	6.21	2.47	1.74	7.02	4.58
310	N/A	10.54	-1.84	-2.45	2.10	-1.69	-0.02	3.90	3.14	2.27	4.03	1.81	1.35	0.72	1.01	3.74	2.73
320	N/A	-30.82	-13.00	-10.40	0.89	-17.49	0.18	-25.47	5.01	5.35	13.25	6.45	2.59	2.91	5.50	18.60	4.32

Table 18. FPJB measured dynamic stiffnesses for 4000 rpm and 0 kPa

Ω (Hz)	Ω/ω	EXPERIMENT															
		Dynamic Stiffness (MN/m)								Uncertainty (MN/m)							
		$Re(H_{xx})$	$Im(H_{xx})$	$Re(H_{xy})$	$Im(H_{xy})$	$Re(H_{yx})$	$Im(H_{yx})$	$Re(H_{yy})$	$Im(H_{yy})$	$Re(U_{xx})$	$Im(U_{xx})$	$Re(U_{xy})$	$Im(U_{xy})$	$Re(U_{yx})$	$Im(U_{yx})$	$Re(U_{yy})$	$Im(U_{yy})$
20	0.30	28.17	12.08	1.67	-0.45	11.91	1.09	32.31	14.07	0.54	0.49	0.17	0.23	0.44	0.38	0.75	0.87
30	0.45	27.31	18.14	1.21	-0.61	12.55	1.96	29.18	19.97	0.30	0.42	0.11	0.19	0.32	0.38	0.35	0.31
40	0.60	25.40	24.82	1.32	-0.15	12.46	2.12	27.63	28.08	0.54	0.26	0.23	0.24	0.27	0.29	0.55	0.44
50	0.75	22.08	31.84	1.60	-0.01	10.97	0.46	24.24	35.45	1.04	1.21	0.25	0.42	0.66	0.93	0.57	0.37
80	1.20	15.37	53.71	1.87	0.98	12.92	4.54	19.09	59.35	1.33	1.32	1.03	0.68	1.15	0.78	0.98	0.48
90	1.35	13.49	62.02	2.58	1.67	10.36	7.30	15.51	67.35	1.96	1.80	0.69	0.37	2.17	1.56	0.75	0.68
100	1.50	12.77	69.93	2.77	0.27	11.40	9.25	10.63	76.73	1.90	2.02	0.66	0.65	2.63	1.36	0.79	0.65
110	1.65	5.72	76.88	2.87	1.02	12.89	10.81	7.55	84.20	1.05	1.33	0.42	0.70	0.82	1.95	0.61	0.67
130	1.95	9.47	94.50	2.44	2.11	13.34	14.18	4.17	103.70	4.45	4.90	3.20	1.70	3.95	4.20	2.73	1.14
150	2.25	-3.53	107.19	0.22	4.24	18.43	19.56	-3.19	120.38	1.22	1.16	0.85	1.21	1.39	0.78	0.77	1.32
160	2.40	-7.10	115.25	0.18	6.43	19.38	21.09	-4.53	130.78	0.95	1.13	0.84	0.53	1.07	0.72	0.65	1.18
170	2.55	-7.76	121.91	-0.92	7.46	21.38	22.07	-8.22	137.73	0.83	1.17	0.94	0.46	0.43	0.51	0.88	1.03
190	2.85	-10.09	131.56	-1.26	11.11	18.05	22.40	-19.12	146.18	1.88	1.04	1.35	0.95	1.71	0.98	1.30	1.36
210	3.15	-33.80	132.37	-7.22	12.26	14.58	28.63	-29.21	164.76	4.61	4.53	4.84	1.79	5.01	3.89	1.96	3.60

Table 19. FPJB measured dynamic stiffnesses for 4000 rpm and 172 kPa

Ω (Hz)	Ω/ω	EXPERIMENT															
		Dynamic Stiffness (MN/m)								Uncertainty (MN/m)							
		$Re(H_{xx})$	$Im(H_{xx})$	$Re(H_{xy})$	$Im(H_{xy})$	$Re(H_{yx})$	$Im(H_{yx})$	$Re(H_{yy})$	$Im(H_{yy})$	$Re(U_{xx})$	$Im(U_{xx})$	$Re(U_{xy})$	$Im(U_{xy})$	$Re(U_{yx})$	$Im(U_{yx})$	$Re(U_{yy})$	$Im(U_{yy})$
20	0.30	31.39	11.90	2.37	-0.19	14.04	0.08	37.91	14.23	0.53	0.38	0.16	0.21	0.53	0.53	0.87	0.86
30	0.45	30.67	17.79	2.53	-0.62	13.51	0.64	34.80	20.00	0.49	0.33	0.18	0.15	0.37	0.27	0.66	0.40
40	0.60	28.87	24.35	2.35	-0.42	13.62	1.15	33.66	28.86	0.33	0.24	0.23	0.20	0.40	0.22	0.70	0.45
50	0.75	26.73	31.10	2.33	-0.30	12.67	1.39	29.02	35.56	1.05	0.80	0.30	0.31	0.82	0.88	0.52	0.33
80	1.20	19.69	52.35	4.62	0.28	12.14	7.80	32.75	78.71	1.60	1.20	1.25	1.07	1.88	2.65	6.87	10.22
90	1.35	18.35	60.37	4.31	-0.21	9.65	4.51	24.63	70.37	2.52	1.43	0.91	0.48	1.88	1.91	1.16	0.65
100	1.50	17.22	67.86	4.04	0.34	12.51	12.87	17.20	77.94	1.72	1.75	0.67	0.56	1.62	1.53	0.60	0.69
110	1.65	11.07	75.51	3.87	0.80	13.61	12.86	11.06	83.69	1.07	1.54	0.46	0.46	0.83	1.18	0.72	0.68
130	1.95	12.13	91.66	3.90	1.79	20.75	16.61	9.76	104.83	2.64	2.10	0.82	2.12	2.80	1.60	1.12	1.67
150	2.25	1.88	104.72	0.97	5.63	19.52	17.06	-15.06	111.41	0.85	1.05	0.87	0.70	1.30	0.88	1.58	1.42
160	2.40	-2.20	112.51	3.96	5.46	23.35	18.34	2.93	133.70	1.15	1.45	0.87	0.58	1.44	0.90	2.57	0.64
170	2.55	-2.15	119.36	2.86	7.65	24.45	22.04	-1.34	142.48	0.97	0.80	0.60	0.52	0.74	0.82	0.89	0.78
190	2.85	-6.70	127.60	1.50	10.50	25.09	21.47	-12.81	137.90	1.07	0.91	0.61	0.41	0.88	1.05	1.12	0.73
210	3.15	-26.58	138.17	1.23	18.67	29.24	26.90	-26.65	152.25	7.73	5.89	4.66	4.55	6.28	8.62	5.47	5.86
230	3.45	-11.20	132.24	6.35	17.63	28.69	30.32	-13.05	185.70	1.00	1.82	0.81	0.79	1.78	1.17	1.67	1.88
250	3.75	-43.57	138.34	4.23	14.84	28.76	30.94	-33.34	184.91	3.09	3.86	2.04	0.64	2.17	4.12	1.55	1.23
260	3.90	-65.73	125.25	-0.77	12.43	17.05	22.13	-45.38	181.01	3.84	5.76	1.81	2.12	3.25	5.50	5.43	3.18

Table 20. FPJB measured dynamic stiffnesses for 4000 rpm and 345 kPa

Ω (Hz)	Ω/ω	EXPERIMENT															
		Dynamic Stiffness (MN/m)								Uncertainty (MN/m)							
		$Re(H_{xx})$	$Im(H_{xx})$	$Re(H_{xy})$	$Im(H_{xy})$	$Re(H_{yx})$	$Im(H_{yx})$	$Re(H_{yy})$	$Im(H_{yy})$	$Re(U_{xx})$	$Im(U_{xx})$	$Re(U_{xy})$	$Im(U_{xy})$	$Re(U_{yx})$	$Im(U_{yx})$	$Re(U_{yy})$	$Im(U_{yy})$
20	0.30	42.67	13.52	5.04	-0.58	16.85	-1.95	57.39	16.57	0.77	0.54	0.32	0.25	0.61	0.87	0.97	0.88
30	0.45	42.18	20.28	5.67	-1.33	15.43	-1.99	53.81	23.66	0.56	0.68	0.46	0.36	0.43	0.35	0.66	0.50
40	0.60	40.54	27.40	5.22	-1.69	15.63	-1.85	52.46	34.12	0.74	0.47	0.22	0.31	0.40	0.56	0.65	0.62
50	0.75	34.39	35.72	5.57	-0.85	12.50	-2.91	44.82	43.20	3.16	2.16	0.44	0.93	2.86	2.71	0.98	0.51
70	1.05	27.24	47.73	0.98	4.63	16.47	-5.45	34.43	58.93	6.90	4.06	3.95	6.55	2.12	6.56	6.30	3.69
80	1.20	30.98	58.79	3.51	-0.52	12.92	1.46	13.00	70.73	1.28	2.29	1.78	1.24	1.47	0.65	1.45	2.09
90	1.35	30.58	68.01	6.64	-3.20	11.60	-2.57	45.02	86.70	2.18	2.51	1.62	1.65	4.37	2.05	2.08	2.53
100	1.50	34.06	76.06	5.83	-2.43	19.05	14.40	30.81	95.74	1.61	2.29	0.98	0.48	2.27	2.79	0.69	2.26
110	1.65	26.28	86.22	6.26	-1.21	18.70	10.71	24.41	104.37	1.85	1.62	0.57	0.72	1.73	1.85	0.47	2.09
140	2.10	21.29	108.13	5.06	3.73	29.27	10.80	15.46	132.53	2.60	2.48	1.07	1.58	2.06	2.25	2.06	3.66
150	2.25	21.72	115.76	5.52	4.44	26.67	9.88	9.38	140.71	1.66	1.53	0.73	0.42	1.13	1.21	1.28	3.49
160	2.40	18.71	124.45	11.72	2.90	30.16	8.40	32.58	172.14	2.12	1.48	1.43	0.90	1.45	2.03	1.74	2.94
170	2.55	21.01	130.25	10.49	5.11	32.35	12.81	18.52	175.91	2.39	1.33	1.02	0.86	1.08	0.78	1.98	4.14
210	3.15	-1.15	150.00	10.84	12.08	39.11	19.24	5.08	186.03	2.88	3.49	1.83	1.16	2.11	2.61	2.99	2.81
220	3.30	-16.19	152.84	7.34	17.95	19.27	11.65	-12.70	180.92	5.86	3.54	2.77	1.71	2.92	2.75	5.10	2.73
230	3.45	5.77	138.10	15.70	14.37	43.02	19.71	17.38	226.94	3.71	2.25	2.38	1.13	3.16	3.79	4.61	2.71

Table 21. FPJB measured dynamic stiffnesses for 4000 rpm and 517 kPa

Ω (Hz)	Ω/ω	EXPERIMENT															
		Dynamic Stiffness (MN/m)								Uncertainty (MN/m)							
		$Re(H_{xx})$	$Im(H_{xx})$	$Re(H_{xy})$	$Im(H_{xy})$	$Re(H_{yx})$	$Im(H_{yx})$	$Re(H_{yy})$	$Im(H_{yy})$	$Re(U_{xx})$	$Im(U_{xx})$	$Re(U_{xy})$	$Im(U_{xy})$	$Re(U_{yx})$	$Im(U_{yx})$	$Re(U_{yy})$	$Im(U_{yy})$
20	0.30	59.92	16.95	4.11	-0.23	14.19	-6.47	86.47	19.68	2.68	1.28	0.70	0.43	1.93	2.58	1.04	1.03
30	0.45	60.56	24.84	5.67	-1.89	12.84	-3.28	83.48	29.13	1.62	0.75	0.68	0.68	1.25	1.40	0.99	1.21
40	0.60	59.03	32.94	5.83	-2.73	13.94	-4.25	81.96	40.30	1.26	1.53	0.89	0.54	1.51	0.60	1.34	1.28
50	0.75	56.95	42.38	7.58	-3.42	11.15	-3.10	75.48	53.37	2.51	5.03	1.31	1.12	3.92	1.90	1.94	2.15
80	1.20	51.13	66.95	7.81	-3.73	14.56	-5.36	45.61	85.00	4.08	3.19	2.46	3.91	1.60	3.38	4.21	0.99
90	1.35	52.55	76.25	9.31	-10.35	17.71	-7.09	76.43	107.77	1.99	2.26	1.30	2.36	1.09	2.28	3.19	2.30
100	1.50	52.60	84.92	9.05	-8.55	15.00	-2.81	62.64	114.96	1.84	2.11	1.68	1.57	2.06	1.30	2.68	2.63
110	1.65	50.96	93.12	9.60	-9.06	20.81	-2.93	58.13	123.19	1.59	2.13	0.95	1.39	1.24	0.77	1.96	2.97
150	2.25	46.98	126.82	10.74	-4.81	26.55	-2.57	29.76	168.54	1.87	2.73	1.32	1.21	1.97	1.25	4.07	7.02
170	2.55	45.90	142.04	13.31	-4.75	34.43	-0.82	49.85	200.80	1.09	2.26	1.88	0.98	0.82	1.70	2.23	5.06
190	2.85	42.89	154.84	13.22	-4.52	33.38	-3.54	59.49	190.41	1.41	2.95	1.21	1.46	1.00	1.09	2.46	4.02
220	3.30	39.67	172.30	15.64	-4.06	28.90	0.92	36.28	216.31	1.08	2.86	1.77	1.92	1.27	1.18	2.69	5.46
230	3.45	37.24	173.20	22.99	-3.01	45.29	5.52	60.63	271.52	1.63	2.86	1.33	2.18	1.89	0.61	1.68	6.35
250	3.75	31.64	181.75	15.23	5.63	40.06	8.70	31.98	246.68	1.93	2.59	1.65	2.19	1.36	2.15	3.86	5.47
260	3.90	29.38	183.91	16.64	4.40	38.53	8.26	37.89	239.74	1.18	3.70	3.78	1.76	1.83	2.75	6.04	3.41

Table 22. FPJB measured dynamic stiffnesses for 4000 rpm and 689 kPa

Ω (Hz)	Ω/ω	EXPERIMENT															
		Dynamic Stiffness (MN/m)								Uncertainty (MN/m)							
		$Re(H_{xx})$	$Im(H_{xx})$	$Re(H_{xy})$	$Im(H_{xy})$	$Re(H_{yx})$	$Im(H_{yx})$	$Re(H_{yy})$	$Im(H_{yy})$	$Re(U_{xx})$	$Im(U_{xx})$	$Re(U_{xy})$	$Im(U_{xy})$	$Re(U_{yx})$	$Im(U_{yx})$	$Re(U_{yy})$	$Im(U_{yy})$
20	0.30	65.49	12.49	9.75	0.55	20.94	-3.15	105.18	19.23	1.43	2.12	0.63	0.62	1.82	2.66	1.74	2.39
30	0.45	69.69	22.10	12.60	-0.29	18.13	-1.04	102.50	28.34	1.23	0.91	0.90	1.13	2.50	1.29	2.69	2.26
40	0.60	67.19	27.92	12.52	-0.96	20.49	-1.25	99.56	39.70	1.27	1.86	1.36	1.06	1.39	1.61	3.81	1.82
50	0.75	65.45	40.48	14.61	-2.18	19.74	-4.42	93.07	53.29	2.86	2.85	1.61	1.85	3.36	2.90	2.43	3.50
80	1.20	65.05	63.65	14.88	-5.37	19.23	-5.79	75.42	88.20	11.55	4.65	3.07	4.84	4.07	9.73	3.41	4.14
90	1.35	65.81	71.53	15.02	-10.94	21.50	-8.19	102.72	109.57	2.56	2.18	3.14	3.30	1.49	2.28	8.18	7.03
100	1.50	68.66	79.50	15.25	-6.73	18.45	-3.44	83.77	118.04	2.29	2.19	2.73	1.79	2.93	1.24	3.74	6.05
110	1.65	67.67	85.51	14.49	-6.87	22.38	-4.84	81.22	123.69	1.83	1.32	1.46	2.22	1.33	1.29	4.43	6.23
130	1.95	67.31	103.92	15.38	-7.51	16.85	-4.79	85.41	161.67	2.67	2.77	2.28	3.43	3.77	2.97	9.72	9.54
150	2.25	66.29	114.28	14.51	-1.60	24.68	-4.29	59.77	165.71	1.39	3.66	2.07	3.25	3.48	4.76	7.54	12.21
160	2.40	68.98	122.62	17.78	-2.68	30.20	-2.84	82.34	201.71	0.83	2.91	2.47	2.93	2.07	2.05	12.51	14.65
170	2.55	67.08	126.15	15.91	-0.86	29.82	-1.52	69.22	196.32	2.41	1.55	2.25	3.02	3.13	2.95	14.10	8.53
190	2.85	65.00	136.85	14.99	0.69	27.23	-2.28	89.63	183.62	2.05	0.92	1.97	2.13	3.20	2.41	11.58	15.02
200	3.00	65.12	146.07	19.64	-0.18	25.17	-1.88	92.77	205.19	2.56	1.80	1.72	3.17	1.91	2.13	16.70	12.46
220	3.30	63.03	150.95	17.23	-1.61	24.42	1.91	66.58	213.89	6.09	1.39	3.45	2.64	1.87	11.51	15.94	10.31
230	3.45	58.24	152.29	23.67	0.45	37.44	7.49	89.40	270.63	2.48	1.22	3.64	2.16	3.79	3.08	19.80	19.39
250	3.75	53.74	158.31	14.81	9.43	31.89	10.59	61.04	240.32	1.97	1.52	1.76	1.74	1.79	2.99	12.36	11.81
260	3.90	51.96	159.82	14.19	9.23	30.93	11.86	66.17	237.94	1.90	1.85	2.19	2.06	1.41	1.39	8.65	13.61
270	4.05	49.94	161.69	9.87	12.15	29.75	9.42	52.37	228.53	2.31	2.15	3.22	3.23	2.15	1.65	6.67	11.86

Table 23. FPJB measured dynamic stiffnesses for 6000 rpm and 0 kPa

Ω (Hz)	Ω/ω	EXPERIMENT															
		Dynamic Stiffness (MN/m)								Uncertainty (MN/m)							
		$Re(H_{xx})$	$Im(H_{xx})$	$Re(H_{xy})$	$Im(H_{xy})$	$Re(H_{yx})$	$Im(H_{yx})$	$Re(H_{yy})$	$Im(H_{yy})$	$Re(U_{xx})$	$Im(U_{xx})$	$Re(U_{xy})$	$Im(U_{xy})$	$Re(U_{yx})$	$Im(U_{yx})$	$Re(U_{yy})$	$Im(U_{yy})$
20	0.30	28.17	12.08	1.67	-0.45	11.91	1.09	32.31	14.07	0.54	0.49	0.17	0.23	0.44	0.38	0.75	0.87
30	0.45	27.31	18.14	1.21	-0.61	12.55	1.96	29.18	19.97	0.30	0.42	0.11	0.19	0.32	0.38	0.35	0.31
40	0.60	25.40	24.82	1.32	-0.15	12.46	2.12	27.63	28.08	0.54	0.26	0.23	0.24	0.27	0.29	0.55	0.44
50	0.75	22.08	31.84	1.60	-0.01	10.97	0.46	24.24	35.45	1.04	1.21	0.25	0.42	0.66	0.93	0.57	0.37
80	1.20	15.37	53.71	1.87	0.98	12.92	4.54	19.09	59.35	1.33	1.32	1.03	0.68	1.15	0.78	0.98	0.48
90	1.35	13.49	62.02	2.58	1.67	10.36	7.30	15.51	67.35	1.96	1.80	0.69	0.37	2.17	1.56	0.75	0.68
100	1.50	12.77	69.93	2.77	0.27	11.40	9.25	10.63	76.73	1.90	2.02	0.66	0.65	2.63	1.36	0.79	0.65
110	1.65	5.72	76.88	2.87	1.02	12.89	10.81	7.55	84.20	1.05	1.33	0.42	0.70	0.82	1.95	0.61	0.67
130	1.95	9.47	94.50	2.44	2.11	13.34	14.18	4.17	103.70	4.45	4.90	3.20	1.70	3.95	4.20	2.73	1.14
150	2.25	-3.53	107.19	0.22	4.24	18.43	19.56	-3.19	120.38	1.22	1.16	0.85	1.21	1.39	0.78	0.77	1.32
160	2.40	-7.10	115.25	0.18	6.43	19.38	21.09	-4.53	130.78	0.95	1.13	0.84	0.53	1.07	0.72	0.65	1.18
170	2.55	-7.76	121.91	-0.92	7.46	21.38	22.07	-8.22	137.73	0.83	1.17	0.94	0.46	0.43	0.51	0.88	1.03
190	2.85	-10.09	131.56	-1.26	11.11	18.05	22.40	-19.12	146.18	1.88	1.04	1.35	0.95	1.71	0.98	1.30	1.36
210	3.15	-33.80	132.37	-7.22	12.26	14.58	28.63	-29.21	164.76	4.61	4.53	4.84	1.79	5.01	3.89	1.96	3.60

Table 24. FPJB measured dynamic stiffnesses for 6000 rpm and 172 kPa

Ω (Hz)	Ω/ω	EXPERIMENT															
		Dynamic Stiffness (MN/m)								Uncertainty (MN/m)							
		$Re(H_{xx})$	$Im(H_{xx})$	$Re(H_{xy})$	$Im(H_{xy})$	$Re(H_{yx})$	$Im(H_{yx})$	$Re(H_{yy})$	$Im(H_{yy})$	$Re(U_{xx})$	$Im(U_{xx})$	$Re(U_{xy})$	$Im(U_{xy})$	$Re(U_{yx})$	$Im(U_{yx})$	$Re(U_{yy})$	$Im(U_{yy})$
20	0.20	38.69	11.35	1.40	-0.63	14.05	0.78	47.06	12.80	0.58	0.48	0.14	0.23	0.87	0.86	0.75	0.87
30	0.30	38.67	15.94	1.57	-0.89	13.79	1.17	44.94	17.35	0.45	0.53	0.22	0.19	0.53	0.35	0.43	0.36
40	0.40	37.65	21.60	1.30	-0.79	14.35	1.25	43.63	24.40	0.39	0.33	0.29	0.25	0.43	0.37	0.51	0.45
50	0.50	36.70	26.03	1.67	-0.89	14.76	1.96	39.55	30.10	0.56	0.82	0.32	0.27	0.67	1.28	0.45	0.32
70	0.70	32.54	37.77	2.48	-0.46	14.37	3.05	33.75	42.02	0.70	0.75	0.36	0.42	0.57	1.23	0.68	0.53
80	0.80	30.56	43.64	2.69	-0.65	16.42	5.84	45.52	62.35	0.84	0.32	0.52	0.95	1.19	1.45	5.87	4.09
90	0.90	24.25	47.08	2.31	2.68	13.48	-2.38	32.06	58.27	3.01	2.39	0.82	1.23	2.46	2.57	1.54	1.01
110	1.10	17.26	56.78	-3.39	4.96	18.34	2.27	19.05	63.86	3.30	3.54	2.12	1.31	2.90	3.03	1.28	1.59
130	1.30	20.68	70.34	5.42	0.01	19.02	6.89	20.62	83.62	2.45	1.77	1.24	1.36	2.20	2.39	1.32	1.10
140	1.40	13.45	76.52	3.64	-1.43	15.13	10.02	11.25	85.03	0.85	1.20	0.79	0.63	0.64	0.72	1.25	0.76
150	1.50	11.01	81.42	3.14	-0.23	13.87	10.16	-0.90	87.19	0.88	0.54	0.47	0.50	0.59	0.36	1.23	0.84
160	1.60	6.42	87.65	5.80	-1.59	14.41	14.07	15.13	110.12	0.81	0.72	0.64	0.65	0.78	0.48	2.46	0.88
170	1.70	4.13	92.34	3.94	-1.17	15.01	17.06	6.18	108.47	0.59	0.87	0.53	0.59	0.51	0.51	0.90	0.94
190	1.90	-2.95	99.15	2.04	-0.40	16.44	20.36	-9.33	109.42	0.99	1.11	0.58	0.69	0.65	1.27	1.31	0.92
230	2.30	-13.03	106.02	0.93	3.08	22.62	31.09	-13.73	150.08	0.91	2.00	0.63	0.66	0.81	1.81	1.33	0.93
250	2.50	-44.51	105.47	1.48	-1.90	25.51	30.53	-38.52	150.64	2.62	4.67	2.52	0.70	2.87	3.38	1.16	0.93
260	2.60	-65.93	85.85	-2.20	-6.26	14.22	20.64	-49.41	150.52	4.16	4.05	0.82	1.98	2.09	3.42	1.91	1.77

Table 25. FPJB measured dynamic stiffnesses for 6000 rpm and 345 kPa

Ω (Hz)	Ω/ω	EXPERIMENT															
		Dynamic Stiffness (MN/m)								Uncertainty (MN/m)							
		$Re(H_{xx})$	$Im(H_{xx})$	$Re(H_{xy})$	$Im(H_{xy})$	$Re(H_{yx})$	$Im(H_{yx})$	$Re(H_{yy})$	$Im(H_{yy})$	$Re(U_{xx})$	$Im(U_{xx})$	$Re(U_{xy})$	$Im(U_{xy})$	$Re(U_{yx})$	$Im(U_{yx})$	$Re(U_{yy})$	$Im(U_{yy})$
20	0.20	45.76	11.87	1.74	-0.35	16.09	-0.32	58.87	13.96	0.80	0.55	0.29	0.24	0.80	0.86	0.97	0.87
30	0.30	45.74	16.89	2.26	-0.54	15.00	-0.14	57.08	18.58	0.70	0.46	0.27	0.37	0.64	0.94	0.76	0.39
40	0.40	45.03	22.59	2.29	-0.52	15.24	-0.01	55.53	26.51	0.80	0.46	0.54	0.30	0.40	0.49	0.73	0.60
50	0.50	43.36	27.30	2.82	-0.63	15.96	0.98	50.46	33.08	1.34	1.38	0.47	0.36	1.10	1.83	0.77	0.49
70	0.70	40.11	38.98	4.08	-0.85	15.48	2.86	46.52	46.70	1.83	1.01	0.35	0.67	0.75	1.45	1.05	0.79
80	0.80	38.72	44.81	4.75	0.14	11.95	5.96	1.76	76.06	1.31	0.87	1.27	1.10	0.59	1.31	2.21	3.14
90	0.90	32.57	49.80	5.39	0.42	11.34	-2.88	48.39	63.98	8.14	4.61	2.39	6.06	4.66	10.38	5.08	1.99
130	1.30	30.47	72.62	7.11	-0.61	24.20	6.84	34.27	91.85	3.06	2.75	1.54	2.87	1.71	2.23	2.02	1.85
140	1.40	21.97	79.13	5.00	-1.62	19.60	8.67	21.94	91.69	1.65	1.20	1.28	1.49	1.29	1.09	1.73	3.09
150	1.50	20.23	84.26	5.17	-0.95	18.00	8.46	13.55	96.56	0.82	1.51	1.00	0.73	0.48	1.03	1.00	2.77
160	1.60	16.25	90.75	9.77	-2.17	18.57	11.86	35.33	129.71	1.69	1.86	0.88	0.67	0.92	0.78	1.98	3.63
170	1.70	14.39	95.40	6.52	-1.93	19.29	14.68	17.84	117.95	1.40	1.97	0.69	0.85	0.65	0.88	1.08	3.46
190	1.90	6.61	101.41	4.66	-0.67	21.07	18.32	2.94	119.08	0.89	2.75	1.07	1.07	0.95	1.58	1.39	3.61
220	2.20	-26.31	112.93	1.11	6.60	12.86	19.44	-26.14	126.75	2.77	3.82	2.10	2.23	2.40	2.30	2.62	4.19
230	2.30	-7.97	107.73	5.52	3.85	30.09	27.66	-1.08	164.73	0.76	2.04	0.59	1.75	2.46	1.22	2.72	5.35
240	2.40	-13.22	96.32	3.54	4.44	29.29	27.26	-23.88	156.42	2.82	1.77	1.03	2.03	4.53	5.50	3.19	4.89
250	2.50	-36.60	120.12	2.48	4.61	27.91	32.42	-22.86	160.28	2.72	2.87	0.41	1.37	1.21	1.42	0.83	3.58
260	2.60	-65.90	113.50	1.03	5.60	26.44	31.00	-33.15	153.87	2.74	3.43	0.80	1.52	1.38	1.41	1.72	3.87

Table 26. FPJB measured dynamic stiffnesses for 6000 rpm and 517 kPa

Ω (Hz)	Ω/ω	EXPERIMENT															
		Dynamic Stiffness (MN/m)								Uncertainty (MN/m)							
		$Re(H_{xx})$	$Im(H_{xx})$	$Re(H_{xy})$	$Im(H_{xy})$	$Re(H_{yx})$	$Im(H_{yx})$	$Re(H_{yy})$	$Im(H_{yy})$	$Re(U_{xx})$	$Im(U_{xx})$	$Re(U_{xy})$	$Im(U_{xy})$	$Re(U_{yx})$	$Im(U_{yx})$	$Re(U_{yy})$	$Im(U_{yy})$
20	0.20	63.85	14.91	1.43	-0.46	14.30	-5.39	85.81	17.80	1.88	2.13	0.31	0.48	1.90	2.24	1.26	0.91
30	0.30	64.62	23.14	2.77	-1.36	14.23	-2.15	83.59	25.43	1.13	1.50	0.33	0.39	1.65	1.26	1.41	1.14
40	0.40	62.78	30.60	2.88	-1.31	14.64	-2.52	82.06	35.31	1.42	1.74	1.00	0.37	1.11	1.00	1.58	1.30
50	0.50	62.19	36.37	4.62	-1.88	13.41	-0.52	77.20	46.23	1.88	1.30	0.88	0.56	0.56	0.72	1.13	1.22
70	0.70	59.91	50.68	7.13	-3.88	16.64	0.03	74.78	66.23	1.71	1.82	1.23	1.04	1.27	1.16	1.44	1.79
80	0.80	57.41	57.17	8.94	-3.49	15.34	0.13	50.38	74.51	1.29	2.10	1.55	0.92	0.99	0.87	1.16	1.71
90	0.90	55.96	64.98	9.29	-8.29	19.29	-2.40	82.29	91.96	2.40	3.49	2.85	3.42	4.18	2.18	2.77	3.08
110	1.10	51.03	79.97	9.93	-5.82	21.29	-0.86	64.39	101.88	3.01	3.24	2.80	3.61	2.44	2.62	3.46	3.39
130	1.30	48.28	96.90	12.40	-8.80	16.03	0.44	65.07	124.00	1.55	3.35	0.70	1.08	2.27	1.50	1.98	2.69
140	1.40	44.46	103.36	12.75	-8.48	20.82	-1.68	49.98	128.03	1.42	2.01	1.20	1.10	1.22	0.66	1.43	3.24
150	1.50	42.71	109.57	13.22	-6.16	20.17	2.05	27.16	137.49	0.98	2.70	0.93	1.06	0.71	0.91	1.81	2.49
170	1.70	37.01	123.21	13.53	-8.96	27.09	10.57	42.35	156.93	0.85	2.79	1.45	1.79	0.81	0.85	1.95	3.20
190	1.90	28.82	137.76	10.07	-8.18	32.33	11.24	41.74	157.31	1.21	3.06	2.34	2.54	2.39	1.28	3.28	3.97
210	2.10	24.98	152.81	10.69	-3.03	37.68	17.13	24.15	179.46	1.95	3.41	2.73	3.46	2.73	2.23	2.95	5.26
220	2.20	21.61	159.71	9.98	-2.64	33.97	13.56	14.07	180.93	1.19	3.65	1.62	2.16	1.96	1.60	2.06	4.11
230	2.30	20.49	162.44	15.52	-3.42	47.73	20.38	37.78	225.67	1.07	3.38	1.55	1.78	1.39	1.17	2.13	4.74
240	2.40	17.03	166.28	12.65	0.92	41.65	16.31	4.23	206.63	2.22	3.67	4.15	3.14	4.80	2.48	5.83	9.02
250	2.50	14.03	172.79	8.26	4.81	42.12	20.44	7.68	207.98	1.05	3.67	1.08	1.31	1.41	0.96	2.27	4.42
260	2.60	11.46	175.39	9.92	5.72	41.28	17.78	6.47	208.59	1.03	3.68	1.05	1.37	1.45	0.85	1.77	3.88
270	2.70	8.30	178.63	4.89	10.81	36.65	15.51	-14.47	195.66	1.01	3.74	0.84	0.86	1.14	1.02	2.26	3.37
280	2.80	5.99	179.20	18.89	5.51	41.70	25.87	25.26	280.38	0.78	3.52	1.02	1.09	1.50	0.99	2.35	5.95

Table 27. FPJB measured dynamic stiffnesses for 6000 rpm and 689 kPa

Ω (Hz)	Ω/ω	EXPERIMENT															
		Dynamic Stiffness (MN/m)								Uncertainty (MN/m)							
		$Re(H_{xx})$	$Im(H_{xx})$	$Re(H_{xy})$	$Im(H_{xy})$	$Re(H_{yx})$	$Im(H_{yx})$	$Re(H_{yy})$	$Im(H_{yy})$	$Re(U_{xx})$	$Im(U_{xx})$	$Re(U_{xy})$	$Im(U_{xy})$	$Re(U_{yx})$	$Im(U_{yx})$	$Re(U_{yy})$	$Im(U_{yy})$
20	0.20	80.25	16.78	0.54	-0.44	11.02	-6.80	113.94	19.90	2.07	2.72	0.92	0.83	1.84	3.71	1.64	1.23
30	0.30	80.29	25.58	2.27	-1.25	13.58	-2.55	111.57	28.30	2.01	0.90	1.40	1.00	2.24	2.36	1.87	1.13
40	0.40	79.36	34.16	3.20	-1.77	13.43	-5.08	109.51	39.79	2.15	1.70	1.39	1.13	1.65	2.38	1.75	1.18
50	0.50	79.66	40.86	5.40	-2.48	12.11	-1.10	103.79	53.05	1.86	2.06	0.75	1.04	1.55	1.39	1.53	1.87
70	0.70	76.47	55.32	9.00	-4.91	15.58	-2.73	101.36	74.75	1.64	1.61	1.75	1.10	1.05	2.08	2.90	2.21
80	0.80	74.38	62.53	10.35	-4.78	16.06	-1.99	85.56	84.05	3.90	1.16	1.78	2.43	1.82	1.93	3.22	1.98
90	0.90	67.41	73.82	12.30	-2.36	15.35	-11.04	100.06	104.36	4.41	1.55	3.60	7.38	2.76	3.65	8.45	4.21
130	1.30	65.40	103.35	12.37	-9.18	18.57	-5.37	90.87	137.10	4.22	2.00	2.77	6.14	1.78	4.04	5.50	4.42
140	1.40	61.84	109.87	13.52	-12.62	22.72	-7.82	76.55	140.88	2.32	2.22	2.02	2.61	1.53	1.26	2.52	4.17
150	1.50	60.83	115.87	13.62	-10.97	23.36	-3.70	61.12	141.62	1.74	1.54	1.58	2.93	0.86	1.36	3.20	3.72
160	1.60	59.47	122.89	17.27	-13.51	27.82	3.09	65.28	169.77	1.96	2.25	1.80	2.79	0.76	1.64	4.81	5.60
170	1.70	54.94	129.99	14.66	-14.81	28.00	4.15	64.46	172.39	1.30	2.99	1.63	2.10	1.56	0.93	2.23	4.98
190	1.90	47.10	144.32	11.40	-14.66	33.92	6.35	66.84	174.89	1.80	3.00	1.76	2.85	1.63	1.09	2.82	5.82
220	2.20	39.57	166.60	12.20	-9.22	37.89	10.14	40.73	201.20	2.19	2.99	1.74	3.78	1.40	2.33	5.17	4.95
230	2.30	37.10	169.75	19.52	-9.11	52.55	14.08	63.83	255.81	2.07	3.41	2.30	1.67	1.86	3.14	4.36	6.82
240	2.40	34.63	174.55	16.48	-3.35	47.39	11.63	36.03	229.97	3.14	2.90	5.76	6.36	3.92	4.17	9.01	7.83
260	2.60	28.21	183.17	13.98	0.72	46.22	11.78	35.37	228.96	1.80	2.81	1.42	1.03	0.82	1.60	3.36	4.47
270	2.70	25.60	186.10	10.98	4.58	42.36	10.61	21.26	220.29	1.34	2.72	0.85	1.25	0.58	1.60	3.48	4.38
280	2.80	23.34	186.93	25.36	-0.95	44.39	18.91	55.08	322.06	1.51	2.70	1.51	1.39	0.79	1.41	4.76	8.18
290	2.90	17.11	187.60	7.59	4.05	35.59	10.01	27.83	228.65	1.28	2.41	1.02	1.70	0.94	0.97	5.50	4.23

Table 28. FPJB measured dynamic stiffnesses for 6000 rpm and 862 kPa

Ω (Hz)	Ω/ω	EXPERIMENT															
		Dynamic Stiffness (MN/m)								Uncertainty (MN/m)							
		$Re(H_{xx})$	$Im(H_{xx})$	$Re(H_{xy})$	$Im(H_{xy})$	$Re(H_{yx})$	$Im(H_{yx})$	$Re(H_{yy})$	$Im(H_{yy})$	$Re(U_{xx})$	$Im(U_{xx})$	$Re(U_{xy})$	$Im(U_{xy})$	$Re(U_{yx})$	$Im(U_{yx})$	$Re(U_{yy})$	$Im(U_{yy})$
20	0.20	93.74	16.23	-1.45	0.29	10.52	-8.80	144.21	21.09	2.43	1.99	1.44	0.89	4.60	5.60	1.66	1.65
30	0.30	96.17	26.67	0.89	-1.19	11.85	-3.33	141.49	29.40	2.68	2.04	0.82	1.12	2.03	1.44	1.11	1.37
40	0.40	95.11	34.33	1.89	-1.68	11.81	-5.79	138.37	41.57	2.27	1.84	1.84	1.96	2.13	3.18	1.34	1.62
50	0.50	94.96	42.89	5.34	-3.89	9.83	-2.21	132.68	56.87	2.68	1.73	0.87	1.07	2.95	2.41	2.32	1.27
70	0.70	92.67	57.74	8.54	-7.85	13.58	-3.70	130.23	79.70	1.45	2.84	1.48	1.39	2.64	1.75	2.01	2.28
80	0.80	90.69	64.06	9.81	-9.00	17.96	-2.76	123.48	94.47	3.67	1.83	2.38	2.18	2.79	3.01	2.69	2.42
90	0.90	86.35	75.26	12.02	-7.87	16.14	-8.40	132.03	110.25	4.31	3.49	3.58	8.57	5.04	5.01	9.65	4.02
130	1.30	84.02	105.57	12.82	-14.56	20.34	-6.45	111.42	150.72	3.21	2.37	3.22	4.27	2.02	3.69	3.66	6.29
140	1.40	79.02	112.63	13.93	-17.42	22.15	-11.22	104.42	154.97	1.28	1.51	3.09	2.39	2.23	0.74	1.72	5.12
150	1.50	76.93	118.27	14.27	-16.79	23.86	-8.31	89.34	155.27	1.11	1.25	1.84	1.74	1.37	1.15	3.50	2.20
160	1.60	75.99	124.84	20.15	-25.47	31.12	-3.32	135.71	215.70	1.36	2.26	3.09	2.76	1.71	1.54	4.12	5.93
170	1.70	71.53	132.42	14.72	-19.74	29.69	-1.74	94.52	186.30	0.93	1.26	2.16	2.46	1.67	1.22	2.61	4.92
190	1.90	63.77	146.30	13.03	-18.89	34.78	0.58	94.77	189.83	1.77	1.43	3.53	3.17	2.82	1.24	4.42	2.51
220	2.20	55.70	167.71	15.54	-13.71	39.85	4.03	68.95	218.80	1.02	1.61	2.56	2.00	1.71	1.30	6.18	4.69
230	2.30	52.75	171.36	22.01	-14.04	52.73	5.53	92.88	272.47	0.80	1.96	2.38	1.52	1.60	1.47	3.45	3.86
240	2.40	50.13	174.99	17.96	-9.75	46.60	3.97	63.40	247.41	3.16	2.06	5.53	6.15	4.43	3.26	13.21	10.42
250	2.50	46.81	181.51	15.66	-2.85	48.29	6.52	57.75	248.96	0.53	1.65	1.42	1.23	1.18	1.45	4.36	2.15
260	2.60	43.90	183.80	17.80	-3.32	47.17	5.77	64.93	246.89	0.61	1.39	1.20	1.17	0.61	0.58	1.97	3.70
270	2.70	41.31	186.26	15.49	-0.45	43.61	6.28	53.07	240.27	0.39	1.69	0.94	0.73	0.68	0.52	1.79	3.09

Table 29. FPJB measured dynamic stiffnesses for 8000 rpm and 0 kPa

Ω (Hz)	Ω/ω	EXPERIMENT															
		Dynamic Stiffness (MN/m)								Uncertainty (MN/m)							
		$Re(H_{xx})$	$Im(H_{xx})$	$Re(H_{xy})$	$Im(H_{xy})$	$Re(H_{yx})$	$Im(H_{yx})$	$Re(H_{yy})$	$Im(H_{yy})$	$Re(U_{xx})$	$Im(U_{xx})$	$Re(U_{xy})$	$Im(U_{xy})$	$Re(U_{yx})$	$Im(U_{yx})$	$Re(U_{yy})$	$Im(U_{yy})$
20	0.15	47.50	12.51	2.77	-1.29	14.96	2.54	56.45	14.37	0.85	0.62	0.25	0.37	0.83	0.88	0.76	0.92
30	0.23	47.63	18.59	2.24	-2.12	15.91	3.41	54.52	19.48	0.61	0.78	0.27	0.39	0.64	0.58	0.56	0.69
40	0.30	46.79	24.31	1.91	-2.06	17.17	2.80	54.03	25.75	0.59	0.49	0.33	0.25	0.55	0.40	0.52	0.65
50	0.38	44.42	30.16	1.54	-1.70	17.24	2.59	51.44	32.28	1.04	1.08	0.40	0.37	0.59	1.59	0.56	0.64
70	0.53	42.48	42.07	2.63	-0.90	18.75	2.74	45.79	45.31	0.81	0.85	0.55	0.58	0.61	0.80	0.64	0.76
80	0.60	41.29	48.94	1.84	-0.88	19.03	1.51	45.14	53.81	0.56	0.60	0.49	0.29	0.67	0.59	0.56	0.93
90	0.68	39.57	53.69	2.82	-0.01	18.64	2.14	43.65	60.37	1.16	0.79	0.47	0.43	0.73	0.81	0.49	0.91
100	0.75	37.68	60.59	3.93	0.19	17.65	1.75	40.28	67.31	2.95	1.58	0.40	0.64	1.44	1.96	0.89	0.87
110	0.83	34.06	65.22	4.34	1.30	19.98	3.01	37.26	72.97	1.24	1.24	0.76	0.63	0.87	1.24	0.34	1.00
150	1.13	21.94	84.99	3.99	0.13	16.25	8.73	26.29	94.24	0.88	1.46	2.46	1.29	1.14	0.70	1.22	2.55
160	1.20	18.38	91.28	6.50	-0.77	14.74	11.01	25.31	101.89	0.72	1.11	1.38	0.53	0.86	0.26	1.58	1.27
170	1.28	15.23	95.90	8.64	-3.23	13.94	13.73	20.72	108.58	0.60	1.05	1.35	1.00	0.65	0.41	1.71	1.38
190	1.43	11.07	100.11	9.14	-2.61	11.34	20.29	11.92	119.00	1.01	1.29	1.16	0.86	0.82	1.43	1.17	1.77
210	1.58	-1.63	95.25	9.25	-7.74	11.25	31.79	0.67	133.07	1.80	1.41	1.21	0.74	1.80	1.50	0.72	1.24
230	1.73	1.00	92.40	5.43	-18.17	7.44	44.03	-11.28	148.94	2.80	2.14	1.12	1.61	2.22	2.53	1.35	2.27

Table 30. FPJB measured dynamic stiffnesses for 8000 rpm and 172 kPa

Ω (Hz)	Ω/ω	EXPERIMENT															
		Dynamic Stiffness (MN/m)								Uncertainty (MN/m)							
		$Re(H_{xx})$	$Im(H_{xx})$	$Re(H_{xy})$	$Im(H_{xy})$	$Re(H_{yx})$	$Im(H_{yx})$	$Re(H_{yy})$	$Im(H_{yy})$	$Re(U_{xx})$	$Im(U_{xx})$	$Re(U_{xy})$	$Im(U_{xy})$	$Re(U_{yx})$	$Im(U_{yx})$	$Re(U_{yy})$	$Im(U_{yy})$
20	0.15	47.13	11.93	0.87	-1.02	14.89	0.65	57.25	12.65	0.84	0.69	0.32	0.30	0.81	0.91	0.88	0.88
30	0.23	47.36	16.44	0.74	-1.48	14.37	1.53	55.95	17.12	0.72	0.59	0.24	0.29	0.50	0.56	0.81	0.41
40	0.30	46.33	21.68	0.37	-1.15	15.16	1.54	54.17	23.54	0.57	0.32	0.48	0.19	0.26	0.23	0.90	0.58
50	0.38	45.46	26.75	0.76	-1.27	14.99	1.29	50.94	29.60	0.96	1.55	0.35	0.36	1.38	1.11	0.70	0.43
70	0.53	42.13	36.67	1.24	-0.76	15.83	2.36	44.59	40.60	0.65	0.61	0.55	0.35	0.33	0.42	0.99	0.65
80	0.60	40.17	42.37	2.45	-2.12	19.15	5.16	60.91	64.86	0.66	0.48	0.66	0.52	0.87	0.65	5.00	3.19
90	0.68	37.99	46.81	1.66	-0.55	15.97	1.93	46.00	55.90	0.74	0.75	0.53	0.44	0.87	0.21	0.57	0.68
100	0.75	35.60	53.73	2.75	-0.10	13.54	5.18	41.19	62.98	1.72	0.98	0.66	0.63	0.85	1.51	0.52	0.79
110	0.83	32.94	59.58	2.81	-0.32	18.85	5.27	37.17	66.43	0.96	0.98	1.24	0.68	0.99	1.14	0.34	0.65
150	1.13	21.27	77.53	2.70	-0.56	14.39	6.12	10.44	84.41	0.86	1.18	3.55	0.56	0.47	1.28	1.39	2.83
160	1.20	17.92	82.76	6.61	-0.97	16.47	11.41	33.54	106.97	0.87	1.06	1.58	1.52	0.81	0.42	2.00	1.66
170	1.28	15.12	87.29	6.30	-1.47	15.98	11.99	19.74	102.24	0.85	0.44	1.37	0.67	0.60	0.48	1.04	1.52
190	1.43	9.72	88.47	6.12	-1.42	16.55	16.45	9.12	102.43	1.08	0.97	0.96	0.54	0.94	0.84	1.27	1.52
200	1.50	-15.19	110.41	9.56	-2.90	9.88	17.55	0.67	108.06	2.42	1.70	0.81	0.72	1.44	1.13	1.73	2.09
210	1.58	-7.45	92.74	7.27	0.25	16.70	22.31	-19.28	112.20	1.03	1.28	0.52	0.44	1.11	0.90	3.95	2.96
230	1.73	-16.01	96.72	7.34	-1.56	15.73	27.16	-2.48	138.85	0.87	1.04	0.81	0.71	0.84	1.59	2.00	1.96
250	1.88	-41.44	96.69	5.62	-8.37	11.50	26.41	-27.92	132.86	3.54	2.74	1.69	0.62	2.29	1.80	2.02	0.82

Table 31. FPJB measured dynamic stiffnesses for 8000 rpm and 345 kPa

Ω (Hz)	Ω/ω	EXPERIMENT															
		Dynamic Stiffness (MN/m)								Uncertainty (MN/m)							
		$Re(H_{xx})$	$Im(H_{xx})$	$Re(H_{xy})$	$Im(H_{xy})$	$Re(H_{yx})$	$Im(H_{yx})$	$Re(H_{yy})$	$Im(H_{yy})$	$Re(U_{xx})$	$Im(U_{xx})$	$Re(U_{xy})$	$Im(U_{xy})$	$Re(U_{yx})$	$Im(U_{yx})$	$Re(U_{yy})$	$Im(U_{yy})$
20	0.15	51.48	12.75	0.19	-0.58	16.12	-1.42	65.30	14.66	1.18	0.98	0.25	0.37	0.75	1.06	1.23	1.14
30	0.23	51.95	17.84	0.70	-0.98	14.95	0.48	64.63	19.07	1.22	1.83	0.36	0.36	0.89	0.89	0.91	1.88
40	0.30	51.07	22.90	0.28	-0.74	15.70	0.42	62.35	25.51	1.12	2.41	0.53	0.49	0.47	0.48	1.13	2.51
50	0.38	49.93	28.27	0.90	-0.43	15.22	1.15	59.27	32.98	1.26	2.76	0.62	0.53	0.93	1.18	1.09	3.24
70	0.53	47.27	38.79	2.36	-0.23	16.27	2.36	53.29	45.67	1.19	3.71	0.61	0.57	0.67	0.83	1.16	5.13
80	0.60	45.50	44.14	4.21	0.22	13.64	4.80	19.37	70.49	1.24	3.66	0.97	0.59	0.67	1.06	2.19	3.69
90	0.68	42.85	49.14	3.63	-1.00	14.55	0.72	58.67	60.52	2.12	5.15	1.15	1.11	1.44	0.54	1.67	6.75
100	0.75	41.97	57.55	4.15	-0.24	10.29	8.36	49.88	69.66	2.60	6.00	1.54	1.06	1.27	1.95	1.93	7.16
110	0.83	38.23	61.28	4.45	-0.69	20.74	5.61	45.64	72.35	3.25	6.22	2.03	1.48	0.87	1.97	2.22	7.50
160	1.20	24.88	85.30	9.81	-2.04	20.87	11.72	53.87	123.16	1.59	6.72	3.63	2.52	1.35	1.14	2.52	7.08
170	1.28	21.65	90.25	8.62	-1.59	18.52	12.03	27.02	109.34	1.60	7.11	2.98	1.13	1.06	0.71	2.61	9.12
190	1.43	15.46	89.61	8.28	-2.44	19.96	15.59	22.41	108.29	1.48	6.26	2.05	1.52	1.56	1.37	2.08	8.79
200	1.50	-6.12	119.06	12.34	-2.94	12.64	18.12	17.22	115.60	2.12	8.85	2.91	1.57	2.13	2.77	1.92	10.63
210	1.58	-3.52	96.45	8.42	0.05	20.43	23.53	1.46	121.16	2.25	8.03	2.29	1.17	1.81	2.34	1.19	9.46
220	1.65	-12.87	105.51	7.24	0.02	10.22	15.32	-16.07	119.86	1.68	9.55	1.82	1.34	1.43	2.65	1.27	8.71
230	1.73	-13.92	103.51	11.55	-1.71	23.77	25.65	12.10	150.33	0.97	9.73	2.39	1.80	2.21	3.43	1.25	13.09
250	1.88	-40.97	111.46	7.92	0.76	25.24	32.21	-27.41	139.88	2.49	12.41	1.38	3.62	3.17	3.75	4.03	8.81
270	2.03	-6.02	110.24	5.80	0.02	27.09	17.30	-46.38	153.24	2.45	8.09	2.02	2.99	3.32	6.96	4.02	18.25

Table 32. FPJB measured dynamic stiffnesses for 8000 rpm and 689 kPa

Ω (Hz)	Ω/ω	EXPERIMENT															
		Dynamic Stiffness (MN/m)								Uncertainty (MN/m)							
		$Re(H_{xx})$	$Im(H_{xx})$	$Re(H_{xy})$	$Im(H_{xy})$	$Re(H_{yx})$	$Im(H_{yx})$	$Re(H_{yy})$	$Im(H_{yy})$	$Re(U_{xx})$	$Im(U_{xx})$	$Re(U_{xy})$	$Im(U_{xy})$	$Re(U_{yx})$	$Im(U_{yx})$	$Re(U_{yy})$	$Im(U_{yy})$
20	0.15	81.49	19.21	-0.04	0.79	16.68	-5.34	114.87	17.19	2.50	2.17	1.36	1.00	4.58	3.83	2.00	2.01
30	0.23	82.35	27.07	1.09	-0.02	16.19	-2.76	112.85	24.47	0.94	1.30	0.70	1.42	2.96	2.15	1.91	1.97
40	0.30	81.79	34.64	1.49	-0.24	16.65	-4.19	109.95	36.29	1.10	1.43	1.42	0.79	1.52	1.57	1.77	2.39
50	0.38	82.61	42.24	4.19	-0.21	14.35	-0.26	104.60	48.28	3.07	3.09	0.99	0.90	3.58	3.05	1.02	1.77
70	0.53	81.63	53.32	7.67	-1.16	17.70	2.00	101.23	69.01	1.91	2.21	0.98	0.87	1.62	2.12	1.75	1.68
80	0.60	81.79	61.88	10.28	-1.60	16.67	2.19	86.85	78.12	1.54	2.42	1.40	0.48	1.78	1.77	1.38	3.04
90	0.68	79.09	66.30	10.83	-5.59	16.23	-1.64	113.44	92.47	2.73	3.14	1.39	1.45	2.88	1.71	1.34	2.83
110	0.83	74.47	80.71	13.03	-4.48	30.91	5.19	95.76	106.04	3.54	3.61	1.32	2.61	2.54	3.31	2.78	3.05
150	1.13	60.31	105.83	10.23	-1.24	27.36	-1.61	67.24	125.38	2.53	3.78	3.39	4.42	2.22	2.65	4.89	3.84
170	1.28	54.81	119.05	19.59	-8.98	28.16	4.34	77.79	149.93	1.19	3.77	2.46	1.72	1.60	1.25	2.41	3.33
190	1.43	45.22	120.65	17.77	-9.18	29.56	11.07	70.48	145.02	2.97	3.60	1.44	1.32	1.39	3.08	1.36	3.19
200	1.50	31.27	157.92	24.07	-12.97	20.30	16.20	66.85	157.58	2.76	6.68	1.50	1.94	1.95	2.74	2.09	4.23
210	1.58	21.09	129.86	19.32	-8.61	33.51	21.59	47.81	166.20	2.63	3.87	1.64	1.55	1.31	2.94	1.51	4.16
220	1.65	16.97	145.97	18.15	-8.86	22.27	18.11	34.96	169.60	1.73	4.42	1.57	1.49	1.98	1.52	2.06	4.30
230	1.73	9.48	145.24	25.18	-12.38	39.70	24.27	61.93	217.10	1.47	4.11	1.70	1.99	3.56	2.29	2.61	6.81
250	1.88	-20.06	162.18	16.74	-7.70	46.70	33.73	21.73	199.61	2.78	5.89	1.54	1.23	3.48	2.84	1.86	4.56
280	2.10	-56.06	167.22	18.58	-3.89	53.09	36.93	44.44	286.03	4.52	7.98	2.65	2.16	3.34	2.49	2.39	5.56

Table 33. FPJB measured dynamic stiffnesses for 8000 rpm and 862 kPa

Ω (Hz)	Ω/ω	EXPERIMENT															
		Dynamic Stiffness (MN/m)								Uncertainty (MN/m)							
		$Re(H_{xx})$	$Im(H_{xx})$	$Re(H_{xy})$	$Im(H_{xy})$	$Re(H_{yx})$	$Im(H_{yx})$	$Re(H_{yy})$	$Im(H_{yy})$	$Re(U_{xx})$	$Im(U_{xx})$	$Re(U_{xy})$	$Im(U_{xy})$	$Re(U_{yx})$	$Im(U_{yx})$	$Re(U_{yy})$	$Im(U_{yy})$
20	0.15	90.44	15.26	-2.62	3.26	20.21	-3.23	133.15	15.25	3.05	3.25	1.62	0.98	3.55	3.05	1.44	1.98
30	0.23	89.55	21.59	-0.11	2.70	15.56	-2.06	130.45	21.14	2.12	2.67	1.00	1.56	2.85	1.53	1.45	2.36
40	0.30	89.45	27.62	0.69	2.46	18.58	-2.37	126.26	31.14	1.38	1.50	1.10	0.77	1.72	1.10	1.46	1.27
50	0.38	88.66	35.19	3.80	2.21	16.14	-5.44	121.40	43.26	2.60	1.90	0.99	1.67	4.23	4.07	1.76	1.74
70	0.53	87.65	46.74	8.34	0.59	18.29	2.05	115.92	63.00	2.15	2.35	1.68	1.54	2.21	1.62	1.71	2.18
80	0.60	87.41	53.59	10.05	-0.47	20.53	3.80	105.31	73.21	2.86	2.71	1.75	1.93	1.83	2.00	1.34	3.06
90	0.68	80.58	58.96	11.38	-2.90	23.76	-3.32	126.75	86.41	7.01	2.70	1.64	1.49	6.80	5.59	1.63	2.17
110	0.83	78.62	74.02	14.05	-2.00	32.18	3.42	107.41	100.36	4.84	2.37	3.04	2.69	4.07	5.59	1.84	4.25
160	1.20	64.48	103.04	21.25	1.04	34.53	4.89	122.49	189.27	3.41	3.01	4.64	4.12	3.89	4.15	4.61	5.72
170	1.28	61.68	108.00	16.47	-5.20	30.46	3.38	88.14	144.76	1.67	2.95	2.86	2.74	1.84	1.51	2.49	3.37
190	1.43	53.78	111.27	16.68	-5.79	29.06	7.21	79.96	142.16	3.10	2.84	1.99	1.83	2.15	2.34	2.41	2.96
210	1.58	29.84	126.89	18.22	-5.54	34.70	11.67	60.05	158.52	2.32	3.66	1.32	1.44	2.49	2.09	1.91	2.63
220	1.65	15.17	132.49	19.67	-3.76	23.03	16.01	48.85	163.58	3.53	2.64	1.28	1.46	1.29	3.29	1.68	3.04
230	1.73	27.06	122.41	22.69	-8.73	38.62	19.33	78.64	211.29	1.73	2.25	1.98	2.11	2.40	1.60	1.62	3.22
250	1.88	-5.21	151.17	17.14	-5.23	40.57	26.52	37.94	191.01	2.80	4.09	1.69	0.99	1.91	1.05	1.46	2.87

Table 34. FPJB measured dynamic stiffnesses for 10000 rpm and 0 kPa

Ω (Hz)	Ω/ω	EXPERIMENT															
		Dynamic Stiffness (MN/m)								Uncertainty (MN/m)							
		$Re(H_{xx})$	$Im(H_{xx})$	$Re(H_{xy})$	$Im(H_{xy})$	$Re(H_{yx})$	$Im(H_{yx})$	$Re(H_{yy})$	$Im(H_{yy})$	$Re(U_{xx})$	$Im(U_{xx})$	$Re(U_{xy})$	$Im(U_{xy})$	$Re(U_{yx})$	$Im(U_{yx})$	$Re(U_{yy})$	$Im(U_{yy})$
20	0.12	56.18	13.24	0.39	-1.44	15.10	2.28	66.59	14.13	1.19	1.56	0.49	0.44	1.62	1.36	1.10	1.12
30	0.18	55.70	17.81	0.03	-2.47	16.01	3.22	64.70	19.46	1.09	1.52	0.59	0.43	1.44	1.07	0.67	0.63
40	0.24	55.74	23.58	-0.16	-2.56	17.48	3.18	64.35	26.10	0.70	0.81	0.52	0.73	0.87	0.83	0.70	0.73
50	0.30	54.31	29.35	-1.01	-2.64	17.45	4.54	62.09	31.52	1.70	2.76	0.43	1.01	3.20	2.20	1.12	0.92
70	0.42	51.56	39.35	-0.53	-2.58	19.08	3.68	51.79	50.25	1.90	1.66	0.59	0.70	1.07	1.90	2.55	2.07
80	0.48	50.36	44.41	-2.46	-3.05	21.80	2.22	60.22	52.63	1.65	1.05	1.07	0.91	1.43	1.28	1.23	1.46
90	0.54	45.51	54.07	-2.47	-1.08	20.51	1.57	56.08	57.38	2.69	4.41	0.81	1.01	3.95	3.28	1.05	0.85
100	0.60	48.07	58.02	-1.73	-0.51	18.27	0.81	50.18	63.83	3.61	4.54	1.11	0.97	4.13	1.65	1.61	1.16
110	0.66	41.18	65.30	-0.55	0.92	20.06	1.77	46.27	69.75	2.34	3.02	0.91	0.91	1.43	3.54	0.98	1.14
130	0.78	42.98	74.71	-0.31	4.12	16.17	1.70	43.60	82.95	4.39	2.90	1.14	1.88	2.80	4.29	1.47	1.44
140	0.84	32.58	78.85	-2.16	2.57	18.35	3.18	37.84	85.09	2.22	2.12	1.12	1.51	1.98	1.45	1.58	1.45
190	1.14	19.04	91.95	-1.47	-1.23	11.43	10.56	19.74	103.06	2.30	1.59	1.98	2.21	1.78	2.37	1.64	2.42
210	1.26	-3.97	93.30	6.70	-5.94	1.12	16.12	1.62	128.86	2.02	3.72	1.94	3.62	3.00	3.05	3.36	4.53

Table 35. FPJB measured dynamic stiffnesses for 10000 rpm and 172 kPa

Ω (Hz)	Ω/ω	EXPERIMENT															
		Dynamic Stiffness (MN/m)								Uncertainty (MN/m)							
		$Re(H_{xx})$	$Im(H_{xx})$	$Re(H_{xy})$	$Im(H_{xy})$	$Re(H_{yx})$	$Im(H_{yx})$	$Re(H_{yy})$	$Im(H_{yy})$	$Re(U_{xx})$	$Im(U_{xx})$	$Re(U_{xy})$	$Im(U_{xy})$	$Re(U_{yx})$	$Im(U_{yx})$	$Re(U_{yy})$	$Im(U_{yy})$
20	0.12	57.48	12.46	-1.59	-1.55	15.44	1.74	70.24	13.54	1.76	1.22	0.49	0.52	1.94	1.27	1.29	1.12
30	0.18	57.48	16.91	-2.27	-2.27	15.82	2.62	68.79	18.20	1.13	1.53	0.65	0.52	1.53	1.03	1.21	0.74
40	0.24	57.30	22.40	-2.51	-2.18	16.64	2.39	68.01	24.41	0.65	1.02	0.57	0.52	1.11	0.79	0.61	0.72
50	0.30	56.49	27.97	-2.57	-2.23	16.60	2.24	65.22	30.50	1.82	1.73	0.49	0.75	1.80	2.55	1.11	0.79
70	0.42	53.76	37.80	-2.35	-1.45	19.29	2.19	58.86	40.31	1.23	1.91	0.92	0.64	1.57	1.49	0.90	0.83
80	0.48	52.35	42.87	-1.07	-3.24	22.57	4.67	75.36	63.39	1.83	1.82	0.71	0.82	1.24	1.16	1.84	0.71
90	0.54	47.85	50.22	-2.77	-0.80	17.81	3.02	59.99	55.13	2.49	3.18	0.97	0.61	4.46	2.24	0.90	0.73
100	0.60	50.72	54.66	-2.03	0.07	21.04	2.69	53.60	61.29	2.77	2.62	0.82	1.06	3.25	2.98	1.43	1.76
110	0.66	43.71	61.05	-0.91	1.01	21.65	2.48	49.86	66.07	1.76	2.16	0.79	0.81	3.39	1.48	1.49	1.22
130	0.78	44.52	68.50	2.08	2.66	20.61	-0.17	43.15	79.25	3.19	2.67	1.71	1.39	2.48	1.94	1.89	2.19
140	0.84	34.22	74.70	1.50	3.17	20.43	1.65	35.39	82.45	1.91	1.76	3.07	1.83	1.92	1.64	2.53	3.65
190	1.14	19.33	88.36	2.41	2.49	15.36	9.83	20.68	98.81	3.53	2.31	4.95	1.39	2.19	3.20	1.79	5.76
200	1.20	-29.40	118.24	10.01	-3.14	13.96	12.27	14.47	104.87	6.07	3.32	4.37	2.38	6.70	4.10	1.83	4.44
210	1.26	-4.09	97.54	8.84	0.91	15.72	12.44	-4.24	108.43	2.63	1.70	2.22	2.06	1.35	1.99	2.38	2.98
230	1.38	-2.77	92.60	10.12	-0.75	15.90	21.70	15.13	135.23	1.36	1.53	1.15	1.08	1.72	1.97	1.73	2.64
250	1.50	-41.75	108.51	10.17	-12.40	12.11	21.01	-12.80	132.55	2.74	2.48	1.49	1.35	0.75	1.20	1.19	1.53
260	1.56	-92.18	84.01	10.47	-28.50	7.01	18.33	-32.00	127.76	5.59	4.86	1.99	1.04	1.67	3.12	2.45	2.92
280	1.68	-83.53	69.97	10.55	-33.87	0.47	37.27	-21.46	157.43	3.43	4.04	1.37	2.13	1.92	2.24	1.42	1.54

Table 36. FPJB measured dynamic stiffnesses for 10000 rpm and 345 kPa

Ω (Hz)	Ω/ω	EXPERIMENT															
		Dynamic Stiffness (MN/m)								Uncertainty (MN/m)							
		$Re(H_{xx})$	$Im(H_{xx})$	$Re(H_{xy})$	$Im(H_{xy})$	$Re(H_{yx})$	$Im(H_{yx})$	$Re(H_{yy})$	$Im(H_{yy})$	$Re(U_{xx})$	$Im(U_{xx})$	$Re(U_{xy})$	$Im(U_{xy})$	$Re(U_{yx})$	$Im(U_{yx})$	$Re(U_{yy})$	$Im(U_{yy})$
20	0.12	61.20	12.42	-1.99	-1.44	17.41	0.42	76.09	15.97	1.08	1.31	0.54	0.69	2.51	1.25	1.06	1.28
30	0.18	60.77	16.55	-2.29	-1.86	16.68	2.07	75.85	19.35	1.03	0.88	0.74	0.89	1.24	1.43	0.69	0.44
40	0.24	60.77	21.74	-2.84	-1.89	17.76	1.95	74.50	25.24	0.76	0.90	0.41	0.67	0.86	0.62	0.64	0.82
50	0.30	60.62	27.01	-2.80	-2.03	17.39	1.62	71.81	31.67	1.17	2.89	0.70	0.68	1.81	1.58	1.14	0.59
70	0.42	57.06	36.32	-1.79	-0.94	20.50	2.58	66.29	40.87	1.65	1.26	0.64	0.70	1.73	1.22	0.72	1.04
80	0.48	55.92	41.19	0.25	-0.21	16.31	6.34	25.30	82.04	0.92	1.21	0.59	0.56	0.98	1.90	4.64	3.03
90	0.54	50.37	48.55	-1.83	-0.67	17.98	2.94	69.48	54.40	3.40	3.00	1.01	1.00	2.49	2.67	1.17	0.77
100	0.60	55.76	52.69	-1.43	0.00	23.81	7.04	60.99	61.82	1.94	2.22	1.09	0.70	2.21	2.71	1.31	1.08
110	0.66	47.84	59.10	-0.20	0.34	23.07	3.80	56.65	65.75	2.52	1.67	0.41	0.94	1.55	1.38	0.66	0.92
130	0.78	47.81	64.37	2.19	2.67	24.18	-1.60	51.00	79.69	2.33	2.35	1.26	1.06	2.74	1.99	1.12	1.17
140	0.84	37.90	71.30	1.35	2.66	22.63	0.84	42.81	82.14	1.34	1.48	1.63	1.15	1.42	1.54	1.00	1.13
150	0.90	36.34	74.74	-0.86	4.96	18.87	2.35	29.86	82.28	0.91	1.32	3.57	2.72	1.13	1.29	2.37	2.45
190	1.14	22.43	86.75	2.50	2.41	16.25	9.24	27.29	97.73	2.00	1.77	3.11	1.26	1.77	2.63	1.57	2.53
210	1.26	0.45	96.58	6.13	0.88	18.00	14.09	12.33	109.16	1.88	1.61	1.05	1.03	2.50	1.55	1.13	0.96
230	1.38	1.13	92.47	10.24	0.04	20.18	20.19	26.85	138.15	0.77	1.70	0.85	0.81	1.42	1.66	1.74	1.44
250	1.50	-35.62	108.98	9.72	-2.31	18.99	25.87	-5.07	132.90	1.94	2.29	0.82	0.65	1.19	1.61	1.14	1.59

Table 37. FPJB measured dynamic stiffnesses for 10000 rpm and 517 kPa

Ω (Hz)	Ω/ω	EXPERIMENT															
		Dynamic Stiffness (MN/m)								Uncertainty (MN/m)							
		$Re(H_{xx})$	$Im(H_{xx})$	$Re(H_{xy})$	$Im(H_{xy})$	$Re(H_{yx})$	$Im(H_{yx})$	$Re(H_{yy})$	$Im(H_{yy})$	$Re(U_{xx})$	$Im(U_{xx})$	$Re(U_{xy})$	$Im(U_{xy})$	$Re(U_{yx})$	$Im(U_{yx})$	$Re(U_{yy})$	$Im(U_{yy})$
20	0.12	71.95	18.45	-1.80	0.05	18.36	-4.11	95.23	16.91	1.30	2.88	0.72	1.31	4.86	5.08	2.63	1.80
30	0.18	70.23	23.76	-1.39	-0.11	19.21	-1.84	93.96	23.47	2.55	2.29	0.80	1.32	4.04	4.14	1.85	1.80
40	0.24	71.09	31.09	-1.12	0.28	19.80	-2.02	91.26	32.38	1.98	1.91	0.71	1.20	2.72	1.62	2.52	2.36
50	0.30	72.07	37.81	0.12	0.35	17.26	2.35	87.63	42.74	6.61	4.93	1.63	0.95	5.69	7.84	2.43	2.43
70	0.42	71.58	49.22	2.96	0.95	21.22	2.69	82.16	60.08	3.02	3.70	1.41	1.12	3.79	2.80	2.48	3.42
80	0.48	70.81	57.05	5.49	2.40	18.84	1.65	57.07	70.05	2.87	2.74	1.62	1.50	2.98	3.36	2.86	3.19
110	0.66	65.22	78.78	8.93	0.36	26.89	5.16	77.41	96.63	5.78	3.87	2.32	2.33	3.91	5.36	3.75	4.34
130	0.78	65.69	85.15	11.61	2.09	29.92	-1.90	75.68	113.65	5.59	8.00	2.38	3.69	5.63	5.67	3.95	3.27
140	0.84	53.07	93.73	7.05	4.46	30.00	-0.48	64.56	112.72	3.59	5.68	3.88	3.49	3.26	3.33	5.29	4.80
190	1.14	36.62	109.82	6.66	4.51	25.23	7.54	50.82	122.01	2.94	4.31	4.88	5.20	3.21	5.03	6.66	6.03
210	1.26	10.61	125.44	15.92	0.29	26.33	11.24	38.29	137.16	2.73	5.28	3.45	1.17	4.68	2.61	2.93	4.89
230	1.38	11.52	120.53	22.50	-2.67	26.86	19.78	51.71	176.08	1.65	4.51	3.15	1.53	2.41	2.45	4.18	5.97
250	1.50	-24.39	143.58	22.54	-3.81	25.77	31.54	7.59	162.75	4.19	6.39	2.50	1.90	2.04	2.04	3.24	4.67

Table 38. FPJB measured dynamic stiffnesses for 10000 rpm and 689 kPa

Ω (Hz)	Ω/ω	EXPERIMENT															
		Dynamic Stiffness (MN/m)								Uncertainty (MN/m)							
		$Re(H_{xx})$	$Im(H_{xx})$	$Re(H_{xy})$	$Im(H_{xy})$	$Re(H_{yx})$	$Im(H_{yx})$	$Re(H_{yy})$	$Im(H_{yy})$	$Re(U_{xx})$	$Im(U_{xx})$	$Re(U_{xy})$	$Im(U_{xy})$	$Re(U_{yx})$	$Im(U_{yx})$	$Re(U_{yy})$	$Im(U_{yy})$
20	0.12	87.32	21.47	-2.37	0.91	19.77	-9.05	122.85	18.34	2.82	4.42	1.66	1.66	4.37	7.58	2.36	2.50
30	0.18	86.83	26.64	-1.08	0.98	19.58	-3.42	121.35	25.53	2.53	3.23	1.90	2.05	5.58	3.89	2.50	3.55
40	0.24	86.53	35.71	-0.34	1.20	20.84	-6.08	117.98	35.30	3.26	2.62	1.69	1.72	3.89	3.30	3.39	2.19
70	0.42	90.86	52.00	6.30	1.85	21.67	4.49	108.10	67.22	3.71	2.68	1.72	1.64	3.32	5.92	1.83	1.57
80	0.48	91.43	62.31	9.04	2.02	19.19	1.89	91.43	77.16	3.32	2.81	1.80	1.44	4.47	2.41	2.24	2.62
110	0.66	83.89	82.83	14.73	-2.15	31.33	4.12	105.92	109.00	4.75	2.91	2.34	2.95	5.12	4.41	2.37	2.86
130	0.78	83.49	86.34	18.19	-5.91	34.09	-3.29	107.85	131.07	6.24	6.73	2.61	1.80	5.77	5.16	3.03	2.22
140	0.84	68.79	97.62	17.00	-4.27	34.77	-2.48	98.46	130.89	4.59	5.13	2.90	2.96	2.40	4.69	3.10	1.75
150	0.90	67.86	102.55	16.24	0.94	29.76	-1.32	81.15	130.52	2.91	4.56	4.33	6.93	4.05	3.04	6.27	3.20
200	1.20	12.19	168.93	28.11	-3.70	25.03	5.32	82.53	148.57	11.31	11.20	4.10	3.27	7.63	4.92	3.65	2.63
210	1.26	26.78	137.41	24.12	-2.99	29.91	7.63	64.91	154.09	3.34	5.60	2.89	2.68	2.76	4.27	2.27	1.49
220	1.32	13.76	145.95	24.96	-1.17	16.98	11.45	50.95	155.12	6.28	5.08	0.82	2.10	3.69	3.06	1.75	1.88
230	1.38	27.01	130.06	29.95	-7.45	32.18	16.15	82.79	199.72	2.53	1.62	2.11	2.39	1.42	2.08	3.56	2.34
250	1.50	-9.22	155.87	28.25	-6.64	30.43	27.98	33.06	178.57	1.59	3.65	0.80	1.83	1.41	1.99	1.91	2.50
260	1.56	-63.68	152.18	30.82	-6.31	31.85	35.63	23.63	186.84	9.20	7.18	1.35	0.85	3.24	4.25	1.88	3.02
280	1.68	-48.48	143.65	26.49	-14.15	30.47	52.65	41.24	268.24	3.44	5.12	1.17	1.35	2.13	1.75	2.07	4.27

Table 39. FPJB measured dynamic stiffnesses for 10000 rpm and 862 kPa

Ω (Hz)	Ω/ω	EXPERIMENT															
		Dynamic Stiffness (MN/m)								Uncertainty (MN/m)							
		$Re(H_{xx})$	$Im(H_{xx})$	$Re(H_{xy})$	$Im(H_{xy})$	$Re(H_{yx})$	$Im(H_{yx})$	$Re(H_{yy})$	$Im(H_{yy})$	$Re(U_{xx})$	$Im(U_{xx})$	$Re(U_{xy})$	$Im(U_{xy})$	$Re(U_{yx})$	$Im(U_{yx})$	$Re(U_{yy})$	$Im(U_{yy})$
20	0.12	97.95	15.14	-5.25	3.53	19.41	-2.45	136.30	14.36	6.69	6.20	1.00	2.40	6.78	6.57	1.68	2.73
30	0.18	93.91	20.61	-3.72	4.10	17.68	-1.45	134.04	18.92	3.61	4.62	1.60	2.53	3.98	4.46	2.46	1.90
40	0.24	94.87	26.30	-1.76	4.92	20.40	-1.30	130.43	28.37	1.79	2.86	2.11	1.52	2.41	2.79	1.59	2.51
50	0.30	95.08	32.89	1.08	4.40	18.21	1.82	124.69	38.98	4.73	4.23	1.43	1.32	6.62	5.05	1.82	2.41
70	0.42	92.26	43.98	5.38	3.95	22.40	2.20	118.43	56.43	3.47	2.91	1.24	1.80	3.95	3.37	2.72	2.69
80	0.48	90.81	50.51	7.71	3.60	22.60	1.75	105.41	67.56	2.98	2.71	1.31	1.50	3.22	2.78	2.12	2.22
100	0.60	91.62	61.87	11.83	3.05	29.88	7.54	111.03	90.28	6.48	8.96	1.43	1.84	7.45	5.22	1.99	2.49
110	0.66	85.47	71.88	13.21	2.20	30.64	5.68	110.29	94.80	3.34	4.28	1.04	1.95	4.54	5.80	2.47	1.77
130	0.78	85.52	77.88	18.26	1.89	32.88	-3.79	101.05	115.76	8.09	3.86	2.90	2.92	8.13	8.39	2.14	3.31
140	0.84	71.47	86.29	14.28	5.28	33.45	-2.51	93.03	116.92	1.44	4.63	2.45	2.33	4.21	3.33	2.56	3.37
150	0.90	69.38	90.64	7.39	20.05	28.25	-0.78	65.34	112.40	3.53	3.86	4.11	2.99	2.39	3.34	2.93	3.55
190	1.14	55.49	104.62	11.75	6.82	31.79	6.65	75.69	127.48	3.28	4.99	2.77	5.80	4.54	3.02	6.72	4.14
200	1.20	25.70	146.84	21.44	1.07	32.92	11.42	81.01	134.85	12.45	7.82	3.04	2.94	7.44	6.66	3.51	3.37
210	1.26	30.90	121.66	17.38	1.23	34.79	6.53	64.59	142.50	3.49	3.08	2.08	2.71	3.22	3.89	3.16	3.38
230	1.38	32.58	117.40	23.64	-1.70	36.11	14.41	85.30	189.06	1.16	2.20	2.51	2.05	1.98	1.88	2.82	3.14
250	1.50	2.53	140.25	21.72	-3.20	33.40	22.10	41.65	166.76	2.10	2.19	0.98	1.27	1.43	1.51	1.02	3.11

Table 40. FPJB measured dynamic stiffnesses for 12000 rpm and 0 kPa

Ω (Hz)	Ω/ω	EXPERIMENT															
		Dynamic Stiffness (MN/m)								Uncertainty (MN/m)							
		$Re(H_{xx})$	$Im(H_{xx})$	$Re(H_{xy})$	$Im(H_{xy})$	$Re(H_{yx})$	$Im(H_{yx})$	$Re(H_{yy})$	$Im(H_{yy})$	$Re(U_{xx})$	$Im(U_{xx})$	$Re(U_{xy})$	$Im(U_{xy})$	$Re(U_{yx})$	$Im(U_{yx})$	$Re(U_{yy})$	$Im(U_{yy})$
20	0.10	68.44	12.89	-2.70	-2.05	13.81	2.67	80.71	14.19	2.29	3.06	0.95	0.57	2.73	3.08	1.90	1.33
30	0.15	69.77	18.70	-3.21	-3.45	16.41	4.05	79.15	19.39	2.81	2.70	0.81	1.04	1.93	2.21	1.45	1.33
40	0.20	68.62	24.54	-3.55	-3.28	17.24	4.17	78.58	25.82	1.55	1.54	1.19	0.67	1.77	1.54	1.75	1.87
50	0.25	70.23	32.08	-4.25	-4.25	18.34	4.31	75.89	32.04	4.52	1.42	1.09	1.42	3.43	4.48	1.03	1.53
70	0.35	64.24	41.15	-4.01	-4.76	20.71	4.28	73.86	52.67	2.84	2.56	1.14	1.21	2.92	2.76	3.34	3.56
80	0.40	67.30	46.50	-6.67	-5.00	22.50	3.82	75.83	51.19	3.85	1.13	1.70	1.53	2.53	1.30	2.28	2.20
90	0.45	67.29	50.78	-8.52	-2.96	21.57	3.83	71.93	54.68	6.87	3.74	1.40	1.25	4.51	4.70	1.13	1.77
100	0.50	63.30	58.79	-7.42	-3.85	21.39	0.41	66.25	61.23	4.49	6.05	1.53	1.61	7.28	4.19	2.78	2.92
110	0.55	57.46	64.35	-6.35	-1.68	24.23	1.95	62.33	67.05	3.30	3.40	1.45	1.79	3.40	2.04	1.93	1.27
130	0.65	57.16	66.74	-6.56	1.76	23.06	-1.16	58.79	80.35	3.76	5.32	3.20	1.25	5.16	5.44	1.62	2.21
140	0.70	43.59	75.92	-4.57	0.99	20.94	-0.74	52.88	84.58	3.39	3.59	1.81	1.96	2.32	2.97	3.16	3.41
150	0.75	43.38	81.21	-2.12	2.72	19.16	2.64	48.26	93.10	1.40	1.24	3.01	3.91	1.90	0.84	3.87	4.74
160	0.80	41.14	87.73	-1.47	5.31	20.15	8.74	49.59	100.38	2.74	2.36	3.02	3.28	2.80	2.51	2.27	5.45
170	0.85	37.30	90.96	-1.47	0.85	18.64	5.17	46.64	100.49	1.23	1.79	6.44	4.17	1.43	1.25	4.21	7.76
230	1.15	25.22	72.70	14.75	-29.39	17.30	47.37	34.47	161.01	18.88	18.01	10.43	18.27	12.47	22.31	18.37	13.66
250	1.25	-71.07	113.04	-41.14	-0.21	28.89	41.23	26.88	163.02	14.10	6.69	5.65	12.34	6.01	9.53	5.85	6.69
270	1.35	14.15	76.52	2.46	-26.40	33.18	39.93	21.91	162.22	8.02	8.04	7.82	5.15	5.01	7.11	5.23	5.94
280	1.40	-122.73	142.80	-49.32	35.89	26.37	39.50	16.88	165.90	12.61	8.85	8.06	10.01	6.00	3.65	5.35	2.60
290	1.45	-43.90	82.25	-43.62	-16.37	27.29	42.78	20.39	167.00	6.95	5.93	5.02	8.16	2.06	2.99	4.38	4.83
300	1.50	-16.56	8.10	-60.64	-42.70	28.16	44.08	3.06	168.96	14.98	26.70	7.09	15.91	12.33	6.65	9.75	8.90

Table 41. FPJB measured dynamic stiffnesses for 12000 rpm and 172 kPa

Ω (Hz)	Ω/ω	EXPERIMENT															
		Dynamic Stiffness (MN/m)								Uncertainty (MN/m)							
		$Re(H_{xx})$	$Im(H_{xx})$	$Re(H_{xy})$	$Im(H_{xy})$	$Re(H_{yx})$	$Im(H_{yx})$	$Re(H_{yy})$	$Im(H_{yy})$	$Re(U_{xx})$	$Im(U_{xx})$	$Re(U_{xy})$	$Im(U_{xy})$	$Re(U_{yx})$	$Im(U_{yx})$	$Re(U_{yy})$	$Im(U_{yy})$
20	0.10	69.34	13.44	-5.01	-1.36	14.34	3.39	82.32	14.10	1.63	2.21	1.61	0.75	2.53	2.54	1.30	1.27
30	0.15	70.16	17.97	-4.87	-2.82	16.46	4.41	81.52	18.19	1.62	2.64	1.23	1.19	2.07	1.80	1.93	1.00
40	0.20	69.79	22.73	-5.46	-2.35	16.97	3.15	80.13	24.19	1.26	1.37	0.84	1.21	1.14	1.37	1.30	1.01
50	0.25	69.50	27.34	-6.07	-3.07	17.55	3.32	77.98	29.53	3.01	3.77	0.95	0.86	3.51	2.74	1.39	1.04
70	0.35	67.52	37.04	-5.38	-2.55	19.15	2.28	71.81	37.69	2.60	2.05	1.30	1.12	1.75	1.90	1.41	0.80
80	0.40	65.79	40.85	-5.33	-5.52	23.36	5.71	95.37	66.11	2.57	2.12	1.81	2.23	3.13	1.74	4.17	1.28
90	0.45	63.23	46.60	-6.05	-2.62	20.38	2.68	73.91	51.18	2.91	4.03	1.68	0.80	3.36	2.21	1.35	1.26
110	0.55	58.83	56.86	-5.71	-2.16	22.89	2.64	63.98	60.94	3.13	2.62	1.22	1.62	2.46	3.37	1.23	1.94
130	0.65	56.55	58.60	-4.58	0.60	23.19	-0.65	55.70	71.83	3.80	3.21	1.44	1.68	3.62	1.97	1.46	1.31
140	0.70	47.27	68.27	-3.78	1.20	21.52	1.08	47.00	76.22	1.77	1.32	1.04	1.43	1.48	2.08	1.08	1.70
150	0.75	45.08	71.40	-3.04	2.75	17.48	4.04	30.92	80.14	0.67	1.41	1.43	1.28	1.09	1.05	2.25	1.78
160	0.80	41.03	75.99	-0.11	1.88	21.73	5.44	57.56	100.72	1.25	1.78	1.86	1.67	2.16	2.00	2.38	5.52
170	0.85	37.62	79.62	0.12	2.75	21.11	6.39	44.32	96.92	1.02	1.49	2.13	2.43	0.69	0.86	1.84	1.74
190	0.95	29.78	82.51	0.48	2.04	19.16	7.02	30.62	96.15	3.37	4.80	4.72	5.45	3.87	1.95	3.85	3.65
210	1.05	9.52	90.05	3.77	-0.18	16.11	8.12	4.43	100.74	4.16	4.19	3.51	5.70	3.27	3.48	2.94	2.23
230	1.15	15.15	87.99	11.14	-1.88	19.33	19.93	28.17	134.33	2.62	3.10	1.62	1.80	2.27	2.11	2.39	2.70
250	1.25	-29.19	71.19	7.66	-36.26	13.12	11.98	-5.16	129.21	7.81	12.71	3.46	6.37	3.45	3.31	2.76	1.77

Table 42. FPKB measured dynamic stiffnesses for 12000 rpm and 345 kPa

Ω (Hz)	Ω/ω	EXPERIMENT															
		Dynamic Stiffness (MN/m)								Uncertainty (MN/m)							
		$Re(H_{xx})$	$Im(H_{xx})$	$Re(H_{xy})$	$Im(H_{xy})$	$Re(H_{yx})$	$Im(H_{yx})$	$Re(H_{yy})$	$Im(H_{yy})$	$Re(U_{xx})$	$Im(U_{xx})$	$Re(U_{xy})$	$Im(U_{xy})$	$Re(U_{yx})$	$Im(U_{yx})$	$Re(U_{yy})$	$Im(U_{yy})$
20	0.10	69.69	19.94	-0.51	-1.18	18.05	-1.68	87.86	20.43	2.46	2.22	0.52	1.06	4.71	3.82	1.38	1.96
30	0.15	69.85	26.32	-0.46	-1.65	19.47	1.26	86.95	28.93	1.70	2.38	0.90	1.13	4.11	3.02	1.37	1.50
40	0.20	69.72	35.42	-0.99	-1.64	20.93	-0.71	86.08	37.70	1.32	1.74	1.01	1.29	2.41	1.80	2.19	1.53
50	0.25	72.38	42.15	-0.77	-1.17	19.10	2.84	83.01	47.35	4.76	4.04	1.50	0.96	5.03	5.61	1.61	2.50
70	0.35	72.74	54.83	1.50	-0.35	24.69	3.56	79.07	64.97	3.33	3.31	1.85	1.20	3.84	4.00	2.89	2.88
90	0.45	63.84	67.56	3.32	0.02	23.14	0.57	85.30	87.32	7.24	6.91	2.10	2.34	6.37	5.01	1.90	3.55
100	0.50	75.30	74.16	5.35	0.38	31.46	3.77	78.08	97.11	6.79	6.86	2.37	2.17	4.64	7.77	2.45	2.97
110	0.55	66.52	86.69	6.26	1.02	30.92	2.68	75.40	102.84	3.77	5.36	1.93	2.44	5.29	3.47	2.79	3.49
130	0.65	60.21	93.31	7.24	1.42	32.93	-8.55	74.15	116.85	4.15	4.95	2.38	2.03	3.95	5.92	1.78	3.58
140	0.70	55.43	106.65	8.39	2.16	30.92	-1.78	66.84	122.07	1.84	3.04	1.52	1.33	2.71	2.31	2.34	2.02
150	0.75	57.94	109.45	9.45	4.09	27.18	1.49	55.46	127.28	2.32	2.85	2.19	0.50	2.67	1.96	1.88	3.76
160	0.80	53.12	119.15	11.47	5.26	27.04	2.03	86.89	166.59	3.09	2.08	3.93	2.20	2.03	3.53	3.11	4.06
170	0.85	51.57	121.71	4.38	5.84	27.64	2.95	66.29	137.65	2.32	2.87	5.15	3.79	2.64	2.13	3.66	5.52
220	1.10	11.15	135.77	0.85	-0.95	13.43	13.63	20.85	126.40	5.13	6.70	3.15	3.29	4.02	2.82	3.49	3.13
230	1.15	25.37	132.61	17.43	-2.63	22.84	17.72	60.89	174.70	2.79	2.34	2.27	2.83	2.35	2.52	4.13	2.47

Table 43. FPJB measured dynamic stiffnesses for 12000 rpm and 517 kPa

Ω (Hz)	Ω/ω	EXPERIMENT															
		Dynamic Stiffness (MN/m)								Uncertainty (MN/m)							
		$Re(H_{xx})$	$Im(H_{xx})$	$Re(H_{xy})$	$Im(H_{xy})$	$Re(H_{yx})$	$Im(H_{yx})$	$Re(H_{yy})$	$Im(H_{yy})$	$Re(U_{xx})$	$Im(U_{xx})$	$Re(U_{xy})$	$Im(U_{xy})$	$Re(U_{yx})$	$Im(U_{yx})$	$Re(U_{yy})$	$Im(U_{yy})$
20	0.10	81.10	20.67	-2.65	-0.11	20.53	-4.62	106.88	18.96	2.49	3.44	2.07	1.24	3.75	4.44	2.06	2.62
30	0.15	79.42	27.57	-2.46	0.46	20.36	-1.78	104.97	27.34	1.87	2.00	1.62	1.28	3.91	4.23	1.85	1.56
40	0.20	80.77	37.10	-2.25	0.46	21.09	-3.42	103.22	36.61	1.63	2.92	1.42	1.44	1.81	2.21	2.32	2.34
50	0.25	85.43	39.11	-1.48	0.98	21.13	2.64	99.36	46.97	7.61	6.96	1.54	1.29	6.11	7.96	2.82	2.02
70	0.35	84.72	54.00	2.33	3.11	24.96	3.98	94.17	66.45	3.21	1.89	2.27	1.78	4.16	2.33	3.14	1.87
80	0.40	83.86	66.35	5.25	4.42	19.32	3.29	61.82	75.88	2.22	2.52	1.91	1.65	3.70	1.63	2.19	2.24
100	0.50	86.03	73.29	8.36	0.86	34.74	5.52	94.46	101.19	8.54	10.05	2.23	1.38	9.22	6.73	1.88	2.32
110	0.55	78.88	85.88	9.60	1.62	31.74	3.19	90.86	106.13	4.34	2.70	2.79	1.67	4.13	3.94	2.30	3.21
130	0.65	71.45	90.76	11.56	0.35	34.71	-8.07	92.42	123.81	6.09	4.63	2.54	2.48	5.68	5.53	4.13	2.67
140	0.70	65.29	103.80	13.32	1.01	33.25	-1.11	84.21	128.97	2.69	4.18	2.23	2.93	3.38	3.03	2.49	1.07
150	0.75	67.38	107.70	14.32	2.75	29.80	0.69	68.41	137.04	1.63	2.87	3.80	2.35	2.04	2.09	2.21	2.99
160	0.80	64.26	116.62	22.11	3.74	29.05	1.46	104.74	209.93	3.04	4.08	3.44	4.40	3.12	3.42	4.33	6.83
170	0.85	62.74	119.22	13.09	3.89	30.99	3.99	83.54	148.66	1.51	2.48	6.57	5.79	2.80	2.41	5.60	4.25
230	1.15	32.69	133.97	21.04	-1.39	28.75	15.76	78.26	184.02	3.12	2.66	6.01	3.16	2.97	2.24	4.31	6.11
250	1.25	3.80	144.51	25.46	-0.47	24.85	21.92	37.48	173.67	2.11	2.56	1.65	1.57	1.82	1.52	1.84	1.23

Table 44. FPJB measured dynamic stiffnesses for 12000 rpm and 689 kPa

Ω (Hz)	Ω/ω	EXPERIMENT															
		Dynamic Stiffness (MN/m)								Uncertainty (MN/m)							
		$Re(H_{xx})$	$Im(H_{xx})$	$Re(H_{xy})$	$Im(H_{xy})$	$Re(H_{yx})$	$Im(H_{yx})$	$Re(H_{yy})$	$Im(H_{yy})$	$Re(U_{xx})$	$Im(U_{xx})$	$Re(U_{xy})$	$Im(U_{xy})$	$Re(U_{yx})$	$Im(U_{yx})$	$Re(U_{yy})$	$Im(U_{yy})$
20	0.10	92.31	16.49	-7.42	0.50	18.21	-1.26	120.52	16.37	3.24	2.95	1.13	1.22	6.50	3.53	3.82	2.09
30	0.15	92.75	21.02	-7.34	0.51	18.08	1.34	119.11	20.50	5.40	2.98	2.44	2.31	4.29	6.67	3.34	2.30
40	0.20	93.38	26.81	-6.90	1.17	19.49	1.59	117.13	27.52	3.43	3.66	1.87	1.52	3.76	3.92	3.14	2.90
50	0.25	91.63	33.95	-6.08	1.81	21.96	1.22	112.44	37.33	5.67	3.22	2.14	1.10	8.47	8.24	4.99	2.48
70	0.35	90.95	43.26	-4.69	3.62	24.59	4.81	107.08	50.35	3.21	3.16	1.43	2.64	5.90	3.29	3.84	2.80
80	0.40	91.41	48.33	-2.48	5.22	25.74	5.65	84.02	58.11	3.28	2.43	1.26	2.11	4.26	4.09	2.84	2.20
110	0.55	82.27	66.73	1.39	5.93	35.23	2.69	96.97	84.17	5.90	2.30	2.72	1.47	4.10	4.95	3.73	3.76
130	0.65	82.81	67.92	7.07	7.51	36.27	-6.64	96.24	102.78	6.19	5.67	3.23	2.68	8.47	6.62	3.15	2.90
140	0.70	69.65	84.24	6.86	8.13	32.04	-3.61	85.16	106.91	3.72	3.46	1.45	2.67	3.40	4.68	1.72	1.13
150	0.75	68.91	85.85	8.79	8.36	28.82	-0.27	70.18	108.15	2.69	3.11	3.45	2.39	1.71	1.57	3.13	2.82
160	0.80	65.57	91.61	12.75	12.44	33.90	2.21	38.87	183.33	2.69	1.42	4.60	3.81	3.08	2.22	9.12	5.57
170	0.85	63.07	96.77	10.88	9.98	30.82	3.74	80.76	128.85	3.19	2.42	4.04	2.81	1.55	1.82	4.34	5.02
230	1.15	34.21	112.81	12.71	7.44	33.06	14.50	74.78	165.30	3.05	3.52	6.71	5.44	3.50	2.57	4.48	4.78
250	1.25	7.13	126.35	17.78	3.26	29.42	19.44	42.45	154.99	3.90	2.96	1.61	2.29	2.07	2.52	4.85	3.10

Table 45. FPJB measured dynamic stiffnesses for 12000 rpm and 862 kPa

Ω (Hz)	Ω/ω	EXPERIMENT															
		Dynamic Stiffness (MN/m)								Uncertainty (MN/m)							
		$Re(H_{xx})$	$Im(H_{xx})$	$Re(H_{xy})$	$Im(H_{xy})$	$Re(H_{yx})$	$Im(H_{yx})$	$Re(H_{yy})$	$Im(H_{yy})$	$Re(U_{xx})$	$Im(U_{xx})$	$Re(U_{xy})$	$Im(U_{xy})$	$Re(U_{yx})$	$Im(U_{yx})$	$Re(U_{yy})$	$Im(U_{yy})$
20	0.10	114.82	-17.93	-26.73	42.20	8.63	34.85	147.09	-26.24	18.98	33.90	23.21	20.72	18.68	27.40	19.45	19.60
30	0.15	105.19	-10.01	-10.98	35.13	16.67	30.41	132.67	-13.24	10.81	16.17	9.02	10.06	6.37	16.45	9.01	9.08
40	0.20	100.27	0.68	-9.21	26.80	23.15	24.17	128.42	3.15	8.35	9.99	13.01	9.20	5.97	9.84	8.50	5.73
50	0.25	98.89	11.70	-4.45	23.28	27.57	17.40	125.94	14.35	12.10	6.66	8.20	8.96	12.01	7.81	6.67	6.23
70	0.35	92.69	28.32	0.63	18.17	33.82	13.33	115.11	29.92	7.89	2.47	5.79	6.38	6.93	4.59	4.31	6.47
80	0.40	93.13	32.95	2.21	15.66	35.00	12.56	100.15	40.82	6.11	3.41	4.15	2.44	4.66	3.30	4.31	4.34
90	0.45	86.06	40.11	4.39	12.85	38.50	11.20	120.38	50.37	4.43	5.17	4.86	8.18	7.75	9.60	5.42	6.96
100	0.50	93.92	45.70	4.76	14.17	41.34	11.36	108.44	60.37	5.38	7.67	6.88	4.43	6.58	7.45	5.38	3.59
110	0.55	83.49	51.09	3.35	13.26	42.95	4.43	106.29	63.56	3.25	5.37	2.81	2.84	2.58	6.90	1.83	5.95
130	0.65	82.08	50.80	12.04	10.31	43.09	-2.68	96.02	91.69	6.34	3.85	6.64	4.66	6.11	3.92	7.69	2.67
140	0.70	70.46	67.54	9.25	13.69	38.62	-1.12	89.11	88.38	2.26	4.14	2.40	1.74	3.08	4.08	4.26	4.41
150	0.75	67.67	71.72	10.07	12.34	34.59	1.05	75.11	92.00	1.80	2.46	3.69	1.90	2.29	1.50	1.77	5.97
160	0.80	64.62	77.01	16.31	12.92	36.77	5.64	79.00	122.07	1.40	3.63	2.81	2.60	2.11	2.90	4.21	4.76
170	0.85	62.35	82.28	15.05	13.04	35.64	3.15	82.11	111.11	1.09	2.49	5.96	5.21	1.92	1.83	6.41	8.97
230	1.15	35.28	100.43	20.43	8.92	37.71	15.41	82.87	163.50	2.20	3.09	8.58	5.23	2.92	2.85	7.23	10.64
240	1.20	27.41	95.16	15.67	5.32	31.15	17.88	49.53	140.81	4.06	4.19	4.92	2.42	5.79	8.06	5.14	5.82
250	1.25	8.37	118.59	18.19	7.43	34.62	18.69	47.07	147.96	2.08	3.57	3.22	3.33	1.53	1.80	2.41	5.18

Table 46. Damper-bearing measured baseline dynamic stiffnesses for 0 rpm and 0 kPa

Ω (Hz)	Ω/ω	EXPERIMENT															
		Dynamic Stiffness (MN/m)								Uncertainty (MN/m)							
		$Re(H_{xx})$	$Im(H_{xx})$	$Re(H_{xy})$	$Im(H_{xy})$	$Re(H_{yx})$	$Im(H_{yx})$	$Re(H_{yy})$	$Im(H_{yy})$	$Re(U_{xx})$	$Im(U_{xx})$	$Re(U_{xy})$	$Im(U_{xy})$	$Re(U_{yx})$	$Im(U_{yx})$	$Re(U_{yy})$	$Im(U_{yy})$
20	N/A	3.46	0.14	-0.03	-0.02	-0.12	-0.04	4.56	0.68	0.15	0.13	0.02	0.02	0.05	0.07	0.04	0.17
30	N/A	3.46	0.21	-0.04	0.01	-0.14	-0.01	4.73	0.53	0.09	0.05	0.04	0.02	0.02	0.01	0.06	0.05
40	N/A	3.39	0.35	-0.03	-0.07	-0.19	0.00	4.81	0.48	0.08	0.10	0.05	0.10	0.03	0.01	0.23	0.04
50	N/A	3.39	0.42	-0.04	-0.02	-0.20	-0.01	4.56	0.45	0.22	0.17	0.10	0.22	0.01	0.02	0.20	0.04
60	N/A	0.52	-0.86	7.48	-4.19	-0.06	-0.13	4.38	1.54	54.79	61.48	29.15	34.37	3.95	3.05	1.82	2.14
70	N/A	3.15	0.58	-0.10	-0.03	-0.27	-0.04	4.36	1.00	0.29	0.20	0.27	0.20	0.04	0.02	0.10	0.04
80	N/A	2.86	0.64	-0.01	-0.07	-0.27	-0.08	3.80	1.04	0.09	0.12	0.04	0.12	0.02	0.01	0.10	0.06
90	N/A	3.00	0.96	-0.15	-0.25	-0.46	-0.20	3.70	1.49	0.07	0.08	0.04	0.08	0.03	0.01	0.18	0.07
100	N/A	2.72	0.95	-0.39	-0.23	-0.55	-0.16	3.59	0.86	0.05	0.06	0.07	0.10	0.01	0.02	0.07	0.07
110	N/A	2.47	1.07	-0.43	-0.21	-0.73	-0.15	2.97	1.48	0.06	0.04	0.09	0.04	0.03	0.02	0.08	0.06
120	N/A	2.26	1.17	-0.54	-0.24	-0.87	-0.02	2.98	2.03	0.17	0.15	0.10	0.18	0.18	0.13	0.29	0.22
130	N/A	1.97	1.23	-0.63	0.02	-0.94	-0.01	2.39	1.35	0.04	0.05	0.06	0.05	0.02	0.01	0.03	0.04
140	N/A	1.55	1.40	-0.70	0.03	-1.09	-0.02	1.98	1.77	0.04	0.05	0.04	0.05	0.01	0.01	0.09	0.06
150	N/A	1.01	1.52	-0.87	-0.03	-1.29	-0.02	1.36	2.29	0.06	0.05	0.09	0.06	0.01	0.01	0.07	0.10
160	N/A	0.60	1.63	-1.02	0.03	-1.45	-0.06	0.40	2.33	0.06	0.10	0.08	0.07	0.01	0.03	0.04	0.05
170	N/A	-0.07	1.87	-1.20	0.03	-1.83	-0.06	-0.06	2.51	0.17	0.15	0.12	0.11	0.05	0.06	0.06	0.06
180	N/A	0.55	3.50	-0.12	-1.56	-2.09	0.29	-0.31	3.04	8.04	9.00	5.66	5.86	0.98	1.57	0.93	0.90
190	N/A	-0.98	2.21	-1.80	0.00	-2.48	0.33	-1.48	3.82	0.15	0.10	0.12	0.19	0.07	0.11	0.12	0.20
200	N/A	-1.43	2.04	-2.06	0.14	-2.45	0.32	-2.16	4.34	0.07	0.11	0.12	0.10	0.10	0.11	0.30	0.25
210	N/A	-2.48	2.15	-2.23	0.06	-2.88	0.32	-3.06	4.18	0.05	0.07	0.21	0.07	0.10	0.03	0.48	0.07
220	N/A	-1.61	2.61	-2.73	-0.02	-3.76	0.01	-4.16	6.10	0.07	0.08	0.08	0.06	0.08	0.23	0.24	0.14
230	N/A	-2.67	1.66	-3.65	-0.04	-3.40	0.83	-4.28	7.16	0.08	0.06	0.14	0.12	0.08	0.05	0.41	0.30
240	N/A	-3.10	1.22	-4.50	0.00	-3.80	0.49	-5.65	7.62	0.13	0.09	0.24	0.21	0.17	0.08	0.50	0.24
250	N/A	-3.75	0.90	-5.09	0.50	-4.23	0.23	-6.55	8.56	0.05	0.13	0.12	0.29	0.09	0.11	0.41	0.64
260	N/A	-4.68	0.37	-5.47	1.04	-5.28	0.17	-6.94	10.10	0.11	0.10	0.20	0.16	0.13	0.06	0.59	0.24
270	N/A	-5.19	0.07	-6.44	1.07	-5.92	0.17	-9.00	11.22	0.10	0.10	0.30	0.17	0.10	0.12	0.90	0.51
280	N/A	-5.36	-0.77	-6.90	1.07	-6.61	0.52	-10.53	12.12	0.16	0.18	0.22	0.28	0.05	0.09	0.45	0.66
290	N/A	-7.17	-1.50	-8.75	0.71	-7.89	0.40	-13.45	12.06	0.09	0.07	0.27	0.35	0.10	0.20	0.68	0.89
300	N/A	-9.18	-2.02	-9.94	3.06	-9.78	1.36	-15.99	18.68	0.83	1.31	2.03	1.80	0.19	0.35	1.47	0.69
310	N/A	-17.96	8.03	-8.62	-0.98	-10.07	1.82	-14.06	22.79	3.23	1.34	1.67	1.79	1.32	1.24	4.40	4.32
320	N/A	-7.16	44.73	-5.82	6.44	-0.34	0.50	-21.53	64.01	1.01	1.00	1.56	2.55	1.01	1.03	2.94	6.23

Table 47. Damper-bearing measured dynamic stiffnesses for 4000 rpm and 0 kPa

Ω (Hz)	Ω/ω	EXPERIMENT															
		Dynamic Stiffness (MN/m)								Uncertainty (MN/m)							
		$Re(H_{xx})$	$Im(H_{xx})$	$Re(H_{xy})$	$Im(H_{xy})$	$Re(H_{yx})$	$Im(H_{yx})$	$Re(H_{yy})$	$Im(H_{yy})$	$Re(U_{xx})$	$Im(U_{xx})$	$Re(U_{xy})$	$Im(U_{xy})$	$Re(U_{yx})$	$Im(U_{yx})$	$Re(U_{yy})$	$Im(U_{yy})$
20	0.30	24.23	18.50	-1.94	-1.91	4.79	7.10	24.66	14.77	0.97	1.67	0.32	0.47	0.48	0.78	0.36	0.45
30	0.45	24.20	21.55	-3.55	-0.92	6.85	2.43	20.70	17.76	0.74	0.65	0.44	0.46	0.52	0.62	0.27	0.39
40	0.60	17.51	24.27	-0.70	1.87	6.13	2.65	23.51	26.83	0.75	1.65	1.28	0.98	0.73	0.64	0.64	1.27
50	0.75	18.46	27.73	-2.59	-1.50	5.64	0.48	18.27	28.13	0.77	1.18	0.25	0.34	0.55	0.87	0.61	0.37
70	1.05	9.11	35.98	-0.25	2.52	5.29	-1.39	14.22	41.60	1.55	1.39	0.71	0.87	0.74	1.83	0.54	0.69
80	1.20	15.77	44.31	2.37	6.16	6.45	2.69	7.81	50.85	0.71	0.86	1.39	1.03	0.65	0.80	0.48	0.88
90	1.35	19.25	45.57	3.10	0.70	10.04	1.30	8.30	58.74	2.06	2.03	1.22	0.90	0.66	0.88	0.53	1.49
100	1.50	22.37	58.52	6.44	3.34	13.47	3.03	13.84	64.89	2.23	1.96	0.79	1.11	1.10	1.72	1.06	2.50
140	2.10	11.45	76.54	6.29	-5.79	13.53	4.68	-5.47	90.45	4.45	0.84	2.24	1.01	2.10	2.04	1.09	1.17
150	2.25	10.59	74.13	8.07	-12.34	15.03	7.02	-2.92	96.70	2.29	1.14	1.41	2.25	3.69	0.93	0.73	2.70
160	2.40	9.72	79.49	4.75	-5.24	9.28	5.58	-2.99	99.24	2.74	2.27	1.39	1.82	2.59	4.55	0.90	1.50
170	2.55	-2.00	87.18	7.46	-3.71	9.60	6.04	-2.49	106.54	1.85	1.41	1.34	1.75	0.93	3.42	1.34	0.87
190	2.85	-5.11	93.01	2.13	-2.85	12.47	5.33	-11.87	145.26	1.74	1.31	3.17	2.27	3.63	2.38	3.26	3.25
200	3.00	-11.37	97.55	-0.80	5.31	7.57	9.65	-1.28	142.02	4.86	3.35	1.67	2.45	3.54	2.70	1.57	1.69
210	3.15	-19.51	103.57	9.37	13.16	13.85	15.42	-5.94	137.01	1.14	1.45	1.12	0.87	1.63	1.36	1.46	4.00
220	3.30	-20.75	103.00	-2.88	17.48	16.05	23.97	-5.82	142.80	1.98	4.07	2.47	2.26	1.70	2.06	1.23	2.73
230	3.45	-27.07	110.03	1.64	28.49	16.09	25.50	7.27	142.84	2.61	3.92	1.97	3.56	2.82	1.88	1.27	4.46

Table 48. Damper-bearing measured dynamic stiffnesses for 4000 rpm and 172 kPa

Ω (Hz)	Ω/ω	EXPERIMENT															
		Dynamic Stiffness (MN/m)								Uncertainty (MN/m)							
		$Re(H_{xx})$	$Im(H_{xx})$	$Re(H_{xy})$	$Im(H_{xy})$	$Re(H_{yx})$	$Im(H_{yx})$	$Re(H_{yy})$	$Im(H_{yy})$	$Re(U_{xx})$	$Im(U_{xx})$	$Re(U_{xy})$	$Im(U_{xy})$	$Re(U_{yx})$	$Im(U_{yx})$	$Re(U_{yy})$	$Im(U_{yy})$
20	0.30	22.85	18.23	-2.47	-2.80	3.84	2.52	26.62	13.06	0.79	0.70	0.17	0.15	0.37	0.48	0.18	0.23
30	0.45	20.42	17.45	-2.21	-1.72	3.81	0.05	25.17	17.42	0.34	0.38	0.11	0.17	0.37	0.34	0.14	0.14
40	0.60	19.49	21.96	-2.09	-1.21	5.16	1.67	23.16	24.78	0.43	0.40	0.17	0.16	0.25	0.16	0.27	0.24
50	0.75	19.52	25.15	-1.98	-1.24	4.80	-0.36	20.27	29.63	0.64	0.55	0.22	0.25	0.30	0.50	0.30	0.37
70	1.05	9.03	37.28	-1.94	1.97	5.58	-2.77	11.12	41.60	1.43	1.15	0.68	0.83	0.77	1.23	0.69	0.70
80	1.20	14.18	42.41	1.94	-1.13	7.41	3.81	21.73	63.71	0.55	0.79	0.29	0.40	0.81	0.60	0.59	0.47
90	1.35	10.62	49.43	2.54	-1.92	6.14	2.87	12.81	58.80	0.35	0.70	0.27	0.21	0.25	0.44	0.44	0.45
100	1.50	10.20	55.05	2.27	-2.56	5.75	1.17	11.44	64.33	0.36	0.76	0.21	0.28	0.37	0.34	0.34	1.05
110	1.65	8.16	61.72	3.48	-2.80	7.49	4.78	4.55	69.42	0.55	0.93	0.32	0.29	0.34	0.46	0.42	0.85
140	2.10	3.69	83.72	5.51	-2.01	8.22	7.23	-10.29	89.93	0.93	1.42	0.56	0.60	0.37	0.68	0.65	1.02
150	2.25	-0.05	89.17	3.68	1.14	9.10	0.67	-21.52	88.21	0.53	1.43	0.54	0.56	0.45	0.31	0.95	0.73
160	2.40	-1.64	98.34	9.05	-1.13	7.46	11.50	1.97	122.68	0.88	1.44	0.67	0.39	0.84	0.35	1.37	1.92
170	2.55	-6.87	102.30	3.41	1.61	9.19	10.62	-12.23	109.18	0.85	1.36	0.50	0.67	0.45	0.62	0.56	1.09
190	2.85	-9.04	113.01	8.10	0.37	1.11	7.18	-13.63	121.00	1.24	1.03	1.20	1.52	1.62	1.08	1.88	3.39
200	3.00	-10.74	116.43	5.93	3.40	-4.62	11.98	-20.96	124.86	3.17	3.54	1.85	2.25	2.72	1.51	1.90	1.57
230	3.45	-11.14	123.79	9.42	6.12	3.12	25.91	-23.32	169.20	0.97	3.06	0.73	0.56	2.25	1.11	1.26	1.81
250	3.75	-24.62	125.66	-5.46	8.00	12.34	35.89	-54.34	134.69	1.54	2.16	1.83	2.17	1.73	1.65	4.30	5.81

Table 49. Damper-bearing measured dynamic stiffnesses for 4000 rpm and 345 kPa

Ω (Hz)	Ω/ω	EXPERIMENT															
		Dynamic Stiffness (MN/m)								Uncertainty (MN/m)							
		$Re(H_{xx})$	$Im(H_{xx})$	$Re(H_{xy})$	$Im(H_{xy})$	$Re(H_{yx})$	$Im(H_{yx})$	$Re(H_{yy})$	$Im(H_{yy})$	$Re(U_{xx})$	$Im(U_{xx})$	$Re(U_{xy})$	$Im(U_{xy})$	$Re(U_{yx})$	$Im(U_{yx})$	$Re(U_{yy})$	$Im(U_{yy})$
20	0.30	28.46	12.88	-1.09	-0.83	7.56	0.52	28.79	13.24	0.92	2.44	0.13	0.29	0.71	0.72	0.25	0.54
30	0.45	22.55	16.71	-0.16	-0.48	3.64	0.44	27.65	16.22	0.58	0.65	0.13	0.17	0.83	0.31	0.30	0.25
40	0.60	20.51	21.99	0.04	-0.17	5.55	1.34	25.99	23.83	0.58	0.65	0.28	0.24	0.38	0.27	0.34	0.45
50	0.75	22.97	22.17	-0.33	0.23	5.85	0.93	24.78	27.14	0.88	0.95	0.28	0.34	0.60	0.21	0.42	0.73
70	1.05	7.58	34.57	-2.07	4.65	5.54	-4.95	14.30	37.35	3.41	1.43	1.90	1.86	1.34	2.22	1.29	1.83
90	1.35	15.20	45.39	4.09	-0.41	8.23	3.16	18.57	53.73	0.46	1.14	0.22	0.32	0.43	0.34	0.55	0.84
100	1.50	12.32	51.98	4.60	-0.27	6.63	3.59	16.16	59.42	0.70	0.44	0.22	0.46	0.26	0.25	0.68	1.02
110	1.65	12.30	58.99	5.60	-0.72	8.83	5.52	10.20	63.18	0.89	1.31	0.36	0.35	0.30	0.35	0.61	1.10
130	1.95	7.34	69.76	7.12	0.37	8.29	5.20	4.94	78.76	1.38	2.25	0.94	0.65	0.70	0.24	0.69	1.29
140	2.10	5.70	74.27	7.51	1.64	11.87	8.39	-4.76	84.05	1.32	1.83	1.43	0.94	0.96	0.62	0.79	1.53
150	2.25	3.03	80.81	6.80	2.33	10.56	6.76	-10.30	83.52	0.46	1.11	0.27	0.50	0.42	0.33	0.75	1.28
160	2.40	-0.84	87.51	11.69	1.11	9.71	7.92	11.64	109.99	1.03	0.75	0.82	0.67	0.40	0.38	0.74	1.85
170	2.55	-3.04	93.37	8.58	3.08	10.87	11.01	-7.24	96.36	1.22	1.71	0.65	0.84	0.31	0.24	0.74	1.49
190	2.85	-6.53	102.55	14.23	1.89	12.22	9.30	2.68	112.65	1.02	0.85	0.53	0.87	0.67	0.48	0.68	1.75
210	3.15	-10.08	112.99	10.51	8.97	3.30	16.04	-21.95	121.81	1.83	1.33	1.38	0.48	1.27	1.45	1.74	2.60
220	3.30	-10.97	115.54	6.79	14.03	0.29	10.96	-39.42	119.41	2.61	1.11	0.84	0.87	1.39	1.13	0.66	1.83
230	3.45	-3.64	118.75	13.95	9.98	7.06	22.45	-11.74	144.24	2.37	1.19	1.25	0.91	0.50	1.07	0.88	3.08

Table 50. Damper-bearing measured dynamic stiffnesses for 4000 rpm and 517 kPa

Ω (Hz)	Ω/ω	EXPERIMENT															
		Dynamic Stiffness (MN/m)								Uncertainty (MN/m)							
		$Re(H_{xx})$	$Im(H_{xx})$	$Re(H_{xy})$	$Im(H_{xy})$	$Re(H_{yx})$	$Im(H_{yx})$	$Re(H_{yy})$	$Im(H_{yy})$	$Re(U_{xx})$	$Im(U_{xx})$	$Re(U_{xy})$	$Im(U_{xy})$	$Re(U_{yx})$	$Im(U_{yx})$	$Re(U_{yy})$	$Im(U_{yy})$
20	0.30	36.71	12.81	-1.02	1.49	8.90	0.40	39.43	17.23	3.55	1.17	0.22	0.22	0.66	1.45	0.82	0.71
30	0.45	27.93	18.12	1.46	1.20	3.50	-1.00	37.63	20.37	0.92	0.71	0.35	0.19	0.54	0.61	0.74	0.50
40	0.60	24.83	25.03	2.19	1.36	6.83	0.36	35.44	28.90	0.33	0.70	0.21	0.15	0.80	0.47	0.79	0.59
50	0.75	30.08	29.00	2.50	0.89	6.50	1.51	33.20	33.41	1.68	1.46	0.37	0.30	0.37	0.55	0.78	0.58
70	1.05	11.75	41.24	-1.30	7.26	4.05	-6.67	20.61	45.26	1.65	1.94	0.97	0.85	1.84	1.66	0.91	0.95
80	1.20	20.45	43.56	7.31	2.34	5.21	-6.88	-1.76	88.96	0.67	0.62	0.55	0.49	1.51	1.03	2.96	0.94
90	1.35	21.57	51.65	7.10	0.05	9.80	2.77	29.06	66.08	0.93	0.63	0.22	0.32	0.37	0.26	0.61	0.53
100	1.50	20.60	56.70	7.90	0.00	8.37	3.47	25.57	71.58	0.56	0.66	0.22	0.30	0.40	0.31	0.71	0.78
110	1.65	18.71	66.42	9.38	0.20	11.02	4.76	19.09	78.21	1.03	0.64	0.26	0.37	0.66	0.42	0.88	0.70
130	1.95	13.73	77.97	11.56	0.79	10.22	4.31	13.83	95.53	0.66	0.66	0.75	1.02	0.92	0.80	0.49	1.60
140	2.10	12.15	82.79	12.51	2.39	13.78	8.02	2.05	103.71	0.87	0.81	0.73	1.03	1.18	1.21	1.13	1.56
150	2.25	10.81	87.12	11.41	4.04	12.74	7.38	-3.29	101.67	0.85	1.20	0.53	0.28	0.51	0.43	0.59	0.90
160	2.40	7.41	94.90	17.03	2.22	14.37	10.24	21.35	134.94	0.93	0.89	0.35	0.39	0.52	0.63	1.60	1.05
170	2.55	4.41	101.73	14.36	5.30	16.62	12.17	-0.92	118.73	0.98	0.97	0.49	0.52	0.43	0.32	0.48	1.15
190	2.85	0.64	110.89	19.99	4.45	19.03	10.24	10.04	137.10	0.60	1.37	0.50	0.58	0.62	1.29	0.97	1.42
200	3.00	2.94	116.73	21.26	6.75	18.51	12.99	-1.14	148.70	1.18	1.97	1.70	1.42	1.18	1.53	3.23	4.21
210	3.15	-1.86	124.50	18.61	10.38	14.03	15.12	-13.42	149.73	1.67	0.79	0.90	0.92	0.74	0.71	1.47	1.87
220	3.30	-2.11	127.12	17.93	14.57	11.49	15.12	-29.01	149.97	1.22	0.80	0.56	0.51	1.10	0.83	0.83	1.69
230	3.45	1.13	131.11	24.33	9.23	16.83	22.02	-4.35	181.36	1.70	0.65	0.57	0.66	0.85	0.91	1.73	2.31

Table 51. Damper-bearing measured dynamic stiffnesses for 4000 rpm and 689 kPa

Ω (Hz)	Ω/ω	EXPERIMENT															
		Dynamic Stiffness (MN/m)								Uncertainty (MN/m)							
		$Re(H_{xx})$	$Im(H_{xx})$	$Re(H_{xy})$	$Im(H_{xy})$	$Re(H_{yx})$	$Im(H_{yx})$	$Re(H_{yy})$	$Im(H_{yy})$	$Re(U_{xx})$	$Im(U_{xx})$	$Re(U_{xy})$	$Im(U_{xy})$	$Re(U_{yx})$	$Im(U_{yx})$	$Re(U_{yy})$	$Im(U_{yy})$
20	0.30	36.89	10.48	3.10	1.36	10.70	2.74	44.48	22.25	4.84	3.27	0.88	0.82	1.15	2.09	0.65	0.62
30	0.45	29.77	18.80	4.35	2.23	4.15	0.65	44.26	24.13	3.97	1.76	0.29	0.59	1.30	1.00	1.30	1.13
40	0.60	27.91	24.74	4.80	2.28	9.98	1.09	41.88	32.14	1.72	0.95	0.29	0.36	0.40	1.53	1.29	0.66
50	0.75	32.58	29.80	5.68	2.62	7.44	1.50	38.77	37.32	1.08	2.68	0.28	0.46	1.07	0.94	1.00	0.64
80	1.20	28.51	42.24	8.44	4.73	7.89	1.03	4.48	69.87	1.82	1.12	0.72	0.60	0.87	0.61	1.20	1.56
90	1.35	28.70	48.36	8.51	3.07	9.83	4.60	39.31	71.13	1.17	1.29	0.35	0.75	0.36	1.03	1.31	1.15
100	1.50	27.84	55.68	9.84	4.15	6.80	6.51	35.07	77.39	1.93	1.13	0.22	0.35	0.68	0.71	0.92	1.01
110	1.65	28.45	62.22	10.69	5.02	10.04	8.54	29.52	84.69	1.15	1.35	0.50	0.53	0.64	0.60	0.78	1.05
130	1.95	22.57	73.77	11.07	5.84	7.51	8.15	23.56	103.60	1.03	2.11	0.35	0.35	0.82	0.82	1.34	1.95
150	2.25	20.99	81.99	12.15	10.07	10.66	10.75	6.28	107.27	1.29	1.82	0.37	0.54	0.57	0.98	1.44	1.62
160	2.40	20.50	89.90	16.38	6.85	11.00	14.65	35.69	146.29	1.16	0.87	0.91	0.91	1.11	0.87	2.49	2.67
170	2.55	18.74	92.89	13.88	11.69	13.08	16.98	8.19	126.38	2.24	1.54	1.02	0.36	0.54	0.72	0.79	1.82
190	2.85	12.50	101.80	16.37	12.14	16.70	15.86	26.17	145.08	2.38	1.48	0.99	0.54	0.66	1.04	1.96	2.04
200	3.00	15.71	106.16	18.39	13.66	14.04	19.05	15.91	157.85	2.01	2.76	0.66	0.88	0.71	0.99	2.08	2.79
220	3.30	8.65	118.33	16.46	21.71	10.16	21.08	-15.47	160.32	5.08	2.70	1.19	0.77	0.93	0.93	1.12	2.32
230	3.45	11.51	123.27	24.77	19.17	14.44	28.40	7.94	193.19	5.29	1.24	0.91	1.84	0.79	1.25	2.19	2.88

Table 52. Damper-bearing measured dynamic stiffnesses for 6000 rpm and 0 kPa

Ω (Hz)	Ω/ω	EXPERIMENT															
		Dynamic Stiffness (MN/m)								Uncertainty (MN/m)							
		$Re(H_{xx})$	$Im(H_{xx})$	$Re(H_{xy})$	$Im(H_{xy})$	$Re(H_{yx})$	$Im(H_{yx})$	$Re(H_{yy})$	$Im(H_{yy})$	$Re(U_{xx})$	$Im(U_{xx})$	$Re(U_{xy})$	$Im(U_{xy})$	$Re(U_{yx})$	$Im(U_{yx})$	$Re(U_{yy})$	$Im(U_{yy})$
20	0.20	35.96	20.87	-0.23	-5.22	4.19	6.80	36.97	19.41	2.01	3.99	0.57	0.73	1.55	2.28	0.45	0.45
30	0.30	36.27	27.11	-2.46	-3.85	6.08	3.11	32.71	20.62	3.42	1.98	0.64	0.34	1.16	0.83	0.45	0.54
40	0.40	29.73	29.20	0.23	0.05	7.11	4.31	38.02	28.85	1.35	1.34	1.05	0.95	1.39	1.26	0.51	0.97
50	0.50	31.37	29.66	-3.43	-4.42	6.23	2.18	30.86	30.48	1.41	1.15	0.44	0.44	0.42	0.59	0.48	0.74
70	0.70	25.15	41.62	0.51	-1.57	5.12	2.63	27.43	44.19	1.36	1.71	0.62	0.64	0.76	0.62	0.70	0.97
80	0.80	30.47	48.82	1.43	7.56	9.28	2.62	20.35	56.15	1.63	2.82	1.12	1.32	0.71	0.81	0.75	1.88
90	0.90	33.09	45.07	5.35	-1.96	15.65	-0.14	24.32	66.16	2.92	2.47	1.48	1.35	2.78	1.21	0.72	2.39
130	1.30	21.52	53.23	6.33	-8.30	8.80	-1.44	14.21	83.67	1.73	5.21	0.82	2.39	3.40	0.90	1.18	2.68
140	1.40	20.87	71.12	8.40	-11.01	13.54	2.55	9.76	91.74	6.11	5.26	1.49	1.64	4.22	1.22	1.24	2.86
150	1.50	20.88	70.69	9.03	-15.19	11.61	6.10	9.18	93.95	2.61	4.93	2.35	0.95	2.65	1.53	0.87	4.36
160	1.60	15.99	73.13	6.77	-10.50	6.87	5.99	6.90	99.33	3.31	4.02	1.57	1.64	2.29	4.64	0.94	3.35
170	1.70	4.78	84.90	9.78	-11.71	6.92	8.95	8.18	105.49	1.88	3.04	1.52	2.67	0.83	4.06	1.86	2.27
190	1.90	-0.48	90.98	1.90	-9.75	9.37	9.62	-0.03	146.04	3.33	4.24	1.94	2.17	2.65	3.31	2.40	3.07
200	2.00	-14.77	97.10	-0.52	-3.27	12.95	20.48	8.47	141.48	3.77	3.67	4.12	3.56	1.63	4.16	3.99	4.85
220	2.20	-20.46	108.25	-1.07	8.77	19.35	26.97	3.56	146.37	1.50	2.84	2.17	2.72	1.55	2.04	1.09	3.22
230	2.30	-24.14	113.40	6.15	27.11	20.84	28.93	12.27	140.00	2.94	4.48	3.06	2.06	2.27	1.78	2.10	3.53
250	2.50	-34.77	124.74	13.11	32.06	20.19	28.67	-10.97	152.53	2.02	3.93	1.87	1.78	2.00	1.46	1.72	4.39
260	2.60	-48.05	133.45	26.30	22.44	27.06	32.64	-20.48	160.21	1.61	1.70	3.30	3.53	1.17	0.93	1.56	3.95
270	2.70	-43.29	130.67	13.43	21.54	24.06	41.56	-21.22	169.35	1.73	3.62	2.56	3.69	2.40	0.69	1.62	4.65
280	2.80	-54.68	141.57	33.32	12.02	28.06	35.41	-27.51	172.49	2.01	3.43	1.74	2.84	2.59	0.84	1.45	3.50
290	2.90	-43.34	141.42	26.07	28.48	23.68	35.15	-11.91	178.55	2.17	3.60	2.59	3.93	1.59	1.12	2.02	5.87

Table 53. Damper-bearing measured dynamic stiffnesses for 6000 rpm and 172 kPa

Ω (Hz)	Ω/ω	EXPERIMENT															
		Dynamic Stiffness (MN/m)								Uncertainty (MN/m)							
		$Re(H_{xx})$	$Im(H_{xx})$	$Re(H_{xy})$	$Im(H_{xy})$	$Re(H_{yx})$	$Im(H_{yx})$	$Re(H_{yy})$	$Im(H_{yy})$	$Re(U_{xx})$	$Im(U_{xx})$	$Re(U_{xy})$	$Im(U_{xy})$	$Re(U_{yx})$	$Im(U_{yx})$	$Re(U_{yy})$	$Im(U_{yy})$
20	0.20	30.74	23.88	-2.43	-5.26	2.56	3.35	36.85	16.67	1.09	1.20	0.36	0.39	1.10	1.34	0.87	0.87
30	0.30	29.86	22.23	-3.00	-3.99	2.93	0.44	35.86	19.47	0.37	0.88	0.23	0.33	0.52	0.90	0.89	0.45
40	0.40	30.29	26.05	-3.64	-3.48	5.13	2.50	34.47	27.92	0.82	1.06	0.43	0.34	0.97	0.63	0.72	0.47
50	0.50	29.95	28.39	-3.75	-3.76	5.43	0.39	31.17	32.71	1.10	0.64	0.35	0.39	0.40	0.44	0.68	0.88
70	0.70	23.91	42.11	-1.50	-2.88	5.68	0.51	24.65	47.37	0.75	1.15	0.47	0.25	0.44	0.39	0.47	0.52
80	0.80	25.58	45.23	0.66	-3.75	9.17	2.97	35.03	68.31	0.84	0.55	0.41	0.80	0.87	1.36	2.20	0.98
90	0.90	21.30	53.08	1.15	-3.31	6.96	1.13	26.19	63.62	0.84	0.77	0.71	0.25	0.56	0.74	0.84	0.92
100	1.00	12.78	52.82	-5.70	4.18	10.56	-9.50	17.16	62.14	2.86	2.27	3.42	2.38	2.43	2.07	3.01	2.95
110	1.10	14.52	59.84	-2.87	1.34	10.32	-3.33	13.67	68.91	3.01	2.98	4.18	3.06	2.16	2.97	2.32	4.35
130	1.30	18.33	75.91	6.63	-4.92	4.75	3.37	12.31	84.84	1.17	1.15	0.81	1.01	0.71	0.36	1.04	1.43
140	1.40	15.53	82.57	8.47	-6.68	4.20	6.21	4.20	91.63	0.97	1.61	0.60	0.69	1.08	0.85	1.66	1.40
150	1.50	10.70	86.47	7.33	-3.44	5.54	0.37	-11.66	89.47	1.47	1.09	0.53	0.82	0.90	1.01	2.86	1.66
160	1.60	8.91	96.74	11.66	-10.17	1.59	14.71	11.99	123.67	0.99	1.30	1.00	0.69	1.37	1.31	1.10	2.45
170	1.70	1.36	100.23	8.97	-7.52	5.62	13.82	0.02	112.11	1.22	0.96	0.85	0.92	0.61	0.85	1.45	1.08
190	1.90	-4.13	110.82	8.01	-10.46	0.02	14.06	-7.05	120.03	1.35	1.83	1.03	1.66	1.84	1.42	2.18	1.13
200	2.00	-7.53	112.97	5.72	-9.06	-5.00	19.06	-13.54	120.38	2.45	1.88	2.73	1.91	2.17	2.25	4.17	1.01
230	2.30	-9.84	125.31	-0.45	-7.76	4.74	35.69	-20.77	172.54	3.35	2.81	3.31	2.72	2.80	3.11	1.60	1.61
250	2.50	-20.42	133.50	-21.27	1.21	13.72	44.56	-54.45	137.87	1.37	1.13	2.41	5.08	2.38	2.35	5.55	4.10
260	2.60	-40.37	135.82	-25.51	13.39	10.07	63.76	-80.93	156.07	2.49	6.14	2.08	10.41	4.99	5.84	6.41	11.45
280	2.80	-48.19	127.29	-16.88	22.52	19.48	63.22	-49.07	218.94	3.11	6.21	3.66	6.95	4.36	3.20	3.45	6.83

Table 54. Damper-bearing measured dynamic stiffnesses for 6000 rpm and 345 kPa

Ω (Hz)	Ω/ω	EXPERIMENT															
		Dynamic Stiffness (MN/m)								Uncertainty (MN/m)							
		$Re(H_{xx})$	$Im(H_{xx})$	$Re(H_{xy})$	$Im(H_{xy})$	$Re(H_{yx})$	$Im(H_{yx})$	$Re(H_{yy})$	$Im(H_{yy})$	$Re(U_{xx})$	$Im(U_{xx})$	$Re(U_{xy})$	$Im(U_{xy})$	$Re(U_{yx})$	$Im(U_{yx})$	$Re(U_{yy})$	$Im(U_{yy})$
20	0.20	32.65	14.04	-2.55	-2.80	6.62	-0.56	31.65	13.29	2.46	2.06	0.24	0.25	0.68	1.67	0.62	0.75
30	0.30	27.37	16.01	-1.60	-1.92	2.75	-0.42	30.99	15.59	1.23	0.75	0.17	0.24	0.61	0.31	0.30	0.54
40	0.40	25.54	21.29	-1.93	-1.73	4.39	0.95	29.82	21.68	1.24	0.55	0.16	0.20	0.38	0.13	0.39	0.55
50	0.50	27.46	20.23	-1.86	-1.33	5.19	1.37	28.63	24.99	0.78	0.64	0.33	0.28	0.29	0.35	0.41	0.65
70	0.70	23.43	32.56	0.27	-1.27	5.48	1.86	23.25	34.62	0.71	0.61	0.34	0.34	0.27	0.36	0.51	0.53
90	0.90	19.49	38.99	1.47	-1.70	7.23	2.11	23.62	46.04	2.73	0.74	1.02	2.13	0.42	2.25	2.69	1.11
110	1.10	17.61	50.46	2.92	-3.05	8.18	3.66	17.28	54.70	1.20	1.42	0.76	0.81	0.40	1.03	1.43	1.27
130	1.30	13.17	59.70	4.83	-2.34	6.54	4.16	11.79	65.24	0.61	0.32	0.31	0.32	0.21	0.57	0.84	0.57
140	1.40	11.37	62.55	5.16	-2.49	8.56	6.29	4.74	71.36	0.44	0.33	0.31	0.26	0.42	0.24	0.79	0.86
150	1.50	7.72	68.65	5.37	-1.71	8.06	5.62	-2.79	70.36	0.60	0.29	0.31	0.32	0.37	0.23	0.58	0.74
160	1.60	4.06	74.24	8.72	-3.43	6.21	6.88	16.51	90.70	0.36	0.31	0.31	0.37	0.30	0.31	0.73	0.67
170	1.70	0.93	78.20	6.71	-2.69	8.26	9.63	-0.05	81.86	0.38	0.47	0.36	0.40	0.28	0.34	0.63	0.73
190	1.90	-4.06	87.49	10.62	-3.95	9.13	9.84	0.92	93.88	1.10	0.81	1.17	1.68	0.77	0.39	0.65	0.83
230	2.30	-6.61	104.23	9.13	1.17	6.90	18.28	-7.73	118.46	1.03	1.35	0.38	0.74	0.55	1.12	0.57	1.54

Table 55. Damper-bearing measured dynamic stiffnesses for 6000 rpm and 517 kPa

Ω (Hz)	Ω/ω	EXPERIMENT															
		Dynamic Stiffness (MN/m)								Uncertainty (MN/m)							
		$Re(H_{xx})$	$Im(H_{xx})$	$Re(H_{xy})$	$Im(H_{xy})$	$Re(H_{yx})$	$Im(H_{yx})$	$Re(H_{yy})$	$Im(H_{yy})$	$Re(U_{xx})$	$Im(U_{xx})$	$Re(U_{xy})$	$Im(U_{xy})$	$Re(U_{yx})$	$Im(U_{yx})$	$Re(U_{yy})$	$Im(U_{yy})$
20	0.20	40.58	18.18	-2.12	-3.21	6.28	-0.94	42.75	20.67	3.09	1.17	0.30	0.85	0.83	1.51	0.65	1.19
30	0.30	36.02	20.50	-1.08	-1.96	2.31	-0.92	42.22	23.34	0.61	0.94	0.38	0.18	0.64	0.74	0.95	0.40
40	0.40	32.27	27.92	-0.82	-1.77	5.39	0.10	40.81	32.03	0.90	0.87	0.34	0.44	0.64	0.42	1.00	0.64
50	0.50	35.18	32.52	-0.38	-1.68	5.78	1.16	38.24	37.21	1.08	0.72	0.37	0.53	0.59	0.48	0.82	0.97
70	0.70	32.51	44.36	2.89	-1.38	6.97	2.18	34.05	53.34	1.22	0.94	0.41	0.63	0.73	0.47	1.10	0.69
80	0.80	28.36	46.44	6.96	-0.80	1.96	-7.13	8.16	102.36	1.14	0.96	0.48	0.91	1.37	1.17	0.66	1.87
90	0.90	27.45	53.40	5.36	-1.20	8.79	1.25	37.55	70.59	4.18	1.29	2.01	4.22	1.69	3.16	5.20	1.83
110	1.10	26.13	68.07	7.77	-3.94	10.44	2.80	29.33	80.21	2.33	1.15	1.52	1.46	0.83	1.59	2.12	1.13
130	1.30	20.12	79.67	11.21	-3.77	8.70	3.09	24.24	95.12	0.90	0.91	0.48	0.78	0.79	0.45	1.71	1.05
140	1.40	18.14	83.74	12.73	-4.23	10.65	5.77	12.22	102.67	0.97	0.89	0.47	0.66	0.46	0.74	1.59	1.08
150	1.50	14.24	89.09	12.09	-3.32	9.49	6.42	4.34	99.54	1.02	1.13	0.78	0.39	0.62	0.89	1.11	0.78
160	1.60	11.71	97.15	17.43	-8.02	9.76	9.08	32.12	134.13	0.91	1.04	0.46	0.74	0.73	0.66	1.28	1.93
170	1.70	6.18	102.71	14.30	-5.44	12.14	12.77	6.34	117.91	0.82	1.18	0.61	0.61	0.76	0.78	1.08	1.65
190	1.90	0.00	114.66	16.65	-6.79	16.50	13.91	12.13	130.04	1.45	1.63	1.27	1.21	1.61	1.21	2.33	3.29
210	2.10	-4.22	128.82	13.64	0.11	15.98	17.66	-10.23	142.24	0.69	1.42	0.91	1.39	1.13	0.39	1.17	1.69
220	2.20	-3.69	136.37	14.22	5.17	13.63	14.67	-29.14	146.83	0.89	1.41	0.57	1.51	0.58	0.60	0.48	1.44
230	2.30	-0.31	140.30	18.43	-2.29	18.69	20.68	-0.76	175.15	1.17	1.44	0.71	1.32	1.02	0.97	1.91	2.13

Table 56. Damper-bearing measured dynamic stiffnesses for 6000 rpm and 689 kPa

Ω (Hz)	Ω/ω	EXPERIMENT															
		Dynamic Stiffness (MN/m)								Uncertainty (MN/m)							
		$Re(H_{xx})$	$Im(H_{xx})$	$Re(H_{xy})$	$Im(H_{xy})$	$Re(H_{yx})$	$Im(H_{yx})$	$Re(H_{yy})$	$Im(H_{yy})$	$Re(U_{xx})$	$Im(U_{xx})$	$Re(U_{xy})$	$Im(U_{xy})$	$Re(U_{yx})$	$Im(U_{yx})$	$Re(U_{yy})$	$Im(U_{yy})$
20	0.20	43.40	20.45	-1.50	-3.01	8.35	-1.59	49.38	25.44	1.22	1.34	0.61	0.44	2.34	3.28	0.63	0.90
30	0.30	40.16	22.22	-0.48	-1.51	1.70	-1.05	49.92	28.96	1.20	1.14	0.61	0.51	1.21	2.01	0.58	0.74
40	0.40	36.69	30.94	-0.20	-1.43	5.84	-0.29	47.63	38.08	0.70	0.93	0.79	0.37	0.93	0.38	0.82	0.81
50	0.50	40.30	36.48	0.91	-1.30	5.86	1.19	45.99	44.54	0.95	0.93	0.46	0.33	1.36	1.14	0.48	0.87
70	0.70	38.14	48.24	3.56	-1.41	7.78	2.42	43.61	62.14	0.92	1.24	0.71	0.53	1.03	1.53	0.79	1.35
80	0.80	35.17	50.82	7.75	0.43	9.45	-2.42	9.95	81.77	0.44	0.70	0.84	0.56	1.42	1.17	0.61	1.42
90	0.90	34.37	57.78	8.01	-2.24	10.18	2.58	47.60	80.31	1.73	1.30	1.70	2.02	1.29	1.49	2.07	2.60
130	1.30	25.44	85.21	13.26	-4.33	10.68	2.60	35.23	107.63	0.57	2.00	1.87	1.46	0.96	0.88	1.30	3.04
140	1.40	24.91	90.34	15.75	-4.67	12.71	4.60	24.43	116.55	0.51	2.63	1.81	1.06	1.22	1.31	0.83	2.89
150	1.50	21.09	95.00	15.35	-3.84	11.69	5.69	14.76	112.70	0.41	2.19	1.47	0.66	0.55	0.48	1.03	2.89
160	1.60	19.27	103.97	20.44	-8.97	11.46	8.34	40.87	149.89	0.83	2.35	1.10	0.80	0.81	1.23	1.65	4.87
170	1.70	13.63	108.93	18.06	-6.04	14.56	12.31	16.21	131.80	1.11	2.83	0.91	0.80	1.32	1.32	0.72	4.33
190	1.90	6.99	121.83	20.82	-6.37	19.41	14.28	20.59	148.14	0.92	4.10	1.39	1.16	2.27	0.82	1.42	5.29
220	2.20	2.82	145.89	18.77	5.25	18.21	15.50	-18.64	161.22	1.29	4.37	1.34	2.38	1.72	2.45	1.37	4.27
230	2.30	6.06	150.50	24.72	-2.05	24.09	20.29	3.51	194.48	1.97	4.11	1.71	2.05	1.02	3.17	2.45	6.44

Table 57. Damper-bearing measured dynamic stiffnesses for 6000 rpm and 862 kPa

Ω (Hz)	Ω/ω	EXPERIMENT															
		Dynamic Stiffness (MN/m)								Uncertainty (MN/m)							
		$Re(H_{xx})$	$Im(H_{xx})$	$Re(H_{xy})$	$Im(H_{xy})$	$Re(H_{yx})$	$Im(H_{yx})$	$Re(H_{yy})$	$Im(H_{yy})$	$Re(U_{xx})$	$Im(U_{xx})$	$Re(U_{xy})$	$Im(U_{xy})$	$Re(U_{yx})$	$Im(U_{yx})$	$Re(U_{yy})$	$Im(U_{yy})$
20	0.20	43.16	19.03	-1.57	-1.81	7.47	0.69	53.01	26.28	2.62	4.14	0.48	0.40	2.89	3.39	0.39	1.99
30	0.30	41.22	22.40	-0.48	-0.69	1.49	0.96	55.89	32.37	1.67	1.36	0.46	0.25	1.15	1.37	0.39	1.29
40	0.40	39.93	30.32	0.10	-0.58	6.01	0.53	52.33	41.80	2.48	0.81	0.35	0.39	1.51	1.38	0.35	1.64
50	0.50	42.14	37.38	1.46	0.09	5.75	1.52	52.13	46.28	1.19	3.29	0.42	0.48	1.16	0.93	0.34	2.20
70	0.70	39.91	47.41	5.05	-0.09	7.76	3.18	49.08	64.96	1.45	1.07	0.83	0.42	1.61	1.74	0.49	2.43
80	0.80	37.87	51.08	7.54	1.22	10.25	1.51	29.12	75.10	0.80	2.13	0.98	0.57	1.32	1.15	0.94	2.51
90	0.90	37.91	56.47	8.79	-0.95	10.29	3.28	53.83	84.12	1.71	2.35	0.95	1.18	1.10	1.61	1.46	2.74
130	1.30	28.09	83.13	13.96	-2.91	12.34	3.15	40.72	114.85	1.34	2.93	1.77	0.93	1.64	1.69	1.31	4.50
140	1.40	29.42	88.34	16.41	-3.34	14.62	4.74	31.48	121.81	1.17	4.07	1.66	0.70	1.12	1.18	1.09	4.50
150	1.50	25.32	93.25	16.08	-2.33	13.56	5.09	23.69	115.75	0.63	2.04	0.72	0.59	1.11	0.97	1.79	3.91
160	1.60	23.25	102.53	22.11	-6.34	14.22	7.45	46.36	155.93	0.77	3.75	1.52	1.27	1.29	1.23	2.28	5.23
170	1.70	19.01	107.27	19.56	-3.60	16.22	10.45	22.40	134.60	1.06	3.41	0.91	0.77	1.08	0.97	2.13	5.55
190	1.90	12.12	117.64	23.70	-4.44	19.78	12.56	29.84	152.95	0.60	4.66	1.09	1.16	2.01	1.47	2.08	7.16
220	2.20	7.11	139.31	21.72	6.91	19.15	16.33	-10.17	165.69	1.25	7.04	1.38	2.11	1.78	1.27	1.51	8.00
230	2.30	9.28	144.55	29.11	0.71	24.57	21.12	12.15	198.77	2.85	6.95	1.72	1.82	1.84	1.42	2.05	8.26
240	2.40	7.37	148.83	23.18	3.28	21.67	20.38	-4.58	188.03	4.52	3.75	3.38	2.26	2.30	3.20	5.64	9.38
250	2.50	7.67	152.35	24.07	4.71	19.21	21.87	-8.56	190.49	4.56	2.58	1.92	0.64	1.17	2.08	1.54	9.23

Table 58. Damper-bearing measured dynamic stiffnesses for 8000 rpm and 0 kPa

Ω (Hz)	Ω/ω	EXPERIMENT															
		Dynamic Stiffness (MN/m)								Uncertainty (MN/m)							
		$Re(H_{xx})$	$Im(H_{xx})$	$Re(H_{xy})$	$Im(H_{xy})$	$Re(H_{yx})$	$Im(H_{yx})$	$Re(H_{yy})$	$Im(H_{yy})$	$Re(U_{xx})$	$Im(U_{xx})$	$Re(U_{xy})$	$Im(U_{xy})$	$Re(U_{yx})$	$Im(U_{yx})$	$Re(U_{yy})$	$Im(U_{yy})$
20	0.15	42.82	23.34	-1.55	-7.63	5.09	6.36	41.77	22.48	4.88	2.13	1.60	1.82	1.85	1.36	1.94	2.19
30	0.23	40.03	29.62	-2.73	-3.74	5.68	1.73	38.10	24.71	5.86	3.01	0.52	0.81	1.42	0.96	2.54	1.36
40	0.30	37.05	34.21	0.18	-1.48	8.71	4.09	44.37	31.97	2.91	1.65	1.09	1.72	1.51	0.85	1.45	1.98
50	0.38	34.82	33.45	-3.79	-4.72	6.85	2.13	37.43	35.57	2.51	4.90	1.03	0.97	0.72	0.51	2.10	2.32
70	0.53	31.56	45.86	-1.68	-3.71	7.09	1.67	34.84	49.06	4.10	5.14	1.01	2.37	1.33	0.76	2.30	3.88
80	0.60	38.18	49.96	2.64	3.10	10.18	2.38	28.74	60.37	2.52	3.66	1.64	4.62	0.97	1.57	3.14	4.59
90	0.68	42.72	53.70	1.56	-0.08	13.84	1.72	30.51	71.63	3.54	4.26	3.74	2.04	2.22	3.55	1.70	4.17
100	0.75	40.77	57.44	6.16	-3.53	13.37	1.46	35.72	73.56	7.97	5.22	9.67	4.85	8.22	3.44	4.39	8.38
110	0.83	43.33	60.76	18.44	-7.22	17.29	1.34	35.09	80.81	15.94	8.57	10.29	4.56	6.22	5.56	4.51	1.17
150	1.13	28.44	75.36	9.02	-15.49	9.68	0.49	22.63	96.42	4.50	9.24	5.24	3.59	5.97	4.21	3.27	5.93
160	1.20	22.87	81.92	10.69	-13.54	5.77	2.22	22.52	101.93	3.54	4.24	3.44	4.15	2.86	2.87	6.67	4.97
170	1.28	14.71	85.94	13.33	-11.87	6.10	5.66	20.54	109.71	2.81	5.21	1.86	2.45	1.41	2.17	3.14	3.18
190	1.43	8.06	91.87	10.22	-14.73	7.11	8.76	13.70	143.37	2.95	5.01	5.24	4.22	1.08	4.32	4.95	10.76
200	1.50	-5.40	98.93	5.09	-6.73	7.06	18.41	18.22	138.91	5.60	4.34	3.43	2.49	2.07	6.31	3.72	9.15
210	1.58	-8.68	102.55	18.26	-1.06	7.35	22.45	8.06	137.78	4.28	7.01	1.95	1.58	3.18	5.10	4.77	9.61
220	1.65	-13.18	107.46	7.13	0.82	12.67	29.77	7.82	146.86	5.28	6.42	6.84	3.92	4.56	6.54	1.65	13.68
230	1.73	-22.33	113.77	9.60	15.48	16.47	33.33	14.34	145.64	2.53	9.65	4.75	8.30	5.50	5.00	1.99	8.40
240	1.80	-26.29	121.33	25.14	25.76	17.75	31.00	11.63	141.11	3.87	8.88	4.44	8.78	6.87	4.41	3.83	8.16
260	1.95	-45.69	135.81	33.41	19.25	23.45	42.42	-14.02	162.85	13.80	16.06	4.06	7.16	11.72	3.83	2.87	15.43
270	2.03	-42.30	135.12	18.81	15.52	22.84	50.13	-15.61	173.66	2.33	6.63	6.33	7.31	9.42	2.20	2.31	12.72
280	2.10	-52.69	141.39	42.27	3.49	27.15	48.48	-20.56	175.34	7.74	13.04	5.50	4.27	10.99	4.72	4.38	14.00
290	2.18	-41.19	145.10	30.59	21.13	27.36	47.16	-6.52	181.91	1.12	8.30	3.04	9.65	6.77	4.18	2.36	9.31
300	2.25	-49.84	147.60	18.75	8.16	30.26	53.97	-11.07	192.04	2.28	10.06	4.66	8.89	6.04	3.05	2.18	13.15

Table 59. Damper-bearing measured dynamic stiffnesses for 8000 rpm and 172 kPa

Ω (Hz)	Ω/ω	EXPERIMENT															
		Dynamic Stiffness (MN/m)								Uncertainty (MN/m)							
		$Re(H_{xx})$	$Im(H_{xx})$	$Re(H_{xy})$	$Im(H_{xy})$	$Re(H_{yx})$	$Im(H_{yx})$	$Re(H_{yy})$	$Im(H_{yy})$	$Re(U_{xx})$	$Im(U_{xx})$	$Re(U_{xy})$	$Im(U_{xy})$	$Re(U_{yx})$	$Im(U_{yx})$	$Re(U_{yy})$	$Im(U_{yy})$
20	0.15	32.85	25.90	-3.03	-5.79	2.11	1.94	40.20	18.31	1.46	1.66	0.34	0.53	0.76	0.88	1.47	1.31
30	0.23	33.35	24.41	-3.20	-4.56	3.03	-0.87	39.77	21.76	1.20	1.31	0.23	0.57	0.62	0.74	1.39	1.32
40	0.30	34.69	28.94	-3.93	-4.35	4.37	1.54	38.06	29.49	1.49	1.40	0.43	0.26	0.80	0.61	1.11	1.81
50	0.38	34.29	30.15	-4.30	-4.44	5.92	-0.02	36.27	34.28	1.60	1.84	0.26	0.72	0.81	0.86	1.46	2.55
70	0.53	29.18	44.40	-2.17	-3.73	5.74	0.55	29.47	48.62	1.55	2.53	0.66	1.17	0.46	0.71	1.26	3.31
80	0.60	31.18	46.66	0.00	-4.81	8.33	4.24	41.56	71.28	0.83	2.82	0.67	1.15	0.37	0.89	1.58	4.60
90	0.68	27.71	54.35	0.89	-4.51	7.80	1.96	32.10	65.30	0.70	3.09	0.92	0.86	0.40	0.99	0.70	4.45
100	0.75	28.53	59.48	1.45	-4.83	7.16	-2.39	31.81	70.87	0.60	2.62	1.06	1.10	0.77	1.22	0.82	4.46
110	0.83	27.26	64.41	2.65	-4.49	8.40	-0.46	26.09	75.66	1.32	3.30	1.38	1.81	0.64	1.38	1.31	4.21
140	1.05	22.75	81.29	6.78	-4.94	6.40	2.88	13.08	91.81	1.62	7.08	4.08	2.43	3.73	1.02	2.03	6.12
150	1.13	19.54	86.38	8.50	-2.95	5.33	-0.84	-1.12	89.29	0.90	3.61	1.71	0.71	1.38	0.68	1.42	3.53
160	1.20	17.74	96.26	14.39	-8.68	0.01	10.27	23.60	118.02	0.57	3.94	3.39	1.31	2.36	0.85	1.80	5.27
170	1.28	11.03	98.57	12.85	-6.26	3.33	9.78	10.04	108.10	1.15	3.91	2.26	0.64	1.33	1.49	1.69	4.37
190	1.43	4.81	105.56	14.47	-11.34	-1.90	11.79	4.96	115.21	2.28	4.51	1.69	2.27	1.79	2.28	2.42	4.65
200	1.50	0.76	108.33	13.73	-11.31	-6.88	17.91	-3.47	117.52	2.07	5.00	1.25	2.50	2.16	2.81	2.46	6.57
210	1.58	-5.87	121.34	12.54	-7.37	-20.50	36.44	-22.27	115.33	2.24	6.18	1.06	2.41	2.10	4.91	4.24	5.22
220	1.65	-1.98	128.93	21.07	-1.49	-42.69	67.27	-63.43	147.52	2.81	6.73	2.59	1.39	7.02	6.71	5.70	7.19
230	1.73	-7.14	121.47	11.79	-14.50	2.24	33.07	-11.74	159.65	2.02	6.32	1.89	1.67	1.83	3.83	3.99	10.68

Table 60. Damper-bearing measured dynamic stiffnesses for 8000 rpm and 345 kPa

Ω (Hz)	Ω/ω	EXPERIMENT															
		Dynamic Stiffness (MN/m)								Uncertainty (MN/m)							
		$Re(H_{xx})$	$Im(H_{xx})$	$Re(H_{xy})$	$Im(H_{xy})$	$Re(H_{yx})$	$Im(H_{yx})$	$Re(H_{yy})$	$Im(H_{yy})$	$Re(U_{xx})$	$Im(U_{xx})$	$Re(U_{xy})$	$Im(U_{xy})$	$Re(U_{yx})$	$Im(U_{yx})$	$Re(U_{yy})$	$Im(U_{yy})$
20	0.15	37.77	15.53	-3.82	-4.69	6.23	-0.85	37.66	15.23	1.09	1.26	0.25	0.21	0.99	1.12	0.28	0.44
30	0.23	34.78	18.09	-2.87	-3.36	2.96	-0.70	37.18	16.89	0.77	1.00	0.20	0.19	0.31	0.61	0.49	0.26
40	0.30	32.64	22.65	-3.37	-3.75	4.40	0.21	36.82	22.35	0.62	0.54	0.25	0.21	0.30	0.23	0.40	0.27
50	0.38	34.39	21.31	-3.46	-3.08	5.39	1.37	35.13	25.22	0.73	0.84	0.21	0.25	0.37	0.57	0.67	0.32
70	0.53	31.60	32.84	-2.03	-2.78	5.62	1.59	30.27	34.02	0.71	0.51	0.42	0.37	0.30	0.45	0.39	0.27
90	0.68	28.43	38.12	-0.51	-3.40	7.52	2.50	32.51	45.03	0.39	0.23	0.24	0.31	0.16	0.20	0.40	0.30
100	0.75	26.88	44.10	0.25	-3.39	6.97	2.46	30.00	48.94	0.63	0.52	0.41	0.41	0.32	0.25	0.42	0.40
110	0.83	26.59	48.39	1.07	-3.97	8.16	2.32	25.90	53.85	0.57	0.47	0.42	0.28	0.20	0.30	0.41	0.38
150	1.13	15.65	63.20	2.82	-2.54	8.98	3.78	6.30	66.22	0.42	0.66	0.79	0.72	0.40	0.55	0.74	0.75
160	1.20	13.16	68.81	6.33	-4.34	6.68	5.02	26.23	85.60	0.44	0.50	0.51	0.70	0.42	0.39	0.60	0.51
170	1.28	10.52	72.87	5.90	-4.62	8.37	7.46	10.73	77.71	0.59	0.28	0.78	0.34	0.13	0.19	0.74	0.48
190	1.43	5.68	80.34	10.08	-5.28	7.68	7.71	9.91	85.61	0.59	0.54	0.36	0.58	0.22	0.36	0.87	0.38
200	1.50	4.35	83.73	9.35	-3.74	5.70	10.06	3.28	88.74	0.71	0.60	0.37	0.46	0.25	0.25	0.74	0.59
210	1.58	-0.40	88.35	7.45	-0.99	3.14	12.73	-7.98	90.77	0.77	0.45	0.69	0.56	0.57	0.40	0.72	0.88
220	1.65	-2.90	91.29	7.67	2.43	1.03	8.86	-27.67	91.48	0.95	0.52	0.53	0.50	0.78	0.59	0.73	0.32
230	1.73	-1.01	94.03	11.01	-3.85	4.87	16.50	2.03	109.08	0.86	0.70	0.55	0.45	0.28	0.55	0.85	0.84
250	1.88	-10.93	91.80	8.47	-1.83	-1.43	24.29	-16.51	99.16	0.84	0.82	0.84	0.65	0.51	0.96	0.99	1.05

Table 61. Damper-bearing measured dynamic stiffnesses for 8000 rpm and 517 kPa

Ω (Hz)	Ω/ω	EXPERIMENT															
		Dynamic Stiffness (MN/m)								Uncertainty (MN/m)							
		$Re(H_{xx})$	$Im(H_{xx})$	$Re(H_{xy})$	$Im(H_{xy})$	$Re(H_{yx})$	$Im(H_{yx})$	$Re(H_{yy})$	$Im(H_{yy})$	$Re(U_{xx})$	$Im(U_{xx})$	$Re(U_{xy})$	$Im(U_{xy})$	$Re(U_{yx})$	$Im(U_{yx})$	$Re(U_{yy})$	$Im(U_{yy})$
20	0.15	42.63	19.41	-3.34	-4.18	4.54	-1.74	44.58	21.35	4.15	1.59	0.23	0.57	1.07	1.22	0.95	1.40
30	0.23	38.79	23.28	-2.46	-2.91	2.64	-2.23	43.56	23.59	1.51	0.84	0.24	0.35	0.76	1.00	1.29	0.34
40	0.30	36.37	29.72	-2.45	-3.24	4.52	-0.18	42.73	30.97	2.09	0.48	0.45	0.40	0.71	0.59	1.14	0.38
50	0.38	39.76	32.65	-2.65	-2.99	6.00	1.37	40.71	36.06	2.84	1.38	0.56	0.66	0.85	0.86	1.40	0.68
70	0.53	37.44	44.70	-0.01	-1.91	7.03	1.91	35.71	50.56	2.59	0.80	0.71	0.55	0.43	0.63	1.30	0.84
90	0.68	33.77	51.67	3.58	-3.17	9.56	2.58	41.84	67.74	2.56	0.96	0.57	0.46	0.87	0.49	1.11	1.08
100	0.75	32.47	58.97	4.78	-3.59	8.25	2.34	37.70	74.65	3.51	1.21	0.65	1.16	0.59	1.04	2.27	1.03
110	0.83	31.88	65.26	5.29	-4.10	10.65	1.54	33.40	77.85	9.50	1.88	2.27	4.14	0.53	5.79	5.20	2.16
150	1.13	20.33	84.77	10.49	-2.76	9.96	3.65	11.42	96.37	2.87	2.24	2.54	1.69	0.96	1.09	2.62	2.40
160	1.20	18.64	91.19	15.73	-7.14	8.21	5.22	40.90	123.43	2.64	1.17	2.60	0.88	0.84	1.22	3.64	1.79
170	1.28	14.38	95.91	14.96	-5.26	10.39	7.87	17.60	106.82	3.21	1.12	1.11	0.85	0.45	1.65	3.57	1.61
190	1.43	8.31	104.57	18.30	-9.01	10.48	9.56	23.53	114.65	3.54	1.80	1.47	0.83	1.14	1.60	3.51	1.98
200	1.50	5.85	109.14	19.04	-7.99	9.28	13.32	13.92	123.68	3.53	2.05	1.74	0.71	1.89	1.52	3.52	3.15
210	1.58	1.07	115.34	16.77	-5.20	7.07	17.44	-2.84	124.73	3.31	2.50	1.61	0.90	1.97	1.65	3.95	2.34
220	1.65	-0.41	121.60	16.18	-2.92	5.49	17.18	-20.24	130.41	2.10	2.37	1.49	2.04	2.35	1.13	3.97	2.61
230	1.73	0.38	125.02	19.85	-9.58	10.42	26.54	4.00	152.72	1.43	2.23	1.13	6.33	1.02	1.09	5.02	2.31

Table 62. Damper-bearing measured dynamic stiffnesses for 8000 rpm and 689 kPa

Ω (Hz)	Ω/ω	EXPERIMENT															
		Dynamic Stiffness (MN/m)								Uncertainty (MN/m)							
		$Re(H_{xx})$	$Im(H_{xx})$	$Re(H_{xy})$	$Im(H_{xy})$	$Re(H_{yx})$	$Im(H_{yx})$	$Re(H_{yy})$	$Im(H_{yy})$	$Re(U_{xx})$	$Im(U_{xx})$	$Re(U_{xy})$	$Im(U_{xy})$	$Re(U_{yx})$	$Im(U_{yx})$	$Re(U_{yy})$	$Im(U_{yy})$
20	0.15	47.76	19.90	-2.85	-4.03	6.80	-3.09	53.46	25.49	3.01	1.61	0.55	0.76	1.60	2.71	0.43	1.24
30	0.23	42.87	22.84	-1.32	-2.35	3.30	-1.75	52.44	27.68	1.05	1.35	0.65	0.16	1.07	1.55	0.81	0.27
40	0.30	40.58	31.99	-1.27	-2.32	5.26	-1.28	50.48	36.07	1.34	0.52	0.53	0.48	0.87	0.84	0.58	0.68
50	0.38	44.90	36.83	-0.49	-1.97	5.85	1.32	48.52	43.45	1.04	1.33	0.61	0.53	1.01	1.11	0.71	1.03
70	0.53	43.29	49.04	2.17	-1.55	8.03	2.26	45.61	61.09	0.55	1.28	0.51	0.61	1.01	1.19	0.43	0.70
80	0.60	39.31	52.04	7.50	0.43	8.04	-4.93	11.50	83.10	0.77	0.70	0.34	0.59	0.53	0.43	0.80	0.96
90	0.68	40.33	57.32	7.24	-3.08	10.19	3.58	51.20	79.50	0.78	0.67	0.33	0.64	0.88	0.68	0.73	0.80
100	0.75	39.13	64.56	8.75	-3.95	9.34	3.71	47.13	87.51	0.44	0.66	0.83	0.94	0.92	0.90	0.91	1.43
110	0.83	37.56	71.55	9.60	-3.97	12.27	2.24	43.04	93.02	1.40	1.55	1.75	1.42	1.49	1.37	1.29	1.66
140	1.05	28.60	87.97	14.55	-4.55	13.78	2.78	31.22	115.26	1.01	1.28	1.63	1.24	1.13	1.02	1.12	1.94
150	1.13	25.63	92.62	14.91	-4.11	12.57	4.03	22.40	110.63	0.42	0.97	0.85	1.21	0.70	0.68	1.24	1.22
160	1.20	24.44	100.84	21.47	-9.30	10.81	4.64	49.95	145.42	0.42	0.78	1.24	0.98	0.52	0.88	1.41	2.51
170	1.28	19.24	105.61	20.32	-6.11	13.25	8.07	25.43	126.88	0.76	0.90	1.04	0.93	0.76	0.84	0.40	1.10
190	1.43	12.34	115.87	23.31	-10.18	13.48	11.59	26.61	136.70	1.08	1.10	0.85	0.93	0.59	0.66	1.14	1.55
200	1.50	10.54	120.97	23.32	-9.46	13.48	16.77	19.12	146.22	0.72	1.06	0.58	1.12	0.67	0.59	1.13	1.79
210	1.58	5.62	128.50	20.63	-6.03	13.22	20.10	3.37	148.41	0.83	1.14	0.51	1.22	0.63	0.56	0.74	1.66
220	1.65	4.49	137.51	20.14	-2.17	12.17	19.74	-14.61	151.23	1.21	1.01	0.80	0.93	0.69	0.45	1.02	1.68
230	1.73	5.87	141.92	24.59	-9.46	19.04	28.04	9.05	181.15	1.74	1.43	1.07	1.47	1.31	1.20	1.07	1.81
250	1.88	5.37	148.22	16.85	-1.78	15.47	30.24	-11.17	171.35	3.45	3.11	2.35	6.38	2.87	1.60	2.14	5.23

Table 63. Damper-bearing measured dynamic stiffnesses for 8000 rpm and 862 kPa

Ω (Hz)	Ω/ω	EXPERIMENT															
		Dynamic Stiffness (MN/m)								Uncertainty (MN/m)							
		$Re(H_{xx})$	$Im(H_{xx})$	$Re(H_{xy})$	$Im(H_{xy})$	$Re(H_{yx})$	$Im(H_{yx})$	$Re(H_{yy})$	$Im(H_{yy})$	$Re(U_{xx})$	$Im(U_{xx})$	$Re(U_{xy})$	$Im(U_{xy})$	$Re(U_{yx})$	$Im(U_{yx})$	$Re(U_{yy})$	$Im(U_{yy})$
20	0.15	47.27	19.34	-6.38	-3.54	6.69	-1.48	57.46	24.47	1.65	1.41	0.73	0.48	0.66	1.20	0.48	0.66
30	0.23	46.43	18.81	-4.11	-0.72	0.83	0.66	58.29	26.20	0.80	0.97	0.55	0.37	1.20	0.93	0.37	0.67
40	0.30	41.89	26.30	-3.54	-0.21	5.25	-0.49	55.85	33.28	0.74	0.84	0.65	0.55	0.73	0.56	0.37	0.91
50	0.38	46.00	31.27	-2.04	-0.11	4.66	3.21	53.49	38.27	0.70	1.00	0.58	0.46	0.76	0.56	0.43	0.92
70	0.53	44.14	40.25	1.16	1.18	7.04	4.03	50.02	52.80	0.88	1.13	0.57	0.61	0.52	0.80	0.69	1.23
80	0.60	40.71	42.95	4.17	2.33	9.74	2.40	27.17	65.80	0.54	0.96	0.44	0.33	0.48	0.32	0.47	1.22
90	0.68	41.51	47.28	5.24	0.12	9.81	5.17	55.79	69.87	0.74	1.36	0.75	0.87	0.33	0.38	0.89	1.70
100	0.75	40.39	54.46	6.04	-0.87	8.57	5.00	52.32	75.40	0.51	1.22	0.72	0.92	0.52	0.56	0.96	1.46
110	0.83	39.74	60.59	7.94	-1.80	11.07	5.37	48.69	82.00	1.28	1.01	0.78	1.35	0.75	0.74	1.39	1.51
150	1.13	27.38	77.30	10.92	0.18	13.72	5.37	26.36	97.21	1.46	2.16	3.00	1.47	0.61	1.11	1.64	3.33
160	1.20	26.46	84.52	16.34	-3.83	14.54	6.80	52.37	127.43	0.74	1.92	1.62	1.60	0.62	0.67	2.28	3.15
170	1.28	23.18	88.96	15.28	-1.19	15.79	8.13	29.53	111.87	0.53	2.11	1.80	1.41	0.34	0.62	0.81	2.75
190	1.43	17.65	99.16	20.96	-3.77	16.15	7.49	36.66	122.81	0.65	1.86	1.16	0.66	0.35	0.30	0.70	2.53
200	1.50	16.49	103.77	21.26	-2.06	14.51	10.20	28.65	128.64	0.78	2.04	0.93	0.67	0.50	0.47	0.63	2.61
210	1.58	13.24	109.16	19.62	1.22	13.15	12.71	12.14	131.36	0.66	2.21	1.00	0.94	0.31	0.65	0.92	2.66
220	1.65	11.92	115.13	21.03	4.76	11.59	14.02	-3.42	131.94	0.58	2.43	0.66	0.87	0.34	0.56	0.64	3.06
230	1.73	12.32	117.91	26.44	-2.53	14.46	19.81	19.43	157.75	0.41	2.44	0.99	0.76	0.32	0.93	0.90	3.72
240	1.80	8.85	121.25	21.28	-0.52	12.71	20.45	3.22	149.53	0.75	2.57	1.35	2.16	1.26	1.62	2.84	2.35
250	1.88	7.23	124.38	20.54	-1.37	11.12	22.67	-2.22	150.72	0.46	2.38	1.16	0.73	0.82	1.14	0.98	4.16

Table 64. Damper-bearing measured dynamic stiffnesses for 10000 rpm and 0 kPa

Ω (Hz)	Ω/ω	EXPERIMENT															
		Dynamic Stiffness (MN/m)								Uncertainty (MN/m)							
		$Re(H_{xx})$	$Im(H_{xx})$	$Re(H_{xy})$	$Im(H_{xy})$	$Re(H_{yx})$	$Im(H_{yx})$	$Re(H_{yy})$	$Im(H_{yy})$	$Re(U_{xx})$	$Im(U_{xx})$	$Re(U_{xy})$	$Im(U_{xy})$	$Re(U_{yx})$	$Im(U_{yx})$	$Re(U_{yy})$	$Im(U_{yy})$
20	0.12	46.62	20.21	-2.85	-8.07	6.91	6.27	43.15	17.23	1.88	4.87	0.75	1.81	1.76	1.54	0.98	0.78
30	0.18	46.04	24.25	-4.58	-5.17	6.60	1.05	39.88	19.69	2.50	2.15	1.48	1.07	1.11	1.20	1.32	0.67
40	0.24	39.82	25.77	-0.49	-3.06	8.22	3.29	45.81	23.15	1.36	1.83	1.38	1.69	1.47	1.50	1.17	1.33
50	0.30	38.63	25.95	-3.47	-6.19	6.83	1.85	40.48	24.60	1.26	2.52	0.98	0.66	0.75	1.22	1.11	0.90
70	0.42	36.05	34.81	-1.94	-4.17	5.89	2.60	38.25	34.77	3.11	1.76	1.04	1.36	0.61	0.69	1.47	1.10
80	0.48	41.80	31.11	-0.53	-2.37	10.53	3.63	32.14	42.89	2.19	2.52	2.33	1.56	1.12	1.12	1.06	1.70
90	0.54	38.62	35.77	-4.80	-4.08	10.60	2.43	33.26	49.52	2.29	1.48	1.66	1.57	2.46	1.72	0.95	2.06
100	0.60	36.21	43.12	-2.17	-8.34	9.66	2.71	36.64	47.02	2.26	1.54	0.73	2.02	2.31	2.22	0.92	1.99
110	0.66	35.01	44.59	3.06	-8.34	12.07	2.08	33.72	54.98	1.76	3.35	2.65	2.40	2.44	1.77	2.15	1.22
130	0.78	34.12	42.18	-2.44	-8.55	11.42	-6.39	27.80	63.74	3.86	2.64	2.50	2.90	2.93	3.80	2.25	3.32
140	0.84	31.77	47.26	0.38	-4.30	10.61	-3.96	24.35	68.06	3.70	5.50	4.62	2.24	3.71	4.34	1.28	3.76
190	1.14	15.90	70.78	7.55	-8.80	10.64	1.33	20.93	101.28	1.97	2.49	3.45	3.22	3.27	4.16	2.24	2.60
200	1.20	6.66	74.89	0.68	-5.64	8.85	7.03	20.49	98.77	2.30	2.61	2.10	1.47	1.36	2.65	1.33	3.13
210	1.26	6.06	75.75	9.51	-0.18	5.68	10.74	15.24	97.17	1.38	3.33	1.45	2.41	0.90	0.84	1.20	2.75
220	1.32	2.41	79.06	-0.03	1.66	9.17	13.74	15.63	103.72	1.14	1.43	1.68	1.11	0.92	0.93	1.09	2.12
230	1.38	-5.00	80.39	2.86	10.93	9.47	16.85	18.22	104.49	2.33	1.29	1.23	2.52	1.44	0.98	1.62	3.65
250	1.50	-16.95	91.54	12.35	21.56	7.82	18.46	7.78	110.86	1.57	2.96	3.37	2.51	0.89	1.01	2.03	2.12
260	1.56	-27.53	93.33	18.93	18.79	7.32	22.95	5.24	116.06	1.25	2.51	4.61	2.80	1.53	1.34	3.28	2.60
270	1.62	-23.08	97.78	10.26	14.17	5.47	25.69	1.95	121.06	1.49	1.92	2.28	3.65	1.58	1.81	2.79	3.02
280	1.68	-27.72	101.36	23.52	15.81	3.40	27.99	3.32	115.36	2.70	2.60	3.93	1.04	1.69	1.68	1.83	4.01
290	1.74	-24.37	103.83	17.90	22.21	6.39	34.60	9.73	121.14	1.82	2.52	3.67	4.82	0.98	1.45	2.61	4.31

Table 65. Damper-bearing measured dynamic stiffnesses for 10000 rpm and 172 kPa

Ω (Hz)	Ω/ω	EXPERIMENT															
		Dynamic Stiffness (MN/m)								Uncertainty (MN/m)							
		$Re(H_{xx})$	$Im(H_{xx})$	$Re(H_{xy})$	$Im(H_{xy})$	$Re(H_{yx})$	$Im(H_{yx})$	$Re(H_{yy})$	$Im(H_{yy})$	$Re(U_{xx})$	$Im(U_{xx})$	$Re(U_{xy})$	$Im(U_{xy})$	$Re(U_{yx})$	$Im(U_{yx})$	$Re(U_{yy})$	$Im(U_{yy})$
20	0.12	33.25	25.53	-3.23	-7.02	1.72	1.66	42.90	18.46	1.09	1.26	0.35	0.38	1.02	0.60	1.21	0.68
30	0.18	36.99	23.26	-4.16	-5.45	2.86	-1.13	41.78	18.31	0.84	1.18	0.28	0.25	0.38	0.69	0.86	1.63
40	0.24	36.95	25.99	-5.06	-5.27	4.81	1.03	41.69	25.04	1.35	2.02	0.36	0.54	0.63	0.89	1.08	1.87
50	0.30	37.55	25.77	-5.15	-5.25	5.21	0.60	39.37	27.97	1.03	2.13	0.32	0.58	0.53	0.44	0.79	2.50
70	0.42	33.32	37.66	-4.30	-5.45	5.49	1.02	33.30	38.82	1.03	3.39	0.61	0.63	0.42	0.49	0.77	3.73
80	0.48	34.57	36.64	-3.55	-6.30	9.02	3.80	43.61	56.51	0.75	3.73	0.37	0.54	0.95	1.14	2.25	4.71
90	0.54	31.86	43.87	-3.76	-5.89	7.89	3.14	34.92	51.38	0.93	4.70	0.55	0.72	0.63	0.83	0.84	5.34
100	0.60	31.01	47.92	-2.84	-5.18	7.38	-1.05	34.77	55.34	0.95	5.24	1.06	0.58	0.44	1.24	0.96	6.46
110	0.66	29.48	52.07	-1.23	-4.79	8.75	-0.09	28.91	61.17	0.73	5.75	1.43	0.44	0.27	0.92	0.86	6.57
130	0.78	28.37	61.71	2.18	-4.74	6.80	1.36	22.61	70.53	1.02	7.27	1.47	0.75	0.81	1.15	0.88	7.58
140	0.84	25.23	66.02	2.96	-5.01	7.52	2.79	17.04	76.81	2.09	6.70	1.41	0.81	1.50	0.98	0.87	7.45
170	1.02	17.62	81.24	4.93	-4.14	6.01	8.07	15.80	86.88	2.24	8.90	2.68	2.41	1.74	2.44	2.19	8.20
190	1.14	12.75	87.84	8.31	-6.52	-0.17	7.20	10.80	95.59	1.75	8.83	2.19	1.11	1.82	0.42	1.56	7.94
200	1.20	9.48	89.62	8.09	-5.85	-6.47	12.39	4.11	95.62	1.83	8.93	1.96	1.18	2.74	1.56	1.12	7.84
210	1.26	5.13	97.88	8.11	-0.36	-11.84	30.77	-14.68	94.96	2.16	9.44	2.41	0.78	3.77	5.68	1.29	7.27
220	1.32	7.72	101.48	19.85	0.38	-21.26	59.39	-30.16	133.69	3.46	7.91	2.68	1.87	4.89	8.29	6.30	10.64
230	1.38	-0.32	96.35	10.43	-7.68	1.87	22.54	-0.28	130.23	1.72	7.53	1.79	1.50	1.76	3.19	2.39	11.38
250	1.50	-9.43	103.07	-2.16	-9.62	2.25	30.11	-29.87	100.95	1.57	7.63	2.51	1.66	1.73	4.50	3.52	7.41
260	1.56	-26.96	103.36	-10.23	-4.07	-3.94	41.65	-56.55	100.54	3.99	5.55	3.30	2.10	2.47	4.54	7.48	7.05
280	1.68	-28.31	97.01	-3.61	2.98	0.10	48.34	-41.14	169.94	4.64	5.65	3.39	3.38	4.16	11.17	13.96	18.52

Table 66. Damper-bearing measured dynamic stiffnesses for 10000 rpm and 345 kPa

Ω (Hz)	Ω/ω	EXPERIMENT															
		Dynamic Stiffness (MN/m)								Uncertainty (MN/m)							
		$Re(H_{xx})$	$Im(H_{xx})$	$Re(H_{xy})$	$Im(H_{xy})$	$Re(H_{yx})$	$Im(H_{yx})$	$Re(H_{yy})$	$Im(H_{yy})$	$Re(U_{xx})$	$Im(U_{xx})$	$Re(U_{xy})$	$Im(U_{xy})$	$Re(U_{yx})$	$Im(U_{yx})$	$Re(U_{yy})$	$Im(U_{yy})$
20	0.12	39.99	19.92	-4.62	-7.40	6.46	-0.89	49.19	19.09	1.18	1.94	0.86	0.57	1.48	2.93	6.01	2.17
30	0.18	39.71	22.83	-4.71	-6.29	1.94	-2.11	53.68	23.95	1.19	1.42	1.17	0.57	2.31	1.55	6.77	4.76
40	0.24	37.96	25.82	-4.84	-6.79	4.94	-0.19	47.60	28.63	0.66	0.96	1.00	0.77	0.87	0.61	6.97	1.88
50	0.30	40.28	25.29	-5.96	-6.06	6.24	0.89	46.80	33.21	1.16	1.57	0.99	0.59	1.06	1.59	6.23	3.40
70	0.42	38.18	37.27	-5.03	-6.16	5.42	1.16	43.62	45.76	0.91	0.95	0.90	0.79	0.85	0.82	4.32	7.82
90	0.54	35.47	41.33	-4.39	-6.82	10.63	3.26	54.63	59.96	0.34	0.62	1.42	0.98	0.72	2.18	13.73	11.01
100	0.60	34.92	47.03	-2.63	-6.57	8.76	2.60	39.72	68.85	0.62	0.81	0.63	1.57	1.73	0.68	3.80	15.34
110	0.66	35.54	50.78	-2.16	-7.27	10.55	2.01	38.06	70.98	0.41	0.56	0.53	0.78	1.20	1.56	1.29	5.66
130	0.78	31.43	59.41	2.81	-5.17	9.36	3.36	27.51	88.40	0.61	0.94	1.14	0.81	1.53	1.57	9.18	10.06
140	0.84	28.01	62.64	2.87	-6.00	10.85	3.99	22.90	91.87	0.66	1.22	1.18	1.53	2.54	1.37	7.69	14.55
150	0.90	24.69	68.30	3.53	-3.12	9.56	2.81	10.61	84.57	0.73	1.00	1.48	1.10	2.86	1.28	11.04	27.78
160	0.96	20.62	70.57	1.31	-2.57	11.24	3.25	36.13	116.17	1.33	1.47	2.50	1.59	3.18	1.88	21.28	16.66
190	1.14	14.95	83.31	9.34	-9.35	12.25	4.52	52.71	111.30	0.77	0.62	3.17	2.62	3.32	3.37	22.18	23.40
200	1.20	13.22	86.68	11.54	-7.14	8.80	9.11	30.84	122.66	0.86	0.85	1.92	3.17	4.39	3.12	27.06	20.16
220	1.32	6.52	93.27	12.36	0.76	-1.79	9.20	-11.98	138.29	0.90	1.22	1.46	1.47	1.18	2.75	26.83	18.78
230	1.38	7.11	93.41	16.41	-6.09	8.14	16.84	22.75	134.27	0.73	0.77	1.94	0.74	0.60	4.66	9.08	14.35
250	1.50	-9.82	93.31	12.06	-3.82	1.22	20.67	1.35	110.97	1.38	2.09	1.43	1.05	6.24	7.80	20.23	19.84
260	1.56	-16.07	92.60	10.92	-0.96	-10.18	18.77	-19.93	131.24	3.55	3.63	0.66	1.30	4.57	5.48	19.08	5.33
290	1.74	-12.61	99.35	-0.80	-2.92	-12.47	58.12	-28.21	117.50	2.50	2.69	1.05	1.40	4.03	3.87	8.81	3.56

Table 67. Damper-bearing measured dynamic stiffnesses for 10000 rpm and 517 kPa

Ω (Hz)	Ω/ω	EXPERIMENT															
		Dynamic Stiffness (MN/m)								Uncertainty (MN/m)							
		$Re(H_{xx})$	$Im(H_{xx})$	$Re(H_{xy})$	$Im(H_{xy})$	$Re(H_{yx})$	$Im(H_{yx})$	$Re(H_{yy})$	$Im(H_{yy})$	$Re(U_{xx})$	$Im(U_{xx})$	$Re(U_{xy})$	$Im(U_{xy})$	$Re(U_{yx})$	$Im(U_{yx})$	$Re(U_{yy})$	$Im(U_{yy})$
20	0.12	43.61	19.97	-4.78	-6.74	5.52	-2.18	46.10	19.92	1.35	1.73	0.73	0.32	1.18	2.24	0.69	0.90
30	0.18	42.46	21.89	-4.51	-4.69	2.73	-1.83	46.21	19.91	1.08	1.37	0.36	0.40	0.99	0.99	0.47	0.56
40	0.24	38.70	26.53	-4.28	-5.49	5.09	-0.99	45.64	26.51	1.04	0.77	0.50	0.42	0.74	0.91	0.53	0.37
50	0.30	41.69	26.36	-5.31	-5.23	6.07	2.04	45.04	29.18	1.06	1.21	0.55	0.47	0.74	0.65	0.62	0.42
70	0.42	41.85	38.22	-4.59	-4.95	5.92	1.54	40.88	38.23	0.79	0.81	0.57	0.41	0.99	0.49	0.41	0.63
90	0.54	37.99	40.14	-3.38	-4.55	7.55	3.10	43.83	49.49	0.75	1.02	0.63	0.26	0.44	0.48	0.46	0.80
100	0.60	38.10	47.15	-3.06	-4.23	7.12	2.72	41.63	52.87	0.48	1.02	0.67	0.54	0.57	0.38	0.44	0.91
110	0.66	39.43	51.12	-2.12	-5.42	8.89	2.67	37.55	58.60	0.47	0.97	0.41	0.34	0.54	0.61	0.75	1.18
130	0.78	32.95	58.68	2.22	-3.06	8.19	3.26	30.54	68.42	0.68	1.42	0.86	0.58	0.52	0.31	0.74	1.07
140	0.84	29.79	60.60	2.68	-3.52	10.17	4.17	25.50	75.70	0.71	1.40	1.27	0.57	0.35	0.70	0.97	1.69
150	0.90	26.61	65.39	3.36	-1.83	9.63	3.83	16.88	73.99	0.59	1.46	1.65	0.62	0.60	0.60	0.82	1.92
200	1.20	14.45	84.63	9.26	-3.23	8.43	7.63	17.61	94.97	1.19	1.75	2.05	0.57	0.83	0.49	0.77	2.67
210	1.26	10.65	89.06	9.05	-0.43	6.77	10.08	6.84	96.56	0.74	1.45	0.87	0.54	0.41	0.52	0.82	2.32
220	1.32	10.00	92.50	10.45	2.43	5.52	9.47	-12.43	99.58	0.63	1.36	0.83	0.60	0.49	0.72	0.72	1.63
230	1.38	9.16	94.50	14.16	-3.32	7.08	12.80	17.51	116.19	0.58	1.22	1.14	0.87	0.52	0.59	0.69	2.77

Table 68. Damper-bearing measured dynamic stiffnesses for 10000 rpm and 689 kPa

Ω (Hz)	Ω/ω	EXPERIMENT															
		Dynamic Stiffness (MN/m)								Uncertainty (MN/m)							
		$Re(H_{xx})$	$Im(H_{xx})$	$Re(H_{xy})$	$Im(H_{xy})$	$Re(H_{yx})$	$Im(H_{yx})$	$Re(H_{yy})$	$Im(H_{yy})$	$Re(U_{xx})$	$Im(U_{xx})$	$Re(U_{xy})$	$Im(U_{xy})$	$Re(U_{yx})$	$Im(U_{yx})$	$Re(U_{yy})$	$Im(U_{yy})$
20	0.12	51.83	22.73	-4.35	-5.82	5.09	-2.48	55.34	25.17	2.41	1.84	0.52	0.51	2.25	1.53	1.13	1.59
30	0.18	46.98	23.76	-3.31	-3.50	3.60	-2.77	54.83	27.18	1.26	0.80	0.71	0.78	2.63	1.45	0.81	1.11
40	0.24	44.77	32.81	-3.20	-4.06	5.08	-1.72	53.47	35.16	1.18	1.65	0.77	1.07	0.75	1.53	0.92	1.84
50	0.30	48.91	35.93	-3.34	-3.64	5.74	1.79	51.96	40.83	1.07	2.21	1.28	1.22	1.13	1.41	0.99	2.67
70	0.42	48.27	47.78	-1.04	-2.33	7.68	2.07	47.45	56.64	1.20	2.88	2.39	0.91	1.11	1.20	0.84	5.15
80	0.48	44.54	51.05	3.79	0.13	8.05	-5.26	13.58	77.23	0.72	4.02	2.20	0.75	0.40	1.09	0.57	4.48
90	0.54	45.18	55.86	3.55	-2.14	9.69	3.74	53.14	74.89	0.62	3.67	2.61	0.62	0.70	0.98	1.34	6.05
100	0.60	45.06	63.66	4.97	-3.19	8.60	3.89	49.08	82.13	0.74	4.26	2.77	0.80	0.56	0.72	0.61	7.14
110	0.66	46.10	69.76	7.10	-4.93	11.20	3.95	46.78	88.79	0.80	4.49	2.77	0.94	0.88	0.86	1.28	7.05
130	0.78	39.25	79.82	11.18	-3.87	10.72	3.50	43.77	103.01	1.44	4.31	2.45	0.83	1.24	1.07	1.18	6.50
140	0.84	37.28	83.75	12.13	-4.83	13.56	4.01	36.97	111.61	2.07	4.58	2.46	1.27	1.80	1.56	1.47	6.67
150	0.90	32.95	85.86	9.74	-1.54	14.33	3.82	26.87	103.90	3.41	3.03	3.19	2.99	2.86	2.85	3.10	3.63
190	1.14	21.87	107.54	18.93	-6.81	15.46	5.63	39.31	125.33	1.00	5.09	3.44	2.77	1.39	0.91	3.27	6.00
200	1.20	20.96	112.40	22.16	-5.74	13.39	8.67	35.24	133.60	0.72	5.84	3.36	1.35	1.01	0.72	1.83	7.57
210	1.26	17.49	118.26	21.37	-3.09	10.92	10.95	19.69	134.68	0.72	6.04	2.03	1.00	0.47	0.81	1.08	6.14
220	1.32	16.92	124.20	23.71	-0.35	7.31	11.40	1.36	135.86	0.96	6.00	2.42	1.63	0.95	1.35	0.78	6.48
230	1.38	16.95	126.07	28.67	-8.56	9.34	17.57	29.37	160.36	0.65	6.23	3.26	2.66	1.19	2.25	1.53	7.70

Table 69. Damper-bearing measured dynamic stiffnesses for 10000 rpm and 862 kPa

Ω (Hz)	Ω/ω	EXPERIMENT															
		Dynamic Stiffness (MN/m)								Uncertainty (MN/m)							
		$Re(H_{xx})$	$Im(H_{xx})$	$Re(H_{xy})$	$Im(H_{xy})$	$Re(H_{yx})$	$Im(H_{yx})$	$Re(H_{yy})$	$Im(H_{yy})$	$Re(U_{xx})$	$Im(U_{xx})$	$Re(U_{xy})$	$Im(U_{xy})$	$Re(U_{yx})$	$Im(U_{yx})$	$Re(U_{yy})$	$Im(U_{yy})$
20	0.12	51.01	22.74	-4.96	-6.33	6.27	-2.74	58.32	26.69	2.35	1.72	0.59	0.54	1.77	1.13	0.75	1.28
30	0.18	50.00	22.03	-4.78	-3.70	1.92	-0.27	60.02	28.76	0.86	0.83	0.35	0.44	1.11	1.20	0.38	0.60
40	0.24	47.08	30.24	-4.36	-4.48	5.59	-1.43	58.13	36.90	0.86	1.13	0.43	0.78	1.11	0.63	0.65	0.85
50	0.30	51.09	35.71	-4.52	-4.14	4.07	2.23	57.55	41.56	1.07	1.82	0.48	0.77	0.70	0.93	0.43	1.22
70	0.42	51.21	44.81	-3.27	-2.58	6.79	4.14	54.35	55.55	1.01	1.13	1.10	0.78	0.74	1.06	0.81	1.46
80	0.48	47.58	47.30	-0.01	-0.28	10.23	1.80	30.85	69.06	0.74	1.04	0.84	0.70	0.89	1.11	0.46	1.51
90	0.54	48.32	51.50	0.26	-1.65	9.74	4.91	60.69	71.84	0.55	1.72	1.16	0.38	0.65	0.87	0.81	2.12
100	0.60	48.28	58.68	1.82	-1.73	8.74	4.41	56.18	78.24	0.74	1.36	0.91	0.88	0.69	0.69	0.61	2.66
110	0.66	48.48	65.13	4.46	-2.69	10.53	4.70	53.06	85.26	0.30	1.17	1.50	0.59	0.78	0.95	0.73	2.88
130	0.78	41.36	73.63	9.87	-1.30	11.10	5.46	48.44	100.12	0.60	1.30	1.38	0.70	0.62	0.45	0.78	2.18
140	0.84	41.39	76.76	11.02	-3.31	13.06	6.27	43.53	109.59	0.72	2.13	1.28	0.83	0.56	0.76	0.67	2.98
150	0.90	37.17	80.29	11.92	-1.10	13.82	6.01	33.31	103.25	1.23	1.70	1.20	1.60	0.89	1.04	0.84	2.02
190	1.14	25.57	100.54	20.18	-5.21	17.49	6.82	45.42	124.87	1.39	1.35	2.23	2.31	1.38	1.03	2.12	3.12
200	1.20	24.06	105.55	21.66	-3.68	16.35	8.55	39.93	130.75	1.14	1.99	1.42	0.69	0.76	0.63	0.91	3.09
210	1.26	20.92	111.08	20.71	-0.91	14.91	10.38	25.11	133.51	0.73	2.28	1.09	0.84	0.53	0.60	1.16	2.21
220	1.32	19.75	116.96	22.64	2.68	12.00	10.76	8.62	132.63	0.40	2.58	0.95	1.23	0.46	0.43	0.86	2.54
230	1.38	20.43	119.30	28.06	-4.54	14.42	15.66	36.07	157.60	0.64	2.17	1.72	1.55	0.49	0.53	0.97	2.87
240	1.44	17.43	121.67	22.91	-2.69	11.78	15.94	18.85	147.73	0.57	2.51	2.49	2.05	0.92	0.99	2.69	3.23
250	1.50	15.26	123.37	23.96	-4.61	9.13	18.35	12.91	146.47	0.65	2.71	1.00	0.79	0.36	0.70	0.84	2.81
260	1.56	14.48	126.17	24.06	-3.51	10.07	17.31	8.61	152.77	0.40	1.98	1.02	1.51	0.33	1.51	0.97	3.37
270	1.62	12.86	123.42	22.46	0.72	3.92	15.89	-13.92	163.41	0.89	2.97	0.74	1.16	1.00	1.52	1.62	3.57

Table 70. Damper-bearing measured dynamic stiffnesses for 12000 rpm and 0 kPa

Ω (Hz)	Ω/ω	EXPERIMENT															
		Dynamic Stiffness (MN/m)								Uncertainty (MN/m)							
		$Re(H_{xx})$	$Im(H_{xx})$	$Re(H_{xy})$	$Im(H_{xy})$	$Re(H_{yx})$	$Im(H_{yx})$	$Re(H_{yy})$	$Im(H_{yy})$	$Re(U_{xx})$	$Im(U_{xx})$	$Re(U_{xy})$	$Im(U_{xy})$	$Re(U_{yx})$	$Im(U_{yx})$	$Re(U_{yy})$	$Im(U_{yy})$
20	0.10	47.95	21.50	-2.62	-8.81	6.24	4.14	47.32	20.81	2.29	2.14	1.10	1.11	1.59	1.39	1.22	0.40
30	0.15	47.97	29.26	-2.89	-9.04	7.08	-0.16	44.96	22.21	4.58	4.39	0.81	1.09	1.45	1.55	1.23	0.68
40	0.20	45.21	29.95	-1.13	-4.86	7.71	2.32	51.19	28.72	2.91	2.84	3.32	1.84	1.02	0.96	0.57	0.62
50	0.25	43.40	27.81	-3.51	-7.35	6.32	2.14	46.30	28.73	1.48	1.91	0.99	1.21	0.91	0.81	0.63	0.81
70	0.35	40.63	36.49	-4.40	-7.23	6.91	1.59	44.63	39.30	1.25	1.03	1.24	0.71	0.83	1.10	1.01	0.84
80	0.40	47.34	37.53	-0.02	-3.20	10.03	3.74	39.19	46.72	1.75	2.22	1.23	2.09	0.94	0.96	0.65	0.58
90	0.45	43.80	40.26	-6.91	-7.53	10.14	3.76	41.22	52.37	1.59	2.31	1.66	1.05	0.92	1.19	0.47	0.92
100	0.50	41.10	44.74	-2.74	-12.06	11.56	1.05	44.91	51.45	1.71	2.22	1.17	4.28	1.02	1.51	0.73	0.76
110	0.55	38.99	47.16	0.06	-10.32	12.52	1.89	39.19	58.57	2.29	2.71	2.71	1.35	1.31	1.59	0.94	1.43
130	0.65	40.27	46.67	-0.73	-10.46	17.28	-4.23	32.44	69.34	3.11	2.29	2.13	1.82	1.44	2.41	1.73	1.14
140	0.70	31.78	43.88	4.78	-8.55	21.02	-12.39	32.77	77.85	4.60	2.41	2.46	2.32	4.30	2.10	0.79	1.86
150	0.75	29.08	52.12	8.13	-10.15	17.35	-9.87	30.95	77.89	3.95	4.99	4.22	3.61	2.80	2.58	1.31	1.51
160	0.80	30.50	70.61	6.41	-8.47	12.19	-0.10	31.99	82.41	1.83	2.38	2.31	1.65	1.25	1.73	2.24	1.04
170	0.85	24.84	73.67	6.07	-11.66	12.20	1.16	29.94	86.55	3.74	2.01	6.29	5.95	1.32	2.15	3.04	2.36
210	1.05	11.03	85.71	17.13	-0.45	6.54	11.12	28.76	107.97	2.38	2.61	4.06	3.44	1.84	1.70	2.61	2.76
220	1.10	8.00	83.57	7.06	-1.85	11.83	13.16	25.52	114.53	2.58	3.82	3.88	3.53	1.39	1.22	1.73	1.47
230	1.15	1.14	90.57	8.92	8.52	14.51	14.10	28.97	110.55	2.27	1.54	3.77	6.39	2.74	1.14	1.10	1.51
260	1.30	-15.30	97.50	17.71	12.65	5.19	18.48	12.44	127.15	2.33	3.53	2.36	6.78	1.46	2.05	1.59	2.25
270	1.35	-16.21	106.71	11.87	7.00	6.79	22.83	13.15	132.07	1.85	3.74	3.55	9.19	1.47	1.93	1.72	1.21
280	1.40	-17.62	107.31	25.22	19.31	2.22	24.78	19.39	125.80	1.69	2.23	3.61	3.45	0.96	0.97	1.69	1.86
290	1.45	-17.97	106.58	23.51	19.70	3.70	33.74	21.92	131.59	1.11	2.25	2.50	6.79	1.69	0.94	1.12	1.80

Table 71. Damper-bearing measured dynamic stiffnesses for 12000 rpm and 172 kPa

Ω (Hz)	Ω/ω	EXPERIMENT															
		Dynamic Stiffness (MN/m)								Uncertainty (MN/m)							
		$Re(H_{xx})$	$Im(H_{xx})$	$Re(H_{xy})$	$Im(H_{xy})$	$Re(H_{yx})$	$Im(H_{yx})$	$Re(H_{yy})$	$Im(H_{yy})$	$Re(U_{xx})$	$Im(U_{xx})$	$Re(U_{xy})$	$Im(U_{xy})$	$Re(U_{yx})$	$Im(U_{yx})$	$Re(U_{yy})$	$Im(U_{yy})$
20	0.10	43.94	25.05	-2.75	-11.33	7.91	1.73	52.47	20.38	2.14	1.43	0.52	0.84	1.43	1.37	1.00	0.52
30	0.15	45.66	27.28	-3.74	-8.93	3.72	-2.85	50.39	19.90	0.92	1.47	0.40	0.84	1.15	1.12	1.05	0.84
40	0.20	45.36	28.02	-5.41	-9.40	8.13	-0.86	54.28	26.86	1.43	0.90	1.32	0.97	0.87	1.05	0.96	0.60
50	0.25	45.29	25.02	-6.89	-9.33	6.69	-0.37	48.33	28.86	0.98	0.91	0.62	0.73	0.83	0.56	0.64	0.43
70	0.35	44.52	39.91	-6.40	-8.49	6.32	0.20	44.37	38.63	1.55	0.63	1.07	0.67	0.76	0.56	0.68	0.63
80	0.40	44.90	36.49	-6.00	-10.58	9.62	2.04	52.95	54.23	1.74	0.89	0.81	0.89	1.29	0.75	0.43	1.11
90	0.45	44.64	44.02	-8.10	-9.58	9.89	2.03	47.52	51.80	1.92	1.17	0.59	0.76	0.84	0.86	1.23	0.66
100	0.50	43.71	46.60	-8.19	-8.77	8.05	-0.27	47.38	51.17	1.40	1.23	1.02	0.77	0.80	0.34	1.17	0.88
110	0.55	41.84	50.13	-6.11	-8.72	9.34	1.27	40.03	58.06	1.77	0.73	1.16	0.64	0.71	0.98	0.87	1.10
130	0.65	38.63	55.67	-3.44	-6.54	9.47	2.68	32.77	66.06	1.87	1.05	1.46	0.49	0.74	0.64	1.18	0.97
140	0.70	36.30	61.21	-2.83	-6.81	10.49	3.35	27.91	72.88	1.57	0.84	0.80	0.60	0.84	0.47	1.38	1.65
150	0.75	31.40	66.96	-1.04	-1.72	9.65	-2.10	11.16	71.05	1.49	0.58	0.86	1.00	1.05	0.41	0.88	2.80
160	0.80	31.61	71.85	0.23	-6.01	9.04	10.70	37.50	102.44	0.95	2.69	1.27	1.28	1.67	1.05	2.14	1.61
170	0.85	28.77	75.23	1.28	-3.77	11.84	6.46	26.65	87.28	1.11	2.43	2.11	1.80	1.03	0.80	1.76	1.06
190	0.95	19.90	81.06	-0.15	-5.69	4.33	4.10	20.20	90.14	2.93	1.71	3.07	4.90	1.28	2.62	4.37	1.58
220	1.10	13.89	91.51	11.38	-4.04	16.07	57.11	-30.21	123.76	3.54	2.04	2.94	9.21	5.03	3.46	8.97	6.30
230	1.15	8.01	95.88	2.34	-3.97	16.77	16.31	35.12	137.93	1.24	1.01	0.98	6.05	1.83	1.54	5.15	2.72
250	1.25	2.65	94.37	-8.93	0.78	11.93	19.58	-20.68	110.42	1.00	1.91	1.75	1.08	1.14	1.86	1.58	1.72
260	1.30	-3.64	104.51	-22.38	17.59	6.00	35.82	-60.61	122.61	2.77	1.79	2.65	3.25	3.82	3.08	5.23	5.34
270	1.35	-2.81	98.29	3.11	20.79	13.72	26.52	-55.26	153.01	1.32	2.68	3.93	1.17	2.14	5.57	4.59	2.83
280	1.40	-17.02	105.01	-5.64	35.32	11.45	34.20	20.41	174.63	1.73	2.98	2.69	3.38	2.35	3.67	7.06	5.55

Table 72. Damper-bearing measured dynamic stiffnesses for 12000 rpm and 345 kPa

Ω (Hz)	Ω/ω	EXPERIMENT															
		Dynamic Stiffness (MN/m)								Uncertainty (MN/m)							
		$Re(H_{xx})$	$Im(H_{xx})$	$Re(H_{xy})$	$Im(H_{xy})$	$Re(H_{yx})$	$Im(H_{yx})$	$Re(H_{yy})$	$Im(H_{yy})$	$Re(U_{xx})$	$Im(U_{xx})$	$Re(U_{xy})$	$Im(U_{xy})$	$Re(U_{yx})$	$Im(U_{yx})$	$Re(U_{yy})$	$Im(U_{yy})$
20	0.10	46.03	22.80	-5.63	-9.22	5.05	-0.67	52.88	22.34	2.78	1.72	0.88	0.63	1.36	2.20	2.00	2.52
30	0.15	45.45	26.12	-5.52	-7.18	2.68	-2.36	53.49	24.09	1.99	1.56	0.72	0.62	1.30	1.33	2.61	1.25
40	0.20	43.48	30.92	-5.71	-8.68	4.83	-0.56	51.71	31.09	1.45	2.09	0.67	0.72	0.90	0.49	3.50	1.20
50	0.25	46.91	28.93	-7.55	-8.55	6.29	0.79	51.88	36.09	1.12	0.85	0.56	0.72	0.78	1.17	2.19	2.52
70	0.35	46.09	42.00	-7.05	-8.36	6.38	1.21	47.21	47.02	1.14	1.17	0.84	1.01	0.65	0.51	1.22	4.17
90	0.45	42.90	45.61	-7.25	-7.87	10.04	2.79	52.29	58.59	0.73	0.41	0.79	1.18	0.91	1.28	4.21	2.85
100	0.50	42.80	51.97	-6.90	-7.71	9.96	1.74	47.26	63.39	0.83	1.00	0.88	1.05	0.93	0.88	2.48	6.55
110	0.55	43.34	55.58	-6.43	-7.82	11.37	1.13	44.64	69.85	1.60	1.39	1.34	1.13	0.97	0.92	3.07	5.50
130	0.65	37.75	65.46	-0.79	-4.89	10.25	1.31	33.98	82.03	1.66	1.61	1.13	0.75	1.44	0.82	4.05	5.34
140	0.70	35.10	69.71	-0.58	-6.22	11.89	2.03	33.15	92.26	1.23	1.43	1.27	0.85	1.14	0.83	5.26	4.18
150	0.75	32.84	76.33	1.02	-2.72	10.26	1.38	21.12	88.44	0.83	1.05	0.94	0.99	1.70	0.85	5.28	6.97
160	0.80	29.82	81.83	4.81	-4.37	8.03	2.49	41.30	115.64	1.09	1.35	1.48	1.24	0.98	1.33	5.14	10.51
170	0.85	27.59	85.20	3.90	-3.80	9.96	4.27	24.38	99.69	1.30	0.72	1.80	0.82	0.95	1.36	9.16	5.26
230	1.15	16.47	101.58	13.08	-3.35	6.12	15.34	25.62	134.71	2.05	1.60	3.01	1.20	1.99	2.62	5.72	13.40
250	1.25	-1.85	100.26	13.54	-1.68	0.88	21.07	3.93	118.50	1.32	1.63	1.03	0.91	2.88	2.82	8.36	7.39
280	1.40	-5.52	112.38	14.13	-3.25	0.82	49.49	-3.46	171.76	1.58	4.39	1.97	1.59	3.35	2.62	6.79	10.95

Table 73. Damper-bearing measured dynamic stiffnesses for 12000 rpm and 517 kPa

Ω (Hz)	Ω/ω	EXPERIMENT															
		Dynamic Stiffness (MN/m)								Uncertainty (MN/m)							
		$Re(H_{xx})$	$Im(H_{xx})$	$Re(H_{xy})$	$Im(H_{xy})$	$Re(H_{yx})$	$Im(H_{yx})$	$Re(H_{yy})$	$Im(H_{yy})$	$Re(U_{xx})$	$Im(U_{xx})$	$Re(U_{xy})$	$Im(U_{xy})$	$Re(U_{yx})$	$Im(U_{yx})$	$Re(U_{yy})$	$Im(U_{yy})$
20	0.10	48.03	22.31	-5.35	-8.22	6.51	-2.83	50.16	22.05	2.68	2.36	0.79	0.28	1.94	2.11	0.94	1.34
30	0.15	46.31	24.25	-4.74	-5.89	2.63	-2.45	50.19	22.80	1.56	1.39	0.43	0.52	1.34	1.43	0.89	0.82
40	0.20	42.63	29.40	-4.81	-6.86	5.59	-1.18	49.79	29.82	0.95	0.62	0.37	0.46	0.96	1.02	0.57	1.16
50	0.25	46.58	30.08	-6.19	-6.91	6.30	1.59	49.33	32.72	1.28	1.61	0.49	0.44	1.47	0.94	0.64	1.39
70	0.35	47.29	42.52	-5.97	-6.65	6.35	1.39	45.59	42.74	1.04	1.17	0.91	0.59	0.92	1.00	0.65	0.50
90	0.45	43.40	45.41	-5.19	-6.03	8.66	3.18	48.37	54.48	1.15	1.08	1.25	0.70	0.69	0.74	0.99	0.74
100	0.50	43.72	52.24	-5.38	-5.70	8.58	2.94	47.27	57.82	1.47	0.77	0.70	1.01	1.17	1.50	1.01	0.89
110	0.55	45.08	56.15	-4.34	-6.77	10.51	2.22	43.04	65.26	1.92	1.74	0.53	0.73	0.69	1.68	0.79	1.06
130	0.65	38.68	64.95	0.96	-3.20	9.56	2.58	35.05	75.04	1.67	1.58	1.05	0.98	0.79	1.47	0.43	0.84
140	0.70	35.60	67.15	1.30	-4.33	11.87	3.10	31.71	84.08	1.51	1.47	1.17	1.14	0.66	1.06	1.20	1.14
150	0.75	32.29	72.18	3.41	-2.18	11.44	2.77	22.84	83.21	0.99	1.53	0.83	0.98	0.97	0.44	0.68	0.63
160	0.80	30.59	77.47	5.80	-4.64	9.81	3.50	45.34	107.22	0.88	2.02	1.16	1.29	0.59	0.97	1.62	1.63
170	0.85	26.77	80.25	4.10	-3.31	13.17	4.11	28.60	94.37	0.61	0.99	1.34	1.11	0.53	0.70	1.20	1.70
210	1.05	17.30	97.25	3.61	-2.51	7.95	9.75	14.50	100.47	1.09	0.70	1.75	1.15	0.75	0.82	1.23	1.24
220	1.10	16.85	100.81	11.03	1.42	6.11	9.45	-3.32	107.67	1.23	1.07	0.82	0.45	0.89	0.95	0.77	1.23
230	1.15	15.54	102.44	15.77	-3.18	7.67	12.27	23.75	127.56	0.92	0.80	1.16	0.60	0.78	1.19	1.70	0.94
250	1.25	8.48	101.05	13.98	-0.95	2.81	18.49	6.64	117.72	1.44	0.88	0.89	1.07	0.56	0.73	0.99	1.09
260	1.30	7.65	100.80	14.57	0.87	2.40	12.87	-2.39	123.06	1.81	2.06	1.35	0.36	0.75	1.01	1.38	1.04
270	1.35	-4.78	101.88	16.21	3.84	-5.65	17.85	-10.81	131.97	1.43	2.97	1.08	0.67	0.68	2.10	1.54	0.69

Table 74. Damper-bearing measured dynamic stiffnesses for 12000 rpm and 689 kPa

Ω (Hz)	Ω/ω	EXPERIMENT															
		Dynamic Stiffness (MN/m)								Uncertainty (MN/m)							
		$Re(H_{xx})$	$Im(H_{xx})$	$Re(H_{xy})$	$Im(H_{xy})$	$Re(H_{yx})$	$Im(H_{yx})$	$Re(H_{yy})$	$Im(H_{yy})$	$Re(U_{xx})$	$Im(U_{xx})$	$Re(U_{xy})$	$Im(U_{xy})$	$Re(U_{yx})$	$Im(U_{yx})$	$Re(U_{yy})$	$Im(U_{yy})$
20	0.10	49.01	24.15	-6.37	-8.95	7.65	-2.52	54.93	25.19	2.32	2.60	0.48	0.76	2.62	2.70	0.60	2.11
30	0.15	52.58	23.96	-6.14	-5.81	0.67	-1.75	55.33	24.35	1.50	1.93	0.66	0.33	1.74	1.67	0.91	0.82
40	0.20	46.61	29.82	-5.70	-7.21	5.21	-1.46	54.53	31.58	1.41	1.33	0.35	0.51	0.71	1.18	0.90	1.31
50	0.25	51.73	31.83	-6.71	-7.68	3.43	2.62	54.53	35.65	1.56	1.73	0.51	0.51	0.57	0.81	0.72	1.52
70	0.35	52.86	40.96	-7.60	-7.58	6.47	4.50	52.26	45.77	1.16	1.48	0.42	0.57	1.06	0.87	0.98	1.18
80	0.40	48.82	40.18	-2.71	-6.59	5.93	-3.36	22.45	73.12	0.92	0.97	0.51	0.79	1.08	0.95	0.93	2.15
90	0.45	48.81	43.33	-7.17	-6.59	8.73	5.35	58.68	57.10	1.01	1.07	0.60	0.70	0.86	0.82	0.52	1.10
100	0.50	49.19	49.68	-6.95	-6.70	9.28	5.43	55.52	61.31	1.02	1.45	0.86	0.85	0.52	1.05	1.18	1.50
110	0.55	50.61	53.73	-6.27	-6.55	11.28	5.30	51.06	66.22	0.71	1.72	0.72	0.74	0.75	1.03	0.87	1.67
130	0.65	42.68	60.96	-2.26	-2.65	11.33	5.83	43.84	76.32	0.60	1.88	0.93	1.19	0.61	0.92	1.17	1.32
140	0.70	39.13	64.23	-1.02	-3.62	13.13	5.83	39.47	86.05	0.73	1.69	1.31	0.65	0.70	0.59	1.02	2.30
150	0.75	35.94	68.61	1.34	-1.40	13.12	5.19	28.19	82.90	0.50	1.82	0.87	0.72	0.64	0.63	1.52	1.90
160	0.80	34.31	74.79	4.08	-2.91	12.67	4.66	53.37	110.33	0.76	1.48	0.92	1.34	0.64	0.74	1.15	0.71
170	0.85	29.83	78.00	3.97	-2.16	15.04	6.07	33.66	96.18	0.57	1.07	0.73	1.01	0.63	0.58	1.24	1.27
210	1.05	20.45	94.42	5.49	1.30	13.01	9.43	18.89	103.20	0.83	1.06	2.45	1.90	0.62	0.81	1.43	1.60
220	1.10	19.62	99.71	12.69	4.66	10.38	9.32	1.13	108.91	0.46	0.97	0.86	1.29	0.36	0.67	0.86	1.44
230	1.15	18.82	102.42	16.99	-0.95	12.20	11.90	29.20	129.32	0.57	1.23	1.05	0.72	0.78	0.68	1.08	1.46
250	1.25	13.37	105.89	15.32	-1.17	7.02	14.28	11.07	121.47	0.28	0.82	0.45	1.05	0.70	0.77	0.78	1.53
260	1.30	13.38	106.91	15.43	1.68	7.55	11.64	5.29	125.42	0.33	0.86	0.76	0.72	0.56	0.83	1.44	1.44
270	1.35	6.67	100.55	15.23	6.32	-3.49	11.89	-8.76	138.98	1.38	1.28	0.73	0.57	0.93	2.13	1.43	1.83
280	1.40	5.36	94.15	22.20	6.11	-30.99	23.40	20.17	204.32	2.43	1.43	0.62	0.93	0.81	1.65	1.08	1.44

Table 75. Damper-bearing measured dynamic stiffnesses for 12000 rpm and 862 kPa

Ω (Hz)	Ω/ω	EXPERIMENT															
		Dynamic Stiffness (MN/m)								Uncertainty (MN/m)							
		$Re(H_{xx})$	$Im(H_{xx})$	$Re(H_{xy})$	$Im(H_{xy})$	$Re(H_{yx})$	$Im(H_{yx})$	$Re(H_{yy})$	$Im(H_{yy})$	$Re(U_{xx})$	$Im(U_{xx})$	$Re(U_{xy})$	$Im(U_{xy})$	$Re(U_{yx})$	$Im(U_{yx})$	$Re(U_{yy})$	$Im(U_{yy})$
20	0.10	54.35	23.93	-5.17	-6.96	4.69	-1.46	60.14	29.66	3.54	3.84	0.49	0.49	3.32	4.69	1.15	1.54
30	0.15	51.31	25.19	-4.80	-4.47	2.00	-1.08	61.74	31.36	1.25	2.10	0.50	0.76	1.30	1.30	0.94	1.28
40	0.20	49.27	33.39	-4.87	-5.39	5.02	-1.47	60.46	40.38	0.77	2.19	0.87	0.65	2.49	1.51	0.86	1.69
50	0.25	53.55	39.44	-5.14	-5.22	5.52	3.02	60.06	45.39	1.72	2.01	0.71	0.65	1.59	1.91	0.83	1.44
70	0.35	54.90	48.82	-4.75	-3.42	8.11	4.21	57.40	59.21	1.15	1.35	0.83	0.93	1.27	1.72	0.76	1.22
80	0.40	51.05	52.41	-0.43	-0.96	10.69	1.13	33.05	73.42	1.08	0.97	0.78	0.80	1.17	1.02	0.51	0.97
90	0.45	52.61	55.64	-0.66	-2.07	10.95	4.95	63.24	76.83	1.55	1.45	0.96	0.65	1.05	1.04	1.02	1.27
100	0.50	53.02	64.66	0.31	-2.16	9.29	3.73	60.03	83.23	2.35	1.71	1.37	0.96	1.15	0.81	1.41	1.24
110	0.55	53.08	70.82	2.89	-2.83	11.78	4.52	56.78	91.12	1.32	1.41	1.14	1.05	1.13	0.69	1.04	1.61
130	0.65	46.31	80.90	9.77	-1.08	11.43	4.56	51.65	106.41	1.88	1.50	1.14	0.93	0.89	0.96	0.92	1.55
140	0.70	46.19	84.35	11.03	-2.38	14.06	5.08	46.27	117.03	1.42	1.85	1.31	0.90	1.25	0.94	1.00	2.19
150	0.75	43.55	87.60	11.81	-0.31	13.97	5.90	37.12	110.52	1.64	1.40	1.58	0.99	0.97	1.18	0.68	2.59
160	0.80	43.19	94.32	15.93	-3.66	14.53	6.04	64.30	140.44	1.88	1.49	2.39	1.87	1.04	1.56	2.15	2.31
170	0.85	38.35	97.94	14.90	-0.62	17.24	7.01	42.59	126.06	2.33	1.93	2.80	1.86	0.78	1.43	2.75	3.31
210	1.05	27.58	115.13	15.56	-0.94	17.16	9.47	30.64	135.91	1.59	1.48	5.63	2.72	2.05	0.95	2.65	5.70
220	1.10	27.03	122.10	22.22	1.11	13.19	10.56	16.00	139.24	0.96	1.09	2.89	1.44	0.92	0.70	2.05	2.96
230	1.15	27.44	124.42	29.26	-4.62	15.88	15.23	44.88	167.07	1.57	1.02	1.76	1.32	1.19	0.72	2.33	3.89
250	1.25	22.75	128.33	26.60	-3.84	10.53	17.79	23.03	154.84	1.36	0.90	1.26	0.94	1.30	0.26	2.08	1.85
260	1.30	22.19	129.91	26.91	-3.38	11.02	16.14	20.52	159.05	1.20	1.07	0.83	0.74	1.20	0.49	2.79	1.21
270	1.35	19.47	124.82	26.32	1.26	3.73	15.08	-2.98	170.00	1.69	1.17	1.14	0.79	1.90	0.67	2.93	1.29
280	1.40	26.07	122.62	36.39	-2.11	-22.12	29.74	18.12	257.87	0.69	0.91	0.60	1.04	2.41	2.41	5.13	1.49

Table 76. Damper-bearing rotating load measured stiffness coefficients

EXPERIMENT		Rotordynamic Coefficients Stiffness (MN/m)				Uncertainties Stiffness (MN/m)			
Running Speed (rpm)	Excitation Amplitude (N)	Kxx	Kxy	Kyx	Kyy	ΔKxx	ΔKxy	ΔKyx	ΔKyy
Baseline	Baseline	3.4	0.5	-0.2	4.7	0.1	0.2	0.0	0.1
12000	222	63.7	-7.3	7.9	74.4	0.2	0.3	0.4	0.5
12000	445	56.2	-0.2	3.1	62.3	0.2	0.4	0.3	0.1
12000	667	49.3	5.2	-1.0	52.9	0.3	0.5	0.5	0.5
12000	890	36.6	12.1	-6.3	37.3	0.2	1.1	0.5	1.5
12000	1112	33.2	9.5	-6.4	37.8	0.5	0.7	0.1	0.9
12000	1334	30.1	6.8	-6.3	33.8	0.5	0.4	0.1	1.0
12000	1557	25.2	0.5	-1.6	30.6	0.4	0.1	0.2	0.6
12000	1779	28.6	0.3	0.1	32.4	0.6	0.4	0.2	0.9

Table 77. Damper-bearing rotating load measured damping coefficients

EXPERIMENT		Rotordynamic Coefficients Damping (kN.s/m)				Uncertainties Damping (kN.s/m)			
Running Speed (rpm)	Excitation Amplitude (N)	Cxx	Cxy	Cyx	Cyy	ΔCxx	ΔCxy	ΔCyx	ΔCyy
Baseline	Baseline	0.4	-1.2	0.4	2.1	0.7	0.5	0.2	0.2
12000	222	89.8	-6.9	-0.9	91.4	0.3	0.7	0.8	0.4
12000	445	85.5	-4.3	0.7	90.8	-0.3	0.2	0.4	0.6
12000	667	83.2	-4.3	6.7	83.3	1.0	0.9	1.1	1.9
12000	890	48.8	-38.9	58.9	65.9	6.5	0.9	7.1	2.1
12000	1112	61.4	-44.4	40.8	66.1	4.9	1.7	1.0	1.0
12000	1334	78.3	-56.1	53.6	68.0	1.8	1.8	1.7	2.4
12000	1557	119.4	-97.0	69.5	108.5	7.9	8.0	3.2	7.1
12000	1779	113.8	-59.1	52.5	127.7	2.9	6.6	6.2	2.3

Table 78. Damper-bearing rotating load measured added mass coefficients

EXPERIMENT		Rotordynamic Coefficients Added Mass (kg)				Uncertainties Added Mass (kg)			
Running Speed (rpm)	Excitation Amplitude (N)	Mxx	Mxy	Myx	Myy	ΔMxx	ΔMxy	ΔMyx	ΔMyy
Baseline	Baseline	4.9	0.5	1.1	4.4	0.6	0.6	0.2	0.2
12000	222	46.0	10.2	-14.6	38.7	-0.1	0.1	1.6	0.9
12000	445	35.5	10.9	-12.5	30.0	-0.2	0.1	0.1	0.8
12000	667	27.6	11.2	-7.7	29.2	0.0	2.7	0.6	2.0
12000	890	40.1	-35.4	-0.2	95.0	0.3	9.9	0.9	9.7
12000	1112	42.8	-16.7	1.6	62.8	0.9	7.6	0.6	1.1
12000	1334	49.8	11.0	-1.0	77.0	0.6	3.1	1.6	2.3
12000	1557	97.8	72.5	-50.1	105.9	6.8	11.5	6.6	6.6
12000	1779	57.7	71.4	-77.1	89.4	10.5	4.3	3.3	9.1

VITA

Name:	Jeffrey Scott Agnew
Address:	P.O. Box 44, Tonawanda, NY 14151-0044
Email Address:	jagnew@live.com
Education:	B.S., Mechanical Engineering, Arkansas State University, 2006 M.S., Mechanical Engineering, Texas A&M University, 2011